STUDIES ON ORGANIC CORROSION INHIBITORS FOR REFINERY INDUSTRY

SUMMARY

Thesis

SUBMITTED FOR THE AWARD OF THE DEGREE OF

Doctor of Philosophy

IN

APPLIED CHEMISTRY

BY

NIDHI SAXENA

DEPARTMENT OF APPLIED CHEMISTRY
FACULTY OF ENGINEERING & TECHNOLOGY
ALIGARH MUSLIM UNIVERSITY
ALIGARH (INDIA)

2007


Maulana Azad Library
J.708

Corrosion is the degradation of metal or alloy by chemical or electrochemical reaction with its environment[1-2]. It is a major problem in several industries. It causes enormous economic wastage of metallic materials, which leads to heavy economic losses all over the world. The direct cost includes the replacement of corroded components, use of corrosion resistant alloys, use of coating and inhibitors etc. The indirect costs are loss of production during downtime, loss of products due to leakage, loss of efficiency, contaminations[3-4] and sometimes it causes loss of human lives due to explosion/fire. The cost of corrosion can be reduced to an extent of 25% by applying some corrosion control techniques[5]. The prevalent corrosion control techniques are materials selection, proper design, electrochemical protection and use of inhibitors and paints/coatings. Among these methods, inhibitors are used in a wide range of applications, such as oil pipelines, domestic central heating systems, industrial water cooling systems and metal extraction plants. The advantage of corrosion inhibitor is that it can be implemented or charged *in situ* without disrupting a process and is also a cost effective method[6]. The major industries using corrosion inhibitors are the oil and gas exploration and production industry, the petroleum refining industry, the chemical industry, heavy industrial manufacturing industry, water treatment facilities, and the product additive industries. Due to ease of application and cost effectiveness, the use of inhibitors has increased manifold during the past several years.

Mild steel[7] is one of the most important engineering metal, owing to its low cost and excellent mechanical properties. It is widely used as a

construction material. In petroleum refineries[8] mild steel is used for the construction of components in fractionation tower, separator drums, heat exchangers shell and tubes, reactor cladding, tubes in furnaces, piping and reboiler tubes etc. The mild steel is severely attacked in acid solutions by hydrogen sulfide, hydrochloric acid, hydrofluoric acid, sulfuric acid, and caustic in oil sector during processes related to drilling and distillation.

The research work described in the thesis deals with the study on some oxygen, nitrogen and sulfur containing heterocyclic organic compounds namely hydrazides, thiosemicarbazides, and imidazolines, triazoles and oxadiazoles derivatives as corrosion inhibitors for mild steel in 1.0 mol dm^{-3} HCl. The name, abbreviation and structure of the studied compounds are given in Tables 1- 2. The techniques such as weight loss, potentiodynamic polarization, electrochemical impedance and scanning electron microscopy were employed for the evaluation of inhibitive properties of hydrazides, thiosemicarbazides, imidazolines, triazoles and oxadiazoles on corrosion inhibition.

The thesis has been divided into six chapters. The first chapter describes the general introduction on corrosion, mechanism of inhibition, corrosion process in refinery and statement of the problem. The introduction also highlights the economic and technological importance of corrosion in refineries.

The materials used and the experimental conditions for the study are given in Chapter 2. The techniques namely, weight loss, potentiodynamic polarization, electrochemical impedance and scanning electron microscopy

used for investigating corrosion inhibition behaviour have also been discussed in Chapter 2. The method for the synthesis of inhibitors alongwith their characterization details are given in this chapter.

The third Chapter describes the results and discussion on the observed inhibition efficiency of hydrazides and thiosemicarbazides. The dependance of inhibition efficiency on [inhibitor], temperature, immersion time and [acid] are presented graphically in Figure 1 (for hydrazides) and Figure 2 (for thiosemicarbazides). The various thermodyanamic parameters[9-11] were determined by using the following relations and the values are given in Table 3.

$$\text{Log (CR)} = \frac{-E_a}{2.303RT} + A$$

$$\Delta G_{ads} = -RT \ln (55.5K)$$

$$CR = \frac{RT}{Nh}\exp\left(\frac{\Delta S}{R}\right)\exp\left(-\frac{\Delta H}{RT}\right)$$

$$t_{1/2} = 0.693/k$$

The values of corrosion density (I_{corr}), corrosion potential E_{corr} and inhibition efficiency[12] were determined with help of Tafel plots and these are given in Table 4. The values of R_t and C_{dl} calculated from Nyquist plot are presented in Table 5. From these studies it is evident that the corrosion inhibiting properties of fatty acid hydrazides is due to molecular adsorption to the metallic surface. These compounds are able to get adsorbed on the steel surface through lone pair of electrons of N and O- atoms. The long hydrophobic chain of hydrocarbon prevents corrosion by keeping acid solution

away from metal surface. The excellent performance of DDH is attributed to the presence of long hydrophobic chain of C_{11}. The increase in carbon atoms above than 11 decreases inhibition efficiency due to increased stearic hindrance to adsorption[13].

Among the investigated thiosemicarbazides, the order of inhibition efficiency has been found as follows

UPTS > NPTS > PPTS > HPTS

It has been observed that the inhibition efficiency of the tested thiosemicarbazides increased with the increase in chain length up to C_{11}. A further increase in chain length up to C_{17} has been found to decreased the inhibition efficiency. UPTS showed highest inhibition efficiency among the studied thiosemicarbazides due to presence of long hydrophobic chain.

In Chapter 4, the dependence of inhibition efficiency on [inhibitor], temperature, immersion time and [acid] (Figure 3) have been discussed. The inhibition efficiency was found to be in following order:

UDI > NI > PDI > HDI > HI

Inhibition efficiency of the studied imidazolines increased with the increase in chain length up to C_{11}. A further increase in chain length up to C_{17} decreased the inhibition efficiency. The inhibitive effect of imidazolines is due to adsorption to the steel surface. The adsorption of imidazolines followed Langmiur adsorption isotherm. The thermodynamic parameters and observed data for electrochemical studies are given in Tables 3-5.

The studies on the inhibitive effect of triazoles and oxadiazoles are presented in Chapter 5. Figures 5-6 shows the dependence of inhibition

efficiency on [inhibitor], temperature, immersion time and [acid] of triazoles and oxadiazoles ,respectively. Table 3-5 gives the information about the various thermodynamic and electrochemical parameters. From these observed results it is inferred that aliphatic triazoles are more effective inhibitor than aliphatic and aromatic oxadiazole. The superior performance of triazoles as compared to oxadiazole derivatives can be attributed to the presence of an additional benzene ring and three nitrogen atoms in comparision with oxadiazoles which possess two hetero atoms (O and N).

The order of inhibition efficiency of triazoles is:

UPMT > NPMT > PPMT > HPMT

The inhibition efficiency of oxadiazoles are:

DMOD > PMOD > AMOD > NMOD

Chapter 6 describes the effect of anionic, cationic and nonionic surfactants of sodium dodecylsulfate (SDS), cetyltrimethylammonium bromide (CTAB), Triton-X-100 (TX-100), respectively on inhibition behaviour of 2-aminophenyl-5-mercapto-1-oxa-3,4-diazole (AMOD) and 2- Heptyl-1,3 imidazoline(HI). Inhibition efficiency of AMOD and HI increased appreciably in presence of surfactants[14]. The effect of inhibitor concentration, solution temperature, immersion time and acid concentration on inhibition efficiency of AMOD and HI were studied by weight loss method and potentiodynamic polarization studies. The dissolved surfactant helps inhibitor to adsorb onto the iron surface due to their hydrophilic property and leads to the strong bonding between the metal surface and inhibitor along with head group of surfactant[15-16]. The hydrophobic surfactant tails prefer to adsorb together to

form a coherent hydrophobic film that serves as a barrier to block the reaction between the iron surface and the external environment, thus inhibits the corrosion reaction between the metal and aqueous medium is inhibited. Further, the surfactant and inhibitor molecules inhibit the dissolution of metal either by blocking the cathodic or the anodic reaction of metal by occupying reactive sites, or by simply providing resistance to the supply of oxidant or the transport of the reaction products. Thus, corrosion is inhibited more effectively with increasing surfactant concentration. At further high [surfactant] the inhibition efficiency is decreased due to increase in ionic concentration in the surface region by incorporation of more hydrogen ions as coions or counter ions[17].

Table 1: Name, Abbreviation and structure of the studied compounds

S. No	Name of the compounds (Abbreviated)	Structure
1.	Decanohydrazide (DH)	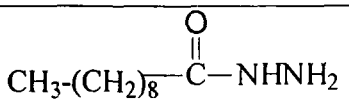
2.	Dodecanohydrazide (DDH)	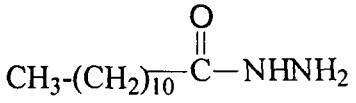
3.	Hexadecanohydrazide (HDH)	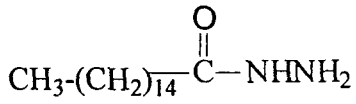
4.	Octadecanohydrazid (ODH)	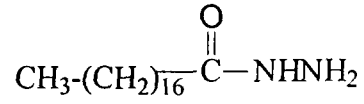
5.	1-Undecyl-4-phenyl thiosemicarbazide (UPMT)	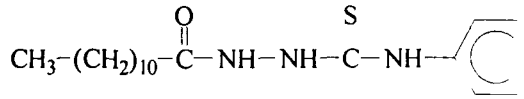
6.	1-Pentadyl-4-phenyl thiosemicarbazide (PPMT)	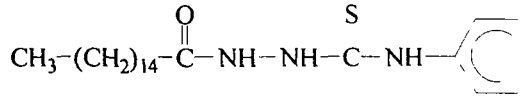
7	1-Heptadecyl-4-phenyl thiosemicarbazide (HPMT)	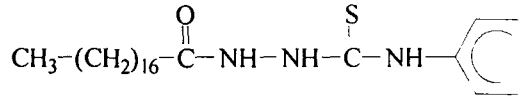
8	1- Nonyl -4-phenyl thiosemicarbazide (NPMT)	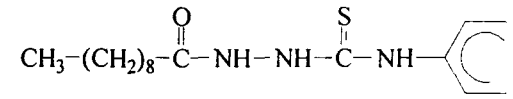

Table 2: Name, Abbreviation ,and structure of the studied compounds

S. No.	Name of the compounds (Abbreviated)	Structure
9.	2- Heptyl-1,3 imidazoline (HI)	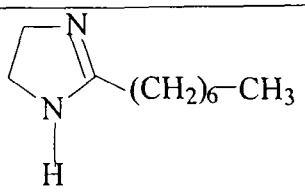
10.	2- Nonyl-1,3 imidazoline (NI)	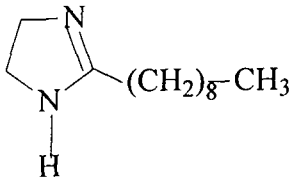
11.	2-Undecyl -1,3 imidazoline (UDI)	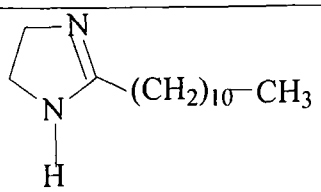
12.	2- Pentadecyl-1,3 imidazoline (PDI)	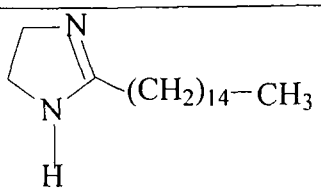
13.	2-Heptadecyl-1,3 imidazoline (HDI)	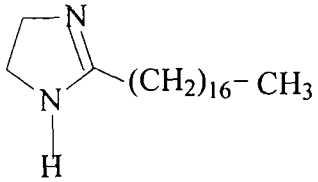
14.	5-Nonyl-4-phenyl-3-mercapto -1,2,4 triazole (NPMT)	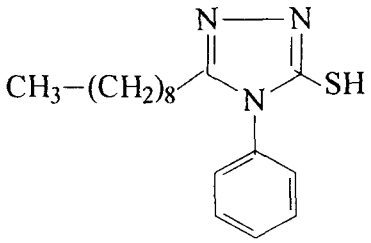

15.	5-Undecyl-4-phenyl-3-mercapto-1,2,4 triazole (UPMT)	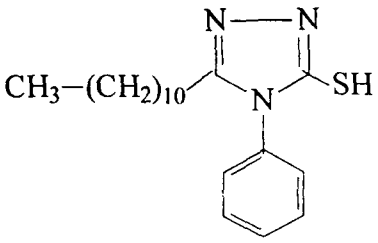
16.	5-Pentadecyl-4-phenyl-3-mercapto-1,2,4 triazole (PPMT)	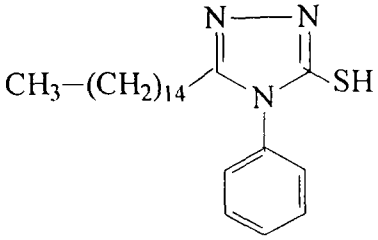
17.	5-Heptadecyl-4-phenyl-3-mercapto-1,2,4 triazole (HPMT)	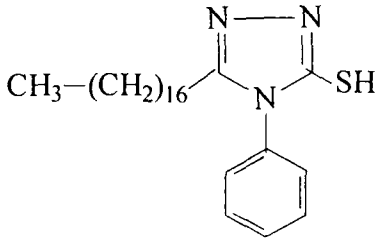
18.	2-Pentadecyl-5-mercapto-1-oxa-3,4-diazole (PMOD)	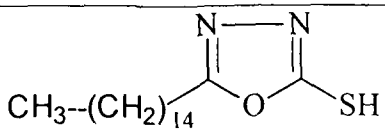
19.	2-Undecyl-5-mercapto-1-oxa-3,4- diazole (UMOD)	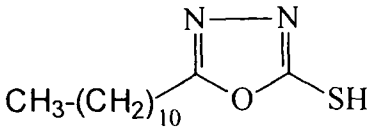
20.	2-Aminophenyl-5-mercapto-1-oxa-3,4-diazole (AMOD)	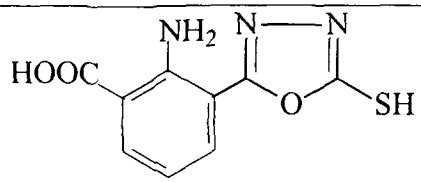
21.	2-Nitrophenyl-5-mercapto-1-oxa-3,4-diazole (NMOD)	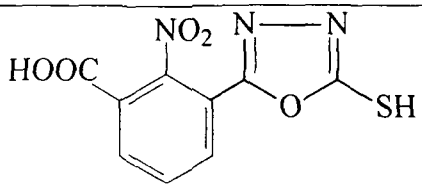

Table 3: Thermodynamic activation parameters for corrosion of mild steel in HCl in the absence and presence of inhibitors

System	E_a (kJ mol^{-1})	ΔH (kJ mol^{-1})	ΔS (J $mol^{-1}K^{-1}$)	ΔG_{ads} (kJ mol^{-1})	-Q (kJ mol^{-1})
HCl	51.18	48.56	200.40	-	-
DDH	86.3	40.32	248.34	36.26	33.02
DH	74.3	41.32	232.07	35.84	32.30
HDH	74.1	61.27	218.66	24.07	23.20
ODH	66.9	59.03	215.79	23.62	22.97
UPTS	75.23	77.88	198.56	39.75	28.72
NPTS	68.10	70.72	196.07	39.47	26.48
PPTS	58.32	60.95	195.31	38.88	19.78
HPTS	42.00	44.65	192.43	36.93	14.87
UDI	23.71	26.35	203.73	38.41	23.66
NI	24.76	27.40	202.20	37.12	23.04
PDI	23.77	32.42	196.75	36.25	18.08
HDI	29.75	32.39	192.43	35.81	18.62
HI	30.73	33.37	186.19	32.10	17.40
UPMT	63.73	40.32	241.60	36.26	30.02
NPMT	60.40	42.32	238.77	35.84	26.30
PPMT	55.53	28.30	235.90	24.07	21.20
HPMT	54.30	27.96	233.00	23.62	21.22
UMOD	55.04	80.03	220.58	34.90	30.43
PMOD	52.13	87.85	217.52	33.71	23.36
AMOD	51.12	101.41	215.98	30.24	18.02
NMOD	48.08	103.50	210.24	29.30	14.35

[Inhibitor] = 500 ppm; [HCl] = 1.0 mol dm^{-3}; Time = 3 hours

Table 4: Electrochemical polarization parameters for the corrosion of mild steel in HCl containing inhibitors.

System	E_{corr} (mV)	I_{corr} ($mAcm^{-2}$)	IE (%)
1N HCl	-461	0.360	-
DDH	-454	0.08	77.8
DH	-452	0.11	69.4
HDH	-456	0.13	63.9
ODH	-456	0.16	55.5
UPTS	-497	0.025	94.44
NPTS	-508	0.072	80.12
PPTS	-493	0.082	77.07
HPTS	-495	0.100	72.05
UDI	-480	0.033	90.83
NI	-476	0.037	89.72
PDI	-466	0.085	76.38
HDI	-479	0.120	66.66
HI	-493	0.150	58.33
UPMT	-492	0.004	98.78
NPMT	-490	0.002	94.49
PPMT	-487	0.048	86.77
HPMT	-485	0.082	77.22
UMOD	-552	0.027	92.50
PMOD	-533	0.031	91.38
AMOD	-526	0.036	89.85
NMOD	-517	0.045	87.52

[Inhibitor] = 500 ppm; [HCl] = 1.0 mol dm^{-3}; Temp = 30°C

Table 5: Dependence of electrochemical impedance parameters on [UPTS] for mild steel in HCl.

System	R_t (ohm cm^2)	C_{dl} ($\mu F\ cm^{-2}$)	IE (%)
HCl	36	1511.50	-
DDH			
100	88.17	105.14	59.17
300	103.53	45.78	65.23
500	140.72	2.58	73.18
UPTS			
100	157.38	769.72	77.12
300	208.69	708.96	82.74
500	286.95	501.87	87.45
UDI			
100	86.95	946.84	58.48
300	141.30	776.92	74.45
500	304.34	315.22	88.13
UPMT			
100	223.07	105.14	83.78
300	346.15	45.78	89.57
500	392.30	27.58	91.07
UMOD			
100	139.13	769.72	74.11
300	167.64	708.96	78.52
500	243.47	501.87	85.15

[HCl] = 1.0 mol dm^{-3}; Temp = 30°C

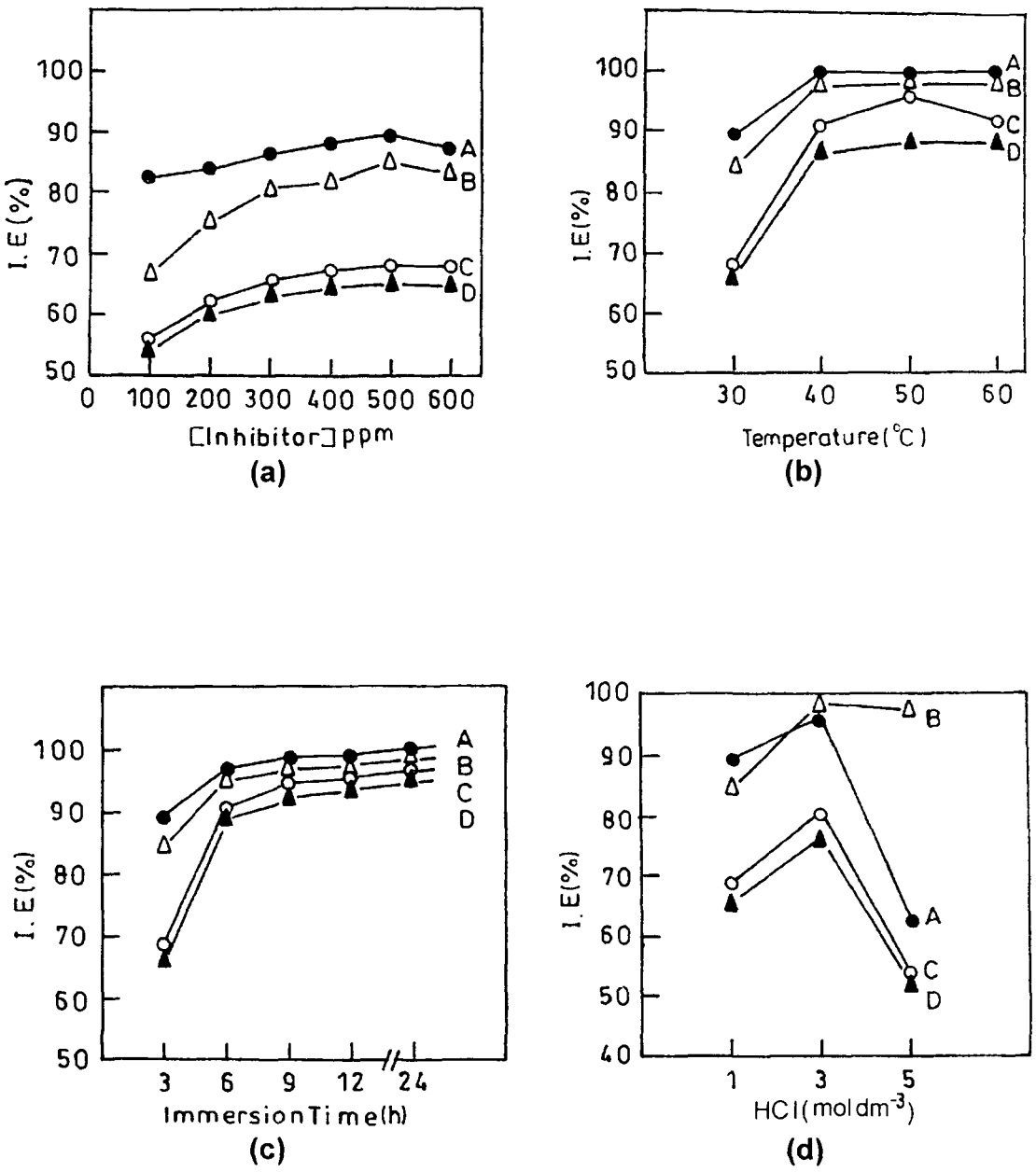

Fig. 1. Plot of variation of inhibition efficiency on (a) hydrazides concentration (b) temperature (c) immersion time and (d) [HCl] for the corrosion of mild steel in HCl.

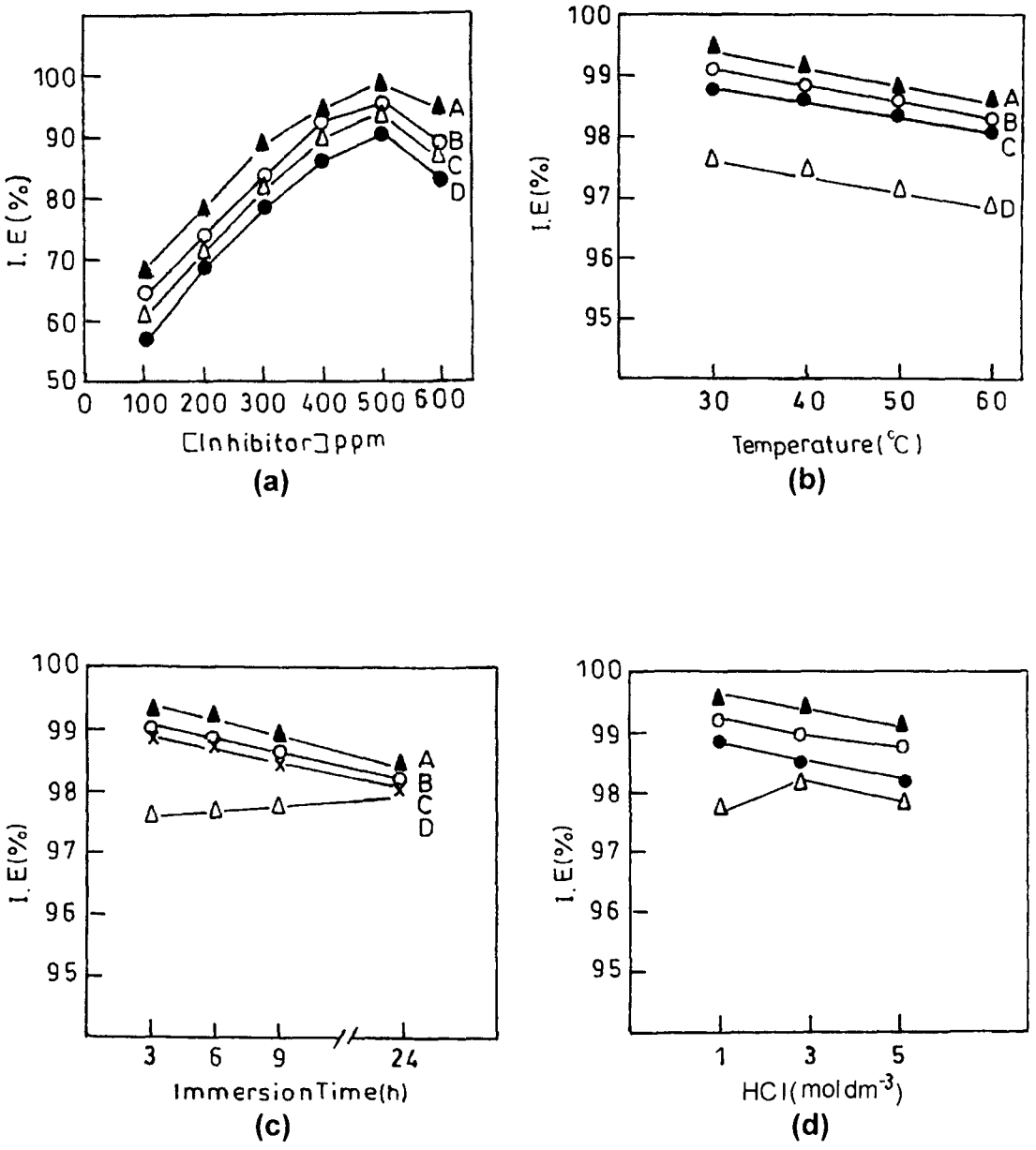

Fig. 2. Plot of variation of inhibition efficiency on (a) thiosemicardazides concentration (b) temperature (c) immersion time and (d) [HCl] for the corrosion of mild steel in HCl.

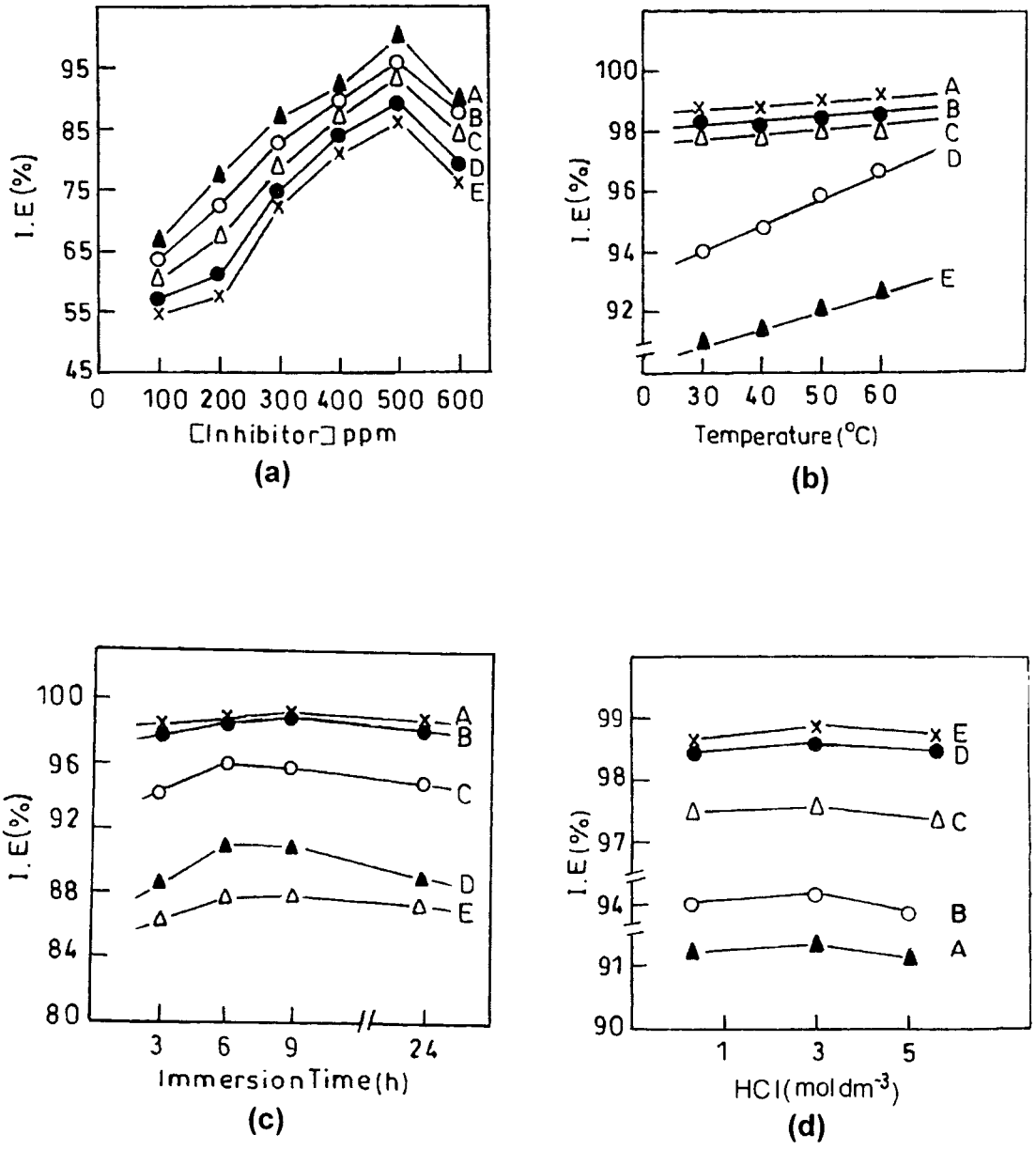

Fig. 3. Plot of variation of inhibition efficiency on (a) imidazolines concentration (b) temperature (c) immersion time and (d) [HCl] for the corrosion of mild steel in HCl.

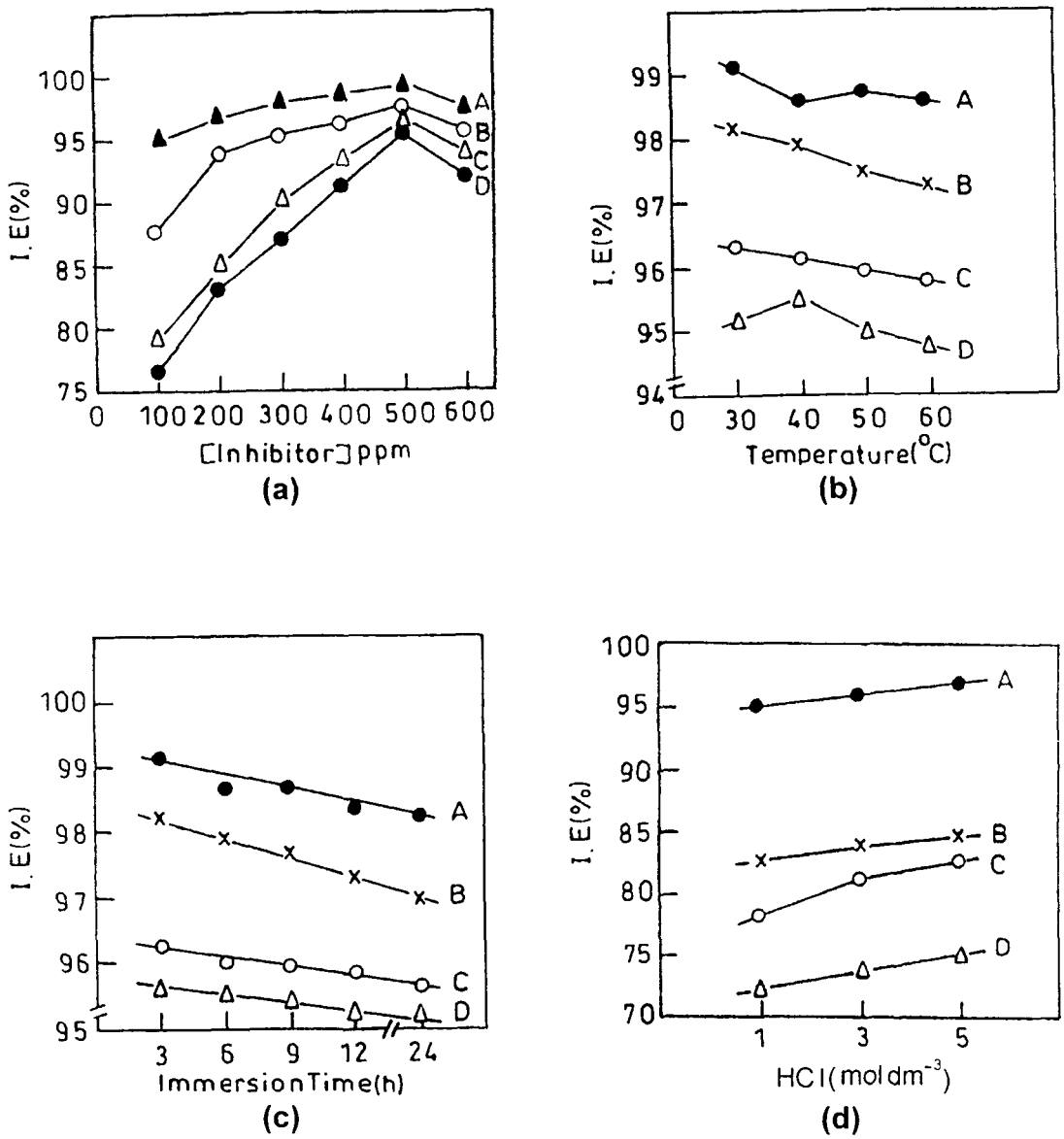

Fig. 4. Plot of variation of inhibition efficiency on (a) triazoles concentration (b) temperature (c) immersion time and (d) [HCl] for the corrosion of mild steel in HCl.

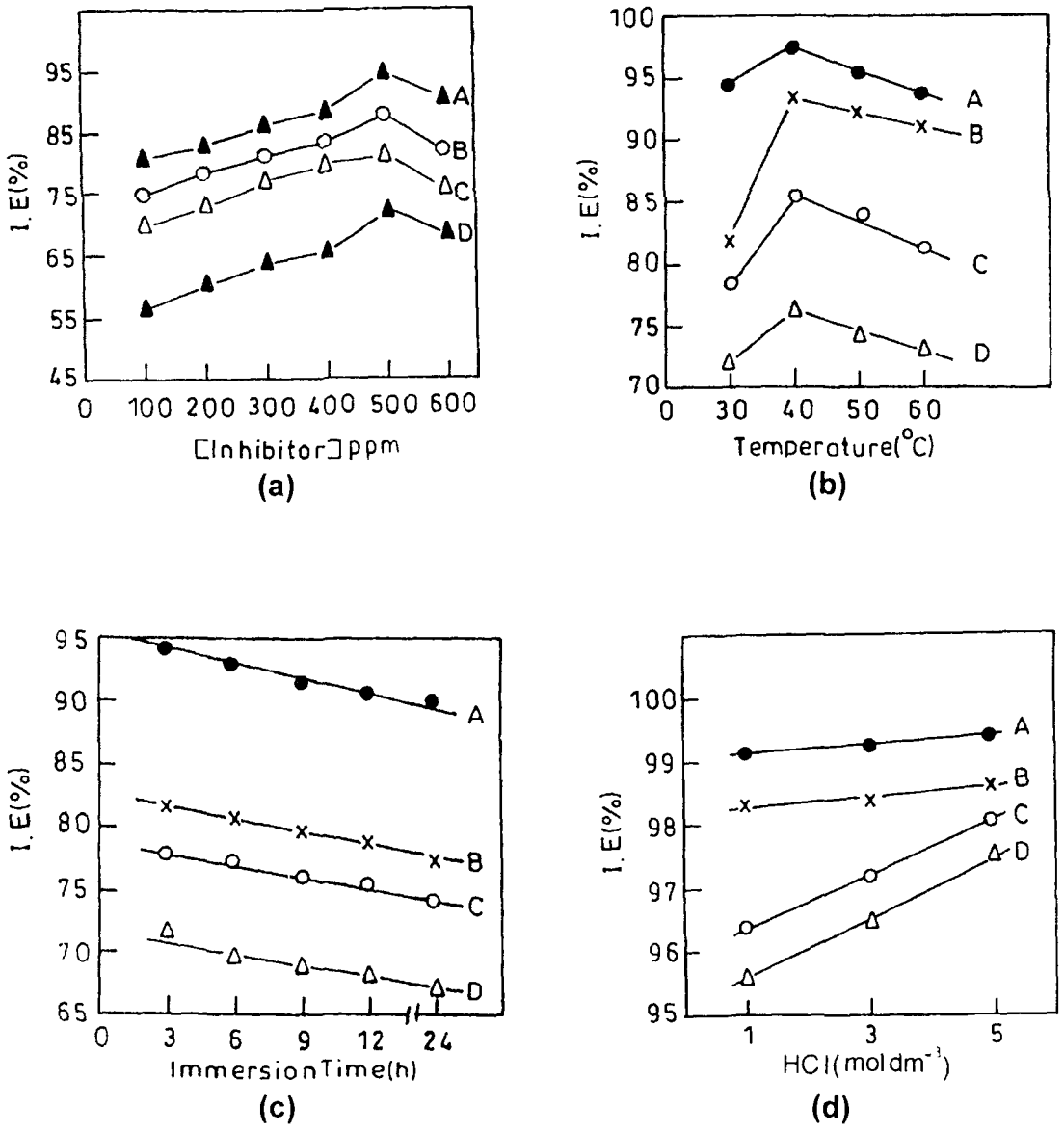

Fig. 5. Plot of variation of inhibition efficiency on (a) oxadiazoles concentration (b) temperature (c) immersion time and (d) [HCl] for the corrosion of mild steel in HCl. .

REFERENCES

1. L. Shreir, *Corrosion*, 1 (1978) 16.

2. F.N. Spellar, "*Corrosion: causes and prevention- An Engineering Problem*", Mc Graw Hill, New York 1935.

3. K. Elayapursemal, *Trans.SAEST*, 17 (1982) 2.

4. K.S. Rajagopalan, "An *Introduction to Corrosion Control*", Colour Publication, Bombay 1988.

5. O.L. Riggs and C.E. Locks, "Anodic Protection Theory and Practice in the Prevention of Corrosion", Premium Press, New York 1981.

6. NACE- Glossary of Corrosion Terms, *Mat. Prot*, 4 (1965) 79.

7. G. L. Cherepakhova, A. V. Shreider and G. P. Charikova, *Chemical and Petroleum Engineering*, 6 (1970) 490.

8. J.H. Martin, "*Concise Encyclopedia of the Structure of Materials*", Elsevier 2006 p. 418.

9. M .A. Quraishi and S Khan, *Ind.J. Chem. Technol*, 12 (2005) 576.

10. M. Schorr and J. Yahalom, *Corros. Sci*, 12 (1972) 876.

11. O.K.Orubite and N.C. Oforka, *J. Appl. Sci. Environ*, 8 (2004) 57.

12. A. Raman and P. Labini, "*Reviews on Corrosion Inhibitiors Science & Technology*", Houston, NACE 1986.

13. M. A. Quraishi, N. Saxena and D. Jamal, *Ind.J. Chem. Technol,* 11 (2005) 220.

14. W. L. Wang and M.L. Free, *Anti-Corr. Method Mater*, 50 (2003)186.

15. A.C. Zettlemoyer, *J.Colloid Interface Sci,* 28 (1968) 343.

16. D.W. Fuerstenau, *J.Phys. Chem*, 60 (1956) 981.

17. M.A. Mighad, E.M.S. Azzam, A.M.A. Sabagh, *Mater. Chem. Phys*, 85 (2004) 273

STUDIES ON ORGANIC CORROSION INHIBITORS FOR REFINERY INDUSTRY

Thesis

SUBMITTED FOR THE AWARD OF THE DEGREE OF

Doctor of Philosophy

IN

APPLIED CHEMISTRY

BY

NIDHI SAXENA

DEPARTMENT OF APPLIED CHEMISTRY
FACULTY OF ENGINEERING & TECHNOLOGY
ALIGARH MUSLIM UNIVERSITY
ALIGARH (INDIA)

2007

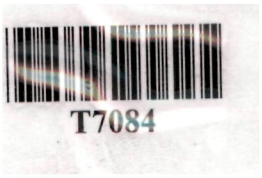

Dedicated to
Cherished feet of
Maa
&
Sai Baba

DEPARTMENT OF APPLIED CHEMISTRY
FACULTY OF ENGINEERING & TECHNOLOGY
ALIGARH MUSLIM UNIVERSITY, ALIGARH - 202 002 (INDIA)

M.Z.A. Rafiquee
M.Sc., Ph.D.

Off. : 0571-2700920-23 Ext. 3000
Mobile : 9411040047
University Fax : (0571) 2400528
E-mail : drrafiquee@gmail.com

Dated:.. Nov. 3, 2007

Certificate

This is to certify that the thesis entitled **"Studies on Organic Corrosion Inhibitors for Refinery Industry"**, submitted for the award of the degree of Doctor of Philosophy in Applied Chemistry, is a faithful record of the bonafide research work carried out at the Department of Applied Chemistry, Zakir *Hussain College of Engineering and Technology, Aligarh Muslim University*, Aligarh by **Ms Nidhi Saxena** under my supervision and guidance

(Dr. M.Z.A. Rafiquee)
Supervisor

Residence : B-2, Nazir Ahmad Road, A.M.U., Aligarh-202002

Acknowledgement

First of all I would like to thank Almighty God for giving me enough courage and strength to complete this research work. It gives me immense pleasure to express my sincere gratitude to my supervisor, Dr. M.Z.A. Rafiquee for rendering the esteemed guidance, never failing inspiration, constant support and encouragement in completing the work.

I am thankful to Dr Ali Mohammad, Chairman, Department of Applied Chemistry, Z. H. College of Engineering and Technology, A. M. U, Aligarh for providing necessary facilities and help during the period of study. It is a matter of priviledge to thanks Prof M. Ajmal and Prof. M. A. Quraishi for their help and guidance.

I am thankful to my seniors and my lab colleagues Dr Rana Sardar, Dr. Farhat Aisha Ansari, Mr. Vikas Bhardwaj, Ms. Fauzia Rehman & Mr. Rajeev for their helpful attitude and encouragement throughout the tenure of this work. I would like to place special thanks to my friend Ms. Sadaf Khan, for her invaluable suggestion, encouragement and moral support in my stress and strain. I sincerely acknowledge the encouragement and, intellectual help of Dr Jaya Rawat.

From oceanic depths of my heart I wish to express thanks to my Parents, Sisters, brother and friends for their love and support. I am grateful to Ujagar for his invaluable contribution and motivation.

Nidhi Saxena

(Nidhi Saxena)

LIST OF PUBLICATIONS

1 Inhibition of mild steel corrosion by oleochemical based hydrazides, M A Quraishi, **N Saxena** & D Jamal, Indian Journal of Chemical Technology, 11 (2005) 220

2 Inhibition of mild steel corrosion in presence of fatty acid imidazolines in hydrochloric acid, M A Quraishi, M Z A Rafiquee, **Nidhi Saxena** & Sadaf Khan, Protection of Metal (Russia) – Accepted in Dec 2006

3 Some fatty acid oxadiazoles for corrosion inhibition of mild steel in HCl, M Z A Rafiquee, **Nidhi Saxena**, Sadaf Khan and M A Quraishi, Indian Journal of Chemical Technology- Accepted in Sept 2007

4 Influence of surfactants on the corrosion inhibition behaviour of 2-aminophenyl-5-mercapto-1-oxa-3,4-diazole (AMOD) on mild steel, M Z A Rafiquee, **Nidhi Saxena**, Sadaf Khan and M A Quraishi, Mater Chem Phys (2007) doi 10 1016/j matchemphys 2007 08 022

5 Corrosion inhibition of aluminium in acid solutions by some imidazoline derivatives, M A Quraishi, M Z A Rafiquee, Sadaf Khan & **Nidhi Saxena**, Journal of Applied Electrochemistry (Springer Publication) –Accepted in July 2007

6 Influence of some thiadiazole derivatives on corrosion inhibition of mild steel in formic and acetic acid media, M Z A Rafiquee, Sadaf Khan, **Nidhi Saxena** & M A Quraishi, Journal of Portugaliae Electrochimica Acta – Accepted in July2007

7 Fatty acid thiosemicarbazides as corrosion inhibitors for Mild steel in Hydrochloric acid solution, M A Quraishi*, M Z A Rafiquee, **Nidhi**

Saxena, Sadaf Khan, Journal of Chemical Science and Engineering (UK Publication) – Preprint published (2006).

8. Inhibitive Effect of Some New Triazole Derivatives on Mild Steel Corrosion in Formic and Acetic acid, M.A Quraishi, M.Z.A Rafiquee, Sadaf Khan & **Nidhi Saxena**, Journal of Chemical Science and Engineering (UK Publication) – Preprint published (2006).

9. Inhibition Effect of Fatty acids Triazoles on Mild Steel Corrosion in Hydrochloric Acid Solution, M Z A Rafiquee, **Nidhi Saxena**, Sadaf Khan and M A Quraishi, Bulletin of Material Science- Communicated 2007

10. Inhibition of mild steel corrosion by azathione derivatives in organic acid Solutions,M.A Quraishi, M.Z.A Rafiquee, Sadaf Khan, **Nidhi Saxena**. Anti-Corrosion - Methods & Material (Emerald Publication) Communicated 2006.

11. Effect of fatty acid imidazoline derivative on corrosion inhibiton on mild steel in sulphuric acid, M.Z.A Rafiquee, Sadaf Khan, **Nidhi Saxena** & M.A Quraishi, Bulletin of Electrochemistry (CECRI)- Communicated 2007.

CONTENTS

Chapter- 1
Introduction

CORROSION

Corrosion is deterioration of essential properties in a metal or alloys due to reaction with its surroundings[1]. Physiochemical interaction between metals and its environment leads to changes in the properties of metal and which may often lead to impairment of the function of the metal, the environment, or the technical system of which these form a part. Corrosion is the natural process of deterioration and most metals corrode on contact with water (and moisture in the air), acids, bases, salts, oil, other solid and liquid chemicals. Metals are also susceptible to corrosion when exposed to gaseous materials like acid vapours, formaldehyde gas, ammonia gas and sulfur containing gases. Thus corrosion is the tendency of metals to return to their naturally occurring forms or it is a reversion or a partial reversion from the metastable condition of the metal to the stable condition of the mineral accompanied by a decrease in the free energy of the system.

Trends in corrosion research have changed rapidly over the years. In Fifties, polarization studies and their applications were the topic of research having considerable interest[2-3]. In Seventies, the work on corrosion research was devoted to the mechanistic studies on metal dissolution, localized corrosion and high temperature corrosion[4-7]. Now the corrosion research has been diversified into several fields including the analysis of the corrosion product and use of paints and enamels, inhibitors, metallic coating to control the corrosion reaction. Application of optical techniques and surface analytical techniques give better insight in understanding the nature of corrosion products and their influence over metal surface and their oxides formed.

These techniques are helpful in characterization of the thickness, structure and composition of the films formed as corrosion product.

In most of the cases metallic state represents the metastable state. Therefore, metals have a natural tendency to react with other substances and go back to lower energy state with subsequent release of energy. All metals show decrease in free energy by undergoing reaction with the environment except noble metals, which are found in native state in nature. Thermodynamic stability of metals / chemical compounds is determined by the sign and the change in the free energy value (ΔG), during their transformation from one state to another[8].

$$\Delta G = \Delta H - T\Delta S$$

where ΔH is the change in enthalpy, ΔS is the change in entropy and T is absolute temperature. For the reaction at equilibrium change in free energy is represented by the following relationship:

$$\Delta G = - RT \ln K_{eq}$$

where ΔG° is standard free energy, R is gas constant and K_{eq} is equilibrium constant. The potential of a reaction is related to its free energy change (ΔG) by:

$$\Delta G = - zFE$$

A negative value for the energy corresponds to a spontaneous reaction, whereas a positive value of ΔG indicates that the reaction has no tendency to proceed.

Corrosion has a major impact on the economy of a nation. According to NACE (International) bulletin[9] the annual losses due to corrosion in USA were estimated to be more than $300 billion The loss due to corrosion has been

estimated to be in the order of 2 – 5% of the GNP of any country. In India the annual losses due to corrosion is more than Rs.25, 000 crores per year[10].

It is estimated that 25% of the total product of the metal and alloys go waste due to corrosion. Corrosion may lead to loss of capital assets such as industrial equipments and machinery requiring higher maintenance and replacement of various parts of equipments and plants. It may lead to shutting down of industries and hence causing great economic loss to workers and owners of industries. Corrosion in pipelines can hamper essential services like supply of water to many places and it further cause contamination of water leading to various health hazards. In this way corrosion actually affects many spheres of our everyday life.

1.1. FACTORS INFLUENCING CORROSION

The nature and extent of corrosion depend largely on the metal and the environment. Factors like structural features of the metal, nature of the environment and the type of reactions that occur at the metal/environment interface have to be considered for the understanding of the corrosion phenomenon[11].

The important factors, which influence the corrosion process, are

(i) **Nature of the metal:** includes oxidation potential, overvoltage, relative areas of anode and cathode, purity of metal, physical state of metal, nature of oxide film and solubility of product of corrosion.

(ii) **Temperature:** As a general rule, increasing temperature increases corrosion rate. The increase in temperature increases the reaction rates as well as the diffusion rate of many corrosive byproducts. The corrosion rates in some system decreases with increasing temperature.

This occur because of many gases have lower solubility in open systems at higher temperatures. As temperatures increase, the resulting decrease in solubility of the gas causes corrosion rates to go down.

(iii) **pH:** Corrosion rates almost always increase with decreasing pH (increasing acidity). This is a direct result of increasing the concentration of an aggressive ion (H^+) and increasing the solubility of most potentially corrosive products.

(iv) **Oxygen Concentration:** Oxygen's role in corrosion is as an aggressive gas or oxidizing agent. As its concentration increases, corrosion rates increase until the rates of diffusion to the surfaces reach a maximum. The same principles apply to most other oxidizing agents, such as Cl_2, H^+, Br_2.

(v) **Fluid Velocity:** It is observed that the corrosion rate increases with the increase in the velocity of fluid. At very low velocities, even zero, there are diffusion effects that cause corrosion. As fluid velocities increase from stagnant to moderate values, the corrosion rate increases. Then, as the limit of diffusion at a particular temperature is reached, further increase in velocity has little effect on the corrosion rate. At some point, however, the velocity reaches such high values that the surface film of the metal begins to be damaged. At these velocities, the corrosion rates resume increasing with the higher velocities.

(vi) **Suspended Solids:** An increase in suspended solids levels accelerates corrosion rates. These solids include any inorganic or

organic contaminants present in the water e.g. clay, sand, silt or biomass.

(vii) **Corrosion Inhibitors:** The corrosion rate is reduced by the presence of corrosion inhibitors. Corrosion inhibitors incorporate themselves to corrosion product films in such way as to increase the film's capacity to prevent corrosion. The process of corrosion inhibition is related to the metal surface and the processes occurring in water. The polar nature of some molecules promotes adsorption. An inhibitor molecule usually is in constant motion, being adsorbed and desorbed between the fluid and the corrosion product film. The rate of adsorption onto the surface is dependent on the nature of the molecule, as well as the concentration of the inhibitor in the fluid.

1.2. FORMS OF CORROSION

It is convenient to classify corrosion by the forms in which it manifests itself, the basis for this classification is the appearance of the corroded metal[12]. Eight forms of corrosion are unique, but all of them are more or less interrelated. The eight forms are: (1) Uniform or general attack (2) Galvanic or two metal corrosion (3) Crevice corrosion (4) Pitting (5) Intergranular corrosion (6) Selective leaching or parting (7) Erosion corrosion and (8) Stress corrosion cracking. This listing covers practically all corrosion failures and problems. The characteristics, mechanisms, and preventive measures of these forms of corrosion are:

(i) **Uniform Attack:** Uniform attack is the most common form of corrosion. It is normally characterized by a chemical or electrochemical reaction which proceeds uniformly over the entire exposed surface or over a

large area. The metal becomes thinner and eventually fails. A sheet iron roof will show essentially the same degree of rusting over its entire outside surface. Uniform attack, or general overall corrosion, represents the greatest destruction of metal on a tonnage basis. This form of corrosion, however, is not of too great concern from the technical standpoint, because the life of equipment can be accurately estimated on the basis of comparatively simple tests. Merely immersing specimens in the fluid involved is often sufficient. Uniform attack can be prevented or reduced by selecting proper materials, coatings, using inhibitors, or by cathodic protection.

(ii) **Galvanic or Two-Metal Corrosion:** A potential difference usually exists between two dissimilar metals when they are immersed in a corrosive or conductive solution. If these metals are placed in contact (or otherwise electrically connected), this potential difference causes electron flow between them. Corrosion of the less corrosion-resistant metal is usually increased and attack of the more resistant material is decreased, as compared with the behavior of these metals when they are not in contact. The less resistant metal becomes anodic and the more resistant metal behaves cathodic.

(iii) **Crevice Corrosion:** Intense localized corrosion frequently occurs within crevices and other shielded areas on metal surfaces exposed to corrosives. This type of attack is usually associated with small volumes of stagnant solution caused by holes, gasket surfaces, tap joints, surface deposits, and crevices under bolt and rivet heads.

(iv) **Pitting:** Pitting is a form of extremely localized attack that results in holes in the metal. These holes may be small or large in diameter, but in most cases they are relatively small. Pits are sometimes isolated or so close together that they look like a rough surface. Generally a pit may be described as a cavity or hole with the surface diameter about the same as or less than the depth. Pitting is one of the most destructive and insidious forms of corrosion. It causes equipment to fail because of perforation with only a small percent weight loss of the entire structure. It is often difficult to detect pits because of their small size and because the pits are often covered with corrosion products. In addition, it is difficult to measure quantitatively and compare the extent of pitting because of the varying depths and numbers of pits that may occur under identical conditions. Pitting is also difficult to predict by laboratory tests. Sometimes the pits require a long time, several months or a year-to show up in actual service. Pitting is particularly vicious because it is a localized and intense form of corrosion, and failures often occur with extreme suddenness.

(v) **Intergranular Corrosion:** Grain boundary effects are of little or no consequence in most applications or uses of metals. If a metal corrodes, uniform attack results since grain boundaries are usually only slightly more reactive than the matrix. However, under certain conditions, grain interfaces are very reactive and intergranular corrosion results. Localized attack at and adjacent to grain boundaries, with relatively little corrosion of the grains, is intergranular corrosion. The alloy disintegrates (grains fall out) and/or loses its strength.

Intergranular corrosion can be caused by impurities at the grain boundaries, enrichment of one of the alloying elements, or depletion of one of these elements in the grain-boundary areas.

(vi) **Selective Leaching:** Selective leaching is the removal of one element from a solid alloy by corrosion processes. The most common example is the selective removal of zinc in brass alloys (dezincification). Similar processes occur in other alloy systems in which aluminum; iron, cobalt, chromium, and other elements are removed. Selective leaching is the general term to describe these processes, and its use precludes the creation of terms such as dealuminiumzication, decobaltification, etc. Parting is a metallurgical term that is sometimes applied, but selective leaching is preferred.

(vii) **Erosion Corrosion:** Erosion corrosion is the acceleration or increase in rate of deterioration or attack on a metal because of relative movement between a corrosive fluid and the metal surface. Generally, this movement is quite rapid, and mechanical wear effects or abrasion are involved. Metal is removed from the surface as dissolved ions, or it forms solid corrosion products which are mechanically swept from the metal surface. Sometimes, movement of the environment decreases corrosion, particularly when localized attack occurs under stagnant conditions, but this is not erosion corrosion because deterioration is not increased. Erosion corrosion is characterized in appearance by grooves, gullies, waves, rounded holes, and valleys and usually exhibits a directional pattern. In many cases, failures because of erosion corrosion occur in a relatively short time, and they are

unexpected largely because evaluation corrosion tests were run under static conditions or because the erosion effects were not considered.

(viii) **Stress Corrosion Cracking:** Stress-corrosion cracking refers to cracking caused by the simultaneous presence of tensile stress and a specific corrosive medium. Many investigators have classified all cracking failures occurring in corrosive mediums as stress-corrosion cracking, including failures due to hydrogen embrittlement. However, these two types of cracking failures respond differently to environmental variables. Cathodic protection is an effective method for preventing stress-corrosion cracking whereas it rapidly accelerates hydrogen- embrittlement effects. Hence, the importance of considering stress-corrosion cracking and hydrogen embrittlement as separate phenomena is obvious.

During stress-corrosion cracking, the metal or alloy is virtually unattacked over most of its surface, while fine cracks progress through it. This cracking phenomenon has serious consequences since it can occur at stresses within the range of typical design stress. Exposure to boiling $MgCl_2$ at 310°F (154°C) is shown to reduce the strength capability to approximately that available at 1200°F.

The two classic cases of stress-corrosion cracking are "season cracking" of brass, and the "caustic embrittlement" of steel. Season cracking refers to the stress-corrosion cracking failure of brass cartridge cases. During periods of heavy rainfall, especially in the tropics, cracks were observed in the brass cartridge cases at the point where the case was crimped to the bullet. It was later found that the

important environmental component in season cracking was ammonia resulting from the decomposition of organic matter.

Many explosions of riveted boilers occurred in early steam-driven locomotives. Examination of these failures showed cracks or brittle failures at the rivet holes. These areas were cold-worked during riveting operations, and analysis of the whitish deposits found in these areas showed caustic, or sodium hydroxide, to be the major component. Hence, brittle fracture in the presence of caustic resulted in the term caustic embrittement. While stress alone will react in ways well known in mechanical metallurgy (i.e., creep, fatigue, tensile failure) and corrosion alone will react to produce characteristic dissolution reactions; the simultaneous action of both sometimes produces the disastrous results.

1.3. THEORIES OF CORROSION

The corrosion may be classified[13] as

(i) **Dry Corrosion:** Dry corrosion occurs in the absence of a liquid phase. It involves direct chemical reaction of a metal with its environment and involves no transport of electric charge and the metal remains film free. Vapours and gases are the corrodents and such corrosion occurs at high temperature. Examples of dry corrosion are tarnishing of copper and silver, corrosion in liquid metals, fused halides and organic liquids.

(ii) **Wet Corrosion:** Most of the corrosion reactions, especially those occurring in aqueous media are electrochemical in nature. The

overall corrosion process is accompanied by considering the formation of cathodic and anodic areas on the metal surfaces in which less aerated part acts as a anode[14].

$$M \rightleftharpoons M^{n+} + ne^-$$

This reaction constitutes the basis of corrosion of metals.

In a similar fashion, a reduction reaction is indicated by the consumption of electrons. For every oxidation reaction there must be a corresponding reduction reaction. In aqueous solutions, various reduction reactions are possible depending upon the environment. Some of the possible reduction reactions are:

Hydrogen reduction:

$$2H^+ + 2e^- \rightarrow H_2$$

(Evolution of hydrogen in acidic solution)

Oxygen reduction:

$$O_2 + 4H^+ + 4e^- \rightarrow 2\ H_2O$$

(in acidic solution)

$$O_2 + 2H_2O + 4\ e^- \rightarrow 4\ OH^-$$

(in neutral and alkaline solution)

Metal ion reduction: $M^{n+} + e^- \rightarrow M^{(n-1)+}$

Metal deposition: $M^{n+} + ne^- \rightarrow M$

During corrosion process, more than one anodic and cathodic reaction may occur. The corrosion reactions of mild steel in sulfuric acid contaminated by ferric ions occur as follows[15]:

$Fe \rightleftharpoons Fe^{2+} + 2\,e^-$ (anodic reaction)

$M \rightleftharpoons Mn^{2+} + 2\,e^-$ (anodic reaction)

All the constituent metals of mild steel (e.g. Fe, Mn, etc.) go into the solution as their respective ions. The electrons produced by these anodic (oxidation) reactions are consumed by the following cathodic (reduction) reactions:

$Fe^{3+} + e^- \rightarrow Fe^{2+}$

Removal of the Fe^{3+} ions reduces the corrosion rate.

When a metal or alloy is immersed in a conductive or corrosive environment, different potential zones are developed on the surface of metal or alloy due to the presence of different metallic phases, grain boundaries, segregates, crystalline imperfections, impurities, etc. This difference in potential leads to the formation of anodic and cathodic areas on the metallic surface where oxidation and reduction reactions occur, respectively. These areas are helpful in the formation of local action cells on the metallic surface[16]. Local action cell can also be formed in situations where there is a variation in the environmental factor such as temperature. The electrode potential can be calculated by using the Nernst equation:

$$E = E_0 + \frac{RT}{zF} \ln \frac{[ox]}{[red]}$$

where,

E_o = Standard electrode potential

R = Gas constant (1.98 cal/g Equivalent)

F = Faraday constant (96,500 coulombs)

T = Absolute temperature (Kelvin, K)

z = Number of the electrons transferred during the reaction

[ox] = Concentration of oxidized species (mol dm^{-3})

[red] = Concentration of reduced species (mol dm^{-3})

1.4. CORROSION CONTROL METHODS

The corrosion reaction that takes place at the metal / environment interface, can be controlled by the following method[17]:

(i) **Modifying the composition of metal:** Materials selection has a significant effect on the operability, economics and reliability of refinery assets. Criteria for selection of ferrous and non-ferrous materials in equipment construction is largely dependent on suitability for the intended service, availability, ease of fabrication and cost – economics. Carbon and low alloy steels[18] are the most widely used materials of construction as they satisfy all the criteria i.e., inexpensive, easy of fabrication, commonly available material etc. In petroleum refineries, carbon steel is used for the construction of fractionation towers, separator drums, heat exchanger shells, storage tanks, most piping and almost all the structures. Generally these steels are suitable up to

400 °C. The C-0.5Mo steels are suitable in the temperature range of 425-540 °C and are used in several applications. The alloy Cr-Mo steels i.e., steels having Cr less than 10% are extensively used where resistance to long term exposure to high temperature sulfide corrosion and high temperature hydrogen attack is required. The common grades of 5Cr-0.5 Mo, 9%Cr-1Mo are used widely in the construction of furnace tubes, heat exchanger shells, piping, separator drums etc.

Stainless Steels[19] are extensively used in petrochemical plants because of the highly corrosive nature of the catalysts and solvents that are often used. In refineries, stainless steels have been primarily limited to applications involving high temperature sulfide corrosion and other forms of high temperature attack. Martensitic stainless steels[20], such as type 410 (S41000) are used in construction of pump components, fasteners, valve trim, turbine blades and tray valves and other tray components in fractionation towers Austenitic stainless steels[21], such as type 304 (S30400) or type 316 (S31600), have excellent corrosion resistance, but are subject to stress corrosion cracking by chlorides. Typical applications include linings and tray components in fractionation towers; piping heat exchanger tubes; reactor cladding; tubes and tube hangers in furnaces; various components for compressors, turbines, pumps and valves and reboiler tubes.

High silicon cast irons[22] (with 14% Si) are extremely corrosion resistant because of a passive surface layer of silicon oxide that forms during exposure to many chemical environments. Typical refinery applications

include valve and pump components for corrosive service. High-nickel cast iron[23] (with 13 to 36% Ni and upto 6% Cr) have excellent corrosion, wear and high temperature resistance because of the relatively high alloy content.

Copper alloys[24] are extensively used in sea water service which is the prime medium of cooling in the refinery. 70-30 Copper Nickel , 90-10 Copper Nickel , Nickel Aluminum Bronze etc standard materials of construction for tubes , tube sheets in condensers, coolers and other heat exchanger service with sea water as the cooling medium.

Nickel[25] also forms the basis for many high temperature alloys. Alloy 400 is extensively used as a lining for carbon steel equipment to prevent corrosion by hydrochloric acid and chloride. Alloy 400 (NO4400) tubes have been used in overhead condensers. High-nickel alloys, including alloy 625 (NO6625) and alloy 825 (N08225), are used in high temperature service e.g., flare tips, reformer pig tails etc.

(ii) **Modifying the metal surface:** The coating is one of the popular option in which structure is protected from corrosion by using protective coating[26]. The coating acts as a physical barrier to prevent aggressive chemicals from contacting the structure and thus protects the structure. The commercially used barrier coatings in refineries are Zinc metal coating, Aluminum metal coating, Electroplated metal coating and Conversion metal coating. Paints and enamels are also used to coat metals. The limitations associated in the barrier coating are mechanical, thermal damage, high cost involved in its monitoring and maintenance etc.

(iii) **Modifying the environment by using inhibitors:** Steel constitutes an estimated 99% of the material used in the oil industry such as in oil pipelines, domestic central heating systems, industrial water cooling systems and metal extraction plants. Yet its corrosion resistance is poor in aggressive environments, and the one of cost effective method is addition of corrosion inhibitor to the environment. Most inhibitors are organic substances[27], which possess at least one functional group considered as the reaction center for the adsorption process. The molecular structure of organic compounds used as inhibitors has been found to exert a major influence on the extent of inhibition of corrosion[28-29]. The major industries using corrosion inhibitors are the oil and gas exploration and production industry, the petroleum refining industry, the chemical industry, heavy industrial manufacturing industry, water treatment facilities, and the product additive industries. The largest consumption of corrosion inhibitors is in the oil industry, particularly in the petroleum refining industry. The total consumption of corrosion inhibitors in the United States has doubled from approximately $600 million in 1982 to nearly $1.1 billion in 1998.

1.5. CORROSION CONTROL BY APPLICATION OF INHIBITORS

One of the most prevalent methods used for corrosion control in closed system is corrosion inhibitors. Corrosion inhibitor may be defined, as a substance which, when added in a small concentration to an environment[30], effectively reduces the corrosion rate of a metal exposed to that environment A particular advantage of corrosion inhibition is that it often can be implemented or changed *in situ* without disrupting a process. Despite the

extensive use of inhibitors in controlling corrosion of metals and alloys, little is known of their functions because of the complexity of the process[31]. Several mechanisms have been proposed to explain the action of corrosion inhibitors in which the adsorption theory[32] is the most pertinent. Recently the nature of the action of corrosion inhibitors at the metal solution interface has been evaluated by adsorption characteristics and also by the thermodynamics of adsorption. Selection of a suitable inhibitor for a given corroding system depends on the type of the corrosion medium, the nature of the metal, the magnitude of the charge at the metal/ solution interface, and the cathodic reaction etc.

Classification of Inhibitors

(i) **Inorganic Inhibitors:** In strong acid solutions, Br^-, I^- have found to be effective inhibitors[33]. The oxides like As_2O_3, Sb_2O_3 have also been reported as inhibitors in acidic media. These substances get deposited[34] in the form of metal on iron and increase the hydrogen over-voltage and subsequently reduce the corrosion rate. The addition of heavy metal ions like Pb^{2+}, Mn^{2+}, Cd^{2+} is found to inhibit corrosion on iron in acid medium. This may be due to the deposition of these metal ions over the iron surface[35].

(ii) **Organic Inhibitors:** It includes a large number of organic substances containing N, S, or O. The organic inhibitors are adsorbed on the metal surface and inhibit corrosion of metals in acidic environment. The prominent examples of acid inhibitors are acetylinic alcohols, aldehydes, mercaptans, heterocyclic compounds and thiourea

derivatives[36-37]. An organic corrosion inhibitor may be anodic, cathodic or both depending on its reaction mechanism and the potential of the metal at the interface[38]. Generally cathodic inhibitors increase cathodic polarization and shift the corrosion potential to more negative values, while anodic inhibitors enhances anodic polarization and shift the corrosion potential to more positive values.

The effectiveness of an organic inhibitor depends mainly on its size, carbon chain length, bonding strength to metal surface, aromaticity and or presence of conjugated bond, nature and number of bonding atoms[39]. Most organic inhibitors are substances, which possess at least one functional group considered as the reaction center for the adsorption process. The adsorption of inhibitor is related to the presence of heteroatom such as nitrogen, oxygen, phosphorous and sulfur as well as a triple bond or an aromatic ring in their molecular structure through which they can adsorb on the metal surface[40-43]. The molecular structure of organic compounds used as inhibitors has been found to exert a major influence on the extent of inhibition of corrosion [44-45]. In addition to this, other different characteristics such as molecular size and the nature of the substituent groups and heteroatom present in the organic compounds containing nitrogen have found to function as very effective corrosion inhibitors[46-53]. The efficiency of these compounds as corrosion inhibitors can be attributed to the number of mobile electron pairs present[54], the π orbital character of free electron[55] and the electron density around the nitrogen atom[56]. Organic compounds containing both nitrogen or sulfur atoms are of

particular interest as they give better inhibition efficiencies than those containing nitrogen or sulfur alone[57-64].

Nitrogen containing compounds exhibit high inhibition efficiencies in hydrochloric acid, such as alkyl and aryl amines, saturated and unsaturated nitrogen ring compounds, condensation products of amines with aldehydes[65 -72] and ketones[73], ethoxylated amines[74], nitriles, aldoximes and imidazolines derivatives[75-76]. The influence of organic compounds containing nitrogen, such as amines and investigated by several workers[77-80]. It is well known that heterocyclic compounds containing nitrogen atom are good corrosion inhibitors for many metals and alloys in various aggressive media[81-85].

(iii) **Neutral/Alkaline Inhibitors:** These inhibitors include cathodic inhibitors (which increase cathodic polarization), anodic inhibitors (which enhance the anodic polarization) and mixed or general inhibitors[86] (which act on both cathodic and anodic areas). Anodic inhibitors form an oxide or some other insoluble film. Insufficient concentration of anodic inhibitors will lead to severe pitting. Sodium chromate is one of the most widely used and efficient inhibitor. Sodium silicate is generally used in hot water systems. The other compounds used in neutral and alkaline media are borates, molybdates and salts of organic acids like benzoates and salicylates.

(iv) **Vapour Phases Inhibitors (VPI):** Those substances whose vapour pressure is sufficiently high act as vapour phase inhibitors[87]. The vapour pressure of these compounds at room temperature is usually

between 0.1 and 1.0 mm mercury, so that the inhibitors become sufficiently fast moving to ensure its adequate availability in the vicinity of the metal surface e.g. Dicyclohexyl ammonium nitrite, benzothiazole are used for protecting copper, phenylthiourea and cyclohexylamine chromate are used for brass. Dicyclohexylamine nitrite protects both ferrous and non-ferrous parts. The inhibitor vapour condenses on metal surface when comes in contact and is hydrolyzed by moisture present to liberate nitrite and benzoate ions, which in presence of available oxygen are capable of passivation of steel.

(v) **Anodic Inhibitors:** The substances, which retards the anodic area by acting on the anodic sites and polarize the anodic reaction, are called anodic inhibitors[88]. In the presence of anodic inhibitors, displacements in corrosion potential (E_{corr}), takes place in positive direction (Figure 1.1) and suppress corrosion current (I_{corr}) and reduces corrosion rate. Anodic inhibitors which cause a large shift in the corrosion potential are called passivating inhibitors, if used in insufficient concentration, they cause pitting and sometimes increases corrosion rate.

Anodic inhibitors may be oxidizing anodic inhibitors in which they inhibit corrosion by passivating the metal surface. e.g. chromate, nitrite[89] and non-oxidizing anodic inhibitors which include inorganic anions such as molybdate, benzoate and phosphate[90] etc. These inhibitors slow down anodic reaction by forming passive film on the metal surface in presence of oxygen.

(vi) **Cathodic Inhibitors:** Those substances, which reduce the cathodic area by acting on the cathodic sites and polarize the cathodic reactions, are called cathodic inhibitors[91]. They displace the corrosion potential (E^c_{corr}) in the negative direction and reduce corrosion current, thereby retard cathodic reaction and suppress the corrosion rate (Figure 1.2).

Cathodic inhibitors can be divided into three categories:

Cathodic poisons – The substances which interfere with the formation of hydrogen atoms or recombination of hydrogen atoms to H_2 gas are known as cathodic poisons e.g. arsenic and antimony salts.

Oxygen scavangers – The substance which inhibit the corrosion by removing dissolved oxygen in water are called oxygen scavangers e.g. sodium sulphite and hydrazine

$$2Na_2SO_3 + O_2 \rightarrow Na_2SO_4$$

$$N_2H_4 + O_2 \rightarrow N_2 + 2H_2O$$

The advantage of hydrazine over sulphite is that it does not increase the total dissolved solids in water that prevents the salt deposits in boilers & other capillary steam outlets.

Cathodic precipitate (Filming inhibitor) - Calcium bicarbonate and zinc sulphate are the examples of filming type inhibitors. The cationic parts of these inhibitors migrate towards cathode and deposits produce insoluble protective film on cathode and thereby inhibit cathodic reaction.

$Ca^{++} + 2HCO_3 + OH^- \rightarrow CaCO_3\downarrow + HCO_3^- + H_2O$

$Zn^{++} + OH^- \rightarrow Zn(OH)_2\downarrow$

(vii) Mixed Inhibitors: There are a number of inhibitors, which inhibit corrosion by interfering with both the anodic and cathodic reactions and are called mixed inhibitors. This type of inhibition can be represented by Figure 1.3. Gelatin, Glue and other high molecular weight substances fall in this category. Machu[92-93] claimed that inhibition is mainly due to the formation of non-porous layer, which increases the electrical resistance of the surface layer.

(viii) Miscellaneous: These inhibitors include material such as scale inhibitor and biological growth inhibitor which reduce corrosion by interfering with other processes[94].

The above classification of inhibitor types by function appears to give a fairly simple and concise approach, although it has limitations in cases where the mechanism is not known. In general the use of neutralizing and scavenging type inhibitors seems to be the best suited for closed systems where such chemicals are not lost in the system. In open systems however the use of inhibitors is difficult to justify.

1.6 MECHANISM OF INHIBITION IN ACIDS

The inhibitive action of organic compounds occurs on the metallic surface due to interaction between the inhibitors and the metal surface by adsorption phenomenon or by altering the corrosion potential. During adsorption[95] the molecules are held on the surface of the adsorbent by valence forces i.e., variation in the charge from one phase to the other.

Therefore, the molecular structure of the inhibitors assumes special significance[96]. The electron density at atoms of functional group constituting a reaction centre affects the strength of the adsorption bond [97].

The addition of inhibitor may alter the corrosion potential resulting into decrease in the rate of anodic process, the cathodic process or both. The shift of the corrosion potential in positive direction indicates mainly the retardation of the anodic process (anodic control) whereas shift in the negative direction indicates retardation of the cathodic process (cathodic control). Little change in the corrosion potential suggests that both anodic and cathodic processes are retarded. In the presence of an inhibitor, a shift of polarization curves without change in the Tafel slope indicates that the adsorbed inhibitor acts by blocking active sites so that reaction cannot occur[98]. A change in the Tafel slope is the indication of affecting the mechanism of the reaction.

The following factors influence the adsorption of molecule to the metal surface.

(i) **Surface charge on the Metal:** The magnitude and sign of the surface charge on the metal play an important role in the adsorption process. The effect of organic inhibitor on the electrode reactions must be connected with the modification induced in the structure of the electrochemical double layer because of their adsorption. In solution, the charge on a metal is usually expressed in terms of zeta potential. It is more important than the potential on a hydrogen scale and sign of these potentials are different[99]. As the potential becomes more

positive, the adsorption of anions is favoured and as the potential becomes more negative, the adsorption of cations is favoured.

(ii) **Reaction of Adsorbed Inhibitors:** In some cases, the adsorbed corrosion inhibitors may react to form a product by electrochemical reduction, which may be inhibitive in nature. Inhibition due to the added substances has been termed as primary inhibition and that due to the reaction product as secondary inhibition[100]. In such case, the inhibition efficiency may increase or decrease with time depending upon the effectiveness of primary and secondary inhibition[101].

(iii) **Interaction of Adsorbed Inhibitor Species:** Lateral interactions between adsorbed inhibitor species become significant with increase in surface coverage of the adsorbed species. This lateral interaction may be either attractive or repulsive. Attractive interaction occurs between molecules containing large hydrocarbon components. Repulsive interactions occur between ions or molecules containing dipoles. The repulsive interaction leads to weaker adsorption[102].

(iv) **Interaction of the Inhibitors with Water Molecules:** The surface of metal is in contact with adsorbed water molecules. Adsorption of inhibitors takes place by the displacement of adsorbed water molecules from the surface, which involves free energy change during adsorption process. It is found to increase with the increase in energy of solvation of the adsorbing species[103].

(v) **Structure of Inhibitors and their Adsorption:** Inhibitor bound to metal surface by electron transfer forms adsorption bond. Generally,

the inhibitors are the electron donors and the metal is the electron acceptor. The strength of such bond depends on the characteristics of both the metal and inhibitor. Electron transfer from the adsorbed inhibitor species is favoured by the presence of relatively loosely bound electrons, as in case of anions and neutral organic molecules containing lone pair of electrons in π-electron systems associated with multiple, especially triple bonds or aromatic rings.

Most organic inhibitors have at least one polar atom i.e. nitrogen, sulfur, oxygen etc. The polar atom is regarded as the reaction centre for the establishment of the adsorbed film over metal through chemisorption or physisorption of inhibitor[104]. The extent of adsorption is determined by the electron density of the atom acting at the reaction centre and by the polarizability of the polar atoms. The effectiveness of the polar atoms with respect to the adsorption process varies in the following order[105].

Selenium > Sulphur > Nitrogen > Oxygen

The availability of electron pairs for the formation of bonds in chemisorption process can thus be altered by regular and systematic variations in the molecular structure.

The corrosion inhibition reactions in acidic solution are influenced by the following factors:

(i) **Formation of a Diffusion Barrier:** The adsorbed inhibitor forms a surface film on the metal surface and acts as a physical barrier to restrict the diffusion of ions or molecules to or from the metal surface and thus retard the corrosion reaction.

(ii) **Blocking of Reaction Sites:** The inhibitors may adsorb on the metal surface to prevent the surface metal atoms from participating in either the anodic or cathodic reaction of corrosion. The mechanisms of such reactions are not affected and the Tafel slopes of the polarization curves remain unchanged. Adsorption of inhibitors at low surface coverage tends to occur at anodic sites, causing retardation of the anodic reaction. At high surface coverage, adsorption occurs on both anodic and cathodic sites, and both reactions are inhibited.

(iii) **Participation in the Electrode Reactions:** The electrode reactions may involve the formation of adsorbed intermediate species with the surface of metal atoms. The presence of adsorbed inhibitor interferes with the adsorbed intermediate but the electrode processes may then proceed by alternative paths through intermediates containing the inhibitor. In these processes, the inhibitor affects the reaction rate and remains unchanged with a change in the Tafel slope[106]. Inhibitors may retard the rate of hydrogen evolution on metals by affecting the mechanism of the reaction with the increases in Tafel slopes of cathodic polarization curve. This effect has been observed on iron in the presence of inhibitors such as phenylthioureas[107].

(iv) **Alternation of the Electrical Double Layer:** The adsorption of ions or species on metal surface change the electrical double layer at the metal solution interface, and this in turn affect the rates of the electrochemical reactions i.e. electrochemical corrosion.

1.7 CORROSION PROCESSES IN REFINERIES

Corrosion has been an integral and unavoidable part of petroleum refining operations. Most petroleum refining operations involve inflammable hydrocarbon streams, highly toxic or explosive gases, strong acids or caustics that operate usually at elevated temperatures and pressures. In view of the complexity of operations present in a refinery several types of corrosion occur. Some of the corrosion processes are due to faulty materials of construction and some can occur when equipment are shutdown for maintenance. Corrosion problems increase operating and maintenance costs substantially. Unexpected and sudden failures of equipment due to corrosion can be extremely expensive and can lead to other associated problems e.g. health, safety and environment. The study shows that direct corrosion costs in oil and gas exploration and production is $1.4 billion/year, in petroleum refining $3.7 billion/year, in gas and liquid transmission pipelines $7.0 billion/year, in gas distribution $5.0 billion/year, in hazardous materials transport $0.9 billion/year, and in hazardous materials storage $7.0 billion/year. The corrosion cost includes costs for new construction, the maintenance costs on ageing/corroding equipment, the costs of inspections and structural integrity evaluations, the costs associated with corrosion-related failures and outrages, Thus from economic point of view, it is necessary for corrosion specialists to study corrosion mechanism and various ways and means to minimize corrosion damage[108].

Most corrosion problems in Refineries are not caused by hydrocarbons that are processed but by various inorganic compounds, such as water, hydrogen sulfide, hydrochloric acid, hydrofluoric acid, sulfuric acid, and

caustic. There are two principal sources of these compounds; feed stock contaminants and process chemicals, including solvents, neutralizers and catalyst. In addition, corrosion problems are caused by the atmosphere, cooling water, boiler feed water, steam condensate and soil.

Low temperature corrosion occurs in those areas whose temperature is less than 150°C. The types of corrosion that occurs may be uniform, pitting and stress corrosion cracking, depending on alloy and environment. Carbon steel is used to handle most hydrocarbon streams in this temperature range, except where aqueous corrosion by hydrogen chloride or hydrogen sulfide, which requires selective application of more resistant alloys. High temperature corrosion takes place above approximately 250°C and is the result of direct reaction between metal and environment.

The major cause of low temperature corrosion is the presence of contaminants in crude oil. Although some contaminants are removed during preliminary treatment in the fields, most end up in refinery tanks, along with contaminants picked up in pipelines or marine tankers. In most cases, the actual corrosives are formed during initial refinery operations.

Water is primarily responsible for various forms of corrosion in fractionation tower overhead systems. Water and air can be especially detrimental. Moisture and air are drawn into storage tanks during normal breathing as a result of pumping and changes in temperature and cause severe corrosion if the tanks are unprotected by painting etc. Because crude and heavy oils form a protective oil film on the working areas of a tank shell, corrosion is generally limited to the top shell ring and the underside of the

roof. Corrosion occurs primarily at the middle shell courses because these are exposed to more wetting and drying cycles than other tank areas. The rate of corrosion is proportional to the water and air content of light stocks. Contamination from chloride and hydrogen sulfide accelerates attack. The most effective way of corrosion control in tanks is by application of high performance painting / tank linings[109].

Corrosion of steel by hydrogen sulfide[110] is a very common phenomenon and is observed in almost all refinery equipment. Sour water which has large quantities of H_2S can cause severe corrosion problems in overhead systems of certain fractionation towers, in hydrocracker and hydrotreater effluent streams, in the vapor recovery (light ends) section of fluid catalytic cracking unit, in sour water stripping units, and in sulfur recovery units. In general, carbon steel has fairly good resistance to aqueous sulfide corrosion because a protective iron sulfide film is formed but usually due to contamination with chlorides, cyanides the carbon steels are subjected to corrosion. More recently, titanium grade 2 (R50400) tubes have been used as replacements for carbon steel tubes to control aqueous sulfide corrosion[111].

Corrosion by hydrogen chloride[112] is primarily a problem in the overhead condensing systems of both the crude and vacuum towers of crude distillation units. The general material of construction is carbon steel. The overhead section of distillation towers is usually lined with monel and the upper five trays and components made from monel can be used for to combat aqueous chloride corrosion. Addition of chemicals for neutralizing the HCl to control the aqueous corrosion and filming the steel surfaces by forming a

physical barrier to prevent the HCl coming into contact with the equipment surfaces is the usual practice of corrosion management of overhead systems.

Usually sour water is an aggregate of various types of process water containing primarily hydrogen sulfide, ammonia and hydrogen cyanide, often in combination with certain other organic and inorganic compounds, including phenols, mercaptans, chlorides and fluorides. Sour water corrosion is a major problem in sour water stripping units, in which exceptionally high concentrations of ammonium bisulfide can cause severe corrosion in the overhead condenser tubes/ air fin cooler tubes. Corrosion problems of carbon steel components are often closely associated with hydrogen blistering *viz.*, in coolers, separator drums, absorber / stripper towers, and, occasionally, overhead condensers at a number of locations. Corrosion management of aqueous ammonium bisulfide corrosion is carried out by providing higher corrosion allowances for carbon steel equipment , selective alloying[113] with alloy 925 (N08825), alloy 400 (N04400) or titanium grade 2 (R50400) may be required for heat exchangers , separator drums and stripper towers trays are of SS316 (S31600) stainless steel depending on corrosion experience. Most corrosion problems have been in overhead condensers of condensing sour water strippers. Although a variety of alloys have been used for overhead condenser tubes, only aluminium and titanium grade (R50400) can be relied on to provide adequate resistance to the highly corrosive conditions encountered in main overhead systems.

Sodium hydroxide[114] is widely used in refinery operations to neutralize acidic constituents. At ambient temperature and under dry conditions, caustic can be handled in carbon steel equipment and also is satisfactory for aqueous

caustic solutions between 50°C and 80°C depending on concentration. For caustic service above these temperatures upto 120 °C carbon steel is used with post weld heat treatment and for higher temperatures nickel alloys are used. Caustic when gets concentrated in boiler feed water can cause corrosion. Corrosion is not caused by the amine itself, but is caused by dissolved hydrogen sulfide or carbon dioxide and by amine degradation products.

Sulfur compounds originate with crude oils form metal sulfides, certain organic molecules and hydrogen sulfide. The relative corrosivity of sulfur compounds generally increases with temperature. Depending on the process particulars corrosion is in the form of uniform thinning, localized attack or erosion-corrosion. Corrosion control depends almost entirely on the formation of protective metal sulfide scales that exhibit parabolic growth. In general, nickel and nickel rich alloys are rapidly attacked by sulfur compounds at elevated temperatures, while chromium containing steels[115] provide excellent corrosion resistance

Naphthenic acids are organic acids that are present in many crude oils and are corrosive only at temperatures above 230°C. It does not form protective scale. The presence of naphthenic acids may accelerate high-temperature sulfide corrosion that occurs at furnace headers, elbows and tees of crude distillation units because of unfavourable flow conditions. Naphthenic acid corrosion is most easily controlled by blending non-naphthenic with naphthenic crude oils. The usual practice of managing naphthenic acid corrosion is the usage of SS 316 or 317 grades[116] of stainless steels.

Chlorides in the presence of oxygen are perhaps the most common cause of stress corrosion cracking of austenitic stainless steels and nickel alloys. The usual failure mode of stress corrosion cracking in austenitic stainless steels is the transgranular highly branched cracking. Increased oxygen content decreases the critical chloride content for cracking to occur. The severity of cracking increases with increase in temperature. Stainless steel pump impellers in seawater service have shown no cracking problems despite the fact that both chloride and oxygen contents are high because cracking of austenitic stainless steel components rarely occurs at ambient temperatures. In alkaline solutions, the likelihood of chloride stress corrosion cracking is greatly reduced. Chloride stress corrosion cracking in refineries and petrochemical plants often occurs under shutdown conditions when air and moisture enters equipment opened for inspection and repair.

Polythionic acids are formed by the reaction of oxygen and water with the iron/chromium sulfide scale that covers the surfaces of austenitic stainless steel components as a result of high temperature sulfide corrosion. Because neither oxygen nor water is present during normal operation under conditions in which austenitic stainless steels would be used. Stress corrosion cracking evidently occurs during shutdowns. Oxygen and water originate from steam or wash water used to free components of hydrocarbons during shutdown before inspection or simply from atmospheric exposure. Polythionic acid stress corrosion cracking occurs only in austenitic stainless steels and nickel chromium-iron alloys that have become sensitized through thermal exposure. Washing with a soda ash [117] solution is the common method used by refineries in shutdowns to manage polythionic acid corrosion.

Corrosion of carbon and low-alloy steels by aqueous hydrogen sulfide solutions or sour waters can result in one or more types of hydrogen damage. Atomic hydrogen (H) is formed as part of the corrosion process[118]. As the concentration of atomic hydrogen builds up at the surface, it diffuses into the steel and reduces it ductility. Hydrogen atoms preferentially diffuse along grain boundaries and zones where the lattice has already been distorted by cold working or hardening. Atomic hydrogen can also combine to form molecular hydrogen at voids, such as manganese sulfide inclusion or laminations. Cracking does not occur in ductile steels or in steels that have received a proper postweld heat treatment.

Hydrogen Attack or High-temperature hydrogen attack refers to the deterioration of the mechanical properties of steels in the presence of hydrogen gas at elevated temperatures and pressures. It is of particular concern in hydrotreating, reforming and hydrocracking units at above roughly 260°C and hydrogen partial pressures above 689 KPa (100psia). Under these conditions, molecular hydrogen dissociates at the steel surface to atomic hydrogen (H), which readily diffuses into the steel at grain boundaries, dislocations, inclusions, gross discontinuities. Atomic hydrogen reacts with dissolved carbon and with metal carbides to form methane which cannot diffuse owing to its large size. As a result, internal methane pressures become high enough to blister the steel or to cause intergranular fissuring. At high temperatures, dissolved carbon dioxide diffuses to the steel surface and combines with atomic hydrogen to evolve methane. Hydrogen attack now takes the form of overall decarburization rather than blistering or cracking. The overall effect of hydrogen attack is the partial depletion of carbon and the

formation of fissures in the metal. General surface attack occurs when equipment, which is not under stress, is exposed to hydrogen at elevated temperatures and pressures.

Among the various corrosives present in refinery, hydrochloric acid[119] in crude and vacuum units represents a major contribution. It results into loss of production, inefficient operations, high maintenance and additional cost for corrosion control chemicals. HCl plays an important role in a petrochemical industry during butane isomerization, ethylbenzene production and polybutene production etc. In these processes aluminium chloride and other metal chlorides are used as a catalyst. These catalysts hydrolyze to yield hydrochloric acid in presence of traces of water. Corrosion in crude and vacuum units occurs primarily from chlorides. Chloride corrosion is caused by hydrogen chloride, which is formed from hydrolysis of the chloride salts contained in the crude. The majority of the chloride salts present are magnesium, calcium and sodium salts. Sodium chloride is thermally and hydrolytically stable and does not contribute to hydrogen chloride release. However, hydrolysis of calcium chloride and magnesium chloride is significant. The released hydrogen chloride is relatively non-corrosive in the vapour phase; however, below the dew point of water, it becomes very corrosive to many common materials of construction.

Corrosion by chloride can be controlled by using either corrosion resistant material[120] or some corrosion inhibitors[121]. Possible materials of constructions include alloy 400, titanium, nickel alloys or some of the newer super austenitic stainless steel. However, this approach is very situation specific and may be cost prohibitive.

Hackermann[122] suggested that the inhibitive action of N and/or S containing compounds is due to the presence of orbital containing free electrons. The N containing inhibitors are pyridine, quinoline and other amines, S-containing compounds are thiourea and its derivatives, mercaptans and sulfides.

Lee and Hwoejee[123] evaluated the corrosion inhibiting effect of quinoline oxime and 7-Nitroso-80-hydroxyquinoline (7-NHQ) against mild steel in hydrochloric acid solution. 7-NHQ exhibited > 90 % efficiency. Compounds containing N or S have shown vast application as corrosion inhibitors. Machu[124] has shown the use of S -containing compounds as inhibitors for H_2SO_4 and N- containing compounds for HCl solutions are more effective. Walker[125] discussed factors that affect corrosion in fluid catalytic cracking unit (FCC), vapour recovery units and suggested methods for its monitoring and control. Granes and Rosales[126] elucidated the mechanism of corrosion inhibition of iron and steel in HCl media and concluded that nitrogen containing compounds such as alkyl & aryl amines, saturated and unsaturated N-ring compounds are effective inhibitor.

Hettvarchch *et al*[127] evaluated the inhibitive effect of macrocyclic compound as acid corrosion inhibitor for steel by potentiodynamic and impedance studies. Inhibition efficiency was 82 % at 25°C in acid chloride environment. The influence of some of heterocyclic compound containing more than one nitrogen atoms in their molecules on corrosion of carbon steel in 1N HCl was investigated by Trabanelli and Zucchi[128] with view to establish correlation between molecular structure and the inhibition efficiency of the various examined inhibitors. Hashi Omar and Zucchi[129] evaluated the

corrosion inhibition behaviour of acetylenic alcohols in 1N HCl by using weight loss measurements and electrochemical data.

Jayaraman *et al*[130] performed studies on corrosion inhibiting behavior of various known amines & amino amides from non–edible oils. Mehta[131] discussed the application of fatty amines or diamines as corrosion inhibitors.

Granes *et al*[131] studied various heterocyclic compounds in HCl by electrochemical and surface analysis. They inferred that efficiency of these compound increases with number of aromatic systems and electrons availability in the molecule.

Muralidharan *et al*[133] investigated the inhibitive action of 4-amino-5-mercapto- 3 methyl -1,2,4-trizole on corrosion of mild steel in 1 N H_2SO_4 and 1N HCl by using potentiodynamic polarization study, A C impedance and hydrogen permeation method. They found it to be very effective in bringing down the permeation current in both the acid solutions. Kane *et al*[134] simulated chemical process corrosion in the laboratory. They found that testing used intelligently could give significant information to support analysis, troubleshooting and materials selection.

Keera *et al*[135] studied the behaviour of corrosion at carbon steel during distillation process by using N- based inhibitors e.g. ammonia & chlorinated hexadecyl amine, heterocyclic compounds Naphthyl, 1,2,4-triazole-3-thione, Benzyl-1,2,4- triazole -3-thione.

Ajmal *et al*[136] studied the inhibitive action of 2-hydrazino-6-methyl-1-benzothiazole on the corrosion of mild steel in acidic solutions. They found that this compound acts as a mixed inhibitor in H_2SO_4 and behave predominantly as cathodic inhibitor in HCl.

Kane and Cayard[137] proposed guidelines to control corrosion and environmental cracking of process equipment containing sulfur, chlorides and /or naphthenic acids. These feedstocks when processed under high temperature and pressure and alkaline conditions can cause brittle cracks and blisters in susceptible steel fabricated equipments. The observed data showed the process conditions such as temperature, pH and flowrate are key factors in the corrosion mechanisms present within process conditions. The studies help to use process controls, inhibitors and / or metallurgy to control corrosion and environmental cracking to improve material selection and to extend equipment service life.

The inhibitive action of azathiones was studied by Quraishi *et al*[138] on corrosion of mild steel in HCl and H_2SO_4 by weight loss and electrochemical techniques. The inhibiting action of the azathiones depends on the molecular size. Cyclohexyl azathione gave 90% inhibition efficiency at 500 ppm in 1N HCl.

Ram Prasad[139] classified the corrosion in refineries into two broad categories; chemical and electrochemical corrosion. The chemical corrosion results from direct action of aggressive agents (e.g. naphthenic acid, phenols, and aliphatic acids) either due to van der Waal's adsorption or to direct chemical reaction. The electrochemical corrosion is due to presence of water in liquid state, presence of NaCl, $MgCl_2$, HCl, H_2S in water or due to presence of local galvanic elements. Corrosion occurring in refineries may be uniform, galvanic, crevice, pitting, intergranular, selective leaching, erosion and stress corrosion cracking depending upon the conditions. The corrosion can be controlled through chemical treatment which includes oxygen scavengers,

neutralizing inhibitors, filming inhibitors and combination of these. To neutralize amines cyclohexylamine, morpholine, isobutanol amine and diethylamino ethanol are frequently used. The filming amines protect condensate systems from both carbondioxide and oxygen corrosion by forming a mono- molecular, non- wettable, protective film on the metal surface of the pipe. This film is formed by the attraction of the molecules polar group to the metal surface, the long, water insoluble, carbon chain then provides a water repellant barrier. The advantage of using filming amines is that they effectively protect high and low pressure condensate return systems from CO_2 and O_2 attack.

Shastri[140] recommended the use of organic inhibitors for controlling corrosion in primary operations and in refining operations. The organic inhibitors are adsorbed on the metal surface through electron rich functional groups. The non- polar hydrocarbon tail of the inhibitor is positioned vertically to the metal surface. The hydrocarbon chains of the inhibitor molecules mesh together to form a close knit film which repels the aqueous phase. The common inhibitors are amines, diamines, imidazolines, pyridines & their compounds with fatty acids and sulfonates.

Alley and Coble[141] discussed the use of corrosion inhibitors in overhead sections of crude oil distillation units. The corrosion in the overhead system is caused by HCl, which originates as chloride salts in crude oil. The inhibitor used in crude unit overhead includes the barrier or film forming inhibitors and by neutralizing the acidic corrodents. Neutralizing inhibitors inhibit corrosion by neutralizing HCl e.g. NH_3. The film forming inhibitors inhibit

corrosion by forming a barrier between metal and the corrosive element in the environment.

L.J Rokehar[142] discussed the corrosion in refinery units. The main corrodents are hydrochloric acid, naphthenic acid, hydrogen sulfide and hydrogen. He recommended the use of film forming amines and neutralizing amines for controlling corrosion. Nitin Raut and Jignesh Patel[143] studied corrosion in stripper overhead airfin cooler of naptha hydrodesulfurization plant, pretreater unit and catalytic reforming unit at BPCL refinery. Corrosion in the overhead piping and airfin cooler was due to condensation of HCl vapours. They recommended the injection of neutralizing inhibitor in overheads and by provision of water wash facility in stripper to control the corrosion.

Migahed[144] investigated the effect of non-ionic surfactant, namely *N,N*-di(poly oxy ethylene) amino lauryl amide, on the corrosion rate of carbon steel in produced water by various corrosion monitoring techniques. The strong adsorption ability of the surfactant molecules leads to formation of a mono-layer, which isolates the surface from the environment and thereby reduces the corrosion attack on the surface. The adsorption process was found to obey the Langmuir adsorption isotherm. The potentiostatic polarization results clearly revealed that the inhibitor behaves as a mixed type.

The corrosion inhibition behaviour of 4-phenylazo-3-methyl-2-pyrazolon-5-one and three of its derivatives have been investigated by Fouda *et al*[145] for C-steel in 2 M hydrochloric acid solution using weight-loss and galvanostatic polarization techniques. The efficiency of the inhibitors increases with the increase in the inhibitor concentration but decreases with a

rise in temperature. The conjoint effect of the pyrozolone derivatives and KBr, KSCN and KI has also been studied. The apparent activation energy (E_a*) and other thermodynamic parameters for the corrosion process have also been calculated. The galvanostatic polarization data indicated that the inhibitors were of mixed-type, but the cathode is more polarized than the anode. The slopes of the cathodic and anodic Tafel lines (β_c and β_a) were approximately constant and independent of the inhibitor concentration. The adsorption of these compounds on C-steel surface has been found to obey the Frumkin's adsorption isotherm. The authors discussed the mechanism of inhibition in the light of the chemical structure of the inhibitors. Amin *et al*[146] studied the effect of succinic acid (SA) on the corrosion inhibition of a low carbon steel (LCS) electrode has been investigated in aerated non-stirred 1.0 M HCl solutions at 25 °C. Weight loss, potentiodynamic polarization and electrochemical impedance spectroscopy (EIS) techniques were used to study the metal corrosion behaviour in the absence and presence of different concentrations of SA under the influence of various experimental conditions. Measurements of open circuit potential (OCP) were performed as a function of time till steady-state potentials (E_{st}) were established. Surface analysis using energy dispersive X-ray (EDX) and scanning electron microscope (SEM) were carried out. The mechanistic aspects were evaluated and the relative inhibition efficiency were calculated. Results obtained showed that SA is good "green" inhibitor for LCS in HCl solutions. The polarization curves showed that SA behaves mainly as an anodic-type inhibitor. EDX and SEM observations of the electrode surface confirmed existence of a protective adsorbed film of the inhibitor on the electrode surface. The inhibition efficiency increased with

increase in SA concentration, pH of solution and time of immersion. The effect of SA concentration and pH on the potential of zero charge (PZC) of the LCS electrode in 1.0 M HCl solutions has also been studied and the mechanism of adsorption were discussed.

STATEMENT OF THE PROBLEM

Corrosion is the degradation of metal or alloy by chemical or electrochemical reactions with its environment. Its cost is very high on the nation's economy (2 – 5% GNP). The direct cost includes the replacement of corroded components, use of corrosion resistant alloys, use of coating and inhibitors etc. The indirect costs are loss of production during downtime, loss of products due to leakage, loss of efficiency, contaminations and sometimes it causes loss of human lives due to explosion/fire. The cost of corrosion can be reduced to an extent of 25% by applying some corrosion control techniques. The prevalent corrosion control techniques are materials selection, proper design, electrochemical protection and use of inhibitors and paints/coatings. Among these methods, inhibitors are used in a wide range of applications, such as oil pipelines, domestic central heating systems, industrial water cooling systems and metal extraction plants. The advantage of corrosion inhibitor is that it can be implemented or charged *in situ* without disrupting a process and is also a cost effective method. The major industries using corrosion inhibitors are the oil and gas exploration and production industry, the petroleum refining industry, the chemical industry, heavy industrial manufacturing industry, water treatment facilities, and the product additive industries. The highest consumption of corrosion inhibitors is in oil refinery and petroleum processing units. We have synthesized various classes of inhibitors (Hydrazides, thiosemicarbazides, imidazolines, triazoles and oxadiazoles) with the following objectives:-

- Should be effective in hydrocarbon system.

- Should be stable at high temperature
- Should not decompose into toxic products
- Should remain effective for longer period of time.
- Cost effective and environment friendly.

The performances of these inhibitors were evaluated by weight loss method, potentiodynamic polarization and AC impedance technique. The surface morphology was performed by scanning electron spectroscopy.

The works have been divided into the following six chapters.

Chapter I: General Introduction which includes the definition, mechanism, forms of corrosion, method of control, corrosion process in oil refineries, survey of literature etc.

Chapter II: Experimental details which includes the materials and method used during experimental work.

Chapter III: Corrosion inhibition behaviour of Hydrazides and Thiosemicarbazides under the varying conditions of [inhibitor], [HCl], temperature and Immersion time.

Chapter IV: Corrosion inhibition behaviour of Imidazolines under the varying conditions of [inhibitor], [HCl], temperature and Immersion time.

Chapter V: Corrosion inhibition behaviour of Triazoles and Oxadiazoles under the varying conditions of [inhibitor], [HCl], temperature and Immersion time.

Chapter VI: Effect of Surfactants on corrosion inhibition behaviour of 2-aminophenyl-5-mercapto-1-oxa-3,4-diazole (AMOD) and 2- Heptyl-1,3 Imidazoline (HI).

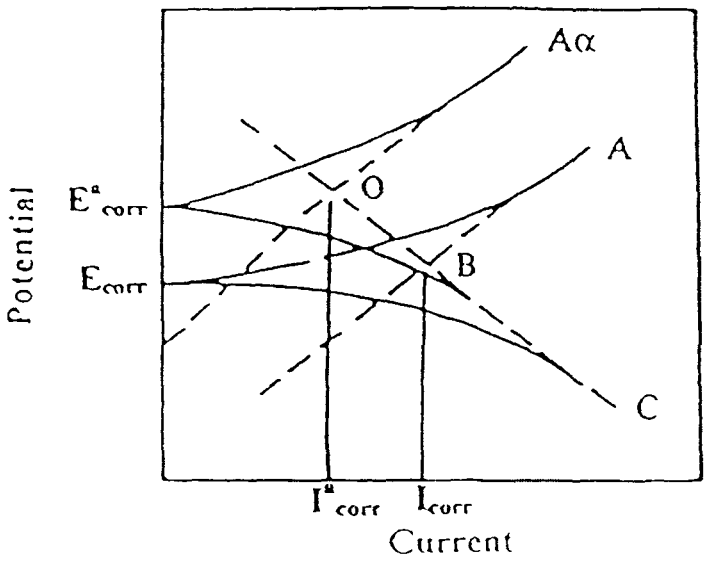

Fig. 1.1. Mechanism of corrosion inhibitors for anodic inhibitors

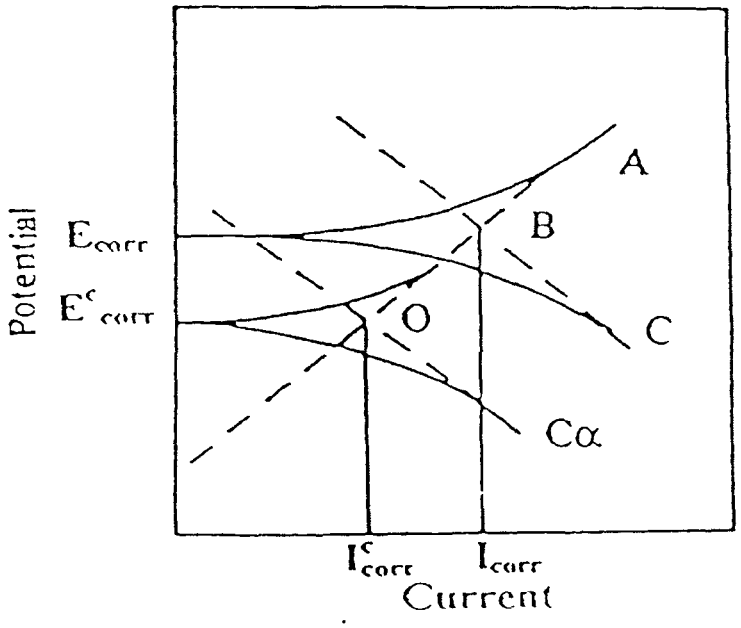

Fig. 1.2. Mechanism of corrosion inhibitors for cathodic inhibitors

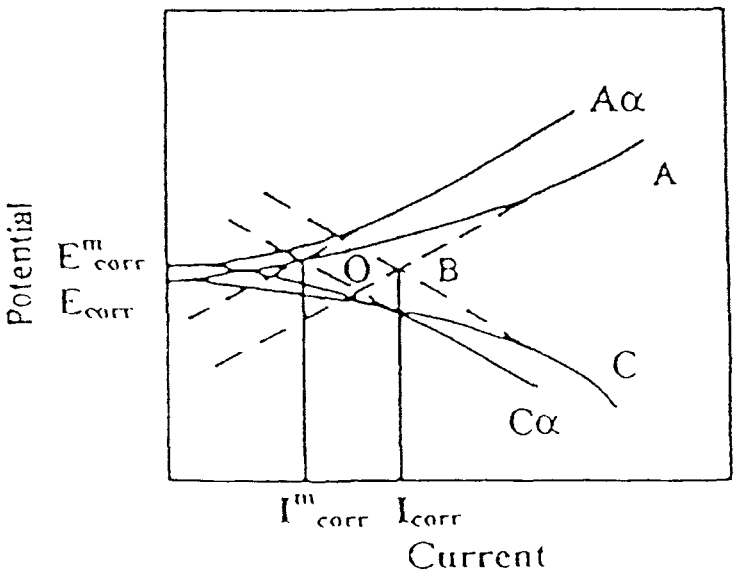

Fig. 1.3. Mechanism of corrosion inhibitors for mixed inhibitors

Chapter- 2
Experimental

2.0 MATERIALS AND METHODS

2.1 CHEMICALS USED

Various chemicals used throughout the experimental work are given in Table 2.1.

2.1.1. Test specimen for weight loss study

Cold rolled mild steel strips of size 2 cm × 2.5 cm × 0.05 cm having the following composition were used for corrosion study in 1.0 mol dm^{-3} acidic solutions by weight loss method.

C	Mn	Si	P	Fe
0.14 %	0.35 %	0.17 %	0.03 %	Remainder

2.1.2. Test specimen for electrochemical study

Cold rolled mild steel strips having the working area of 1 cm^2 and composition same as reported above were used for all electrochemical studies.

2.2 SYNTHESIS OF INHIBITORS

The following inhibitors were synthesized and tested for their inhibition properties in the laboratory. The method of synthesis of these compounds are given in the following sections.

a. Fatty acid Hydrazide

1.	Decanohydrazide	DH
2.	Dodecanohydrazide	DDH
3.	Hexadecanohydrazide	HDH
4.	Octadecanohydrazide	ODH

b. Thiosemicarbazides

5.	1-Undecyl-4-phenyl thiosemicarbazide	UPTS
6.	1-Pentadecyl-4-phenyl thiosemicarbazide	PPTS
7.	1-Heptadecyl-4-phenyl thiosemicarbazide	HPTS
8.	1- Nonyl -4-phenyl thiosemicarbazide	NPTS

c. Imidazolines

9.	2- Heptyl-1,3-imidazoline	HI
10.	2- Nonyl -1,3-imidazoline	NI
11.	2-Undecyl -1,3-imidazoline	UDI
12.	2- Pentadecyl-1,3-imidazoline	PDI
13.	2-Heptadecyl-1,3-imidazoline	HDI

d. Triazoles

14.	5-Nonyl- 4-phenyl -3- mercapto -1,2,4-triazole	NPMT
15.	5-Undecyl- 4-phenyl -3- mercapto-1,2,4-triazole	UPMT
16.	5-Pentadecyl- 4-phenyl- 3-mercapto-1,2,4-triazole	PPMT
17.	5-Heptadecyl -4-phenyl-3-mercapto-1,2,4-triazole	HPMT

e. Oxadiazoles

18.	2-Pentadecyl–5-mercapto-1-oxa-3,4- diazole	PMOD
19.	2-Undecyl-5-mercapto-1-oxa-3,4- diazole	UMOD
20.	2-Aminophenyl-5-mercapto-1-oxa-3,4-diazole	AMOD
21.	2-Nitrophenyl-5-mercapto-1-oxa-3,4-diazole	NMOD

2.2.1 Preparation of Fatty acid Hydrazides [147]

0.01 Moles of the fatty acid was first esterified with 50 ml ethanol. Thus obtained esters of fatty acid was refluxed for 8 hours with 0.03 moles hydrazine hydrate and 25 ml of ethanol. A solid compound that separated (Scheme 2.1) on cooling the reaction mixture was filtered, washed with little ethanol and ether and then dried. These acid hydrazides were recrystallized from ethanol.

The structural formulae, percentage yield, their melting point and R_f value are given in Table 2.2.

IR spectral data (significant bands ν_{max} in cm^{-1} (KBr))

IR recorded for DDH showed peak at 3300 cm^{-1} correspond to presence of N-N bond, CH_3 gave adsorption peak at 2900 cm^{-1}, CH_2 chain at 2845 cm^{-1}, C = O at 1621 cm^{-1} and of C - N at 1152 cm^{-1}

NMR Spectral data (δ $CDCl_3$)

NMR recorded for DDH gave peaks (12 H, $(CH_2)_6$) at 1.36, (2H, $\underline{C}H_2$ - CH =) at 2.1, (2H, CH_2 C = O) at 2.76, (2H, NH_2) at 5.09, (2H, $\underline{C}H_2$ = CH) at 5.2, (1 H, CH_2 - $\underline{C}$H -) at 5.96, (1 H, N - $\underline{H}$) at 8.87.

2.2.2. Preparation of 1-Alkyl- 4- Phenyl Thiosemicarbazide [148]

1.5 x 10^{-2} Moles of fatty acid hydrazide (as obtained in section 2.2.1) was dissolved in 40 ml benzene and 10 ml ethanol and then 12 ml phenyl isothiocyanate was added dropwise with shaking. The mixture was refluxed for 15 hours. Solid mass was separated out (Scheme 2.2) on cooling. It was

filtered, washed with ice cold benzene and dried in air. The product was recrystallized from ethanol.

The Chemical formula, abbreviation, percentage yield, their melting point and R_f value are given in Table 2.3.

IR Spectral data (significant bands ν_{max} in cm^{-1} (KBr))

UPTS = 3280 (N - N), 2875 (CH_3), 2820 (CH_2 chain), 1618 (C = O), 941 (C_6H_5), 1290 (Ar-C - N), 1152 (C - N), 1020 (C - S).

NPTS = 3230 (N - N), 1234 (CH_3), 2855 (CH_2 chain), 1670 (C = O), 925 (C_6H_5), 1303 (Ar-C - N), 1380 (C - N), 1245 (C - S).

PPTS = 3361 (N - N), 1255 (CH_3), 2845 (CH_2 chain), 1691 (C = O), 896 (C_6H_5), 1311 (Ar-C - N), 1446 (C - N), 1311 (C - S).

HPTS = 3316 (N - N), 1199 (CH_3), 2850 (CH_2 chain), 1641 (C = O), 890 (C_6H_5), 1330 (Ar-C - N), 1410 (C - N), 1230 (C - S).

NMR spectral data (δ $CDCl_3$)

UPTS = 1.38 (12 H, $(CH_2)_6$), 2.12 (2H, = CH - $\underline{C}H_2$), 2.38 (2H, $COCH_2$), 4.92 (1H, N - H), 5.19 (2H, $\underline{C}H_2$ = CH -), 5.97 (1 H, CH_2 - $\underline{C}H$ -), 7.59 (5 H, $C_6\underline{H}_5$), 9.18 (2H, NH - N$\underline{H}$), 9.52 (1 H, $\underline{H}N$ - C_6H_5).

2.4.3. Synthesis of 2-Alkyl-1- 3 Imidazoline [149]

0.1 Moles of fatty acid was dissolved in 50 ml absolute alcohol and treated with 12 ml thionyl chloride and was refluxed for 3 hours. The reaction product was then treated with ethylene diamine (6 ml) and was again refluxed for another 4 hours. The solid product formed (Scheme 2.3) was filtered, washed with water and recrystallized in ethanol.

The Chemical formulae, percentage yield, their melting point and R_f value in petroleum ether, ethyl alcohol, methyl alcohol system are given in Table 2.4.

IR spectral data (significant bands ν_{max} in cm^{-1} (KBr)

NI = 1648 (C = N), 1352 (C - N), 2924 (C - H), 3146 (N - H), 1172 (CH_3)

UDI = 1647 (C = N), 1323 (C - N), 2852 (C - H), 3257 (N - H), 1166 (CH_3)

PDI = 1640 (C = N), 1463 (C - N), 2845 (C - H), 3290 (N - H), 1164 (CH_3)

HDI =1665 (C = N), 1372 (C - N), 2845 (C - H), 2921 (N - H), 1250 (CH_3)

NMR spectral data (δ $CDCl_3$)

UDI = 7.350 (1 H, NH), 1.936 (20 H, $(CH_2)_{10}$), 1.253 (3H, CH_3), 2.006 (4 H, $CH_2)_2$).

2.4.4 Synthesis of 3-Alkyl-4-Aryl-5-Mercapto-1, 2,4-Triazole [150]

To a suspension of 1-alkyl-4-aryl thiosemicarbazide (0.01M) in 25 ml ethanol 20.0 ml of 10% ethanolic KOH was added and the mixture was refluxed for 10 - 12 hours on a steam bath. The solution was then cooled, 15 ml. of water was added and mixture was acidified to pH 5-6 with dil HCl. A solid product separated (Scheme 2.4) which was filtered, washed with water and recrystallized from ethanol.

The percentage yield, their melting point and R_f value are given in Table 2.5.

IR spectral data (significant bands ν_{max} in cm^{-1} (KBr)

UPMT =1606 (C = N), 1313 (C -N), 999 (C_6H_5), 1733 (S - H), 2983 (C - H), 1252 (CH_3).

NPMT =1734 (C = N), 1410 (C -N), 924 (C_6H_5), 2362 (S - H), 2848 (C - H), 1233 (CH_3).

PPMT =1640 (C = N), 1311 (C -N), 915 (C_6H_5), 2354 (S - H), 2911 (C - H), 1203 (CH_3).

HPMT =1557 (C = N), 1314 (C -N), 917 (C_6H_5), 2364 (S - H), 2850 (C - H), 1251 (CH_3).

NMR spectral data (δ $CDCl_3$)

UPMT = 7.388 (5 H, C_6H_5), 1.180 (1H,SH), 0.983 (3H, CH_3), 2.295 (16H, $(CH_2)_8$).

2.4.5 Synthesis of 2-Alkyl-5-Mercapto-1- Oxa -3, 4-Diazole[151]

0.03 Moles of carbon disulphide was added dropwise to 10 ml ethanolic KOH solution and the content was heated on water bath. The fatty acid hydrazide was added and the mixture was refluxed for 12 - 14 hours (until evolution of H_2S ceases). The excess solvent was distilled under reduced pressure. The residual mass was poured over crushed ice, and alkaline solution was neutralized with 10%HCl. The separated solid (Scheme 2.5) was filtered and washed with water and recrystallized from ethanol.

The percentage yield, their melting point and R_f value are given Table 2.6.

IR spectral data (significant bands ν_{max} in cm^{-1} (KBr)

UMOD= 1599.98 (C=N), 663.38 (C-S), 2359.34 (SH), 1184.83 (CH_3), 1412.64 (C-O-C), 2648.74 (CH_2) chain cm^{-1}.

PMOD= 1585.43 (C=N), 595.79 (C-S), 2361.62(SH), 1196.62(CH_3), 1403.65 (C-O-C), 2847.63 (CH_2) chain cm^{-1}.

AMOD=1584.77 (C=N), 658.32 (C-S), 2359.34 (SH), 1412.64 (C-O-C), 921.57 (C_6H_5), 3473.11 (NH_2) cm^{-1}.

NMOD=1602.96 (C=N), 669.76 (C-S), 2369.47 (SH), 1420.70 (C-O-C), 932.21 (C_6H_5), 3493.36 (NO_2) cm^{-1}.

NMR spectral data. (δ $CDCl_3$)

UMOD = 1.37 (2H $(CH_2)_6$), 2.16 (2H, $C\underline{H}_2$ - CH=), 5.04 (1H, SH), 5.12 (2H, - CH_2 = CH_2 = CH-), 5.96 (1H, $\underline{C}H$ - CH_2).

2.3 EQUIPMENTS AND TECHNIQUES USED

The following equipments and techniques were used during the experimental work.

2.3.1. Characterization of the synthesized compounds

Determination of melting point: Melting points were recorded on a Kofler hot block apparatus.

Determination of R_f values: R_f values were determined by thin layer chromatography using Silica-Gel G_{254} (MERCK) as support. Petroleum ether, ethyl acetate and methyl alcohol in ratio (5 : 3 : 2) was used as mobile phase. Iodine was used as developer.

Infra red spectroscopy: IR spectra were recorded by spectrophotometer Model No Interspec 2020, UK using KBr as an internal standard.

Nuclear magnetic resonance: The ^{1}H-NMR spectra were recorded in $CDCl_3$ on a Bruker spectrospin 300 mega Hertz spectrometer with TMS (Me_4Si) as an internal standard and its values are given in ppm (δ). The chemical shift was recorded relative to TMS assigned at zero.

2.3.2 Determination of Corrosion Rate and Other related parameters

Weight Loss Method: *The specimens of required size of different steels* were mechanically polished with 1/0 to 4/0 grade of emery papers. In each specimen a 1.5 mm diameter hole was drilled to mount the specimen. After polishing, the specimens were washed with distilled water and degreased with trichloroethylene. The clear and dry specimen were measured for the total surface area with utmost accuracy by using the following equation (as per ASTM method) [152]:

$A = 2$ (length x width + length x thickness + width x thickness $- \pi$ x radius^2 + π x radius x thickness)

The weight of the specimen was measured before exposing it to the corrodent solution on a sartorious balance. The volume of the test solution per square centimeter was maintained at about 20 ml, to avoid any appreciable change in its corrosivity during the test, either through exhaustion of corrosive constituent or by accumulation of corrosion products that might affect further corrosion.

The studies were carried out under varying conditions of immersion time, solution temperature, inhibitor and acid concentration. The experimental conditions were controlled in order to ensure reproducible results. After a definite immersion time, the specimen was taken out and washed with running

water. The corrosion product on the steel surface, if any, was removed mechanically by rubbing with brush. The specimen was then dried and loss in weight was recorded by weighing. Constant temperature bath was used to study the weight loss at desired temperatures (±1°C). Covered beakers containing acidic solutions were used to study corrosion rate. The percentage inhibition efficiency (% I.E.) was calculated using the following equations[153]:

$$\% \text{ I.E.} = \frac{C_R^0 - C_R}{C_R^0} \times 100$$

$$\theta = \frac{C_R^0 - C_R}{C_R^0}$$

Corrosion rate (C.R.) in mmpy was obtained by the use of the following equation.

$$CR = \frac{8.76 \times 10^4 \times \text{weight loss (mg)}}{\text{Surface Area of Specimen (cm}^2\text{)} \times \text{time(h)} \times \text{density of specimen(g cm}^{-3}\text{)}}$$

Potentiodynamic Polarization Technique: Working electrodes of size 1 cm × 1 cm with tag of 4 cm was cut from the steel of same composition and polished with 1/0 to 4/0 of emery papers. The specimens were then washed with distilled water and finally degreased with trichloroethylene. The unwanted area of the working electrode was coated with a commercial lacquer to get a well defined working area of 1 cm^2. The potentiodynamic polarization studies were carried out using EG & G PARC potentiostat / galvanostat (model 173), universal programmer (model 175) and X – Y recorder (model RE 0089) as per ASTM[154]. A platinum foil and saturated calomel electrode were used as auxiliary and reference electrode, respectively. All the experiments were

carried out at constant temperature of 30 ± 1 °C and at a scan rate of 1mV / sec at open circuit potential. The polarization curves were recorded after immersion of the electrode in the solution for 30 minutes (until steady state is reached). Corrosion rate was calculated by using below mentioned relation[155].

$$CR = \frac{0.13 \times I_{corr} \times E.W}{D}$$

The percentage inhibition efficiency was calculated using the following equation:

$$\%I.E. = \frac{I_{corr\,o} - I_{corr\,i}}{I_{corr\,o}} \times 100$$

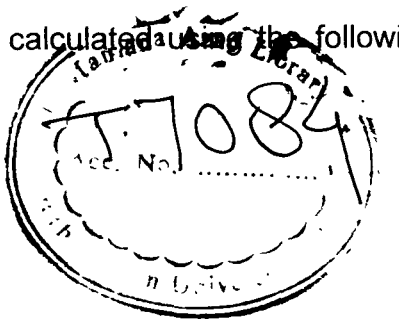

Electrochemical Impedance Technique: In this technique a three electrodes assembly consisting of mild steel strip as working electrode, platinum as auxiliary electrode and calomel as reference electrode was used. The specimen, so called working electrode was polished with emery paper of grade 1/0 to 4/0 and degreased with trichloroethylene and then immersed in the test solution kept in the cell. The connection of these electrodes are shown in the block diagram of the circuit (Figure 2.1). A time interval of 15 – 20 minutes was given for the open circuit potential to reach a steady value.

Impedance measurements were performed at E_{corr} with the ac voltage amplitude + 5mV in the frequency range from 5 Hz – 100 KHz. All the measurements were carried out by Zahner IM-6 electrochemical workstation using an IBM computer[156].

The values of R_t and C_{dl} were obtained using the Nyquist Plot[157].The values of solution resistance (R_S) is negligible for acidic solution and the R_S +

R_t values were taken together as R_t. The percentage inhibition efficiency were calculated using the following equation :

$$\% \text{ I.E.} = \frac{1/R_{to} - 1/R_{ti}}{1/R_{to}} \times 100$$

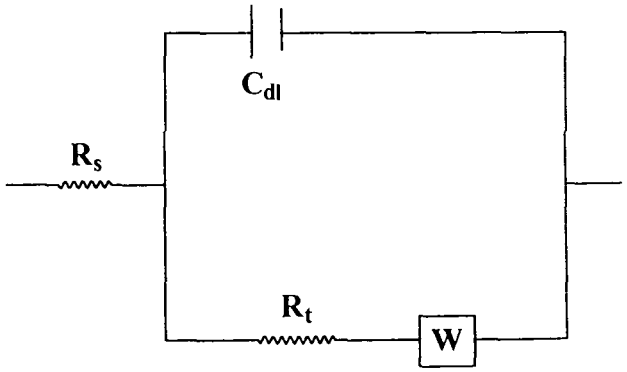

Fig 2.1 Block diagram of impedance set up

C_{dl} values were calculated from the frequency at which the imaginary component of impedance was maximum ($Z_{im\,max}$) using the following equation.

$$C_{dl} = \frac{1}{2\pi f_{max}} \times \frac{1}{R_t}$$

Scanning Electron Microscopy: Scanning electron microscope (SEM) Model No 435 VP LEO, was used to study the morphology of corroded surface in presence and absence of inhibitors. The specimens were thoroughly washed with double distilled water before putting on the slide. The photographs were taken at appropriate magnifications (x 3000μ). To understand the morphology of the steel surface in absence and presence of inhibitors, the following cases have been examined.

i. Polished mild steel specimen

ii. Mild steel specimen after dipping in 1.0 mol dm^{-3} HCl solution for 30 minutes.

iii. Mild steel specimens after dipping 30 minutes in 1.0 mol dm^{-3} HCl solution containing 500 ppm inhibitor.

2.4. DETERMINATION OF THERMODYNAMIC PARAMETERS

Determination of Activation Energy: The corrosion rate at varying temperatures in the range from 30°C to 60°C was determined while keeping all other parameters fixed. The values of activation energy (E_a) were calculated from the slope of the plot of log (CR) versus 1/T by using the Arrhenius equation[158-160].

$$\text{Log (CR)} = \frac{-E_a}{2.303RT} + A$$

Determination of Free Energy of Adsorption: The free energy of adsorption was calculated[161] using the equation given below:

$$\Delta G_{ads} = -RT \ln (55.5K)$$

and K is given by:

$$K = \theta/C\ (1-\theta)$$

Determination of Heat of Adsorption: The value of heat of adsorption of inhibitor at the metal surface was determined by plotting log (θ/1-θ) against 1/T and the slope of the plot gave Q[162].

$$\text{Slope} = \frac{-Q}{2.303R}$$

Determination of Entropy and Enthalpy: To determine ΔH and ΔS from the corrosion rate the following equation[163] was used.

$$CR = \frac{RT}{Nh}\exp\left(\frac{\Delta S}{R}\right)\exp\left(-\frac{\Delta H}{RT}\right)$$

The slope of plot log (CR/T) versus 1/T gave the values of ΔH and the intercept gave the value of ΔS.

Determination of Half-life: The Plot of log (weight loss) versus Immersion time was used to calculate the values of half-life[164]. The half-life ($t_{1/2}$) values were calculated[165] using the following equation.

$$t_{1/2} = 0.693/k$$

where, $k = 2.303 \log \frac{(\text{weight loss})}{t}$

and weight loss is expressed in mg.

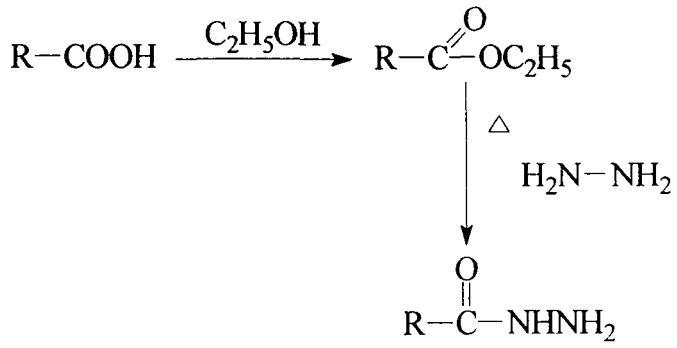

1. R = CH_3–$(CH_2)_8$
2. R = CH_3–$(CH_2)_{10}$
3. R = CH_3–$(CH_2)_{14}$
4. R = CH_3–$(CH_2)_{16}$

SCHEME 2.1

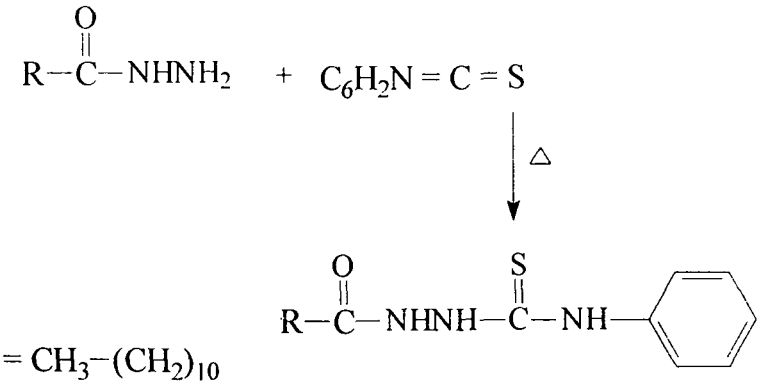

5. R = CH_3–$(CH_2)_{10}$
6. R = CH_3–$(CH_2)_{14}$
7. R = CH_3–$(CH_2)_{16}$
8. R = CH_3–$(CH_2)_8$

SCHEME 2.2

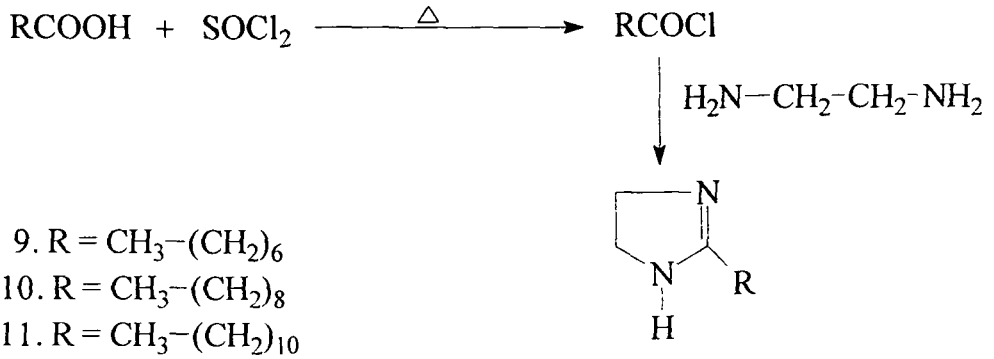

9. R = CH_3–$(CH_2)_6$
10. R = CH_3–$(CH_2)_8$
11. R = CH_3–$(CH_2)_{10}$
12. R = CH_3–$(CH_2)_{14}$
13. R = CH_3–$(CH_2)_{16}$

SCHEME 2.3

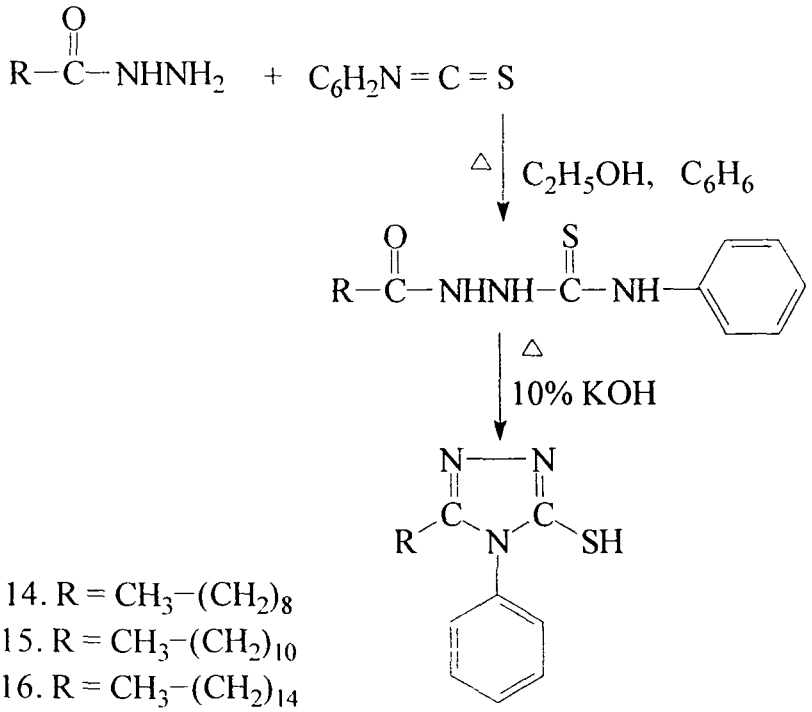

14. R = CH_3–$(CH_2)_8$
15. R = CH_3–$(CH_2)_{10}$
16. R = CH_3–$(CH_2)_{14}$
17. R = CH_3–$(CH_2)_{16}$

SCHEME 2.4

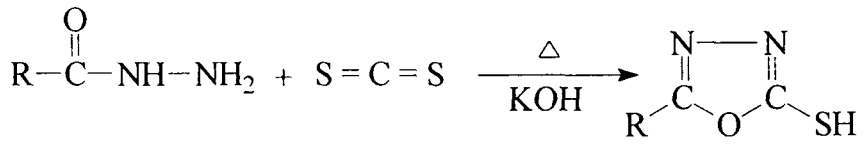

18. R = $CH_3-(CH_2)_8$

19. R = $CH_3-(CH_2)_{14}$

20. R = 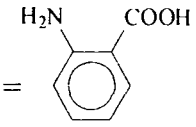

21. R = 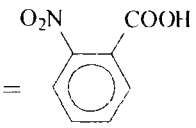

SCHEME 2.5

Table 2.1: Name, Abbreviation and Purity of Chemicals used.

Name	Abbreviation	Make	% Purity
Hydrochloric Acid	HCl	Merck	35
Acetone	Act	Merck	99
Decanoic Acid	DH	CDH	98.5-100.5
Dodecanoic Acid	DDH	CDH	98.5-100.5
Hexadecanoic Acid	HDH	CDH	99.0-101.0
Octadecanoic Acid	ODH	CDH	98-100
Hydrazine Hydrate	Hh	Qualigens	99-100
Ethyl Alcohol	EtOH	Merck	100
Benzene	B	Merck	99
Phenyl isothio-Cyanate	Ph itc	Merck	98
Thionyl Chloride	Tc	Merck	99
Ethylene Diamine	EA	Merck	99.5
Potassium Hydroxide	KOH	Merck	84
Carbon disulfide	CS_2	Thomas Baker	99.5
Silica –gel	Sg	Merck	-
Petroleum Ether	Pet	Merck	90
Methanol	MeOH	Qualigens	99.5
Iodine	I_2	Merck	99.5-100.5

Table 2.2: Structure Formula, % Yield, Melting point and R_f value of synthesized hydrazides.

S.No	Name of the compounds (Abbreviated) and Structure	Yield (%)	M.P. (°C)	R_f value Pet : E.A. : MeOH (5 : 3 : 2)
1	DH 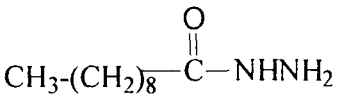	95	113-114	0.31
2	DDH 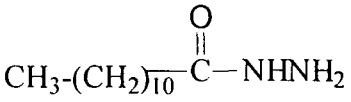	91	92-95	0.34
3	HDH 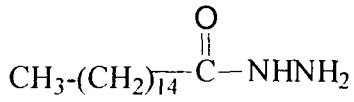	92	78-79	0.37
4	ODH 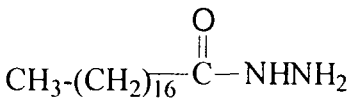	89	73-75	0.40

Table 2.3: Structure Formula, % Yield, Melting point and R_f value of synthesized thiosemicarbazides.

S. No	Name of the compounds (Abbreviated) and Structure	Yield (%)	M.P. (°C)	R_f value Pet:E.A.:MeOH (5 : 3 : 2)
5.	UPMT 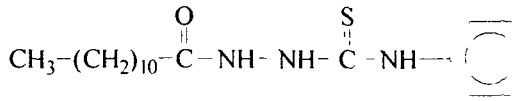	85	104-105	0.08
6.	PPMT 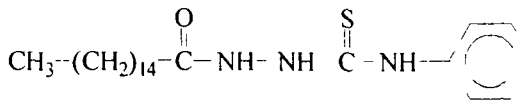	82	60-62	0.11
7.	HPMT 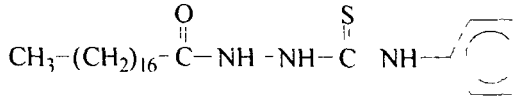	93	65-66	0.10
8.	NPMT 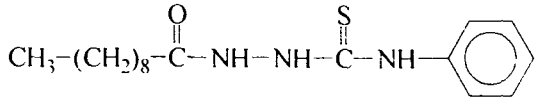	76	82-83	0.07

Table 2.4: Structure Formula, % Yield, Melting point and R_f value of synthesized imidazolines.

S.No	Name of the compounds (Abbreviated) and Structure	Yield (%)	M.P. (°C)	R_f value Pet : E.A. : MeOH (5 : 3 : 2)
9.	HI 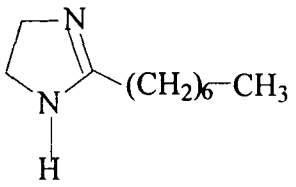	59	69-70	0.43
10.	NI 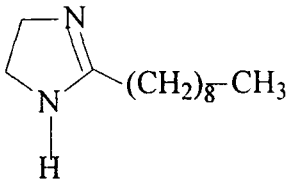	63	77-78	0.35
11.	UDI 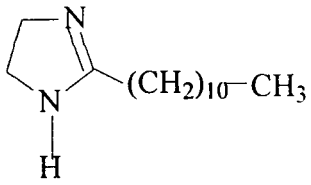	75	91-92	0.28
12.	PDI 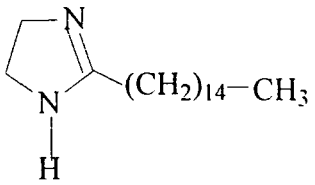	68	135-136	0.52
13.	HDI 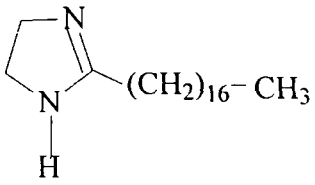	70	110-111	0.45

Table 2.5: Structure Formula, % Yield, Melting point and R_f value of synthesized triazoles.

S.No	Name of the compounds (Abbreviated) and Structure	Yield (%)	M.P. (°C)	R_f value Pet : E.A. : MeOH (5 : 3 : 2)
14	NPMT 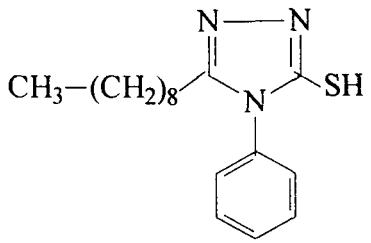	75	130-134	0.49
15	UPMT 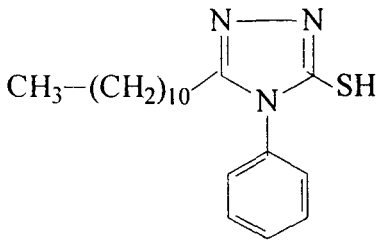	68	250-252	0.38
16	PPMT 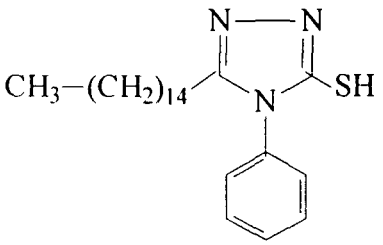	70	145-146	0.45
17	HPMT 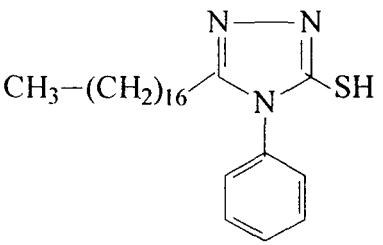	65	293-295	0.52

Table 2.6: Structure Formula, % Yield, Melting point and R_f value of synthesized oxadiazoles :

S.No	Name of the compounds (Abbreviated) and Structure	Yield (%)	M.P. (°C)	R_f value Pet : E.A. : MeOH (5 : 3 : 2)
18	PMOD 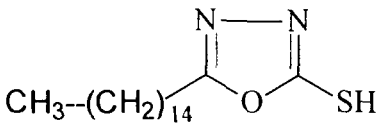	64	86-87	0.55
19	UMOD 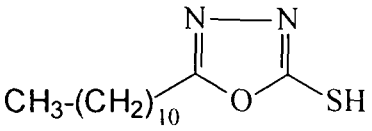	69	92-93	0.26
20	AMOD 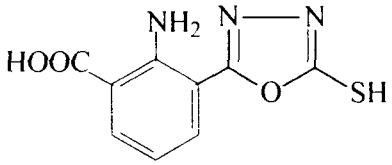	52	144-145	0.30
21	NMOD 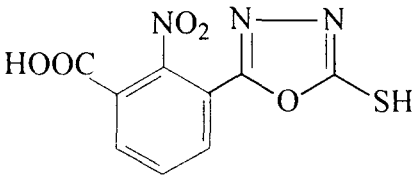	63	130-136	0.41

ABBREVIATION USED

A= Total surface area (cm^2)

I.E = Inhibition efficiency (%)

C.R = Corrosion rate (mmpy)

C_R^o = Corrosion rate in uninhibited system (mmpy)

C_R = corrosion rate in inhibited system (mmpy)

E.W = Equivalent weight

D = Density (gcm^{-3})

$I_{corr\ o}$ = Current density without inhibitor (mA cm^{-2})

$I_{corr\ i}$ = Current density with inhibitor (mA cm^{-2})

C_R = Capacitance ($\mu F\ cm^{-2}$)

R_S = Solution resistance (ohm cm^2)

C_{dl} = Double layer ($\mu F\ cm^{-2}$)

W = Warburg impedance

f= Frequency of component of impedance (s^{-1})

$R_{t\ o}$ = Charge transfer resistance without inhibitor (ohm cm^2)

$R_{t\ i}$ = Charge transfer resistance with inhibitor (ohm cm^2)

θ = Degree of coverage on the metal surface

C = Concentration of inhibitor (mole/litre, ppm)

T = Temperature (K, °C)

R = Universal gas constant ($J\ K^{-1}mol^{-1}$)

K = Equilibrium constant

h = Plank's constant (J-s)

N = Avogadro's number (mol^{-1})

ΔS = Change in entropy of activation ($J\ mol^{-1}K^{-1}$)

ΔH = Change in enthalpy of activation ($kJ\ mol^{-1}$)

E_a = Activation energy ($kJ\ mol^{-1}$)

ΔG_{ads} = Change in free energy of adsorption ($kJ\ mol^{-1}$)

Q = Heat of adsorption ($kJ\ mol^{-1}$)

$t_{1/2}$ = Half Life (hours)

k = Rate constant (s^{-1})

t = Time (hours)

Chapter- 3
Corrosion Inhibition behaviour of hydrazides & Thiosemicarbazides

A persual of literature reveals that corrosion inhibitors derived from fatty acids constitute an important and potential class of corrosion inhibitors[166-168]. Corrosion inhibition of mild steel by nitrogen containing heterocyclic compounds have been reported by many authors[77, 136,169-173]. A.V. Radushev *et al*[174] investigated on the corrosion inhibition properties of hydrazides of fatty, carbonic acids and natural naphthenic acids for steel corrosion in hydrochloric acid, hydrogen sulfide media and actual oil well waters. Test results obtained for specimens of steel demonstrated that these compounds exhibit good corrosion-inhibiting properties in the various solutions studied. E.S. Lower[175] studied various oleochemicals such as ammonium stearate, ethyl stearate, glyceryl monooleate, stearyl maleate and ricinoleic acid hydrazides for their corrosion inhibiting properties. Oleochemicals applications such as dewatering and corrosion preventives, anti-corrosive lubricants, strippable rust preventives, vapor-phase corrosion inhibitors, and oleochemical-containing rust preventives, car protection, engine protectives, and corrosion protection against chemicals have been discussed.

Inhibitors that contain nitrogen and sulfur in their structures are of particular importance, since these compounds provide an excellent inhibition property as compared with the compounds that contain only sulfur or nitrogen[176]. L. Larabi *et al*[177] synthesized N-phenyl oxalic dihydrazide (PODH) and oxalic N-phenylhydrazide N-phenylthiosemicarbazide (OPHPT), and tested for their inhibitive properties on the corrosion of mild steel in 1M HCl by electrochemical measurements. Results showed that both OPHPT and PODH inhibited the corrosion rate but better performances was observed for OPHPT

due to presence of N and S atoms in OPHPT and presence of additional phenyl group.

B.I. Ita *et al*[178] studied the effect of 4-methylthiosemicarbazide (4MTS), pyridoxal-(4) -methylthisemicarbazone) (P4TS) and Zn(II) -pyridoxal-(4-methylthiosemicarbazone) (ZnP4TS) on the corrosion rate of mild steel in hydrochloric acid by weight loss and hydrogen evolution measurements. It has been found that ZnP4TS exhibited maximum inhibition efficiency because of its higher molecular weight.

The influence of thiosemicarbazide, phenylthiosemicarbazide Girad's-T and phenylthiosemicarbazide Girard's-P on the corrosion rate of steel in 2 M HCl has been studied by A.A. El-Shafei *et al*[179]. Thiosemicarbazide and its derivatives showed a higher inhibitive effect on the corrosion of C-steel in hydrochloric acid. The higher inhibition is due to the adsorption of the inhibitor molecules on the steel surface.

Quraishi *et al*[180-181] have studied the corrosion behavior of fatty acid hydrazides and thiosemicarbazides on mild steel and oil-well steel (N-80) in boiling 15% hydrochloric acid solution by weight loss method and potentiodynamic polarization studies. They observed that both hydrazides and thiosemicarbazides inhibited the corrosion of mild steel by the adsorption mechanism. Thiosemicarbazides was effective inhibitor than hydrazides due to the presence of additional phenyl group, N and S atoms in thiosemicarbazides.

The following chapter presents the systematic studies on inhibitive action of hydrazides and thiosemicarbazides on mild steel in acidic medium. Weight loss measurement, potentiodynamic polarization studies and

electrochemical impedance studies were carried out for the determination of corrosion rate under the varying conditions of acidities, temperature, immersion time and inhibitor concentration. Surface morphology was characterized by Scanning Electron microscopy (SEM).

RESULTS AND DISCUSSION

3.1. Weight loss Studies

The influence of hydrazides and thiosemicarbazides on the corrosion rate of mild steel in 1.0 mol dm^{-3} HCl was studied by monitoring the weight loss. The temperature was kept constant at 30°C and the immersion time was 3 hours. The corrosion rate and inhibition efficiency were calculated by using the following equations:

$$CR = \frac{KW}{ATD}$$

$$\%I.E. = \frac{C_R^0 - C_R}{C_R^0} x100$$

The corrosion rate and the inhibition efficiency were determined at different concentrations of hydrazides and thiosemicarbazides and the values are given in Tables 3.1-3.2.

The weight loss studies were carried out under the varying conditions of [acid], solution temperature and immersion time. The effect of variation of concentration of inhibitor on corrosion rate was studied from 100 ppm - 600 ppm. The dependence of inhibition efficiency of hydrazides and thiosemicarbazides on inhibitor concentration, temperature, immersion time and acid concentration are presented in Figures 3.1-3.4, respectively. The addition of hydrazides and thiosemicarbazides decreased the rate of

corrosion of mild steel in HCl solution. It has also been observed that the inhibition efficiency of these compounds increased with the increase in concentration upto 500 ppm and, thereafter, the inhibition efficiency decreased with further increase in [inhibitior]. Thus, these inhibitor displayed maximum inhibition efficiency at 500 ppm (Figures 3.1.a- 3.1.b).

The inhibition efficiencies of hydrazides and thiosemicarbazides were studied at temperatures 30°, 40°, 50° and 60° C by weight loss method and are shown in Figures 3.2 a -3.2 b. All hydrazides significantly increased the inhibition efficiency with an increase in temperature from 30 to 50°C. However, no significant change in inhibition efficiency has been observed for DH and DDH with the increase in temperature upto 60°C indicating that the inhibitive film formed on the metal surface is protective in nature upto this temperature. The inhibition efficiency of HDH and ODH decreased slightly with the increase in temperature from 50°C to 60°C, showing that desorption rate of the inhibitor molecules from metal surface becomes higher at temperature beyond 50°C[182]. The inhibition efficiency for thiosemicarbazide inhibitors decreases slightly with increase in temperature from 30°C to 60°C, indicating that the rate of desorption of inhibitive film is higher than the rate of adsorption at high temperature. All the tested hydrazides showed that an increase in inhibition efficiency with the increase[183] in immersion time from 3h to 24h, as shown in Figure 3.3 a. The thiosemicarbazides displayed no significant change in inhibition efficiency with the immersion time from 3h to 24h. This behaviour shows the persistency of the adsorbed fatty acid thiosemicarbazides over a longer test period (Figure 3.3 b). The dependence of inhibition efficiency on the concentration of acid was carried out by

monitoring the inhibition efficiency at varying acid concentration in the range 1.0 mol dm^{-3} – 5.0 mol dm^{-3}. The observed results suggest that inhibition efficiency increases with increase in acid concentration up to 3 mol dm^{-3} HCl for all the hydrazides tested. Further increase in acid concentration upto 5 mol dm^{-3} HCl caused decreased in inhibition efficiency, except for DH. DH having C_9 has shown almost no change in inhibition efficiency with the increase in acid concentration range from 3 mol dm^{-3} to 5 mol dm^{-3} HCl .The decrease in inhibition efficiency on increasing acid concentration beyond 3 mol dm^{-3} is due to increased aggressiveness of the acid[184]. Figures 3.4a - 3.4.b depict the effect of acid concentration on inhibition efficiency of hydrazides and thiosemicarbazides.

The loss in weight of mild steel at different initial concentrations of inhibitors in 1.0 mol dm^{-3} HCl was investigated at 30°C after 3 hours of immersion time. The data obtained from the weight loss studies were used to evaluate surface coverage (θ).The data were tested graphically by fitting to various isotherms. A straight line was obtained on plotting log (θ /1-θ) versus log C (Figures. 3.5 a - 3.5 b) suggesting that the adsorption of the hydrazides and thiosemicarbazides on mild steel surface follows Langmuir's adsorption isotherm. To obtain the values of heat of adsorption (Q), log (θ/1-θ) was plotted against 1/T as shown in Figures 3.6 a - 3.6 b. The values for the heat of adsorption (Q) were obtained from the slope of the plot and are presented in Tables 3.3 - 3.4. The values of Q, thus obtained suggest the physical nature of adsorption[162].

Different experiments were performed at various temperatures in the range from 30°C to 60°C at fixed concentrations of hydrochloric acid (1.0 mol

dm^{-3}) and inhibitor (500 ppm). The immersion period was 3h and the corrosion rate was determined at temperatures 30°C, 40°C, 50°C and 60°C. Log (corrosion rate) *versus* 1/T was plotted (Figures 3.7.a - 3.7.b) and the slope of the plot gave the values of E_a. The values of activation energy (E_a) for hydrazides and thiosemicarbazides are presented in Table 3.3 - 3.4.

To obtain the values of ΔH and ΔS for the adsorption of hydrazides and thiosemicarbazides on the mild steel surface in presence of HCl, logarithm of (CR /T) was plotted against 1/T (Figures 3.8.a - 3.8.b). The slope and intercept of plots gave the values of ΔH and ΔS respectively. The values of ΔH and ΔS for the adsorption of hydrazides and thiosemicarbazides are listed in Table 3.3 - 3.4 respectively.

The lower E_a values for hydrazides indicate that they exhibit high efficiency at elevated temperature[163]. The higher energy of activation (E_a) values as obtained from slope of Figure. 3.7 b for thiosemicarbazides except HPTS suggest that these inhibitors are more effective at room temperature[185]. The lower value of E_a for HPTS indicates its poor efficiency[163].

The lower values of enthalpies (ΔH) in presence of DDH, DH and HPTS signify both the corrosion reactions as well as the adsorption at the mild steel surface. The lowering in the values of ΔH in the presence of DDH, DH and HPTS may be due to the energy released during the adsorption of DDH, DH and HPTS at mild steel surface[186]. It is evident from the fact that the presence of DDH, DH and HPTS reduces the corrosion rate and increases the inhibition efficiency. The higher values of ΔH in the presence of HDH, ODH and thiosemicarbazides indicate that the presence of more energy barrier is involved in the adsorption of HDH, ODH and thiosemicarbazides on

mild steel surface[187]. Thus, a weak association exists between the mild steel surface and HDH, ODH and thiosemicarbazides and, therefore, it exhibit poor inhibition efficiency. The values of entropy of activation ΔS in the absence and presence of hydrazides and thiosemicarbazides are negative and large[188]. This indicates that the activated complex formed during the corrosion and adsorption of inhibitor processes is an associative in nature rather than dissociative step. Therefore, a decrease in disorderness takes place during the transformation from reactants to the activated complex[189].

The change in free energy of adsorption (ΔG_{ads}) were calculated[190] using the following equation and the values are listed in Tables 3.3 - 3.4.

$$\Delta G_{ads} = -RT \ln (55.5K)$$

and K is given by:

$$K = \theta/C\ (1-\theta)$$

The lower values of ΔG_{ads} also indicate that hydrazides and thiosemicarbazides of fatty acid are physically adsorbed on the metal surface[191]. It further indicates that adsorption of inhibitor on the surface of mild steel is a spontaneous process [31].

In order to determine the dependency of the corrosion rate on immersion time, a number of experiments were performed in which weight losses were monitored as a function of immersion time. The concentrations of HCl and inhibitor were kept constant at 1.0 mol dm^{-3} and 500 ppm, respectively at 30°C. A straight line was obtained for the plot of log (weight loss) *versus immersion time as depicted in Figures 3.9a.- 3.9b showing that*

the reaction obeyed first order kinetics. The rate constant was calculated using the first order rate law[164].

where A_o is the intial mass of the metal and A is the mass of the metal corresponding to time t. The half life ($t_{1/2}$) value was calculated using the following equation[165].

$$t_{1/2} = 0.693 / k$$

The values of the rate constant and half life period ($t_{1/2}$) obtained in the absence and presence of hydrazides and thiosemicarbazides are summarized in Tables 3.5.-3.6. The half life ($t_{1/2}$) values give the information regarding the durability of inhibitor film on the mild steel surface under the corrosive condition[193].

3.2 Potentiodynamic polarization Studies

The cathodic and anodic polarization curves of mild steel in 1.0 mol dm^{-3} HCl in the absence and presence of different compounds of hydrazides and thiosemicarbazides at 500 ppm concentration at 30±1 °C are shown in Figures 3.10.a -3.10b.

Tafel plots were used to calculate corrosion current density (I_{corr}), corrosion potential (E_{corr}) and inhibition efficiency (IE). These values are given in Tables 3.7 - 3.8.

The values of I_{corr} decreased significantly in the presence of inhibitor. Maximum decrease in I_{corr} was observed for DDH (among hydrazides) and UPTS (among thiosemicarbazides). All the hydrazides and thiosemicarbazides do not show any significant change in E_{corr} values suggesting that these compounds are mixed type inhibitors i.e., they retard

the corrosion reaction by blocking both anodic and cathodic sites of the metal[194].

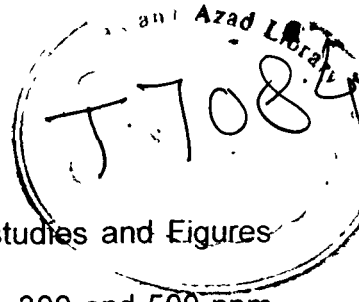

3.3. Electrochemical Impedance Studies

Tables 3.9.- 3.10 gives the results of impedance studies and Figures 3.11a- 3.11b shows Nyquist plots in the presence of 100, 300 and 500 ppm of DDH and UPTS. The Nyquist plots are not perfect semicircles and this difference has been attributed to frequency dispersion[195]. The values of R_t and C_{dl} were calculated from Nyquist plots[157]. The percentage inhibition efficiency was calculated from the following equation[196].

$$\% \text{ I.E.} = \frac{1/R_{to} - 1/R_{ti}}{1/R_{to}} \times 100$$

where R_{to} and R_{ti} are charge transfer resistance without and with inhibitor, respectively and its values are given in Tables 3.9.- 3.10. R_t values increases with increase in inhibitor concentration (DDH and UPTS) and, in turn, it leads to an increase in inhibition efficiency. The addition of DDH and UPTS to 1.0 mol dm^{-3} HCl lowers the C_{dl} values, which shows that the inhibition in corrosion may be due to surface adsorption of the inhibitor [197].

3.4. Scanning electron microscopy

Photograph of the mild steel surface was taken by scanning electron microscope after its immersion in HCl, HCl and DDH, and HCl and UPTS solution. It was observed that the surface of mild steel immersed in hydrazides and thiosemicarbazides solutions was smoother than that in blank 1.0 mol dm^{-3} HCl alone (Figures 3.12-3.13).These observations suggest that

the inhibitors form protective layer over the metal surface and prevent the attack of acid on metal surface[198].

3.5. Mechanism of corrosion inhibition

Inhibition of corrosion of mild steel in the acidic solutions by the hydrazides and thiosemicarbazides can be explained on the basis of their molecular structure and adsorption. It is apparent from the molecular structures that these compounds are adsorbed on the metal surface through π-electrons of aromatic ring and lone pair of electrons of N atoms[199]. The presence of long hydrophobic chain plays an important role in enhancing the protective action and keeps the acid solution away from metal surface. Among the compounds investigated in the present study, inhibition efficiency has been found to be in the following order:

Hydrazides :- DDH > DH > HDH > ODH

(C_{11}) (C_9) (C_{15}) (C_{17})

Thiosemicarbazides:- UPTS > NPTS > PPTS > HPTS

(C_{11}) (C_9) (C_{15}) (C_{17})

It has been observed that inhibition efficiency of the hydrazides and thiosemicarbazides increases with the increase in chain length up to C_{15}. A further increase in chain length decreased the inhibition efficiency[200]. The higher inhibition efficiency of thiosemicarbazides than hydrazides may be attributed to the presence of the CS-NHC_6H_6 in the thiosemicarbazides molecules which enhances the adsorption of thiosemicarbazides to the mild steel surface through polarizable sulfur and phenyl group[201].

Table 3.1: Dependence of corrosion rate and inhibition efficiency on [Hydrazides].

Inhibitor Used	Concentration (ppm)	Weight loss (mg)	IE (%)	CR (mmpy)
DDH	0	60.0	--	22.3
	100	10.7	82.1	4.0
	200	9.7	83.7	3.6
	300	8.3	86.1	3.0
	400	6.9	88.5	2.5
	500	6.4	89.3	2.4
	600	6.1	85.1	3.3
DH	0	60.0	--	22.3
	100	20.3	66.2	7.5
	200	15.3	74.5	5.7
	300	11.7	80.5	4.3
	400	11.2	81.3	4.1
	500	9.6	84.0	3.5
	600	10.5	82.3	3.9
HDH	0	60.0	--	22.3
	100	26.2	56.3	9.7
	200	22.8	62.0	8.5
	300	20.8	65.3	7.7
	400	20.2	66.3	7.5
	500	19.2	68.0	7.1
	600	19.6	67.2	7.3
ODH	0	60.0	--	22.3
	100	27.3	54.5	10.1
	200	24.0	60.0	8.9
	300	21.9	63.5	8.1
	400	21.6	64.0	8.0
	500	21.0	65.0	7.8
	600	21.2	64.2	7.9

[HCl] = 1.0 mol dm^{-3}, Temp. = 30 °C, Immersion time = 3 hours

Table 3.2: Dependence of corrosion rate and inhibition efficiency on [Thiosemicarbazides].

Inhibitor Used	Concentration (ppm)	Weight loss (mg)	IE (%)	CR (mmpy)
UPTS	0	63.5	-	23.62
	100	21.5	66.11	8.00
	200	13.7	78.35	5.11
	300	7.9	87.44	2.96
	400	4.3	93.12	1.62
	500	0.2	.96.65	0.75
	600	4.2	93.21	1.60
NPTS	0	63.5	-	23.62
	100	23.5	62.99	8.74
	200	17.0	73.12	6.34
	300	9.2	85.36	3.45
	400	4.8	92.07	1.82
	500	3.0	95.15	1.14
	600	6.5	89.79	2.43
PPTS	0	63.5	-	23.62
	100	24.9	60.67	9.28
	200	18.3	71.12	6.82
	300	10.2	83.85	3.81
	400	6.2	90.12	2.33
	500	3.7	94.02	1.41
	600	7.8	87.97	2.90
HPTS	0	63. 5	-	23.62
	100	26.6	58.31	9.84
	200	19.2	69.72	7.15
	300	12.5	80.21	4.67
	400	6.8	89.23	2.54
	500	4.4	92.99	1.65
	600	1.1	82.13	4.2

[HCl] = 1.0 mol dm^{-3}, Temp. = 30 °C, Immersion time = 3 hours

Table 3.3: Thermodynamic activation parameters for corrosion of mild steel in HCl in the absence and presence of hydrazides.

System	E_a (kJ mol^{-1})	ΔH (kJ mol^{-1})	ΔS (J $mol^{-1}K^{-1}$)	ΔG_{ads} (kJ mol^{-1})	-Q (kJ mol^{-1})
1N HCl	51.18	48.56	200.40	-	-
DDH	86.3	40.32	248.34	36.26	33.02
DH	74.3	41.32	232.07	35.84	32.30
HDH	74.1	61.27	218.66	24.07	23.20
ODH	66.9	59.03	215.79	23.62	22.97

[Hydrazides] = 500 ppm; [HCl] = 1.0 mol dm^{-3}; Time= 3 hours.

Table 3.4: Thermodynamic activation parameters for corrosion of mild steel in HCl in the absence and presence of thiosemicarbazides.

System	E_a (kJ mol^{-1})	ΔH (kJ mol^{-1})	ΔS (J $mol^{-1}K^{-1}$)	ΔG_{ads} (kJ mol^{-1})	-Q (kJ mol^{-1})
1N HCl	51.18	48.56	200.40	-	-
UPTS	75.23	77.88	198.56	39.75	28.72
NPTS	68.10	70.72	196.07	39.47	26.48
PPTS	58.32	60.95	195.31	38.88	19.78
HPTS	42.00	44.65	192.43	36.93	14.87

[Thiosemicarbazides] = 500 ppm; [HCl] = 1.0 mol dm^{-3}; Time= 3 hours.

Table 3.5: Half-life values (in hours, h) for the corrosion of mild steel in hydrazides.

System	10^3 k (h^{-1})	$t_{1/2}$ (h)
HCl	32.79 ± 0.141	21.13
HCl + DDH	4.61 ± 0.162	150.21
HCl + DH	8.80 ± 0.130	78.68
HCl + HDH	17.62 ± 0.214	39.31
HCl + ODH	20.76 ± 0.122	33.37

[Hydrazides] = 500 ppm; [HCl] = 1.0 mol dm^{-3}; Temp = 30° C

Table 3.6: Half-life values (in hours, h) for the corrosion of mild steel in thiosemicarbazides.

System	10^3 k (h^{-1})	$t_{1/2}$ (h)
HCl	32.79 ± 0.141	21.13
HCl + UPTS	2.09 ± 0.112	134.48
HCl + NPTS	5.80 ± 0.145	119.47
HCl + PPTS	6.62 ± 0.194	104.74
HCl + HPTS	8.20 ± 0.212	84.44

[Thiosemicarbazides] = 500 ppm; [HCl] = 1.0 mol dm^{-3}; Temp = 30°

Table 3.7: Electrochemical polarization parameters for the corrosion of mild steel in HCl containing hydrazides.

System	E_{corr} (mV)	I_{corr} (mA cm^{-2})	IE (%)
HCl	-461	0.360	-
HCl + DDH	-454	0.08	77.8
HCl + DH	-452	0.11	69.4
HCl + HDH	-456	0.13	63.9
HCl + ODH	-456	0.16	55.5

[Hydrazides] = 500 ppm; [HCl] = 1.0 mol dm^{-3}: Temp = 30° C.

Table 3.8: Electrochemical polarization parameters for the corrosion of steel inHCl containing thiosemicarbazides.

System	E_{corr} (mV)	I_{corr} (mA cm^{-2})	IE (%)
HCl	-461	0.360	-
HCl + UPTS	-497	0.025	94.44
HCl + NPTS	-508	0.072	80.12
HCl + PPTS	-493	0.082	77.07
HCl + HPTS	-495	0.100	72.05

[Thiosemicarbazides] = 500 ppm; [HCl] = 1.0 mol dm^{-3}; Temp = 30° C

Table 3.9: Dependence of electrochemical impedance parameters on [DDH] for mild steel in HCl.

System	R_t (ohm cm^2	C_{dl} ($\mu F\ cm^{-2}$)	IE (%)
0	36	1511.50	-
100	88.17	105.14	59.17
300	103.53	45.78	65.23
500	140.72	2.58	73.18

[HCl] = 1.0 mol dm^{-3}; Temp = 30° C.

Table 3.10: Dependence of electrochemical impedance parameters on [UPTS] for mild steel in HCl.

System	R_t (ohm cm^2	C_{dl} ($\mu F\ cm^{-2}$)	IE (%)
0	36	1511.50	-
100	157.38	769.72	77.12
300	208.69	708.96	82.74
500	286.95	501.87	87.45

[HCl] = 1.0 mol dm^{-3}; Temp = 30° C.

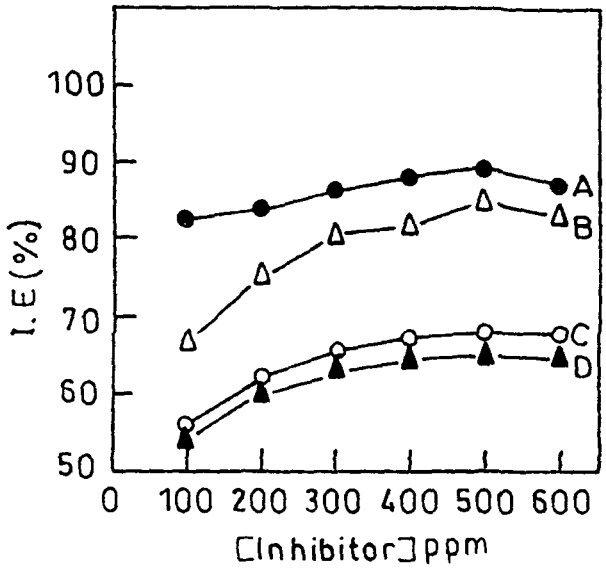

Fig 3.1 a. Plot of variation of inhibition efficiency on hydrazides concentration (●, DDH; Δ, DH; O, HDH; ▲, ODH).
Reaction conditions [HCl] =1.0 mol dm^{-3}, Temp =30°C, Time =3 hours.

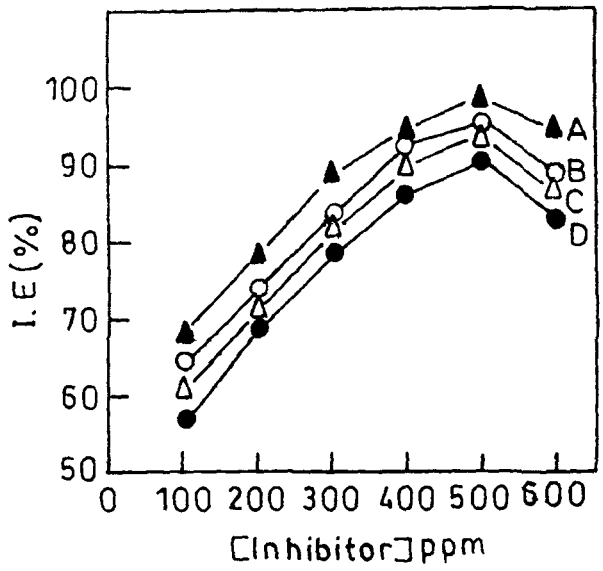

Fig 3.1 b. Plot of variation of inhibition efficiency on thiosemicarbazides concentration. (▲,UPTS; O, NPTS ; Δ, PPTS; ●,HPTS)
Reaction conditions [HCl] =1.0 mol dm^{-3}, Temp =30°C, Time =3 hours.

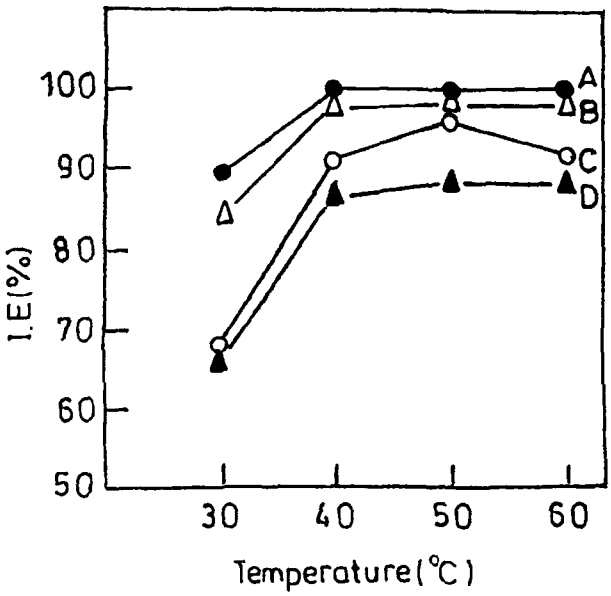

Fig 3.2 a. Plot of variation of inhibition efficiency on temperature for hydrazides (•, DDH; Δ, DH; O HDH; ▲, ODH).
Reaction conditions [HCl] =1.0 mol dm^{-3}, Time =3 hours, [inhibitor]=500 ppm.

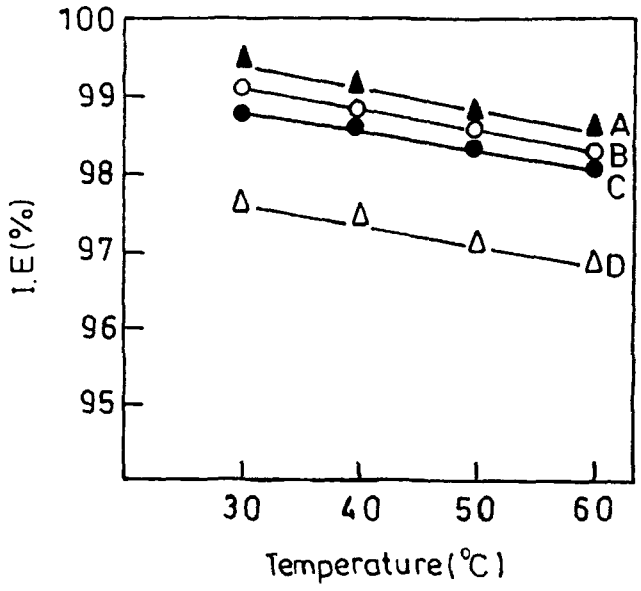

Fig 3.2 b. Plot of variation of inhibition efficiency on temperature for thiosemicarbazides (▲,UPTS; O, NPTS ; •, PPTS; Δ,HPTS)
Reaction conditions [HCl] =1.0 mol dm^{-3}, Time =3 hours, [inhibitor]=500 ppm.

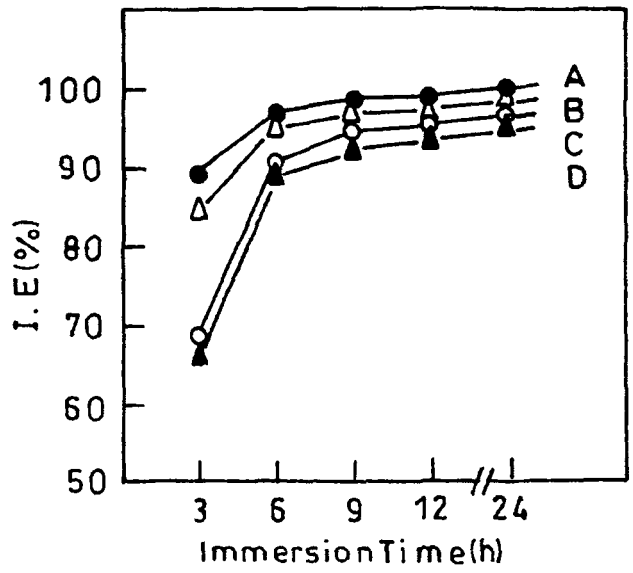

Fig 3.3 a. Plot of variation of inhibition efficiency on immersion time for hydrazides (•, DDH; Δ, DH; O, HDH; ▲, ODH).
Reaction conditions [HCl] =1.0 mol dm^{-3}, Temp =30°C, [inhibitor]=500 ppm.

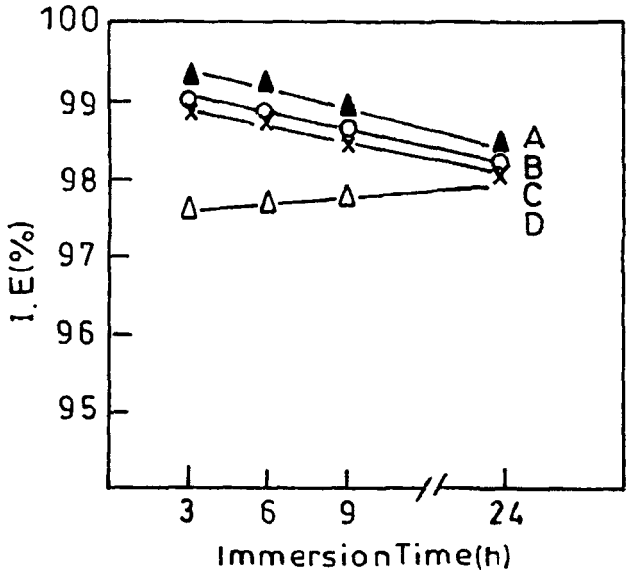

Fig 3.3 b. Plot of variation of inhibition efficiency on immersion time for thiosemicarbazides (▲,UPTS; O, NPTS ; **x**, PPTS; Δ,HPTS)
Reaction conditions [HCl] =1.0 mol dm^{-3}, Temp =30°C, [inhibitor]=500 ppm..

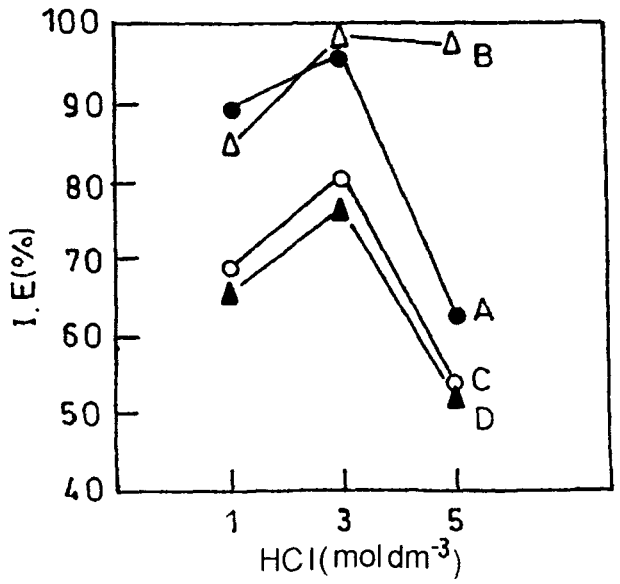

Fig 3.4 a. Plot of variation of inhibition efficiency on [HCl] for hydrazides (●, DDH; ; Δ, DH; O, HDH; ▲, ODH)

Reaction conditions [inhibitor]=500 ppm, Temp =30°C, Time =3 hours.

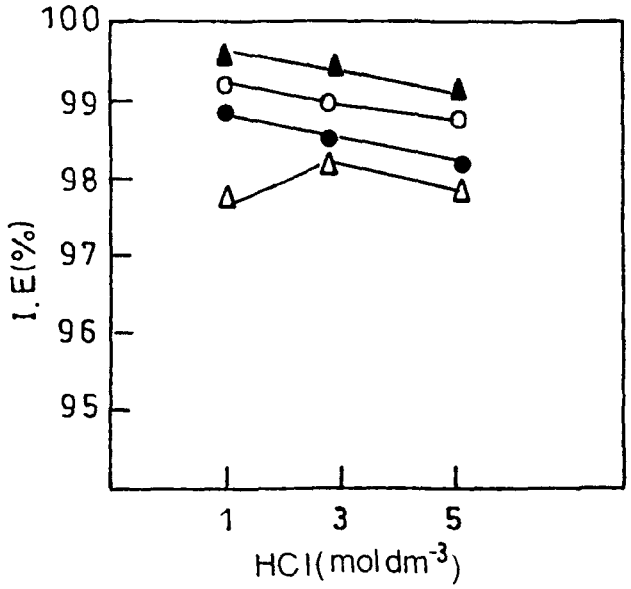

Fig 3.4 b. Plot of variation of inhibition efficiency for thiosemicarbazides [HCl] (▲,UPTS; O, NPTS ; ●, PPTS; Δ,HPTS).

Reaction conditions [inhibitor]=500 ppm, Temp =30°C, Time =3 hours.

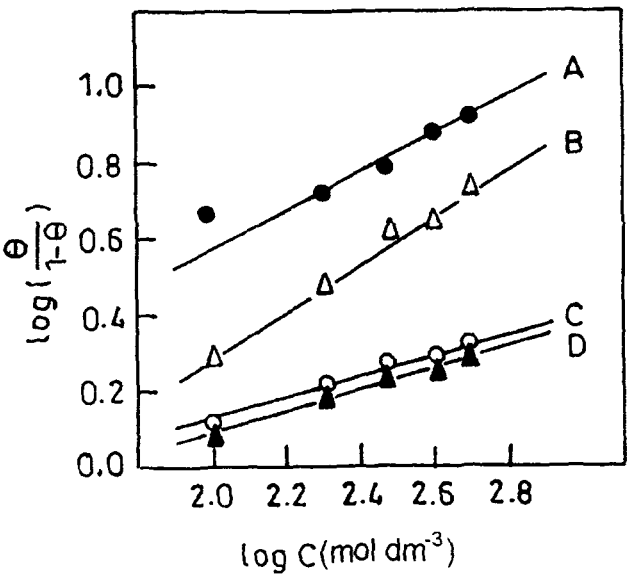

Fig 3.5 a. Langmuir s adsorption isotherm plots for hydrazides (•, DDH; Δ, DH; O, HDH; ▲, ODH).

Reaction conditions [HCl] =1.0 mol dm-3, Temp =30°C, Time =3 hours.

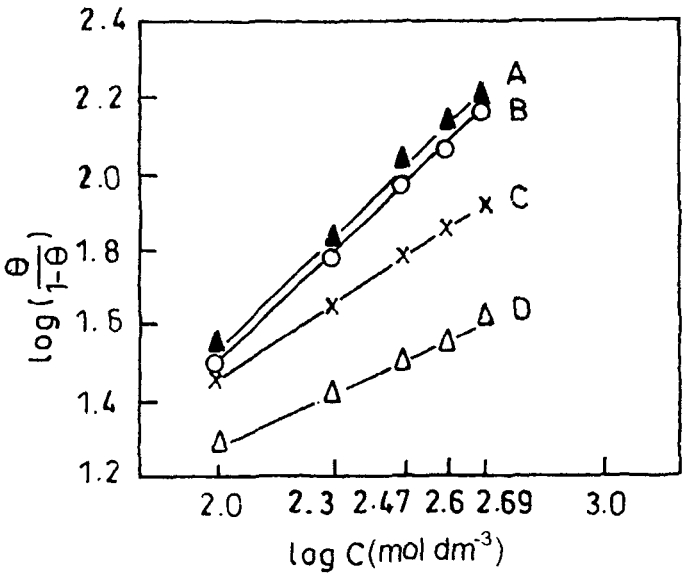

Fig 3.5 b. Langmuir s adsorption isotherm plots for thiosemicarbazides (▲,UPTS; O, NPTS ; x, PPTS; Δ,HPTS) [HCl] =1.0 mol dm-3, T =30°C.

Reaction conditions [HCl] =1.0 mol dm-3, Temp =30°C, Time =3 hours.

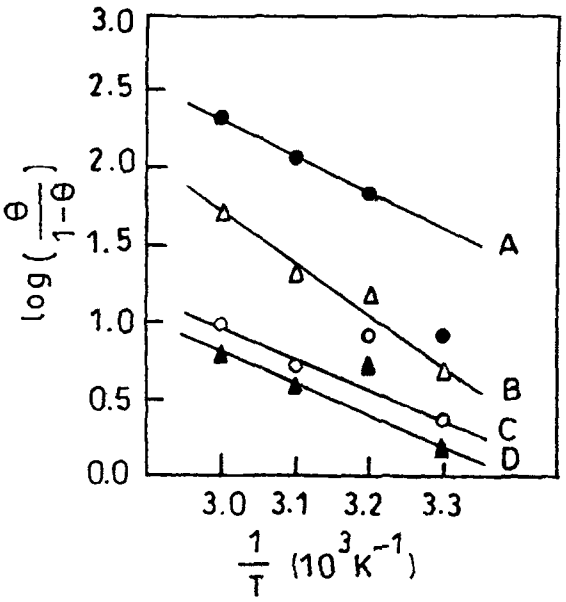

Fig 3.6 a. Adsorption isotherm plot for log (θ /1- θ) versus 1/T for hydrazides (•, DDH; Δ, DH; O, HDH; ▲, ODH)

Reaction conditions [HCl] =1.0 mol dm-3, Time =3 hours, [inhibitor]=500 ppm.

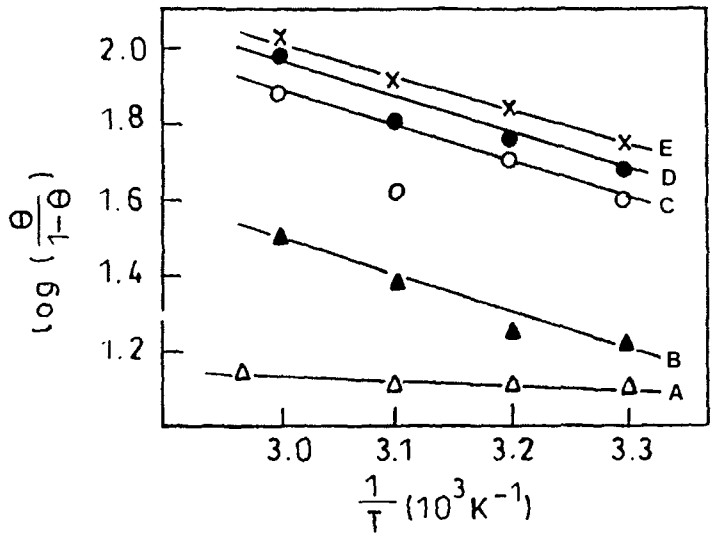

Fig 3.6 b. Adsorption isotherm plot for log (θ /1- θ) versus 1/T for thiosemicarbazides (▲,UPTS; O, NPTS ; **x**, PPTS; Δ,HPTS)

Reaction conditions [HCl] =1.0 mol dm-3, Time =3 hours, [inhibitor]=500 ppm.

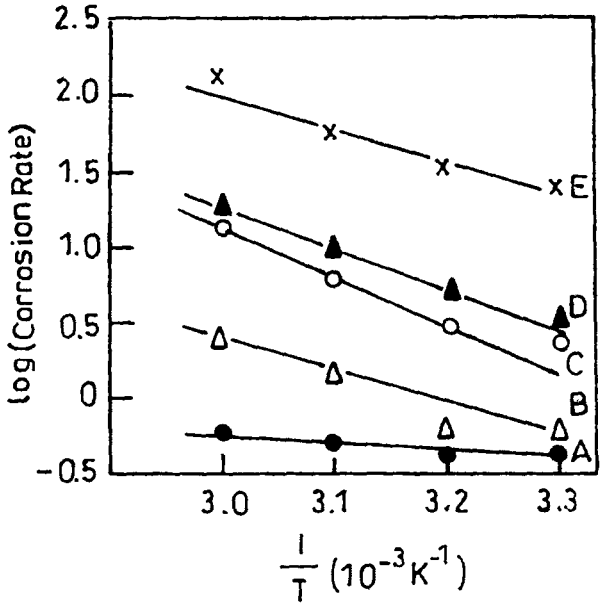

Fig 3.7 a. Adsorption isotherm plot for log (CR) versus 1/T for hydrazides (●,DDH; Δ, DH; ; o, HDH; ▲, ODH; **x**, Blank)
Reaction conditions [HCl] =1.0 mol dm^{-3}, Time =3 hours, [inhibitor]=500 ppm.

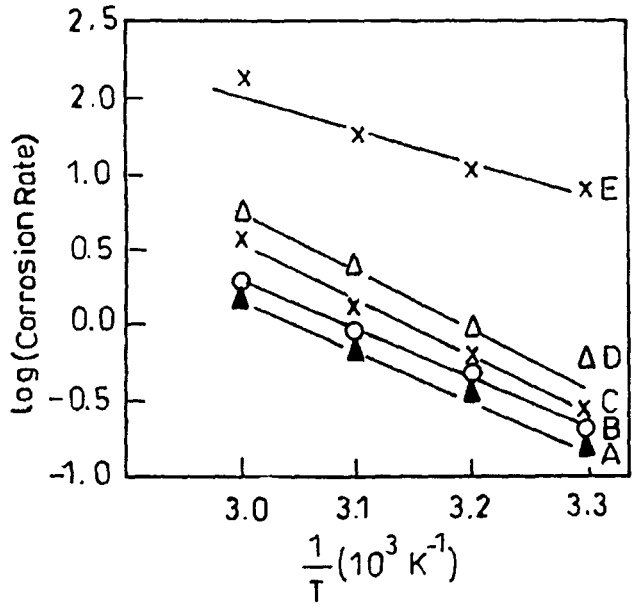

Fig 3.7 b. Adsorption isotherm plot for log (CR) versus 1/T for thiosemicarbazides (▲, UPTS; o,NPTS; **x.** PPTS; Δ, HPTS; **x**, Blank).
Reaction conditions [HCl] =1.0 mol dm^{-3}, Time =3 hours, [inhibitor]=500 ppm.

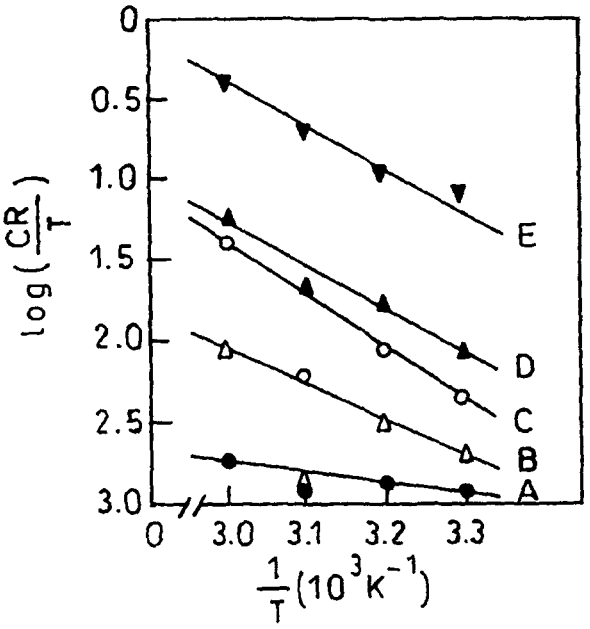

Fig 3.8 a. Adsorption isotherm plot for log (CR/T) versus 1/T for hydrazides (•,DDH; Δ, DH; ; o, HDH; ▲, ODH; ▼, Blank).

Reaction conditions [HCl] =1.0 mol dm-3, Time =3 hours, [inhibitor]=500 ppm.

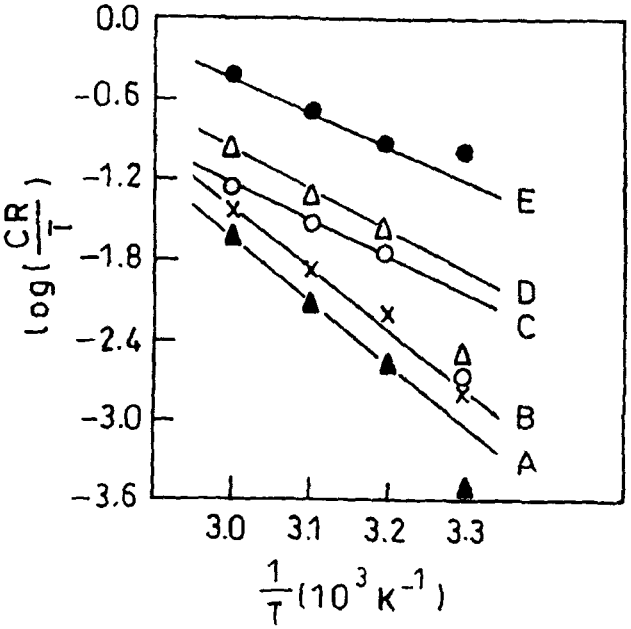

Fig 3.8 a. Adsorption isotherm plot for log (CR/T) versus 1/T for thiosemicarbazides (▲, UPTS; ▼, NPTS; o, PPTS; , Δ ODH; •, Blank)

Reaction conditions [HCl] =1.0 mol dm-3, Time =3hours, [inhibitor]=500 ppm.

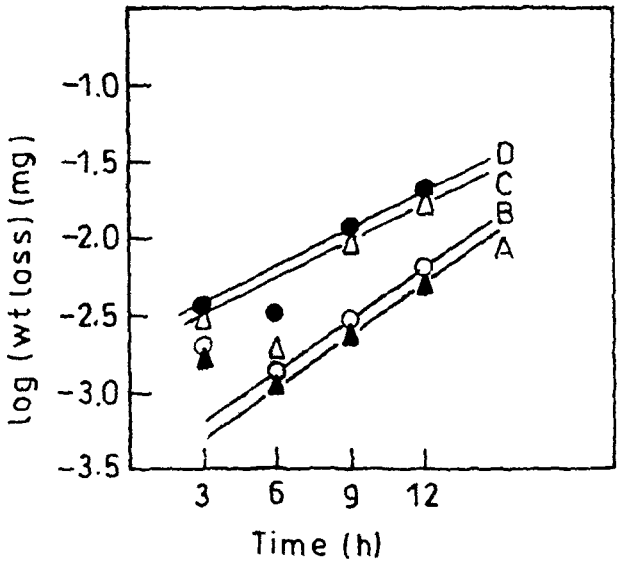

Fig 3.9 a. Plot of log (weight loss) versus immersion time for hydrazides (▲,DDH; o, DH; Δ, HDH; •,ODH)

Reaction conditions [HCl] =1.0 mol dm-3, [inhibitor]=500 ppm ,Temp =30°C.

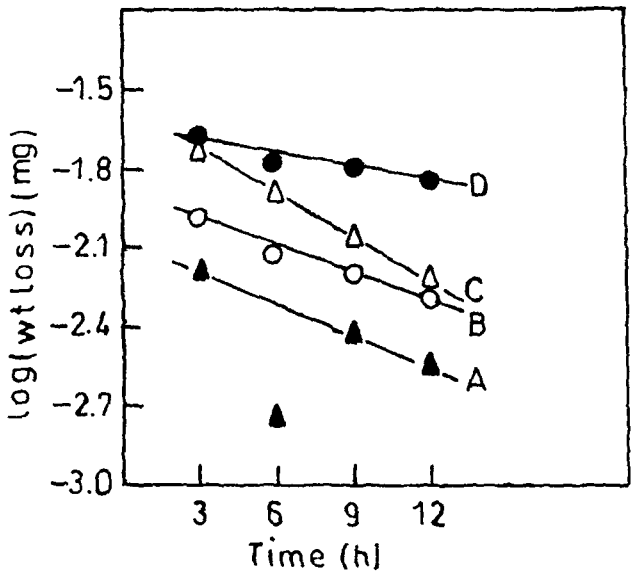

Fig. 3.9 b. Plot of Log (weight loss) versus immersion time for thiosemicarbazides(▲,UPTS; o, NPTS; Δ, PPTS; • ,HPTS)

Reaction conditions [HCl] =1.0 mol dm^{-3}, [inhibitor]=500 ppm ,Temp =30°C..

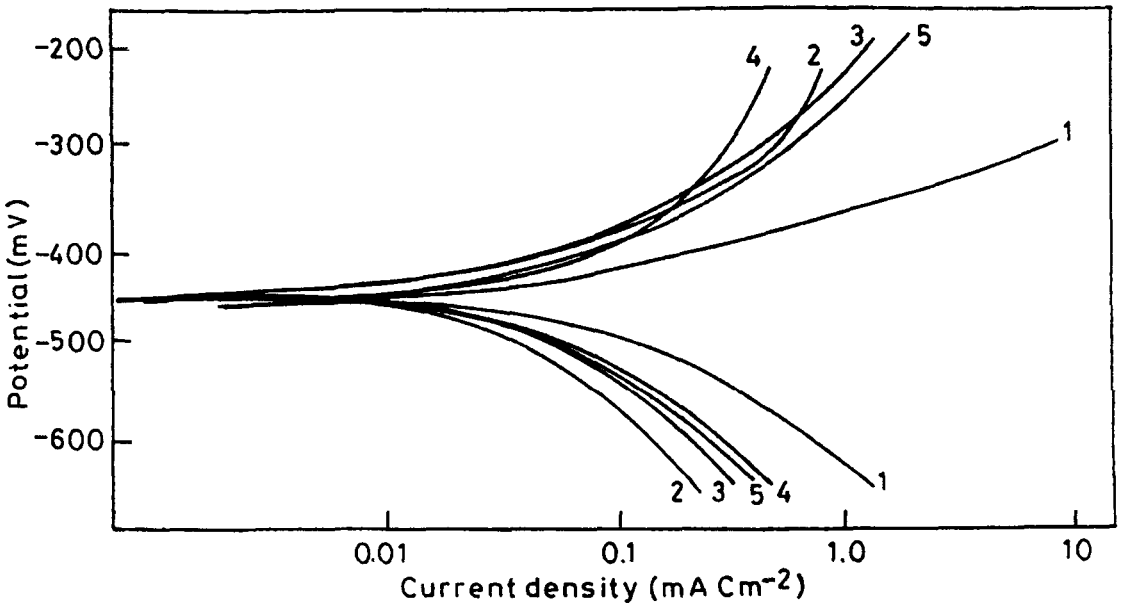

Fig 3.10 a. Potentiodynamic polarization curves for mild steel in presence of hydrazides (1) Blank (2) DDH (3) DH (4) ODH (5) HDH
Reaction conditions [HCl]= 1.0 mol dm^{-3}, Temp =30°C.

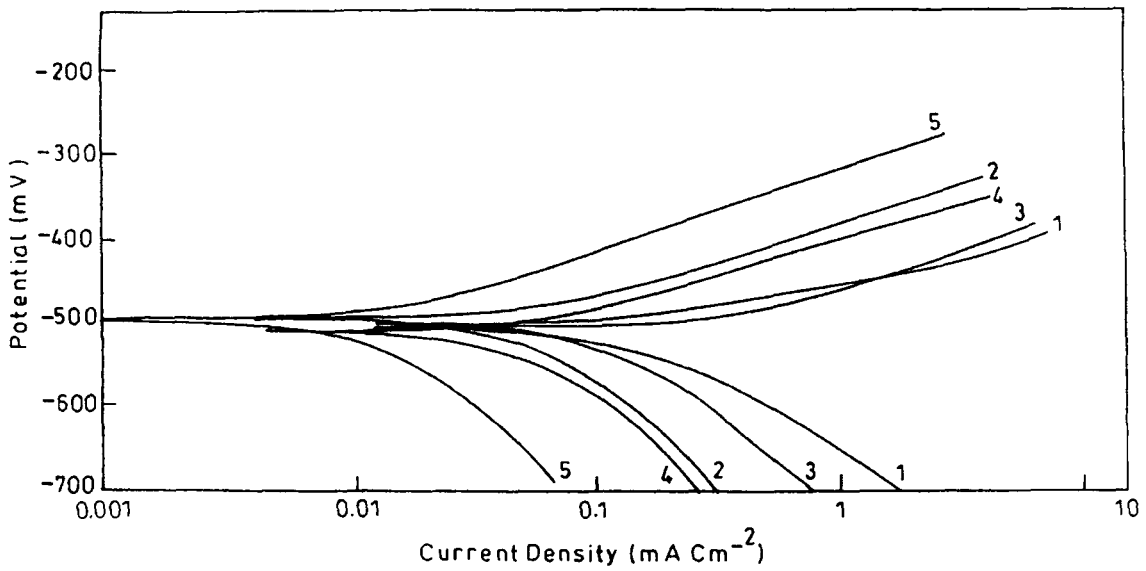

Fig 3.10 b. Potentiodynamic polarization curves for mild steel in presence of thiosemicarbazides on mild steel (1) Blank (2)HPTS (3) PPTS (4) NPTS (5) UPTS Reaction conditions [HCl]= 1.0 mol dm^{-3}, Temp =30°C.

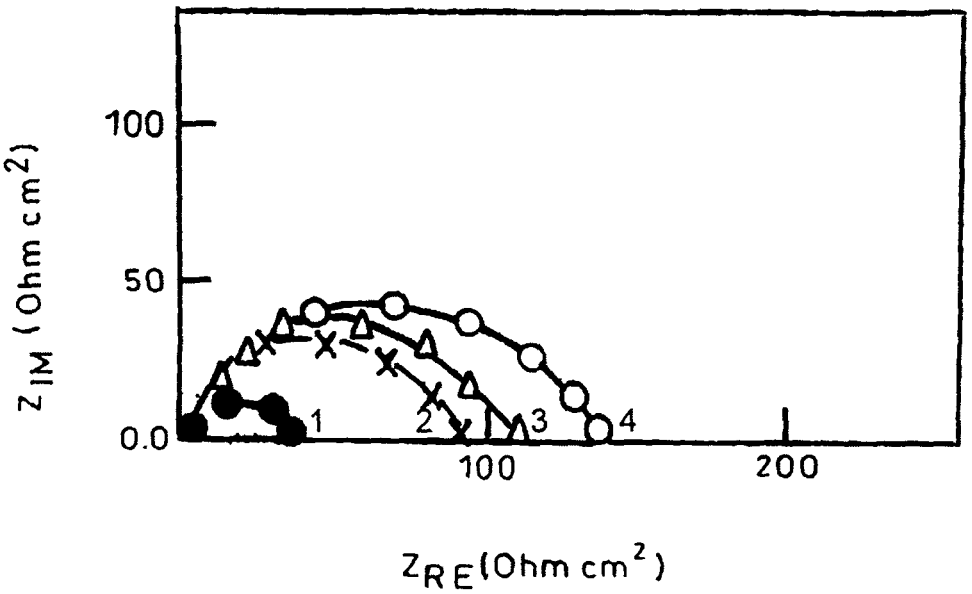

Fig 3.11 a. Nyquist plot of mild steel in 1.0 mol dm^{-3} HCl in the absence and presence of 100, 300 and 500 ppm of DDH (1) Blank (2) 100 ppm (3) 300 ppm (4) 500 ppm.

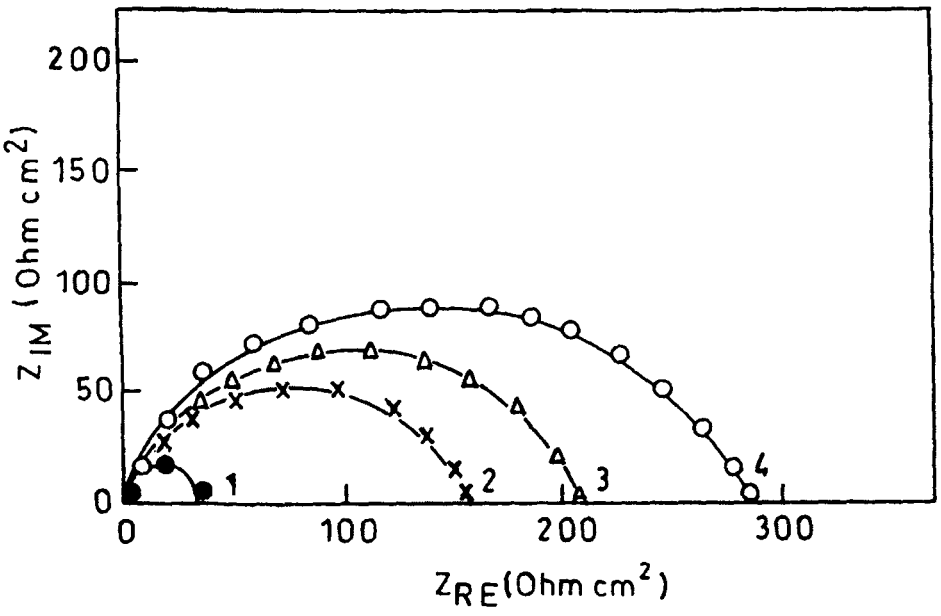

Fig 3.11 b. Nyquist plot of mild steel in 1.0 mol dm^{-3} HCl in the absence and presence of 100, 300 and 500 ppm of DDH (1) Blank (2) 100 ppm (3) 300 ppm (4) 500 ppm.

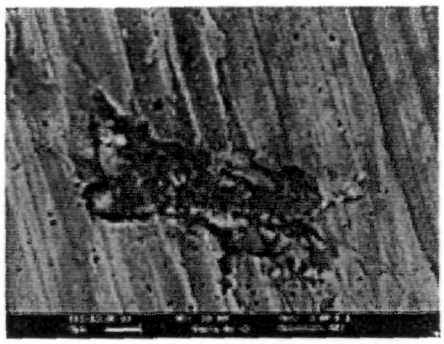

(a)

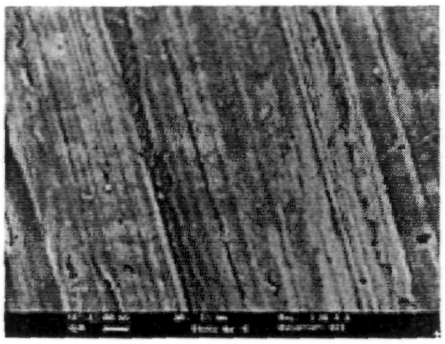

(b)

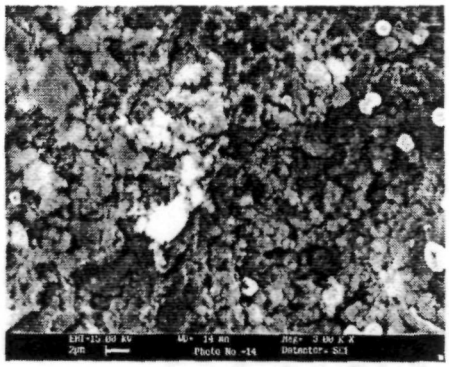

(c)

Figure 3.12. Scanning electron micrographs for mild steel surface in absence and presence of DDH (a) mild steel in 1·0 mol dm^{-3} HCl (b) polished mild steel and (c) mild steel in presence of DDH.

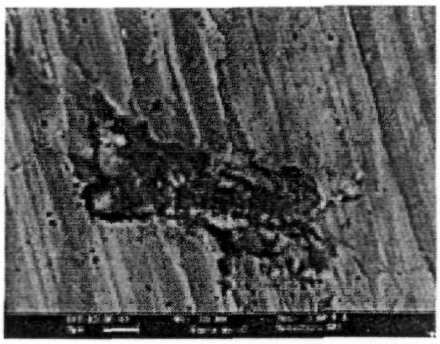

(a)

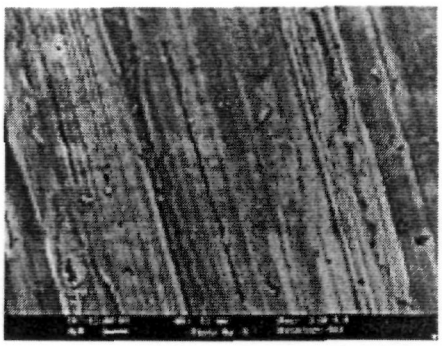

(b)

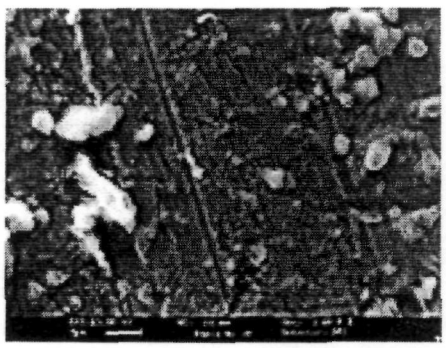

(c)

Fig 3.13. Scanning electron micrographs for mild steel surface in absence and presence of UPTS (a) mild steel in 1.0 mol dm^{-3} HCl (b) polished mild steel and (c) mild steel in presence of UPTS.

Chapter- 4
Corrosion inhibition behaviour of Imidazolines

Nitrogen-based organic compounds are found to be effective inhibitors for mild steel corrosion in acidic solutions [64,202-203]. The presence of lone pairs of electrons on the nitrogen atoms helps to delocalize the electrons and thus stabilizes the compound. The heterocyclic nitrogen are adsorbed to the metal surface through electrostatic interactions between the electron deficient nitrogen atom and the electron rich metal surface[204].

Imidazolines belong to the heterocyclic compounds containing five membered ring having two nitrogen atoms. The ability of imidazolines to form cations helps it to strongly adsorb on to negatively charged surface of metals[205]. They are used as corrosion inhibitors[206] in the oil well, oil pipeline protection and gas industry. Joseph *et al*[207]studied the adsorption of oleic imidazoline (1-(2-aminoethyl)-2(heptadec-8-enyl)-2-imidazoline) on mild steel surface. Imidazoline acts as a strong chemical anchor lying flat on the surface and hydrocarbon tail of oleic imidazoline acts as hydrophobic barrier between metal surface and solution and inhibits corrosion. The authors correlated the relationship between the structure of imidazolines and inhibition efficiency.

Y. Abboud *et al*[208] focused on the efficiency of non-toxic 2,2'-bis(benzimidazole), as steel corrosion inhibitor in hydrochloric acid by electrochemical techniques. The compound possessed fairly good inhibiting property for steel corrosion in hydrochloric acid, and behaves as a mixed inhibitor. The influence of 2-methyl-imidazole and benzimidazole on the corrosion of mild steel in 1N HCl and 1N H_2SO_4 through hydrogen permeation was studied by Muralidharan *et al*[41]. The inhibitors were effective in both 1N HCl and 1N H_2SO_4.

D. Wang and co-workers[209] investigated the corrosion inhibition behaviour of imidazoline derivatives with different electron releasing substituents as acid corrosion inhibitors for iron and steel. They proposed the relationship between the structure and inhibition efficiency. The electron donor substituents particularly the substituent group with conjugated system, introduced to imidazoline ring improved inhibition efficiency because it strengthen the chemical adsorption of the N atom on the metal surface.

Zhang *et al*[210] developed corrosion inhibitor containing imidazoline, non-ionic surfactant, cationic surfactant, ammonium citrate and water. The inhibitor capable of acid mist resistance and etching promotion was used in an HCl solution. They reported the inhibition efficiency 99.6% at 20°C.

This Chapter comprises the studies on the corrosion inhibiting properties of imidazoline derivatives such as 2-Undecyl-1,3 imidazoline (UDI), 2- Nonyl-1,3 imidazoline (NI) , 2- Pentadecyl-1,3 imidazoline (PDI, 2-Heptadecyl-1,3 imidazoline (HDI), 2-Heptyl-1,3 imidazoline (HI). The synthesized compounds were characterized and tested for inhibitive action on mild steel in hydrochloric acid by weight loss method, potentiodynamic polarization method and electrochemical impedance method. The observed results are presented and discussed herewith.

RESULTS AND DISCUSSION

4.1. Weight Loss Studies

The corrosion rate of mild steel in 1.0 mol dm^{-3} HCl was studied by monitoring the weight loss after a constant interval of time in the absence and presence of imidazolines. The temperature was kept constant at 30°C and the

immersion time was 3 hours. The corrosion rate and the inhibition efficiency were determined at different concentrations of imidazolines in the range from 100 to 600 ppm and are given in Table 4.1. The effect of variation in concentrations of inhibitor, solution temperature, acid concentration and immersion time on inhibition efficiency of imidazolines were studied and are presented in Figures 4.1- 4.4.

The imidazoline compounds inhibited the corrosion rate of mild steel in 1.0 mol dm^{-3} HCl solution, at different concentrations in the range 100 ppm – 600 ppm. It has been observed that the inhibition efficiency of these compounds increased with the increase in concentration of inhibitor as shown in Figure 4.1 and gave a maxima in the inhibition efficiency at 500 ppm inhibitor.

The variation of Inhibition efficiency on solution temperature is depicted in Figure 4.2. The inhibition efficiency of imidazolines increased with an increase in temperature from 30°C to 60°C. Thus the adsorption rate increases with increase in temperature and the inhibitive film formed on the metal surface becomes more protective in nature in this temperature range.

The variation of Inhibition efficiency of fatty acids imidazolines on immersion time is shown in Figure 4.3. No significant change in inhibition efficiency was observed with increase in immersion time from 3h to 24h which shows the persistency of the adsorbed fatty acid imidazolines over a longer test period on the metal surface.

The change in acid concentration from 1.0 mol dm^{-3} to 5.0 mol dm^{-3} does not cause any significant change in inhibition efficiency of these compounds as evident from the Figure 4.4. This study suggests that

imidazolines compounds behave as effective inhibitors in acid solution of these concentrations.

The value of weight loss at different initial concentrations of inhibitors in 1.0 mol dm^{-3} HCl was investigated at 30°C after 3 hour of immersion time. The data obtained from the weight loss studies were used to evaluate surface coverage (θ). The data were tested graphically by fitting to various isotherms. A straight line was obtained on plotting log (θ /1-θ) *versus* log C (Figure 4.5) suggesting that the adsorption of the imidazolines on mild steel surface follows Langmuir's adsorption isotherm. The values of the heat of adsorption (Q) were obtained from the slope of the plots of log (θ/1-θ) *versus* 1/T (Figure 4.6) for imidazolines, and the values are given in Table 4.2. The obtained values of Q obtained suggest the physical nature of adsorption.

A number of experiments were performed at different temperatures in the ranging from 30°C to 60°C at fixed concentrations of acid (1 mol dm^{-3}) and inhibitor (500 ppm). The immersion period was 3h and the corrosion rate was determined at temperatures 30°C, 40°C, 50°C and 60°C. Log (corrosion rate) *versus* 1/T was plotted (Figure 4.7) and the slope of the plot gave the values of E_a. The values of activation energy (E_a) obtained from the slope of the plot for imidazolines are given in Table 4.2. To obtain the values of ΔH and ΔS for the adsorption of imidazolines in presence of HCl on the mild steel surface, logarithm of (CR /T) was plotted against 1/T. The slope and intercept of plot (Figure 4.8) gave the values of ΔH and ΔS respectively and the values are listed in Table 4.2.

The lower change in enthalpies, ΔH in presence of imidazolines signify the net values at rate determining step for the corrosion reactions as well as the adsorption of imidazolines at the mild steel surface. The lowering[163] in the values of ΔH in the presence of imidazolines may be due to the energy released during the adsorption of imidazolines on mild steel surface. It is evident from the fact that the presence of imidazolines reduces the corrosion rate and increases the inhibition efficiency. The values of entropy of activation ΔS in the absence and presence of imidazolines are negative and large[188]. This indicates that the activated complex formed during the corrosion and adsorption processes is an associative in nature rather than dissociative step. Therefore, a decrease in disorderness takes place during the transformation from reactants to the activated complex [187].

The change in free energy of adsorption (ΔG_{ads}) were calculated[190] using the equations given in the experimental. The values are listed in Table 4.2. The lower values of ΔG_{ads} indicate that imidazoline of fatty acid are physically adsorbed on the metal surface[191]. It also indicate that the spontaneous nature of adsorption of inhibitor on the surface of mild steel[192].

In order to determine the dependency of the corrosion rate on the activity of mild steel, a number of experiments were performed in which weight losses were monitored as a function of immersion time. The concentrations of HCl, inhibitors were kept constant at 1 mol dm^{-3} and 500 ppm, respectively at 30°C. A straight line was obtained for the plot of log (weight loss) *versus* immersion time as depicted in Figure 4.9, showing that the reaction obeyed first order kinetics. The rate constant was calculated using the first order rate equation[164].

The half life ($t_{1/2}$) values were calculated using following relationship:

$t_{1/2} = 0.693 / k$

The values of the rate constant and half life period ($t_{1/2}$) obtained in the absence and presence of imidazolines are summarized in Table 4.3. The half life ($t_{1/2}$) values indicate the durability of inhibitor film on the mild steel surface under the studied conditions[193].

4.2 Potentiodynamic Polarization Studies

The cathodic and anodic polarization curves were obtained for mild steel in 1.0 mol dm^{-3} in the absence and presence of different inhibitors at 500 ppm concentration at 30±1 °C and are shown in Figure 4.10.

Electrochemical parameters such as corrosion current density (I_{corr}), corrosion potential (E_{corr}) and inhibition efficiency (IE) were calculated from Tafel plots and these values are given in Table 4.4.

The values of I_{corr} decreased significantly in the presence of imidazolines. Maximum decrease in I_{corr} was observed for UDI. All the imidazolines did not show any significant change in E_{corr} values suggesting that these compounds behaves as mixed type inhibitors i.e., they retard the corrosion reaction by blocking both anodic and cathodic sites of the metal[194].

4.3. Electrochemical Impedance Studies

Table 4.5 include the results of impedance studies carried out at different concentration of UDI in 1.0 mol dm^{-3} HCl at 30±1 °C.The results are shown in Figure 4.11 for Nyquist plots in the presence of 100, 300 and 500 ppm of UDI. The Nyquist plots are not perfect semicircles and this difference has been attributed to frequency dispersion[195]. The values of R_t and C_{dl} were

calculated from Nyquist plots[157]. The percentage inhibition efficiency was calculated from the following equation[196].

$$\% \text{ I.E.} = \frac{1/R_{to} - 1/R_{ti}}{1/R_{to}} \times 100$$

The values of R_t, C_{dl} and inhibition efficiency are given in Table 4.5. R_t values increases with increase in inhibitor concentration (UDI) and, in turn, it leads to an increase in inhibition efficiency. The addition of UDI to 1.0 mol dm^{-3} HCl lowers the C_{dl} values, which shows that the inhibition in corrosion may be due to surface adsorption of the inhibitor [197].

4.4. Scanning Electron Microscopy

Scanning electron microscopy were performed for the mild steel surface after dipping it in solution containing HCl; and HCl and UDI (Figure 4.12). The surface of mild steel immersed in inhibited solution was found to be smoother than that in blank 1.0 mol dm^{-3} HCl. This observation suggest that the inhibitor is adsorbed to the metal surface, forms a protective layer and prevent the attack of acid on metal surface[198].

4.5. Mechanism of corrosion inhibition

Inhibition of corrosion of mild steel in the acidic solutions by the fatty acid imidazolines can be explained on the basis of molecular adsorption. The molecules of these compounds are adsorbed on the metal surface through π-electrons of aromatic ring and lone pair of electrons of N atoms and blocks the surface[199]. The presence of long hydrophobic chain keeps the acid solution away from metal surface due to its hydrophobic nature. Thus, the surface is protected from the wetting process by aggressive solution. Among the

compounds investigated in the present study, the order of inhibition efficiency has been found to be in the following order:

UDI > NI > PDI > HDI > HI

(C_{11}) (C_9) (C_{15}) (C_{17}) (C_7)

The inhibition efficiency increased with the increase in chain length up to C_{11} (UDI), however, a further increase in chain length (C_{17}) resulted into decreased inhibition efficiency [200].

Table 4.1 Dependence of corrosion rate and inhibition efficiency on [Imidazolines].

Inhibitor Used	Concentration (ppm)	Weight loss (mg)	IE (%)	CR (mmpy)
UDI	0	68.1	-	25.31
	100	23.6	65.23	8.80
	200	16.7	75.12	6.29
	300	9.9	85.32	3.71
	400	6.3	90.61	2.37
	500	1.1	98.31	0.42
	600	8.5	87.46	3.17
NI	0	68.1	-	25.31
	100	24.8	63.57	9.22
	200	19.6	71.12	7.30
	300	12.0	82.27	4.48
	400	8.1	88.10	3.01
	500	2.7	96.03	1.00
	600	9.1	86.34	3.45
PDI	0	68.1	-	25.31
	100	29.3	60.10	10.91
	200	22.4	67.40	8.34
	300	14.7	78.31	5.48
	400	10.0	85.22	3.74
	500	4.0	93.99	1.52
	600	10.2	84.98	3.80
HDI	0	68.1	-	25.31
	100	27.9	59.01	10.93
	200	24.9	63.41	9.26
	300	16.8	75.20	6.27
	400	10.3	84.81	3.84
	500	6.0	90.87	2.30
	600	14.5	78.62	5.41
HI	0	68.1	-	25.31
	100	29.4	56.80	10.93
	200	27.1	60.90	10.10
	300	18.7	72.50	6.96
	400	12.3	81.93	4.57
	500	9.6	85.80	3.59
	600	16.8	75.32	6.24

[HCl] = 1.0 mol dm^{-3}, Temp = 30 °C, Immersion time = 3 hour

Table 4.2. Thermodynamic activation parameters for corrosion of mild steel in the absence and presence of imidazolines.

System	E_a (kJ mol^{-1})	ΔH (kJ mol^{-1})	ΔS (J $mol^{-1}K^{-1}$)	ΔG_{ads} (kJ mol^{-1})	-Q (kJ mol^{-1})
1N HCl	51.18	48.56	200.40	-	-
UDI	23.71	26.35	203.73	38.41	23.66
NI	24.76	27.40	202.20	37.12	23.04
PDI	23.77	32.42	196.75	36.25	18.08
HDI	29.75	32.39	192.43	35.81	18.62
HI	30.73	33.37	186.19	32.10	17.40

[Imidazolines] = 500 ppm; [HCl] = 1.0 mol dm^{-3}

Table 4.3. Half-life values (in hours h) for the corrosion of mild steel in imidazolines.

System	10^3 k (h^{-1})	$t_{1/2}$ (h)
HCl	32.79± 0.141	21.13
HCl + UDI	3.83± 0.221	180.93
HCl + NI	5.41± 0.201	128.00
HCl + PDI	10.78± 0.187	64.28
HCl + HDI	11.95±0.156	57.99
HCl + HI	14.83±0.134	49.89

[Imidazolines] = 500 ppm; [HCl] = 1.0 mol dm^{-3}; Temp = 30° C

Table 4.4. Electrochemical polarization parameters for the corrosion of mild steel in HCl containing Imidazolines.

System	E_{corr} (mV)	I_{corr} (mA cm^{-2})	IE (%)
HCl	-461	0.360	-
HCl + UDI	-480	0.033	90.83
HCl + NI	-476	0.037	89.72
HCl + PDI	-466	0.085	76.38
HCl + HDI	-479	0.120	66.66
HCl + HI	-493	0.150	58.33

[Imidazolines] = 500 ppm; [HCl] = 1.0 mol dm^{-3}; Temp = 30° C

Table 4.5. Dependence of electrochemical impedance parameters on [UDI] for mild steel in HCl.

System	R_t (ohm cm^2	C_{dl} (μF cm^{-2})	IE (%)
0	36	1511.50	-
100	86.95	946.84	58.48
300	141.30	776.92	74.45
500	304.34	315.22	88.13

[HCl] = 1.0 mol dm^{-3}; Temp = 30° C.

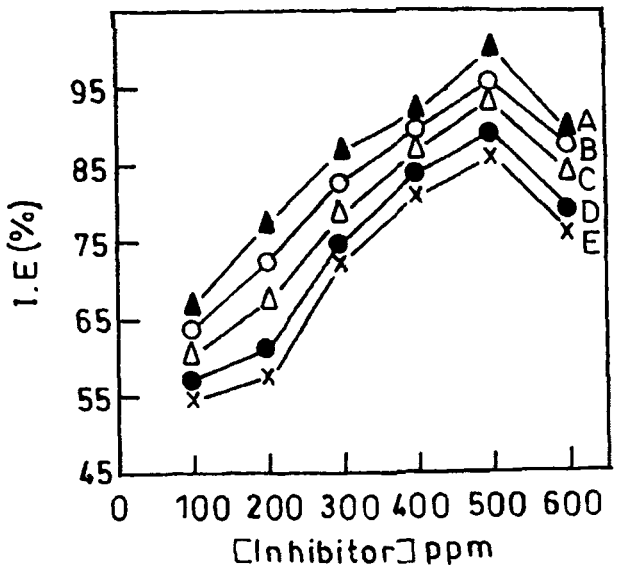

Fig 4.1. Plot of variation of inhibition efficiency on concentration for imidazolines (▲,UDI; o, NI ; Δ,PDI; •, HDI; **x**, HI)
Reaction conditions [HCl] =1.0 mol dm^{-3}, Temp =30°C, Time =3 hours.

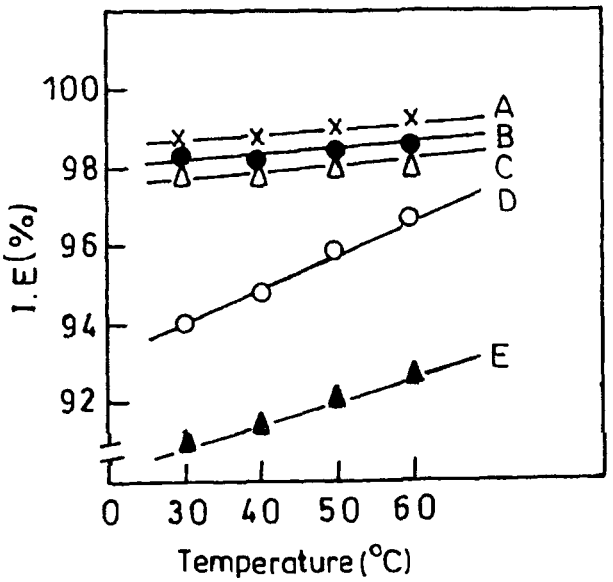

Fig 4.2. Plot of variation of inhibition efficiency on temperature for imidazolines (**x**,UDI; •, NI ; Δ,PDI; o , HDI; ▲, HI).
Reaction conditions [HCl] =1.0 mol dm^{-3}, Time =3 hours, [inhibitor]=500 ppm.

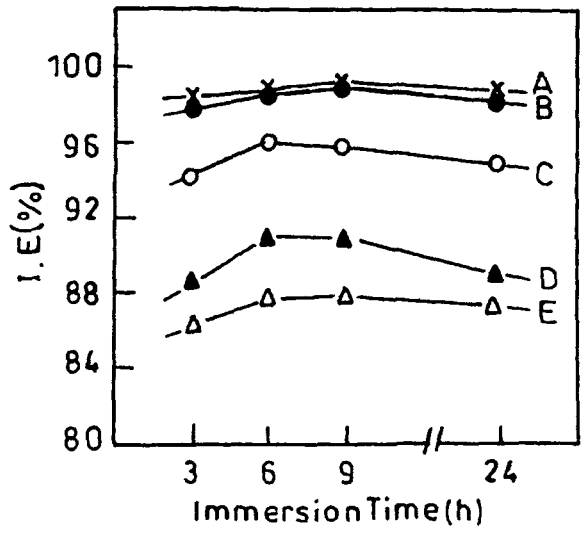

Fig 4.3. Plot of variation of inhibition efficiency on immersion time for imidazolines (**x**,UDI; •, NI ; **Δ**,PDI; O , HDI; **▲**, HI).
Reaction conditions [HCl] =1.0 mol dm^{-3}, Temp =30°C, [inhibitor]=500 ppm.

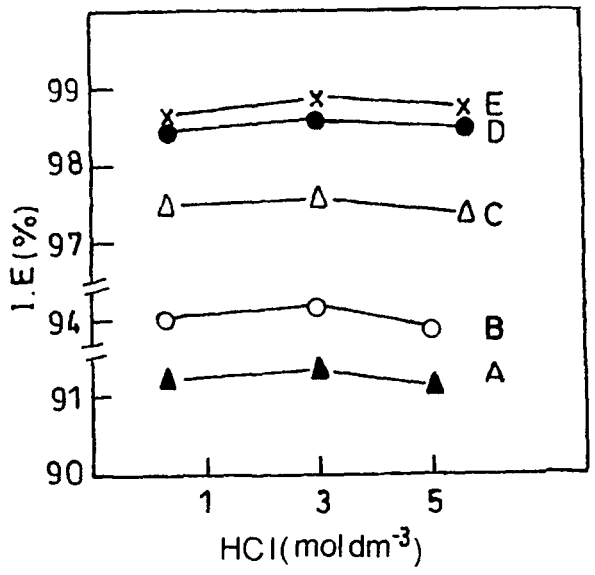

Fig 4.4. Plot of variation of inhibition efficiency on [HCl] for imidazolines (**▲**,UDI; O, NI ; **Δ**, PDI; •,HDI; **x**, HI).
Reaction conditions [inhibitor]=500 ppm, Temp =30°C, Time =3 hours

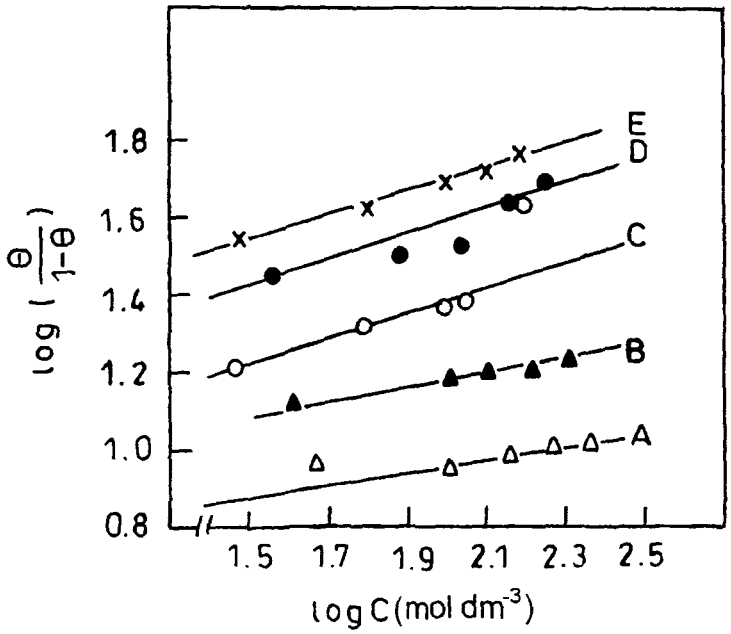

Fig 4.5. Langmuir s adsorption isotherm plots for imidazolines (Δ ,UDI; ▲, NI; o, PDI; •, HD; **x**,HI)

Reaction conditions [HCl] =1.0 mol dm^{-3}, Temp =30°C, Time =3 hours.

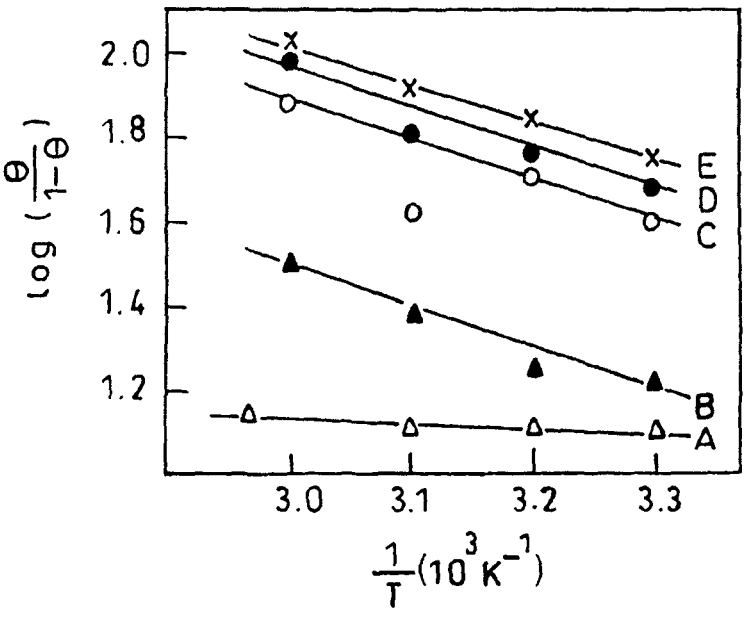

Fig 4.6. Adsorption isotherm plot for log (θ /1- θ) versus 1/T for imidazolines (Δ ,UDI; ▲, NI; o, PDI; •, HD; **x**,HI)

Reaction conditions [HCl] =1.0 mol dm^{-3}, Time =3 hours, [inhibitor]=500 ppm.

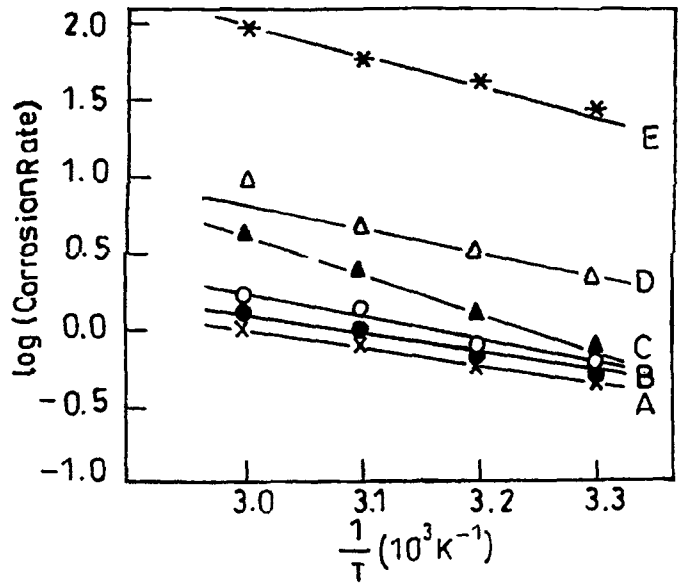

Fig 4.7. Adsorption isotherm plot for log (CR) versus 1/T for imidazolines (**x** ,UDI; •, NI; o, PDI; ▲, HD; Δ,HI; *, Blank)

Reaction conditions [HCl] =1.0 mol dm^{-3}, Time =3 hours, [inhibitor]=500 ppm.

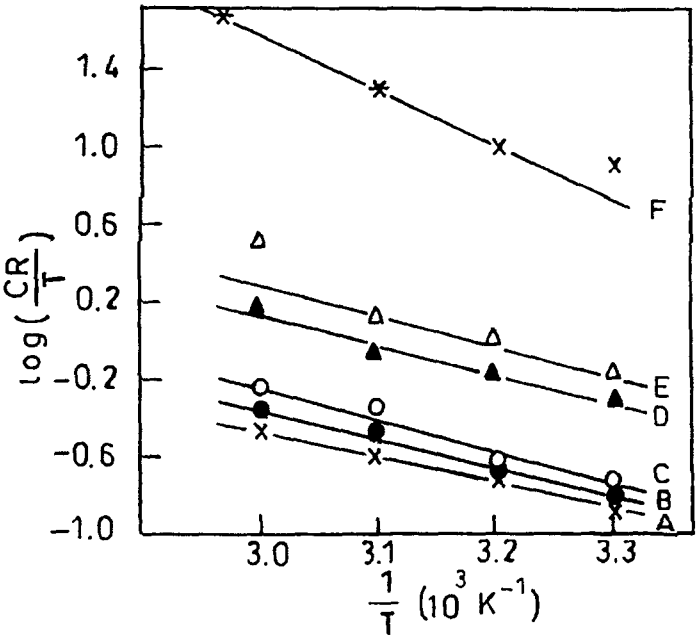

Fig 4.8. Adsorption isotherm plot for log (CR/ T) versus 1/T for imidazolines (**x** ,UDI; •, NI; o, PDI; ▲, HD; Δ,HI; *, Blank)

Reaction conditions [HCl] =1.0 mol dm^{-3}, Time =3 hours, [inhibitor]=500 ppm.

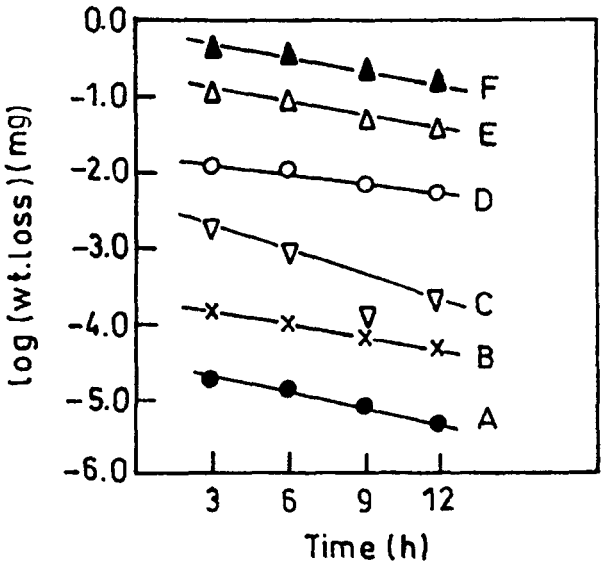

Figure 4.9. Plot of log (weight loss) versus immersion time for imidazolines (● ,UDI; **x**, NI; ▼, PDI; o, HD; Δ,HI; ▲, Blank).
Reaction conditions [HCl] =1.0 mol dm^{-3}, [inhibitor]=500 ppm ,Temp =30°C.

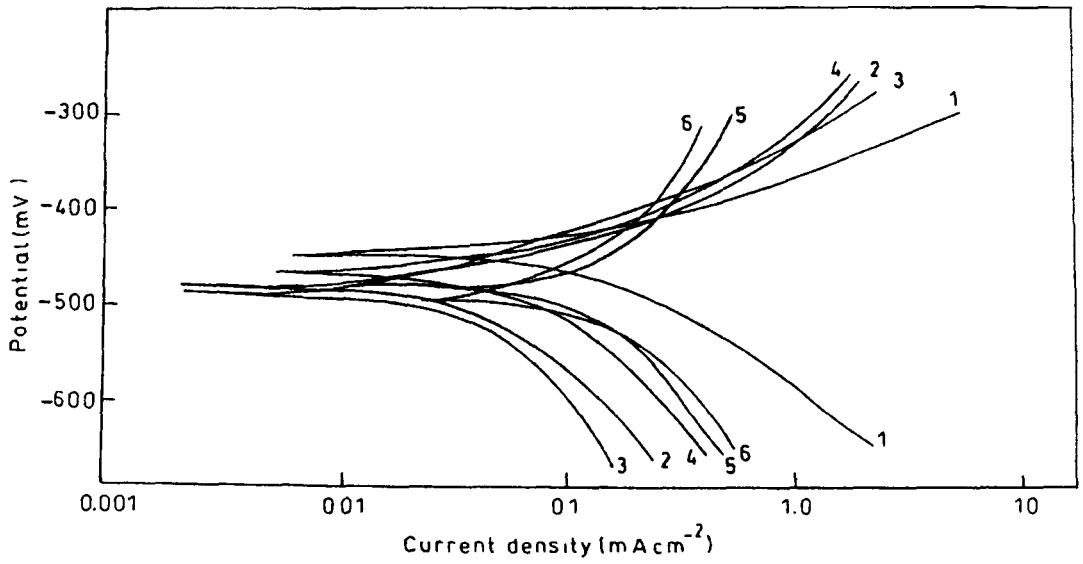

Figure 4.10. Potentiodynamic polarization curves for mild steel in presence of imidazolines (1) Blank 2) NI (3) UDI (4) PDI (5) HDI (6) HI.
Reaction conditions[HCl]= 1.0 mol dm^{-3}, Temp =30°C.

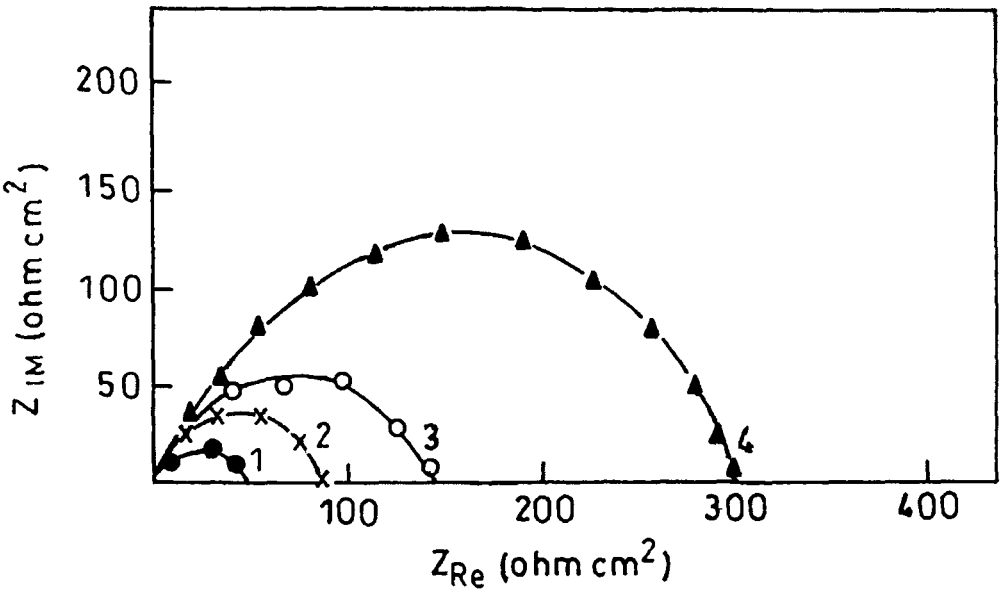

Fig 4.11. Nyquist plot of mild steel in 1.0 mol dm^{-3} HCl in the absence and presence of 100, 300 and 500 ppm of UDI (1) Blank (2) 100 ppm (3) 300 ppm (4) 500 ppm.

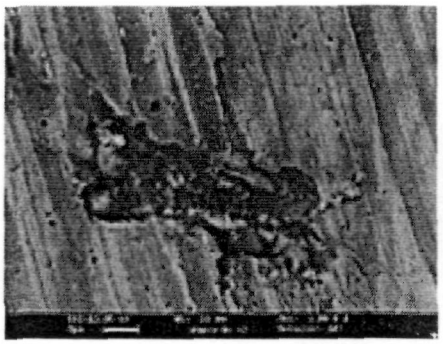

(a)

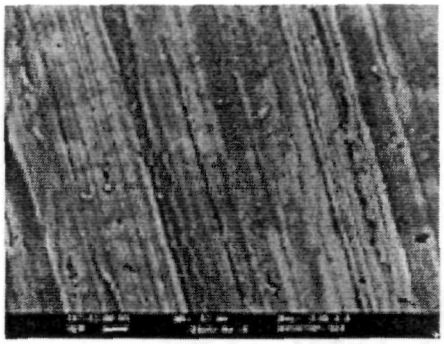

(b)

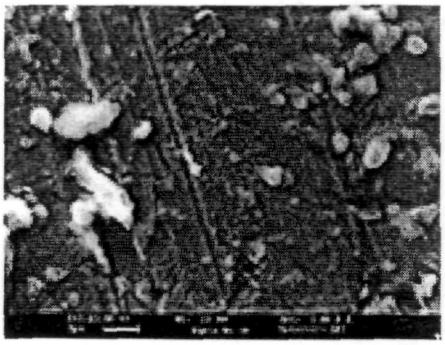

(c)

Figure 4.12. Scanning electron micrographs for mild steel surface in absence and presence of UDI (a) mild steel in 1.0 mol dm^{-3} HCl (b) polished mild steel and (c) mild steel in presence of UDI.

Chapter- 5
Corrosion inhibition behaviour of Triazoles & Oxadiazoles

Fatty acid Triazoles and oxadiazoles are medicinally important heterocyclic molecules, which have been reported to exhibit wide range of biological activities[211-212]. Azoles are excellent corrosion inhibitors for copper[213-214], zinc[215], bronze[216] and steel[217-222]. Triazoles[223-226] and Oxadiazoles[227-230] act as corrosion inhibitors by adsorbing on the metal surface through nitrogen, sulfur, multiple bonds or aromatic rings and block the active sites thereby decreasing the corrosion rate. Triazoles are effective corrosion inhibitors in acidic media[231-232].The substituted N-atoms increase the inhibition efficiency may be due to increase in electron density or blocking the metal surface by stearic hindrance[233].

The inhibitive performance of benzotriazole on the corrosion of stainless steel was studied by Niu *et al*[234] in acidic chloride solution. They studied by using potentiodynamic polarization, electrochemical impedance, spectroscopy and scanning electron microscopy. The inhibitive action was observed due to the blocking of anodic and cathodic sites. The inhibitive effects of 1(benzyl) 1-H-4, 5-dibenzoyl-1, 2, 3-triazole on mild steel in 1% HCl was investigated by Abdennabi *et al* [218-219]. The corrosion rate of mild steel was reduced by > 95% in the presence of 50 ppm inhibitor. Mernari *et al*[235] investigated the corrosion inhibition behaviour of 3, 5-bis (n-pyridyl)-4-amino-1, 2, 4-triazoles on mild steel in 1M HCl. The inhibitive effect of 3, 5-bis-(2-thienyl)-4-amino-1,2,4-triazole on mild steel in 1M HCl and 0.5 M H_2SO_4 was investigated by Bentiss *et al* [82] using weight loss and electrochemical impedance spectroscopy. The electrochemical study revealed that this compound behaves as an anodic inhibitor. They observed that these molecules are strongly adsorbed on the metal surface and suppress its

dissolution reaction. The adsorption leads to the formation of a protective film which grows with increasing exposure time. The influence of some substituted fatty acid triazoles on the corrosion rate of mild steel in 1M HCl and 0.5 M H_2SO_4 was studied by Quraishi *et al* [236]

Bentiss et al[237] synthesized substituted 1, 3, 4-oxadiazole such as 2, 5-bis (2-pyridyl)-1, 3, 4-oxadiazole and 2, 5-bis (2-hydroxyphenyl)-1, 3, 4-oxadiazole and studied their inhibitive action on the corrosion of mild steel in 1M HCl and 0.5 M H_2SO_4. 2, 5-bis (2-hydroxyphenyl)-1, 3, 4-oxadiazole showed more inhibition efficiency than 2, 5-bis (2-pyridyl)-1, 3, 4-oxadiazole due to the presence of an electron releasing -OH group in the aromatic ring at ortho position. These oxadiazoles were found to perform better inhibition characteristics in both acids and the performance was further enhanced in the case of HCl, due to synergistic inhibition.

The present chapter describes the synthesis of aliphatic triazoles and aromatic and aliphatic oxadiazoles and their inhibitive action. The inhibitive behaviour of these compounds on mild steel in 1.0 mol dm^{-3} HCl were investigated by weight loss, potentiodynamic polarization and electrochemical impedance method. Scanning electron spectroscopy techniques have also been perormed for surface characterization of the inhibited mild steel coupons. The observed results are discussed herewith.

RESULTS AND DISCUSSION

5.1. Weight Loss Studies

The corrosion rate of mild steel in 1.0 mol dm^{-3} HCl was studied by monitoring the weight loss after immersion of steel coupon for a fixed interval

of time (3 h) in the absence and presence of aliphatic triazoles and aromatic and aliphatic oxadiazoles. The temperature was kept constant at 30°C. The corrosion rate and the inhibition efficiency were determined at different concentrations of triazoles and oxadiazoles and are reported in Tables 5.1-5.2.

It has been found that triazoles and oxadiazoles decreased the rate of corrosion of mild steel in HCl solution, at all concentrations used in this study ranging from 100 ppm to 600 ppm. It has also been observed that the inhibition efficiency of these compounds increased with the increase in concentration upto 500 ppm and, thereafter, the inhibition efficiencies decreased with increase in [inhibitor]. Thus, the inhibitor displayed maximum inhibition efficiency at 500 ppm concentration for triazoles and oxadiazoles as presented in Figures 5.1 a - 5.1 b. Different experiments were performed at various temperatures in the range of 30°C to 60°C at fixed concentration of acid (1.0 mol dm^{-3}) and inhibitor (500 ppm). The immersion period was 3h and the corrosion rate was determined at temperatures 30°C, 40°C, 50°C and 60°C. The variation of inhibition efficiency with solution temperature is shown in Figures 5.2.a -5.2.b. The inhibition efficiency for all tested fatty acid triazoles decreased slightly with increase in temperature from 30°C to 60°C, showing that desorption rate of the inhibitor molecules from metal surface becomes higher at higher temperatures[182]. The inhibition efficiency for oxadiazoles inhibitors does not change significantly with increase in temperature from 30°C to 60°C indicating that the formation of inhibitive film formed on the metal surface is protective in nature in this temperature range.

In order to determine the dependency of the corrosion rate on immersion time, a number of experiments were performed in which weight losses were monitored as a function of immersion time. The concentrations of HCl, inhibitor were kept constant at 1 mol dm^{-3} and 500 ppm, respectively at 30°C. Triazole showed a significant decrease in inhibition efficiency with the increase in immersion time from 3h to 24h as shown in Figure 5.3.a. The oxadiazoles displayed no significant change in inhibition efficiency with the immersion time from 3h to 24h which shows the persistency of the adsorbed fatty acid oxadiazoles over a longer test period (Figure 5.3.b). Figures 5.4.a - 5.4.b, depict the studies of variation in acid concentration on inhibition efficiency. The concentration of HCl was varied for 1.0 mol dm^{-3} to 5.0 mol dm^{-3} at 500 ppm [inhibitor]. The change in acid concentration does not cause any significant change in inhibition efficiency. Thus triazoles and oxadiazoles are effective corrosion inhibitor in the acid concentration range of 1.0 -5.0 mol dm^{-3}.

The value of weight loss of mild steel at different initial concentrations of inhibitors in 1 mol dm^{-3} HCl was investigated at 30°C after 3 hour of immersion time. The data obtained from the weight loss studies were used to evaluate the surface coverage (θ).The data were tested graphically by fitting to various isotherms. A straight line was obtained on plotting log (θ /1-θ) versus log C (Figures 5.5.a - 5.5.b) suggesting that the adsorption of the triazoles and oxadiazoles on mild steel surface follows Langmuir's adsorption isotherm. From the slope of the plots of log (θ/1-θ) *versus* 1/T (Figures 5.6.a - 5.6.b), the values for the heat of adsorption (Q) were obtained. The values are

presented in Tables 5.3-5.4. The values of Q obtained suggest the physical nature of adsorption.

Log (corrosion rate) *versus* 1/T was plotted (Figures 5.7.a - 5.7.b) to obtain the values of E_a. The slope of the plot gave the values of E_a and these values are given in Tables 5.3-5.4.

To obtain the values of ΔH and ΔS for the adsorption of triazoles and oxadiazoles in presence of HCl on the mild steel surface, logarithm of (CR /T) was plotted against 1/T as given in experimental. The slope and intercept of plots (Figures 5.8.a - 5.8.b) gave the values of ΔH and ΔS respectively. These values are listed in Tables 5.3-5.4 for of triazoles and oxadiazoles respectively.

The higher energy of activation (E_a) suggests that these inhibitors are more effective at room temperature[185]. The lower E_a values for NMOD indicates that its efficiency is high at elevated temperature [163].

The enthalpy change, ΔH in presence of triazoles signifies the net rate determining step of two processes namely; corrosion reactions and the adsorption of triazoles at the mild steel surface. The lowering[186] in the values of ΔH in the presence of triazoles may be due to more energy release during the adsorption of triazoles at mild steel surface. Thus, it results into the lower change in enthalpy and more stronger adsorption. It is evident from the fact that the presence of triazoles reduces the corrosion rate and increases the inhibition efficiency. The higher (ΔH) in the presence of oxadiazoles indicate that the more energy barrier is involved in the adsorption of oxadiazoles on mild steel surface. Thus, a weak association exists between the mild steel

surface and oxadiazoles and, therefore, it exhibit poor inhibition efficiency as compared to triazoles. The change in values of entropy of activation, ΔS in the absence and presence of triazoles and oxadiazoles are negative and large[188] (presented in Tables 5.3- 5.4). This indicates that the activated complex formed during the corrosion and adsorption of inhibitors processes is an associative in nature rather than dissociative step. As a result, a decrease in disorderness takes place during the transformation from reactants to the activated complex [190].

The free energy change of adsorption (ΔG_{ads}) was calculated using the following equations and the values are listed in Tables 5.3-5.4.

$$\Delta G_{ads} = -RT \ln (55.5K)$$

where,

$$K = \theta/C\ (1-\theta)$$

The lower values of ΔG_{ads} indicate that triazole and oxadiazoles of fatty acid are physically adsorbed on the metal surface[191]. It also indicate the spontaneous adsorption of inhibitor on the surface of mild steel [192].

A straight line was obtained for the plot of log (weight loss) *versus* immersion time as depicted in Figures 5.9a- 5.9b, showing that the reaction obeyed first order kinetics. The rate constant was calculated using the first order rate law.

$$k = \frac{2.303}{t} \log \frac{A_o}{A}$$

where A_o is the initial mass of the metal and A is the mass corresponding to time t. The half life ($t_{1/2}$) values were calculated using the equation:

$$t_{1/2} = 0.693 / k$$

The values of the rate constant and half life period ($t_{1/2}$) obtained in the absence and presence of triazoles and oxadiazoles are summarized in Tables 5.5-5.6. The half life ($t_{1/2}$) values give the information regarding the durability of inhibitor film on the mild steel surface under the given condition.

5.2 Potentiodynamic polarization Studies

The cathodic and anodic polarization curves of mild steel in 1.0 mol dm^{-3} in the absence and presence of different inhibitors at 500 ppm concentration at 30±1 °C are shown in Figures 5.10.a -5.10.b.

Electrochemical parameters such as corrosion current density (I_{corr}), corrosion potential (E_{corr}) and inhibition efficiency (IE) were calculated from tafel plots and these values are given in Tables 5.7 - 5.8.

The values of I_{corr} decreased significantly in the presence of inhibitor. Maximum decrease in I_{corr} was observed for UMOD (among oxadiazoles) and UPMT (among triazoles). All the triazoles do not show any significant change in E_{corr} values suggesting that these compounds are mixed type inhibitors i.e., they retard the corrosion reaction by blocking both anodic and cathodic sites of the metal[57]. E_{corr} values changes in presence oxadiazoles in the acid solution suggesting these oxadiazoles are cathodic type inhibitors i.e., they retard the corrosion reaction by blocking cathodic sites of the metal [195].

5.3. Electrochemical Impedance Studies

Tables 5.9.-5.10 includes the results of impedance studies and Figures 5.11a - 5.11b shows Nyquist plots in the presence of 100, 300 and 500 ppm of UPMT and UMOD. The Nyquist plots are not perfect semicircles and this difference has been attributed to frequency dispersion[157]. The values of R_t and C_{dl} were calculated from Nyquist plots[196]. The percentage inhibition efficiency was calculated from the following equation:

$$\% \text{ I.E.} = \frac{1/R_{to} - 1/R_{ti}}{1/R_{to}} \times 100$$

where R_{to} and R_{ti} are charge transfer resistance without and with inhibitor, respectively. The values of R_t ,C_{dl} and inhibition efficiency are given in Tables 5.9. -5.10. R_t values increases with increase in inhibitor concentration (UPMT and UMOD) and, in turn, it leads to an increase in inhibition efficiency. The addition of UPMT and UMOD to 1.0 mol dm^{-3} HCl lowers the C_{dl} values, which shows that the inhibition in corrosion may be due to surface adsorption of the inhibitor [198].

5.4. Scanning electron microscopy

Scanning electron microscopy were taken for the mild steel surface after dipping it in solution containing HCl; HCl and UPMT; and HCl and UMOD for 3 hours at 30°C. Figures 5.12 for triazoles and Figure 5.13 for oxadiazoles suggest that the inhibitors form protective layer over the metal surface and prevent attack of acid on metal surface[63].

5.5. Mechanism of corrosion inhibition

Inhibition of corrosion of mild steel in the acidic solutions by the fatty acid triazole and oxadiazoles can be explained on the basis of molecular adsorption. These triazole compounds are adsorbed on the metal surface through π-electrons of aromatic ring and/ or through the lone pair of electrons of N atoms. The presence of long hydrophobic chain of hydrocarbon keeps the acid solution away from metal surface. The inhibition efficiency has been found to be in the following order:

UPMT > NPMT > PPMT> HPMT

(C_{11}) (C_9) (C_{15}) (C_{17})

The inhibition efficiency of the triazoles increased with the increase in chain length up to C_{15}. A further increase in chain length up to C_{17} decreased the inhibition efficiency.

The oxadiazoles are adsorbed on the metal surface through π-electrons of aromatic ring, and through lone pair of electrons of N, O and S atoms. Additionally, oxadiazoles exist in protonated form in acidic solution and get adsorbed on the cathodic sites of the mild steel and decrease the evolution of hydrogen. While in case of aliphatic oxadiazoles the presence of long hydrophobic chain plays an important role in increasing inhibition efficiency by keeping acid solution away from metal surface[201] (The notational mechanism of adsorption is shown below). The order of the inhibition efficiency of oxadiazoles compounds were found to be in the following order: UMOD > PMOD > AMOD > NMOD

The maximum inhibition efficiency increased was observed for UMOD.

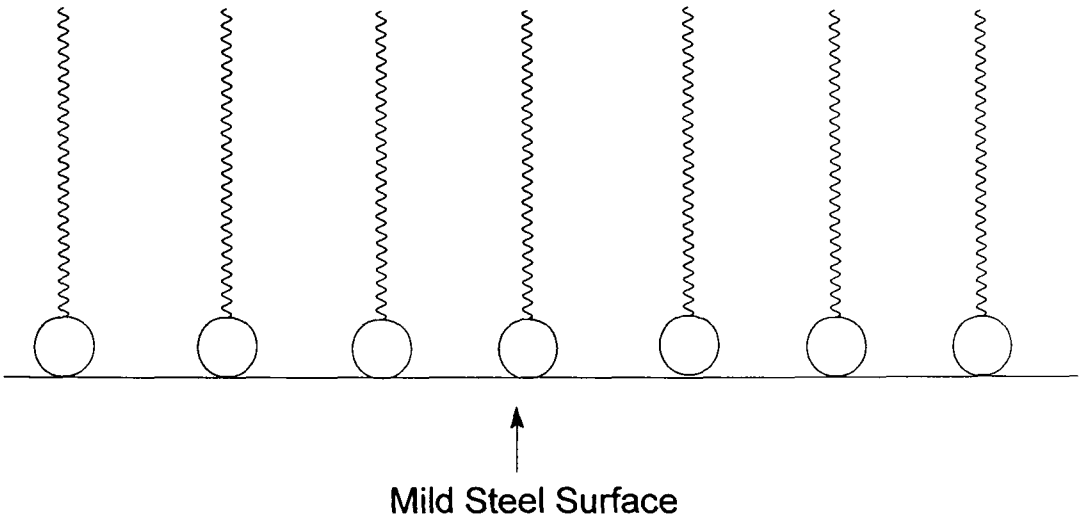

Table 5.1. Dependence of corrosion rate and inhibition efficiency on [Triazoles].

Inhibitor used	Concentration (ppm)	Weight loss (mg)	IE (%)	CR (mmpy)
UPMT	0	59.9	-	22.90
	100	3.4	94.53	1.22
	200	2.0	96.62	0.75
	300	1.6	97.33	0.59
	400	1.1	98.16	0.41
	500	0.5	99.10	0.20
	600	1.5	97.51	0.57
NPMT	0	59.9	-	22.90
	100	7.1	88.09	2.65
	200	3.5	94.01	1.33
	300	2.7	95.49	1.00
	400	2.1	96.38	0.80
	500	1.0	98.21	0.39
	600	3.0	95.08	1.12
PPMT	0	59.9	-	22.90
	100	1.2	79.51	4.56
	200	0.9	85.12	3.31
	300	0.5	90.39	2.14
	400	0.4	93.50	1.44
	500	0.2	96.33	0.81
	600	0.3	93.69	1.42
HPMT	0	59.9	-	22.90
	100	1.4	76.44	5.25
	200	1.1	83.21	3.74
	300	0.7	87.49	2.78
	400	0.5	91.21	1.95
	500	0.2	95.68	0.96
	600	0.4	92.12	1.80

[HCl] = 1.0 mol dm^{-3}, Temp = 30 °C, Immersion time = 3 hours

Table 5.2. Dependence of corrosion rate and inhibition efficiency on [Oxadiazoles].

Inhibitor used	Concentration (ppm)	Weight loss (mg)	IE (%)	CR (mmpy)
UMOD	0	62.4	-	23.20
	100	1.2	80.07	4.62
	200	1.0	82.81	3.98
	300	0.9	85.52	3.35
	400	0.7	88.16	2.76
	500	0.3	94.78	1.21
	600	0.6	89.61	2.41
PMOD	0	62.4	-	23.20
	100	1.5	74.74	5.86
	200	1.3	77.67	5.18
	300	1.1	81.22	4.35
	400	1.0	83.14	3.91
	500	0.7	87.26	2.95
	600	1.2	80.22	4.58
NMOD	0	62.4	-	23.20
	100	1.9	69.92	6.97
	200	1.7	72.14	6.46
	300	1.4	77.08	5.31
	400	1.3	79.42	4.77
	500	1.1	81.85	4.21
	600	1.5	75.11	5.77
AMOD	0	62.4	-	23.20
	100	2.7	56.42	10.11
	200	2.5	59.81	9.32
	300	2.3	63.72	8.41
	400	2.1	65.23	8.06
	500	1.8	75.12	6.70
	600	2.0	67.57	7.52

[HCl] = 1.0 mol dm^{-3}, Temp = 30 °C, Immersion time = 3 hours

Table 5.3. Thermodynamic activation parameters for corrosion of mild steel in HCl in the absence and presence of triazoles.

System	E_a (kJ mol^{-1})	ΔH (kJ mol^{-1})	ΔS (J $mol^{-1}K^{-1}$)	ΔG_{ads} (kJ mol^{-1})	-Q (kJ mol^{-1})
1N HCl	51.18	48.56	200.40	-	-
UPMT	63.73	40.32	241.60	36.26	30.02
NPMT	60.40	42.32	238.77	35.84	26.30
PPMT	55.53	28.30	235.90	24.07	21.20
HPMT	54.30	27.96	233.00	23.62	21.22

[Triazoles] = 500 ppm; [HCl] = 1.0 mol dm^{-3}

Table 5.4. Thermodynamic activation parameters for corrosion of mild steel in HCl in the absence and presence of oxadiazoles.

System	E_a (kJ mol^{-1})	ΔH (kJ mol^{-1})	ΔS (J $mol^{-1}K^{-1}$)	ΔG_{ads} (kJ mol^{-1})	-Q (kJ mol^{-1})
1N HCl	51.18	48.56	200.40	-	-
UMOD	55.04	80.03	220.58	34.90	30.43
PMOD	52.13	87.85	217.52	33.71	23.36
AMOD	51.12	101.41	215.98	30.24	18.02
NMOD	48.08	103.50	210.24	29.30	14.35

[Oxadiazoles] = 500 ppm; [HCl] = 1.0 mol dm^{-3}

Table 5.5. Half-life values (in hours h) for the corrosion of mild steel in triazoles.

System	10^3 k (h^{-1})	$t_{1/2}$ (h)
1N HCl	32.79 ± 0.141	21.13
UPMT	4.61 ± 0.162	150.21
NPMT	8.80 ± 0.130	78.68
PPMT	17.62 ± 0.214	39.31
HPMT	20.76 ± 0.122	33.37

[Triazoles] = 500 ppm; [HCl] = 1.0 mol dm^{-3}; Temp = 30° C

Table 5.6. Half-life values (in hours h) for the corrosion of mild steel in oxadiazoles.

System	10^3 k (h^{-1})	$t_{1/2}$ (h)
1N HCl	32.79 ± 0.141	21.13
UMOD	2.09 ± 0.112	134.48
PMOD	5.80 ± 0.145	119.47
AMOD	6.62 ± 0.194	104.74
NMOD	8.20 ± 0.212	84.44

[Oxadiazoles] = 500 ppm; [HCl] = 1.0 mol dm^{-3}; Temp = 30° C

Table 5.7. Electrochemical polarization parameters for the corrosion of mild steel in HCl containing triazoles.

System	E_{corr} (mV)	I_{corr} (mA cm^{-2})	IE (%)
Blank	-461	0.360	-
UPMT	-492	0.004	98.78
NPMT	-490	0.002	94.49
PPMT	-487	0.048	86.77
HPMT	-485	0.082	77.22

[Triazoles] = 500 ppm; [HCl] = 1.0 mol dm^{-3}; Temp = 30° C

Table 5.8. Electrochemical polarization parameters for the corrosion of mild steel in HCl containing oxadiazoles.

System	E_{corr} (mV)	I_{corr} (mA cm^{-2})	IE (%)
Blank	-461	0.360	-
UMOD	-552	0.027	92.50
PMOD	-533	0.031	91.38
AMOD	-526	0.036	89.85
NMOD	-517	0.045	87.52

[Oxadiazoles] = 500 ppm; [HCl] = 1.0 mol dm^{-3}; Temp = 30° C

Table 5.9. Dependence of electrochemical impedance parameters on [UPMT] for mild steel in HCl.

System	R_t (ohm cm^2)	C_{dl} ($\mu F\ cm^{-2}$)	IE (%)
0	36	1511.50	-
100	223.07	105.14	83.78
300	346.15	45.78	89.57
500	392.30	27.58	91.07

[HCl] = 1.0 mol dm^{-3}; Temp = 30° C.

Table 5.10. Dependence of electrochemical impedance parameters on [UMOD] for mild steel in HCl.

System	R_t (ohm cm^2)	C_{dl} ($\mu F\ cm^{-2}$)	IE (%)
0	36	1511.50	-
100	139.13	769.72	74.11
300	167.64	708.96	78.52
500	243.47	501.87	85.15

[HCl] = 1.0 mol dm^{-3}; Temp = 30° C.

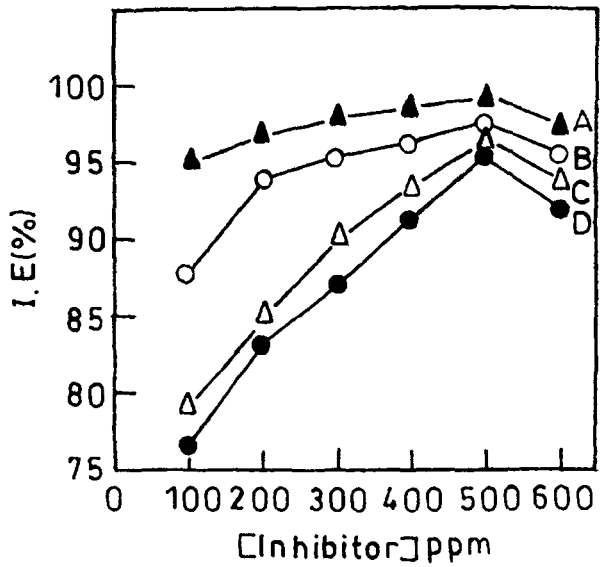

Fig 5.1 a. Plot of variation of inhibition efficiency on triazoles concentration (▲,UPMT; o, NPMT ; Δ, PPMT; •, HPMT).

Reaction conditions [HCl] =1.0 mol dm^{-3}, Temp =30°C, Time =3 hours.

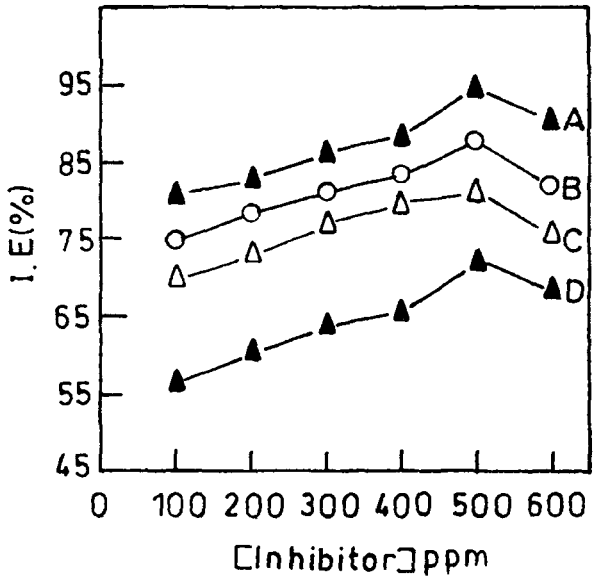

Fig 5.1 b. Plot of inhibition efficiency of oxadiazoles concentration (▲,UMOD; o, PMOD; Δ, NMOD; ▲, AMOD).

Reaction conditions [HCl] =1.0 mol dm^{-3}, Temp =30°C, Time =3 hours.

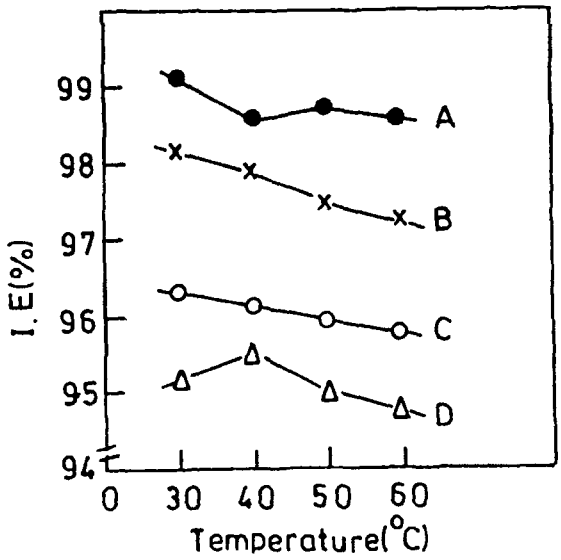

Fig 5.2 a. Plot of variation of inhibition efficiency on temperature for triazoles (•, UPMT; **x**, NPMT ; o, PPMT; **Δ**,HPMT)
Reaction conditions [HCl] =1.0 mol dm^{-3}, Time =3 hours, [inhibitor]=500 ppm.

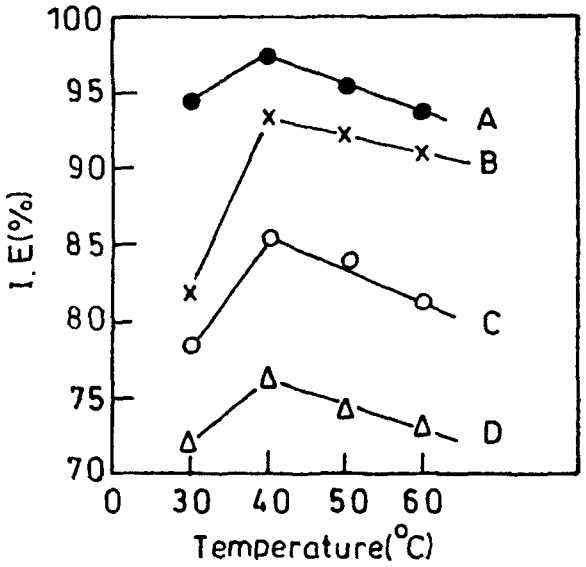

Fig 5.2 b. Plot of variation of inhibition efficiency on temperature for oxadiazoles (•,UMOD; **x**, PMOD ; o, NMOD; **Δ**,AMOD)
Reaction conditions [HCl] =1.0 mol dm^{-3}, Time =3 hours, [inhibitor]=500 ppm.

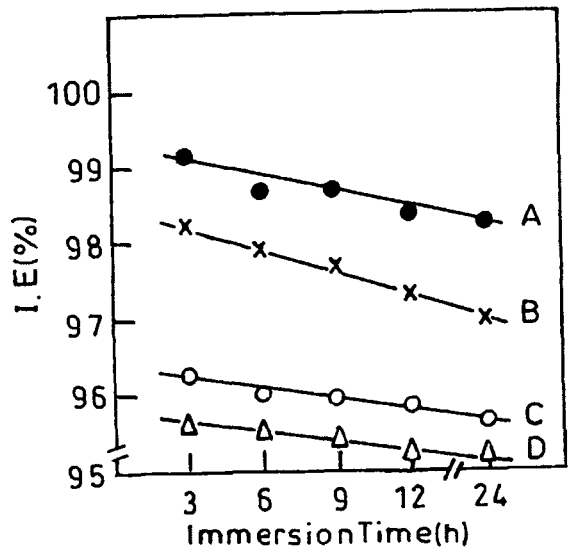

Fig 5.3 a. Plot of variation of inhibition efficiency on immersion time for (•, UPMT; **x**, NPMT ; o, PPMT; **Δ**,HPMT)
Reaction conditions [HCl] =1.0 mol dm^{-3}, Temp =30°C, [inhibitor]=500 ppm.

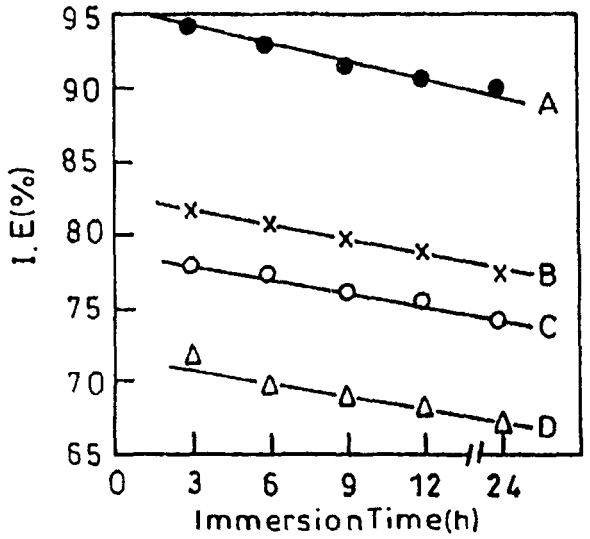

Fig 5.3 b. Plot of variation of inhibition efficiency on immersion time for oxadiazoles (•,UMOD; **x**, PMOD ; o, NMOD; **Δ**,AMOD)
Reaction conditions [HCl] =1.0 mol dm^{-3}, Temp =30°C, [inhibitor]=500 ppm

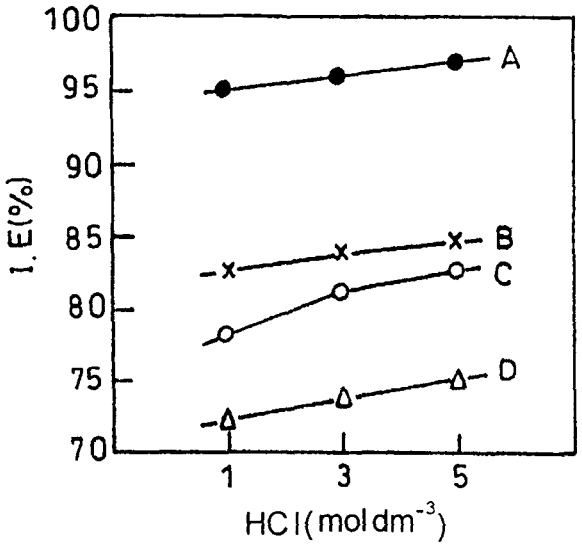

Fig 5.4 a. Plot of variation of inhibition efficiency on [HCl] for triazoles (•, UPMT; **x**, NPMT ; o, PPMT; **Δ**,HPMT.
Reaction conditions [inhibitor]=500 ppm, Temp =30°C, Time =3 hours.

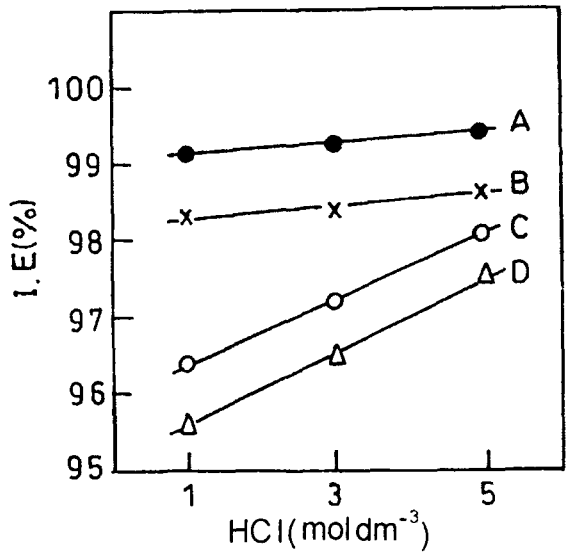

Fig 5.4 b. Plot of variation of inhibition efficiency on [HCl] for oxadiazoles (•,UMOD; **x**, PMOD ; o, NMOD; **Δ**,AMOD) .
Reaction conditions [inhibitor]=500 ppm, Temp =30°C, Time =3 hours.

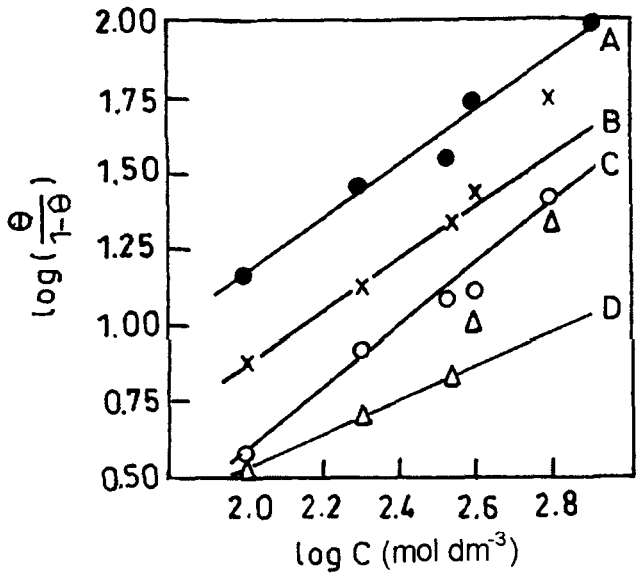

Fig 5.5 a. Langmuir s adsorption isotherm plots for Triazoles (•, UPMT; **x**, NPMT ; o, PPMT; **Δ**,HPMT)

Reaction conditions [HCl] =1.0 mol dm^{-3}, Temp =30°C, Time =3 hours.

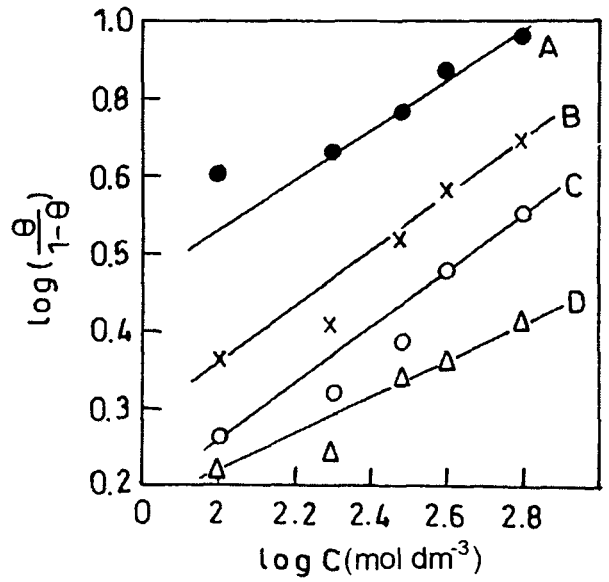

Fig 5.5 b. Langmuir s adsorption isotherm plots for oxadiazoles (•,UMOD; **x**, PMOD ; o, NMOD; **Δ**,AMOD)

Reaction conditions [HCl] =1.0 mol dm^{-3}, Temp =30°C, Time =3 hours.

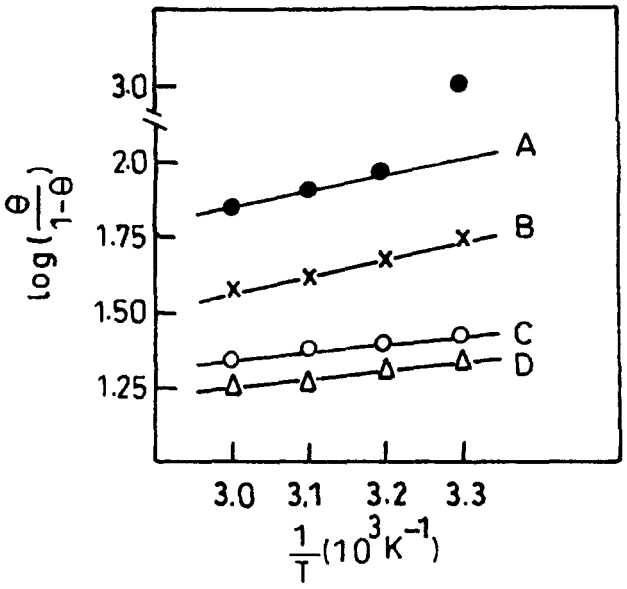

Fig 5.6 a. Adsorption isotherm plot for log (θ /1- θ) versus 1/T for triazoles (•, UPMT; **x**, NPMT ; o, PPMT; **Δ**,HPMT)
Reaction conditions [HCl] =1.0 mol dm^{-3}, Time =3 hours, [inhibitor]=500.

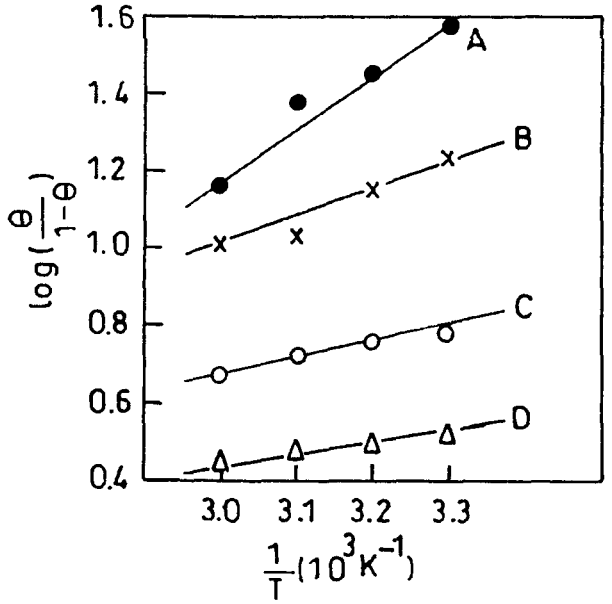

Fig 5.6 b. Adsorption isotherm plot for log (θ /1- θ) vs 1/T for oxadiazoles (•,UMOD; **x**, PMOD ; o, NMOD; **Δ**,AMOD).
Reaction conditions [HCl] =1.0 mol dm^{-3}, Time =3 hours, [inhibitor]=500 ppm.

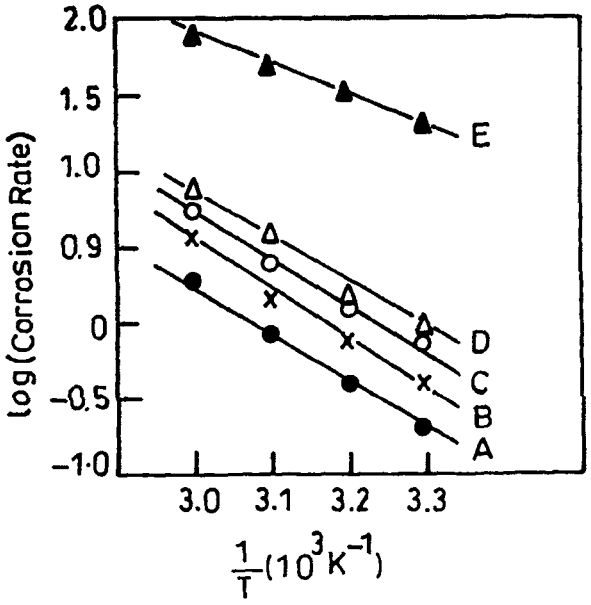

Fig 5.7 a. Adsorption isotherm plot for log (CR) versus 1/T for triazoles (•, UPMT; x, NPMT ; o, PPMT; Δ,HPMT)
Reaction conditions [HCl] =1.0 mol dm^{-3}, Time =3 hours, [inhibitor]=500 ppm

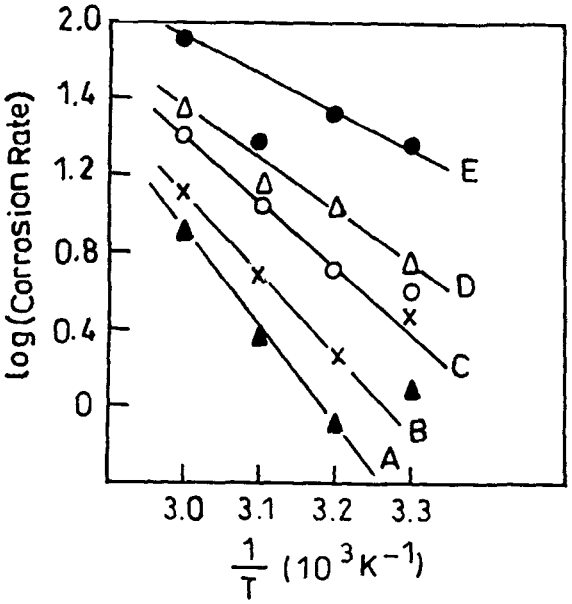

Fig 5.7 b. Adsorption isotherm plot for log (CR) versus 1/T for oxadiazoles (▲, UMOD; x, PMOD ; o, NMOD; Δ,AMOD; •, Blank).
Reaction conditions [HCl] =1.0 mol dm^{-3}, Time =3 hours, [inhibitor]=500 ppm

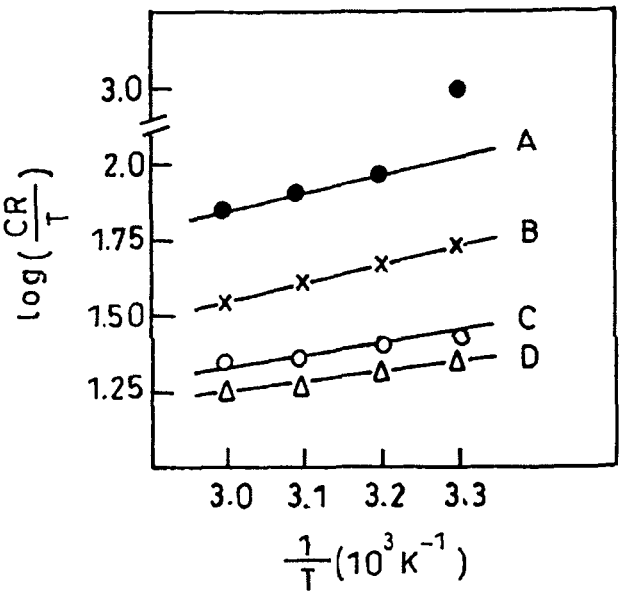

Fig 5.8 a. Adsorption isotherm plot for log (CR/T) versus 1/T for triazoles (•, UPMT; **x**, NPMT; o, PPMT; **Δ**,HPMT; *, Blank).
Reaction conditions [HCl] =1.0 mol dm^{-3}, Time =3 hours, [inhibitor]=500 ppm.

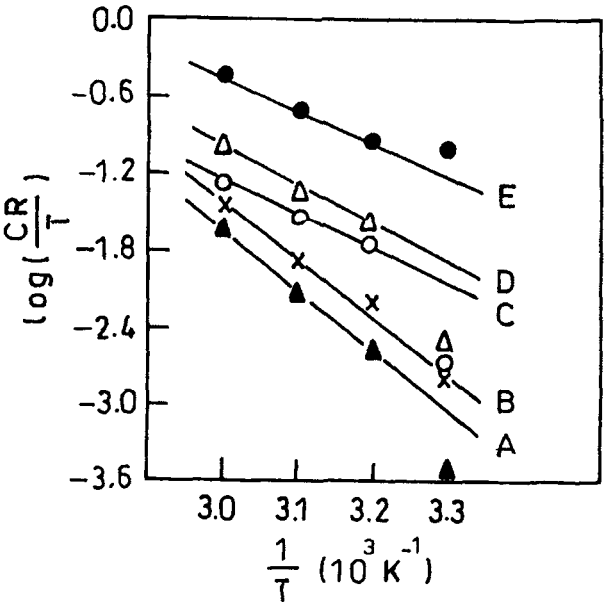

Fig 5.8 b. Adsorption isotherm plot for log (CR/T) versus 1/T for oxadiazoles (▲, UMOD; **x**, PMOD ; o, NMOD; **Δ**,AMOD; •, Blank)
Reaction conditions [HCl] =1.0 mol dm^{-3}, Time =3 hours, [inhibitor]=500 ppm.

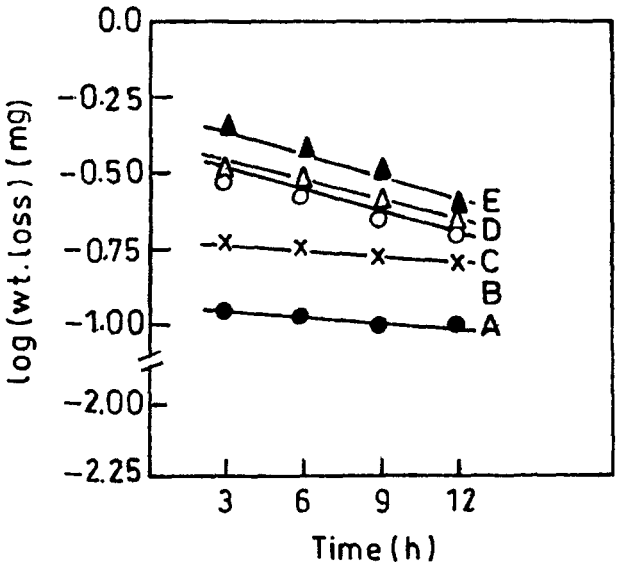

Fig 5.9 a. Plot of log (weight loss) versus immersion time for triazoles (•, UPMT; **x**, NPMT ; o, PPMT; **Δ**,HPMT; **▲**, Blank)
Reaction conditions [HCl] =1.0 mol dm^{-3}, [inhibitor]=500 ppm ,Temp =30°C.

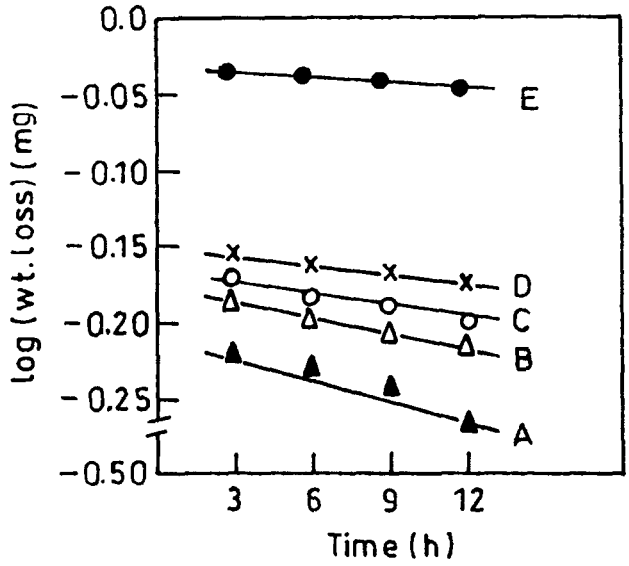

Fig 5.9 b. Plot of Log (weight loss) versus immersion time for oxadiazoles (•, UMOD; **x**, PMOD ; o, NMOD; **Δ**, AMOD; **▲**, Blank)
Reaction conditions [HCl] =1.0 mol dm^{-3}, [inhibitor]=500 ppm ,Temp =30°C.

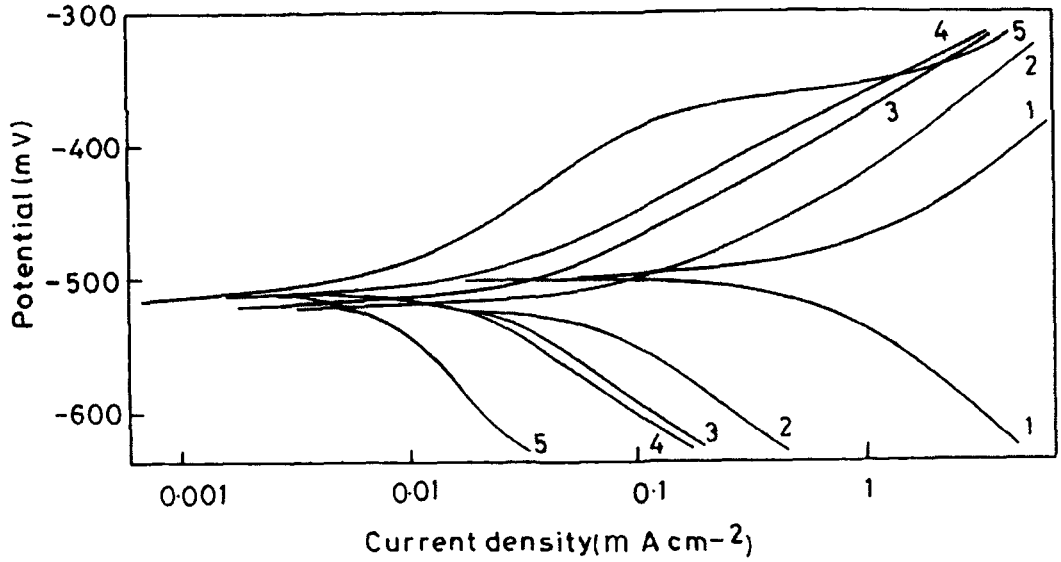

Fig 5.10 a. Potentiodynamic polarization curves for mild steel in presence of triazoles 1) Blank (2) HPMT (3) PPMT (4) NPMT (5) UPMT.
Reaction conditions[HCl]= 1.0 mol dm^{-3}, Temp =30°C.

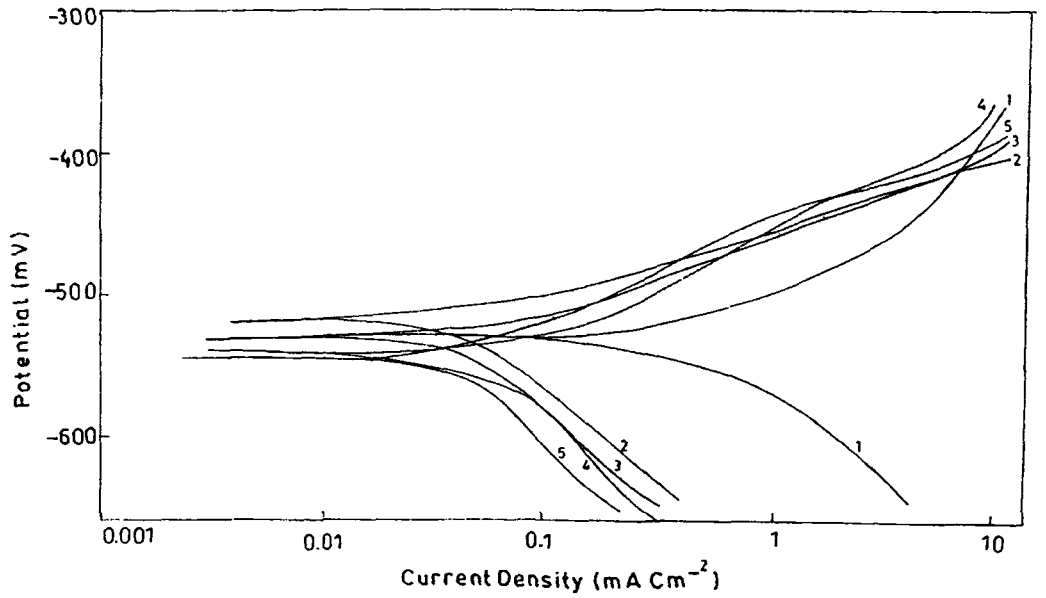

Fig 5.10 b. Potentiodynamic polarization curves of oxadiazoles on mild steel (1) Blank (2) NMOD (3) AMOD (4) PMOD (5) UMOD
Reaction conditions [HCl]= 1.0 mol dm^{-3}, T=30°C.

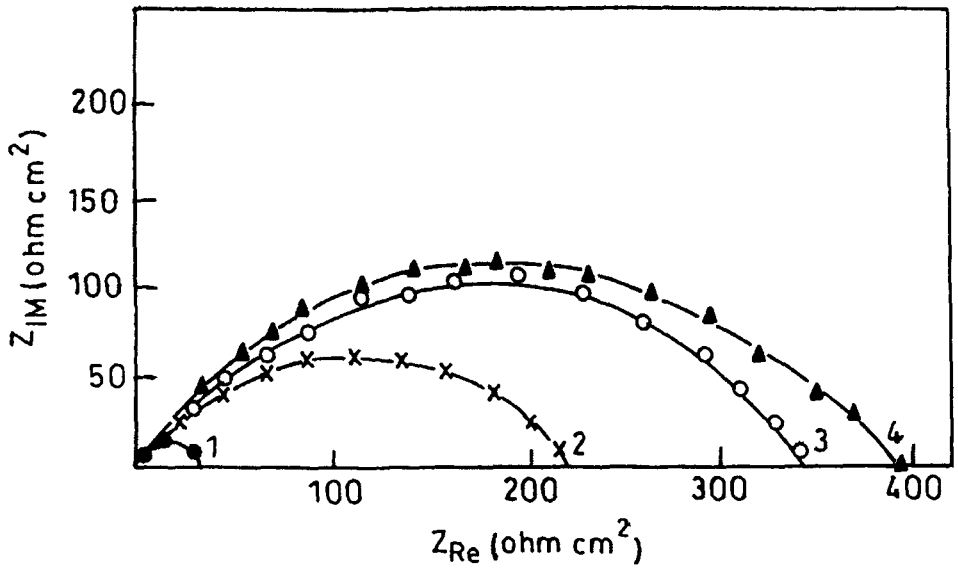

Fig 5.11 a. Nyquist plot of mild steel in 1.0 mol dm^{-3} HCl in the absence and presence of 100, 300 and 500 ppm of UPMT (1) Blank (2) 100 ppm (3) 300 ppm (4) 500 ppm.

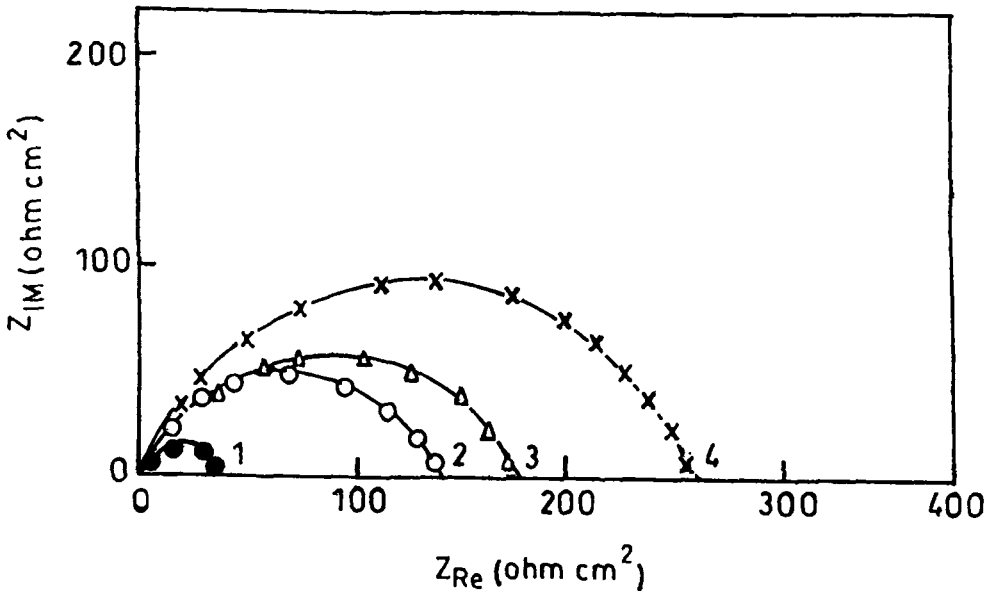

Fig 5.11 b. Nyquist plot of mild steel in 1.0 mol dm^{-3} HCl in the absence and presence of 100, 300 and 500 ppm of UMOD (1) Blank (2) 100 ppm (3) 300 ppm (4) 500 ppm.

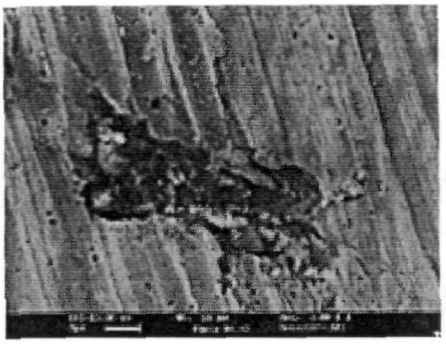

(a)

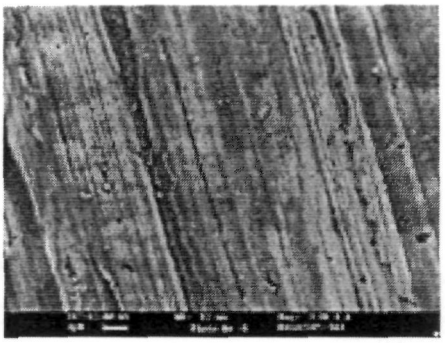

(b)

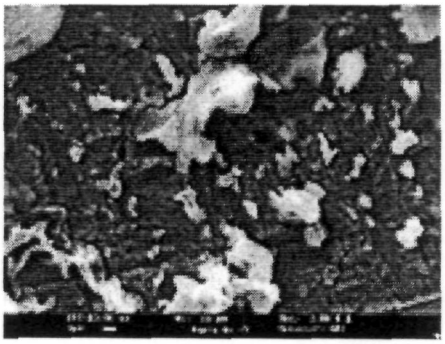

(c)

Figure 5.12 Scanning electron micrographs for mild steel surface in absence and presence of UPMT (a) mild steel in 1·0 mol dm^{-3} HCl (b) polished mild steel and c) mild steel in presence of UPMT.

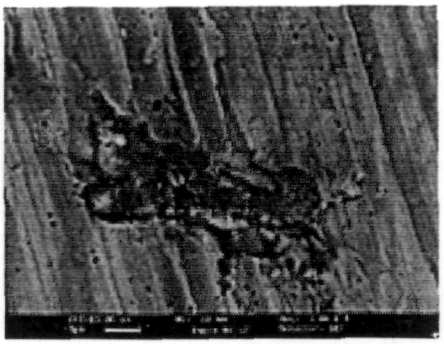

(a)

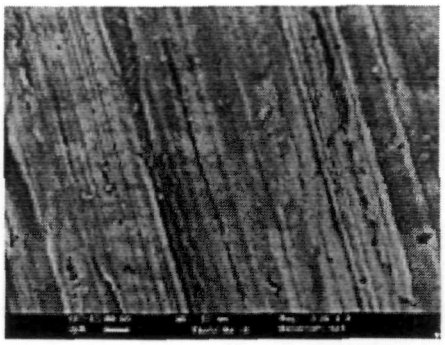

(b)

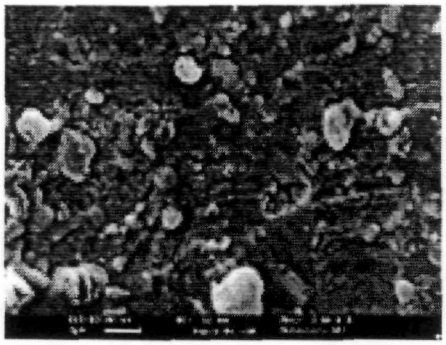

(c)

Figure 5.13. Scanning electron micrographs for mild steel surface in absence and presence of UMOD (a) mild steel in 1·0 mol dm-3 HCl (b) polished mild steel and (c) mild steel in presence of UMOD.

Chapter- 6
Effects of Surfactants on AMOD & HI

Surfactants [238-239] are amphiphile molecule that consists of both hydrophobic tails (usually hydrocarbon chains) and hydrophilic molecular segments. The hydrophobic segment tends to aggregate together to have energetically less expensive state. The shape and size of aggregation depend upon the energetics of interaction between adjacent hydrophilic head groups as well as adjacent hydrophobic tails. They self associate at concentrations above the critical micellar concentration (cmc) to form association colloids, called micelles. Micelles have interfacial regions containing ionic or polar head groups. This polar or ionic head groups plays an important role in the adsorption[240-241] of surfactants onto the solid surfaces and thereby inhibit corrosion by blocking the surface of metal. Surfactant adsorption may occur due to electrostatic interaction, van der Waals interaction, hydrogen bonding and/ or solvation and desolvation of adsorbate and adsorbent species[242]. Studies in surfactant media have demonstrated a marked inhibiting effect on corrosion[243-249]. Depending upon the concentrations the adsorption may occur as individual molecules or as surfactant aggregates of various types.

Surfactant adsorption to the metallic surface is below monolayer level, below cmc and at concentrations above cmc adsorption can consists of multiple layers of physically adsorbed surfactant molecules[250]. Above the cmc, increasing surfactant concentration leads to the gradual formation of multilayer that further reduce the rate of corrosion beyond what can be achieved with monolayer coverage below the cmc. However, concentration changes above the cmc lead to smaller changes in inhibition, since the changes above the cmc result only in additional coverage beyond the monolayer level, which is already sufficient for significant corrosion inhibition.

In the present study the effect of anionic sodium dodecylsulfate (SDS), cationic cetyltrimethylammonium bromide (CTAB), and nonionic Triton-X-100 (TX-100) surfactants on the corrosion efficiency of 2-aminophenyl-5-mercapto-1-oxa-3,4-diazole (AMOD) and 2- Heptyl -1,3 imidazoline (HI) have been studied by weight loss measurements and potentiodynamic measurement studies.

RESULTS AND DISCUSSION

6.1. Weight loss measurements

The effect of variation [surfactants] on the inhibition efficiency (IE) of AMOD and HI were carried out by weight loss method. The concentrations of surfactants (cationic CTAB, anionic SDS and non-ionic TX-100) were varied in the range from 1 x 10^{-2} mol dm^{-3} to 5 x 10^{-1} mol dm^{-3} in the absence and presence of 500 ppm AMOD and HI at 30^{o}C. The results are summarized in Tables 6.1-6.6 and Figures 6.1-6.2. The addition of surfactant enhanced the inhibition efficiency (IE) of AMOD and HI appreciably. The IE first increased with increase in [surfactant], giving maxima at concentrations 0.2 mol dm^{-3} and 0.1 mol dm^{-3} for AMOD and HI respectively. The further increase in [surfactant] decreased the inhibition efficiency. The dissolved surfactant helps inhibitor to adsorb onto the iron surface due to their hydrophilic property and leads to the strong bonding between the metal surface and inhibitor along with head group of surfactant. The hydrophobic surfactant tails prefer to adsorb together to form a coherent hydrophobic film that serves as a barrier to block the reaction between the iron surface and the external environment, thus the corrosion reaction between the metal and aqueous medium is inhibited[251].

At the surfactant concentration below cmc, the surfactant molecules adsorb to the surface to form monolayer coverage on the interface and the surfactant tails are oriented parallel to adsorbent plane[252] as depicted below:

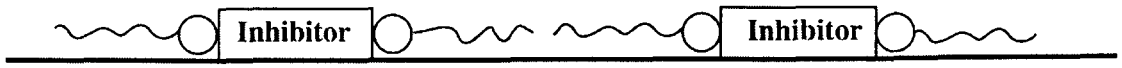

Thus, the surfactant and inhibitor molecules inhibit the dissolution of metal either by blocking the cathodic or the anodic reaction by occupying reactive sites, or by simply providing resistance to the supply of oxidant or the transport of the reaction products. Thus, corrosion is inhibited more effectively with increasing surfactant concentration. The monolayer coverage increases with the increase in surfactant concentration and may lead to the formation of hemimicelles[253].

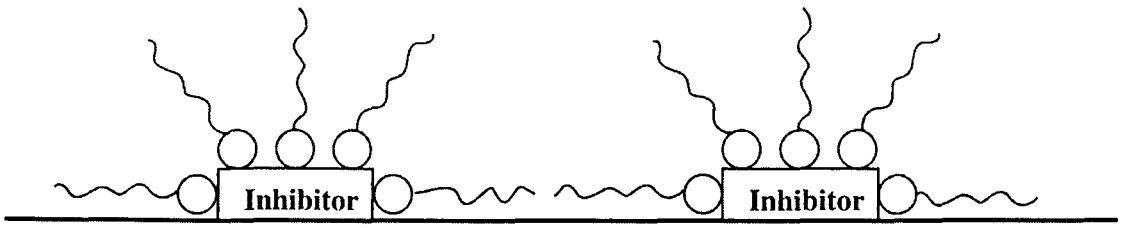

As the concentration of surfactant increases further, surfactant molecules form dimers, and multiple molecules aggregate. The bilayer aggregates are formed with hydrophobic hydrocarbon chains inside and polar head groups outside. A further increase of surfactant concentration, which is already sufficient for significant corrosion inhibition, causes an increase in ionic concentration in the surface region due to the incorporation of ions as counterions or coions. This leads to an increase in concentration of H^+ in the vicinity of surface and therefore, the corrosion efficiency is decreased on increasing the [surfactant].

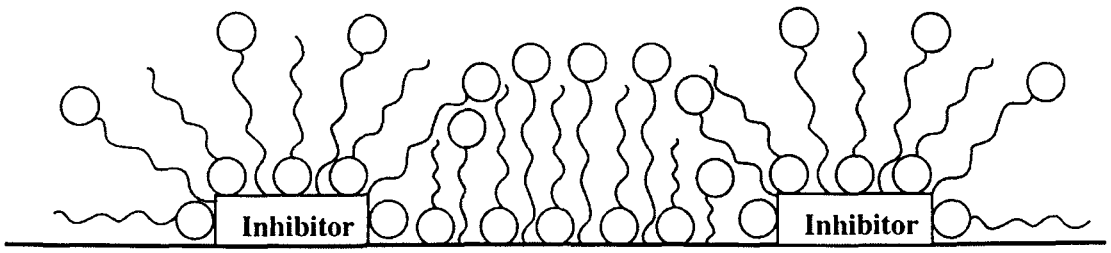

The variation of inhibition efficiency on the acid concentration was studied at [HCl] (1.0 -5.0 mol dm^{-3}). The concentrations of inhibitor (AMOD and HI) was kept constant at 500 ppm at 30°C and the concentration of surfactant was 0.2 mol dm^{-3} for AMOD and 0.1 mol dm^{-3} for HI. The results are presented in Tables 6.7- 6.8 and in Figures 6.3- 6.4. Inhibition efficiency decreased with the increase in acid concentration due to the greater aggressiveness of acid solutions at higher concentration in AMOD. The variation in the acid concentration in presence of HI and surfactants did not cause any significant change in inhibition efficiency as the surface remains blocked by inhibitor and surfactant due to adsorption.

The variation in inhibition efficiency was studied at 500 ppm of inhibitors (AMOD and HI) at different temperature in the range from 30°C to 60°C. The results are presented in Tables 6.9- 6.10 and in Figures 6.5- 6.6. It demonstrates that the surfactants help inhibitor to adhere the surface upto 60°C. The decrease in inhibition efficiency with increase in temperature from 30°C to 60°C (Figure 6.6) in presence of HI and surfactant show desorption of HI and surfactants from metal surface occur at higher temperatures[182].

The surface coverage (θ) at different concentrations of surfactant in the range from 1 x 10^{-2} mol dm^{-3} to 5 x 10^{-1} mol dm^{-3} in the presence of 500 ppm inhibitor (AMOD and HI) have been evaluated by weight loss method. The temperature was kept constant at 30°C and the immersion time was 3h in 1.0 mol dm^{-3} HCl. The data was tested graphically by fitting to various

isotherms. A straight line plot was obtained for log θ /(1-θ) versus log C (Concentration of surfactants in mol dm^{-3}) as shown in Figures 6.7- 6.8. These plots suggest that the adsorption of AMOD and HI in presence of surfactant on mild steel follows Langmuir's adsorption isotherm. The adsorption of inhibitors (AMOD and HI) on mild steel surface is enhanced in presence of the tested surfactants.

The values of the heat of adsorption (Q) was calculated from the slope (-Q/2.303R) of the plot of log θ/1-θ versus 1/T (Figures 6.9- 6.10) in presence of surfactant and inhibitor. The values are given in Tables 6.11- 6.12. The lower values of heat of adsorption for inhibitors (AMOD / HI) and surfactant (SDS, CTAB and TX-100) show the physical nature of adsorption [162].

Figures 6.11- 6.12 show plot of log CR versus 1/T for inhibitor (AMOD and HI) in presence of surfactants. The value of activation energy (E_a) was obtained from the slope. It was observed that the values of E_a for AMOD in presence of surfactants is lower than that of uninhibited system. Values of E_a for HI in presence of surfactants are higher than those in the free acid solution except for TX-100 indicating that HI in presence of surfactants is more effective inhibitor at room temperature[185].

Entropy and enthalpy changes for corrosion reaction was deduced from slope and intercept of plot of log (C.R) / T) versus 1/T (Figures 6.13- 6.14). The values are listed in Tables 6.11- 6.12. The lower values of ΔH in the presence of surfactants and AMOD indicates less energy barrier[186]. The higher values of ΔH for HI in presence of surfactants suggest the high energy barrier for corrosion reaction. The entropy of activation ΔS for AMOD and HI in presence of the surfactant is large and negative. This indicates that the

activated complex in the rate determining step in more ordered form and represents an association rather than a dissociation step. Decrease in disorderness takes place during transformation from reactants to the activated complex[189].

The ΔG_{ads} value calculated for AMOD and HI in presence of surfactant are presented in Tables 6.11- 6.12 respectively. The negative values of ΔG_{ad} reveal the spontaneity nature of adsorption process[190]. Thus the adsorbed layer interacts strongly and is more stable on the steel surface[191]. Values of ΔG_{ads} indicates that AMOD and HI in presence of surfactants are physically adsorbed on the metal surface[192].

6.2. Potentiodynamic Polarization Studies

Various corrosion parameters such as E_{corr}, I_{corr}, IE and CR were obtained by potentiodynamic polarization studies at 30°C in [surfactant] (= 0.20 mol dm^{-3} for AMOD and 0.10 mol dm^{-3} for HI), 500 ppm AMOD and HI after immersion for 3 hours. The results are given in Figures 6.15- 6.16 and the values of E_{corr}, I_{corr}, IE and CR are given in Tables 6.13- 6.14. The presence of surfactants decreased I_{corr}, values. Maximum decrease in I_{corr} was observed for TX-100 indicating that TX-100 is most effective surfactant. E_{corr} values do not change significantly in presence of these surfactants, suggesting that they are of mixed type inhibitors (i.e., they retard the corrosion reaction by blocking both anodic and cathodic sites of the metal[194].

6.3. Mechanism of corrosion inhibition

The presence of surfactants increased the inhibition efficiency of AMOD and HI appreciably as indicated by Figures 6.1- 6.2. The ionic

surfactants (SDS) and CTAB tend to adsorb on the surface of mild steel through electrostatic forces between the head groups and the metal surface. The adsorption of non-ionic surfactants i.e. TX-100 involves hydrogen bonding between surface hydrogen atoms and proton acceptors in polar head group and the hydrophobic bonding between the surface and the hydrocarbon tails. At lower concentration, surfactant molecules are adsorbed alongwith inhibitor to the surface plane. The increase in [surfactant] leads to the association of the adsorbed surfactant into aggregates perpendicular to the surface. Thus the surfactants are effective even at their low concentrations.

At higher concentrations, tail - tail interactions may begin to cause association of the adsorbed surfactants into an additional coverage beyond the monolayer ie. admicelles or bilayer formation. The addition of AMOD and HI to the surfactant solution further increases the inhibition efficiency as illustrated by Figures 6.1- 6.2. AMOD and HI are poorly soluble in water and exist in the protonated form in acidic solution and thereby reduces the aggressiveness of H^+. The non-ionic surfactants, TX-100 and anionic SDS bind with HI through electrostatic interaction and exist in the palisade layer of micelle[254]. Thus TX-100 and SDS help AMOD and HI to adsorb on the steel surface more firmly and, therefore, display higher IE. The IE in CTAB is higher as compared to blank AMOD and HI and lower than SDS and TX- 100. It may be due to the adsorption of AMOD and HI to the surface by binding with CTAB as coions or through hydrophobic interaction.

Table 6.1- Variation of corrosion parameters on [CTAB] for mild steel in the absence and presence of AMOD.

[CTAB] (mol dm^{-3})	In absence of AMOD			In presence of AMOD		
	Weight loss (mg)	IE (%)	CR (mmpy)	Weight loss (mg)	IE (%)	CR (mmpy)
0.0	62.4	-	23.20	11.3	81.85	4.21
0.01	31.0	50.09	11.62	9.1	85.43	3.38
0.05	28.8	54.17	10.69	8.6	86.12	3.20
0.075	29.7	54.89	11.03	7.4	88.14	2.74
0.10	24.7	60.16	9.20	5.2	91.66	1.93
0.20	23.9	61.57	8.91	4.1	93.43	1.52
0.30	24.7	60.31	9.20	6.2	90.05	2.30
0.50	26.0	58.24	9.68	10.9	82.49	4.06

[HCl]= 1.0 mol dm^{-3}; [AMOD] =500 ppm; Temp= 30 °C; Time= 3 hours

Table 6.2- Variation of Corrosion parameters on [SDS] for mild steel in the absence and presence of AMOD.

[SDS] (mol dm^{-3})	In absence of AMOD			In presence of AMOD		
	Weight loss (mg)	IE (%)	CR (mmpy)	Weight loss (mg)	IE (%)	CR (mmpy)
0.0	62.4	-	23.20	11.3	81.85	4.21
0.01	29.8	52.07	11.08	8.8	85.87	3.27
0.05	27.9	55.14	10.37	7.1	88.66	2.63
0.075	26.3	57.64	9.79	6.8	89.11	2.52
0.10	23.8	61.62	8.87	4.3	91.03	2.08
0.20	22.2	64.31	8.25	2.5	95.99	0.92
0.30	23.3	62.47	8.67	4.5	92.74	1.67
0.50	24.6	60.49	9.13	9.6	84.61	3.57

[HCl]= 1.0 mol dm^{-3}; [AMOD] =500 ppm; Temp= 30 °C; Time= 3 hours

Table 6.3- Variation of Corrosion parameters on [TX-100] for mild steel in the absence and presence of AMOD.

[TX-100] (mol dm^{-3})	In absence of AMOD			In presence of AMOD		
	Weight loss (mg)	IE (%)	CR (mmpy)	Weight loss (mg)	IE (%)	CR (mmpy)
0.0	62.4	-	23.20	11.3	81.85	4.21
0.01	23.9	61.45	8.91	7.2	88.47	2.67
0.05	22.3	63.48	8.91	6.1	90.15	2.28
0.075	20.4	67.52	8.44	5.8	90.65	2.16
0.10	16.0	73.12	7.50	2.6	95.67	1.04
0.20	15.0	75.82	6.21	1.4	97.63	0.54
0.30	15.8	74.54	5.59	1.7	97.27	0.63
0.50	17.7	71.43	6.60	4.8	92.15	1.82

[HCl]= 1.0 mol dm^{-3}; [AMOD] =500 ppm; Temp= 30 °C; Time= 3 hours

Table 6.4- Variation of Corrosion parameters on [CTAB] for mild steel in the absence and presence of HI.

[CTAB] (mol dm^{-3})	In absence of HI			In presence of HI		
	Weight loss (mg)	IE (%)	CR (mmpy)	Weight loss (mg)	IE (%)	CR (mmpy)
0.0	62.4	-	23.20	9.6	85.80	3.29
0.01	31.0	50.09	11.62	8.2	87.96	3.04
0.05	28.8	54.17	10.69	7.5	88.98	2.78
0.075	29.7	54.89	11.03	5.4	92.06	2.00
0.10	24.7	60.16	9.20	2.2	96.64	0.85
0.20	23.9	61.57	8.91	3.3	95.02	1.26
0.30	24.7	60.31	9.20	3.9	94.23	1.46
0.50	26.0	58.24	9.68	8.3	87.70	3.11

[HCl]= 1.0 mol dm^{-3}; [HI] =500 ppm; Temp= 30 °C; Time= 3 hours

Table 6.5- Variation of Corrosion parameters on [SDS] for mild steel in the absence and presence of HI.

[SDS] (mol dm^{-3})	In absence of HI			In presence of HI		
	Weight loss (mg)	IE (%)	CR (mmpy)	Weight loss (mg)	IE (%)	CR (mmpy)
0.0	62.4	-	23.20	9.6	85.80	3.29
0.01	29.8	52.07	11.08	7.2	89.66	2.61
0.05	27.9	55.14	10.37	6.1	95.02	2.27
0.075	26.3	57.64	9.79	4.7	92.96	1.78
0.10	23.8	61.62	8.87	1.6	97.53	0.62
0.20	22.2	64.31	8.25	2.6	96.16	0.97
0.30	23.3	62.47	8.67	2.8	95.76	1.07
0.50	24.6	60.49	9.13	6.7	90.02	2.52

[HCl]= 1.0 mol dm^{-3}; [HI] =500 ppm; Temp= 30 °C; Time= 3 hours

Table 6.6-Variation of Corrosion parameters on [TX-100] for mild steel in the absence and presence of HI.

[TX-100] (mol dm^{-3})	In absence of HI			In presence of HI		
	Weight loss (mg)	IE (%)	CR (mmpy)	Weight loss (mg)	IE (%)	CR (mmpy)
0.0	62.4	-	23.20	9.6	85.80	3.29
0.01	23.9	61.45	8.91	6.7	90.06	2.51
0.05	22.3	63.48	8.91	3.1	95.39	1.16
0.075	20.4	67.52	8.44	1.7	97.35	0.66
0.10	16.0	73.12	7.50	1.5	95.67	0.58
0.20	15.0	75.82	6.21	1.4	97.63	0.55
0.30	15.8	74.54	5.59	1.7	97.27	0.11
0.50	17.7	71.43	6.60	6.0	91.07	2.26

[HCl]= 1.0 mol dm^{-3}; [HI] =500 ppm; Temp= 30 °C; Time= 3 hours

Table 6.7. Variation of acid concentration on Inhibition efficiency for AMOD on mild steel in the presence of surfactants at 30 °C for 3 h.

[Acid] (mol dm^{-3})	IE (%)		
	CTAB	**SDS**	**TX-100**
1.0	93.43	95.99	97.63
3.0	87.34	93.59	94.77
5.0	82.97	89.76	91.67

[HCl] = 1.0 mol dm^{-3}; [AMOD] = 500 ppm

Table 6.8. Variation of acid concentration on Inhibition efficiency for HI in mild steel in the presence of surfactants at 30 °C for 3 h

[Acid] (mol dm^{-3})	IE (%)		
	CTAB	**SDS**	**TX-100**
1.0	96.23	97.21	99.34
3.0	96.84	97.59	98.21
5.0	97. 12	98.16	97.87

[HCl] = 1.0 mol dm^{-3} [HI] = 500 ppm

Table 6.9. Variation of Inhibition efficiency on temperature for AMOD in mild steel in the presence of surfactants.

IE (%)	Inhibition efficiency Temperature (°C)			
	30	**40**	**50**	**60**
CTAB	93.43	94.38	95.18	96.51
SDS	87.34	96.27	96.83	97.95
TX-100	82.97	97.90	98.03	98.18

[AMOD] = 500 ppm; [HCl] = 1.0 mol dm^{-3};Time= 3 hours

Table 6.10. Variation of Inhibition efficiency on temperature for HI in mild steel in the presence of surfactants

IE (%)	Inhibition efficiency Temperature (°C)			
	30	**40**	**50**	**60**
CTAB	97.43	95.85	95.38	95.20
SDS	96.64	97.31	96.98	96.73
TX-100	97.79	98.21	98.84	98.53

[HI] = 500 ppm; [HCl] = 1.0 mol dm^{-3};Time= 3 hours

Table 6.11- The thermodynamic activation parameters for the corrosion of mild steel in the absence and presence of surfactants and AMOD.

[Inhibitor] (ppm)	[Surfactant] (mol dm^{-3})	Ea ($kJmol^{-1}$)	ΔH ($kJmol^{-1}$)	$-\Delta S$ ($JK^{-1} mol^{-1}$)	$-\Delta G_{ads}$ ($kJ\ mol^{-1}$)	-Q ($kJmol^{-1}$)
0.0	0.0	50.07	47.41	205.24	-	-
500	0.0	51.12	101.41	215.98	30.24	18.02
500	0.2 (CTAB)	32.51	29.90	231.86	34.90	30.43
500	0.2 (SDS)	31.75	29.16	234.16	33.71	23.36
500	0.2(TX-100)	48.08	40.74	238.18	29.30	14.35

[HCl] = 1.0 mol dm^{-3}; Time= 3 hours

Table 6.12- The thermodynamic activation parameters for the corrosion of mild steel in the absence and presence of surfactants and HI.

[Inhibitor] (ppm)	[Surfactant] (mol dm^{-3})	Ea ($kJmol^{-1}$)	ΔH ($kJmol^{-1}$)	$-\Delta S$ ($JK^{-1}mol^{-1}$)	$-\Delta G_{ads}$ ($kJ\ mol^{-1}$)	-Q ($kJmol^{-1}$)
0.0	0.0	50.07	47.41	205.24	-	-
500	0.0	30.73	47.14	188.88	26.54	27.24
500	0.2 (CTAB)	57.50	46.91	227.97	27.56	10.72
500	0.2 (SDS)	55.52	60.31	229.00	26.01	17.36
500	0.2(TX-100)	26.76	79.14	231.30	25.08	33.09

[HCl] = 1.0 mol dm^{-3}; Time= 3 hours

Table 6.13- Values of E_{corr} , I_{corr} and IE for the corrosion of mild steel under varying conditions of solution composition at 30 °C.

Solution composition	E_{corr} (mV)	I_{corr} (mA cm^{-2})	IE (%)
HCl	507	0.360	-
HCl + AMOD	526	0.036	89.85
HCl + AMOD + CTAB	521	0.032	90.87
HCl + AMOD + SDS	519	0.021	94.12
HCl + AMOD + TX-100	514	0.012	96.53

[AMOD] = 500 ppm; [HCl] = 1.0 mol dm^{-3}; Time= 3 hours

Table 6.14- Values of E_{corr} , I_{corr} and IE for the corrosion of mild steel under varying conditions of solution composition at 30°C.

Solution composition	E_{corr} (mV)	I_{corr} (mA cm^{-2})	IE (%)
HCl	507	0.360	-
HCl + HI	473	0.150	58.33
HCl + HI + CTAB	431	0.032	90.87
HCl + HI + SDS	459	0.021	94.12
HCl + HI + TX-100	484	0.012	96.53

[HI] = 500 ppm; [HCl] = 1.0 mol dm^{-3}; Time= 3 hours

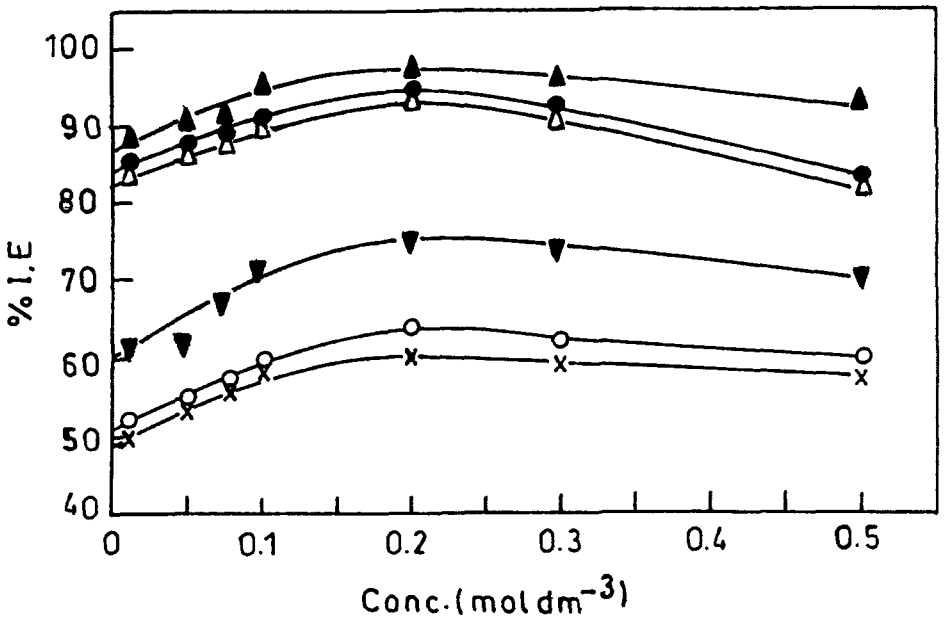

Fig 6.1. Plot of inhibition efficiency on [surfactant] in absence & presence of AMOD (**x**,CTAB; o,SDS; ▼,TX-100; Δ,CTAB+AMOD; •,SDS +AMOD; ▲,TX-100+AMOD).

Reaction conditions [HCl] =1.0 mol dm^{-3}, Temp =30°C, Time =3 hours.

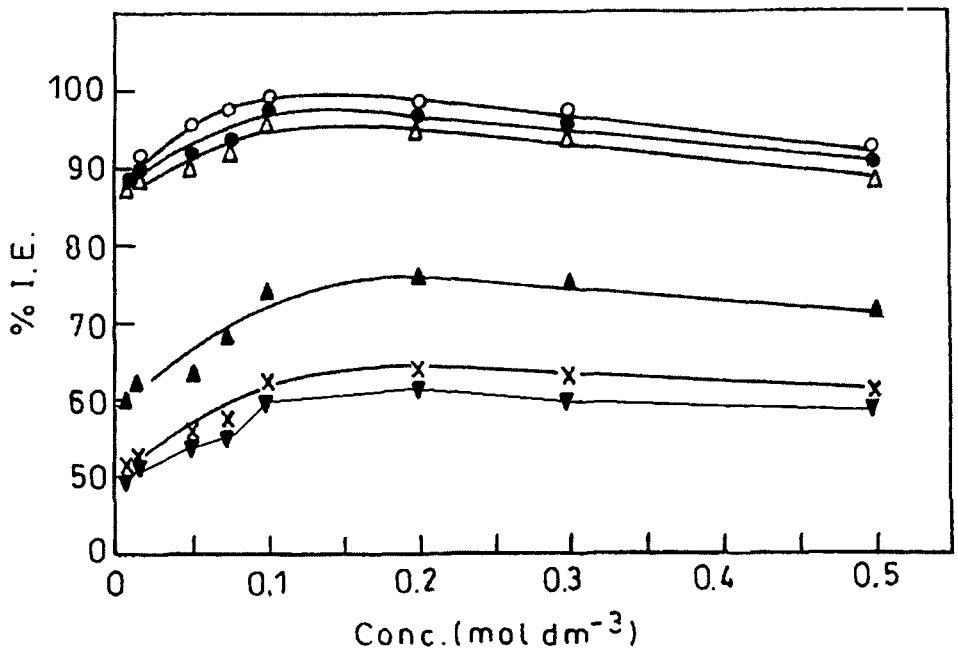

Fig 6.2. Plot of inhibition efficiency on [surfactant] in absence & presence of HI (▼,CTAB; **x**,SDS; ▲,TX-100; Δ,CTAB+HI; •,SDS +AMOD;o,TX-100 +HI)

Reaction conditions [HCl] =1.0 mol dm^{-3}, Temp =30°C, Time =3 hours.

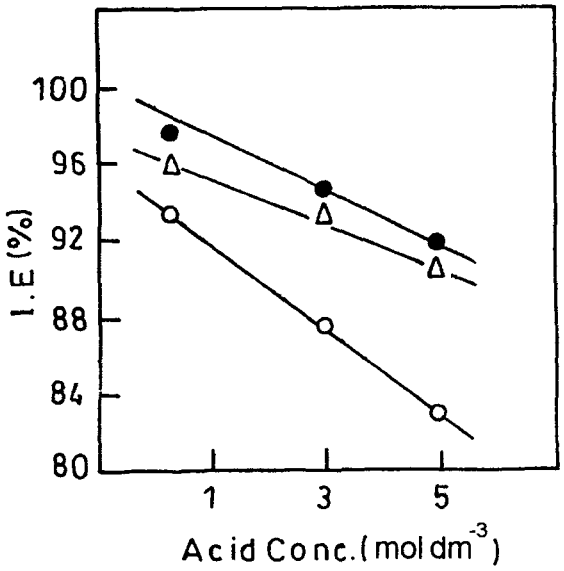

Fig.6.3. Plot of inhibition efficiency on [hydrochloric acid] (●,TX-100+AMOD; Δ,SDS+AMOD; o,CTAB+AMOD).

Reaction conditions [inhibitor]=500 ppm, Temp =30°C, Time =3 hours.

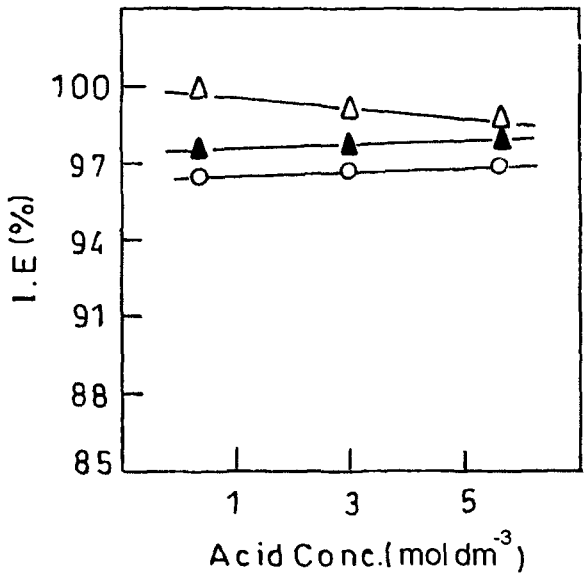

Fig. 6.4. Plot of inhibition efficiency on [hydrochloric acid] (●,TX-100+ HI; Δ,SDS+ HI; o,CTAB+ HI).

Reaction conditions [inhibitor]=500 ppm, Temp =30°C, Time =3 hours.

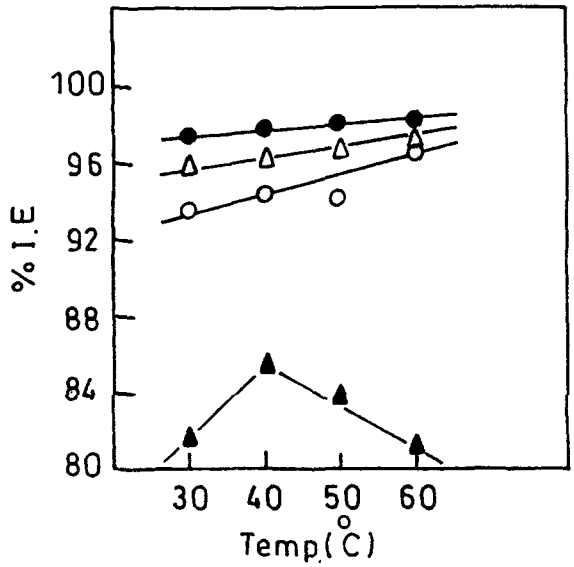

Fig 6.5. Variation of inhibition efficiency on temperature in 1mol dm^{-3} HCl (•,TX-100+AMOD; Δ,SDS+AMOD; o,CTAB+AMOD; ▲, AMOD)
Reaction conditions [HCl] =1.0 mol dm^{-3}, Time =3 hours, [inhibitor]=500 ppm.

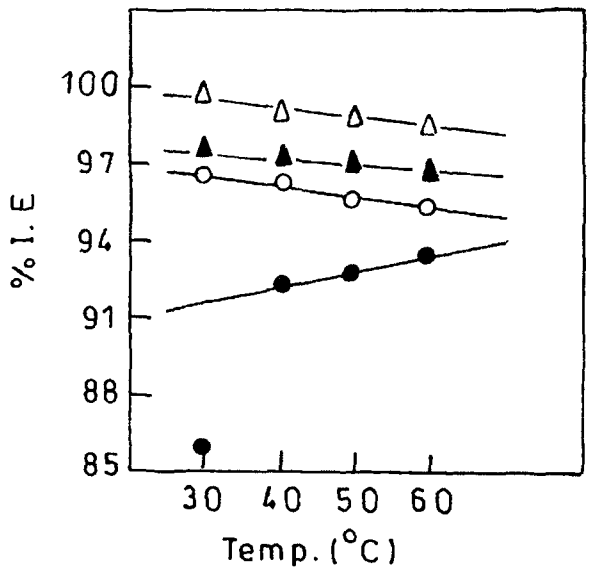

Fig 6.6. Variation of inhibition efficiency on temperature in 1mol dm^{-3} HCl (Δ,TX-100+HI; ▲ ,SDS+HI; o,CTAB+HI; •, AMOD).
Reaction conditions [HCl] =1.0 mol dm^{-3}, Time =3 hours, [inhibitor]=500 ppm.

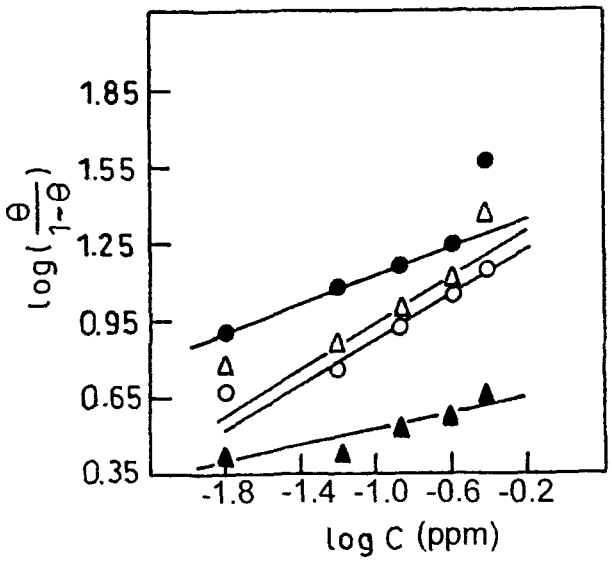

Fig.6.7. Langmuir's isotherm plots for the adsorption of surfactants in presence of AMOD in 1mol dm^{-3} HCl on mild steel (●,TX-100+AMOD; Δ,SDS+AMOD; o,CTAB+AMOD; ▲, AMOD).

Reaction conditions [HCl] =1.0 mol dm^{-3}, Temp =30°C, Time =3 hours.

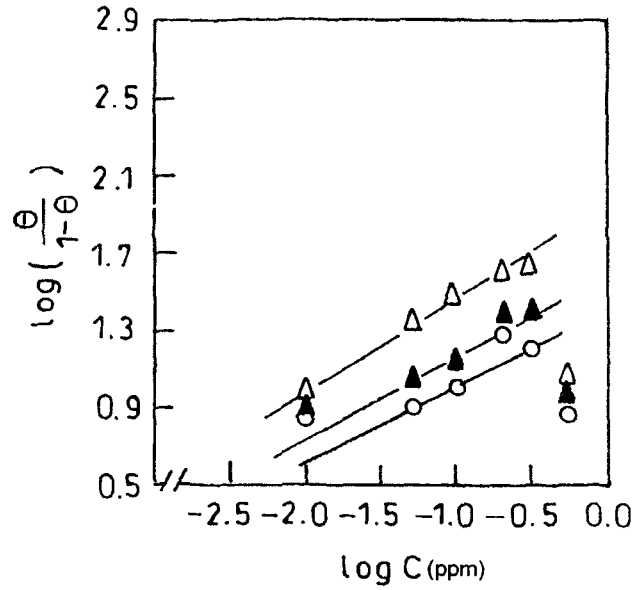

Fig.6.8. Langmuir's isotherm plots for the adsorption of surfactants in presence of HI in 1mol dm^{-3} HCl on mild steel (●,TX-100+HI; Δ,SDS+HI; o,CTAB+HI; ▲, HI).

Reaction conditions [HCl] =1.0 mol dm^{-3}, Temp =30°C, Time =3 hours.

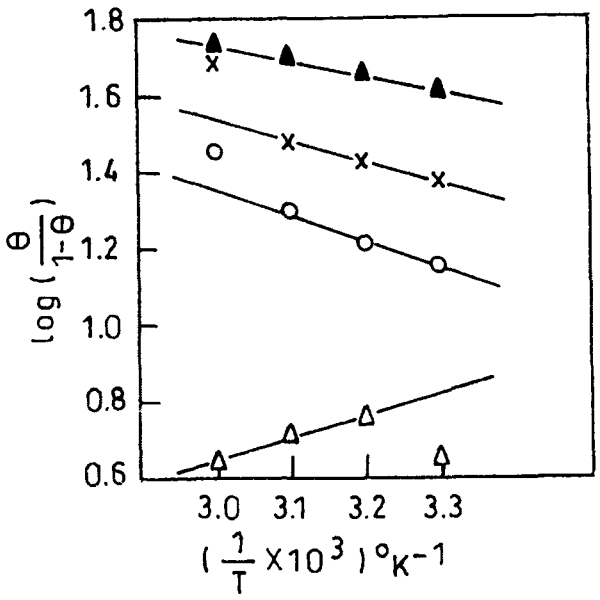

Fig. 6.9. Arrhenius plot for log (θ /1- θ) versus 1/T (▲,TX-100+AMOD; **x**, SDS+AMOD; o, CTAB+AMOD; **Δ**, AMOD).

Reaction conditions [HCl] =1.0 mol dm^{-3}, Time =3 hours, [inhibitor]=500 ppm.

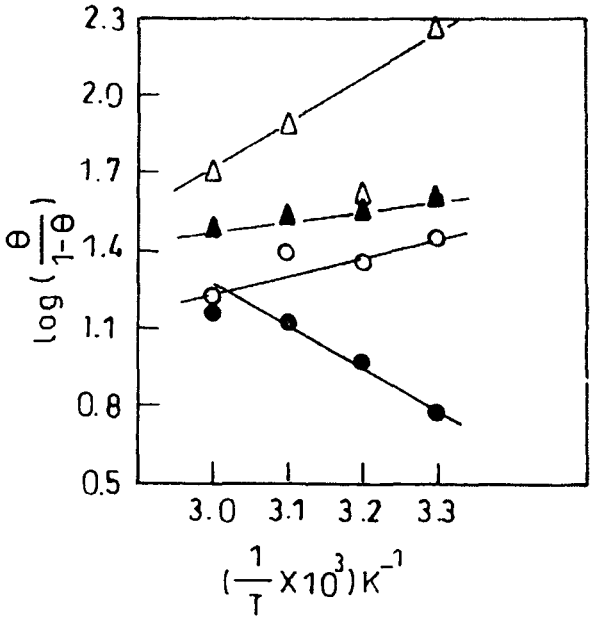

Fig.6.10 Arrhenius plot for log (θ /1- θ) versus 1/T (**Δ**,TX-100+ HI; ▲, SDS+HI; o, CTAB+ HI; •, HI)

Reaction conditions [HCl] =1.0 mol dm^{-3}, Time =3 hours, [inhibitor]=500 ppm.

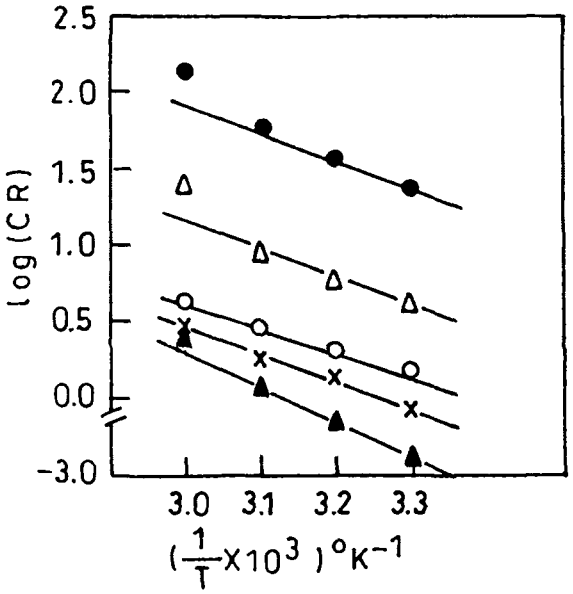

Fig. 6.11. Arrhenius plot for log (CR) versus 1/T (▲,TX-100+AMOD; **x**, SDS+AMOD; o, CTAB+AMOD; **Δ**, AMOD; •, Blank).

Reaction conditions [HCl] =1.0 mol dm^{-3}, Time =3 hours, [inhibitor]=500 ppm.

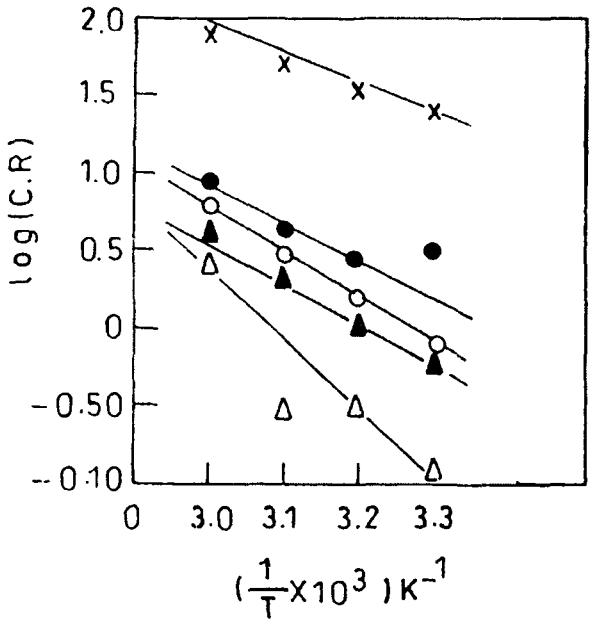

Fig 6.12. Arrhenius plot for log (CR) versus 1/T (**Δ**,TX-100+HI; ▲, SDS+ HI; o, CTAB+ HI; •, HI; **x**, Blank).

Reaction conditions [HCl] =1.0 mol dm^{-3}, Time =3 hours, [inhibitor]=500 ppm.

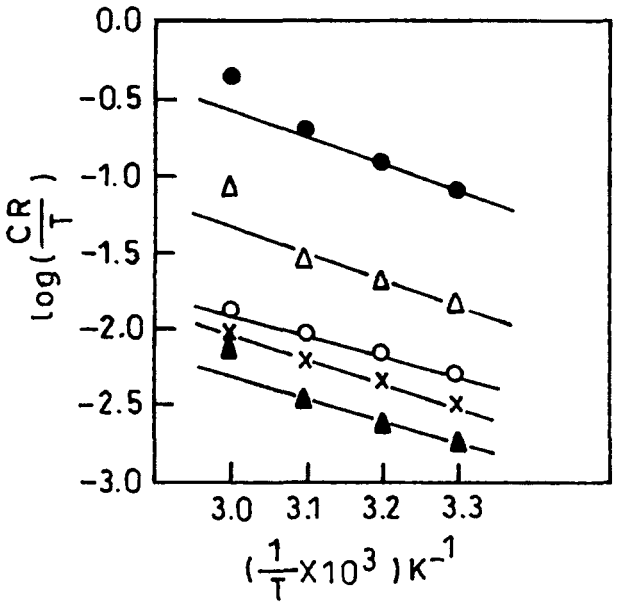

Fig. 6.13. Arrhenius plot for log (CR/T) versus 1/T (▲,TX-100+AMOD; **x**, SDS+AMOD; o, CTAB+AMOD; **Δ**, AMOD; •, Blank).

Reaction conditions [HCl] =1.0 mol dm^{-3}, Time =3 hours, [inhibitor]=500 ppm.

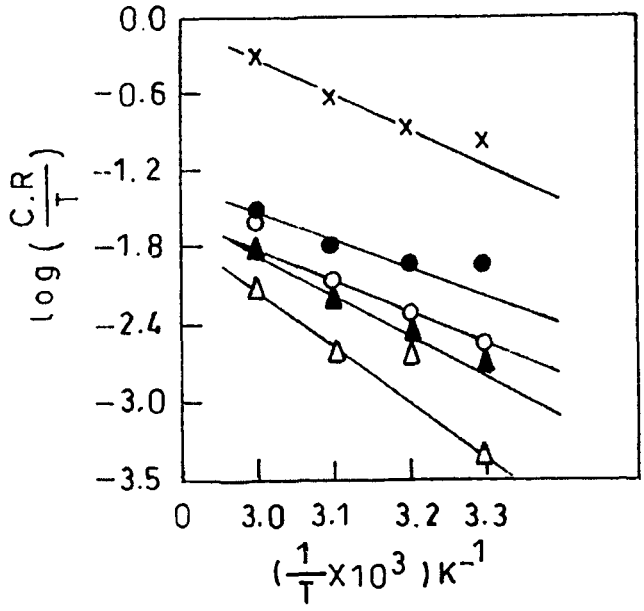

Fig. 6.14. Arrhenius plot for log (CR/T) versus 1/T (**Δ**,TX-100+HI; ▲, SDS+ HI; o, CTAB+ HI; •, HI; **x**, Blank).

Reaction conditions [HCl] =1.0 mol dm^{-3}, Time =3 hours, [inhibitor]=500 ppm.

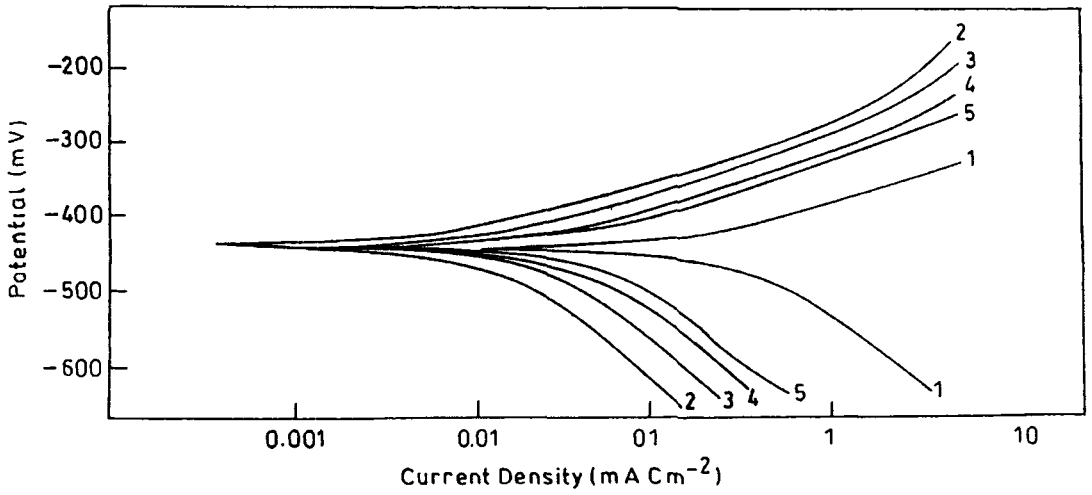

Fig 6.15. Potentiodynamic polarization curves of AMOD on mild steel (1) Blank (2) TX-100+AMOD (3) SDS+AMOD (4) CTAB+AMOD (5) AMOD Reaction conditions[HCl]= 1.0 mol dm^{-3}, Temp =30°C.

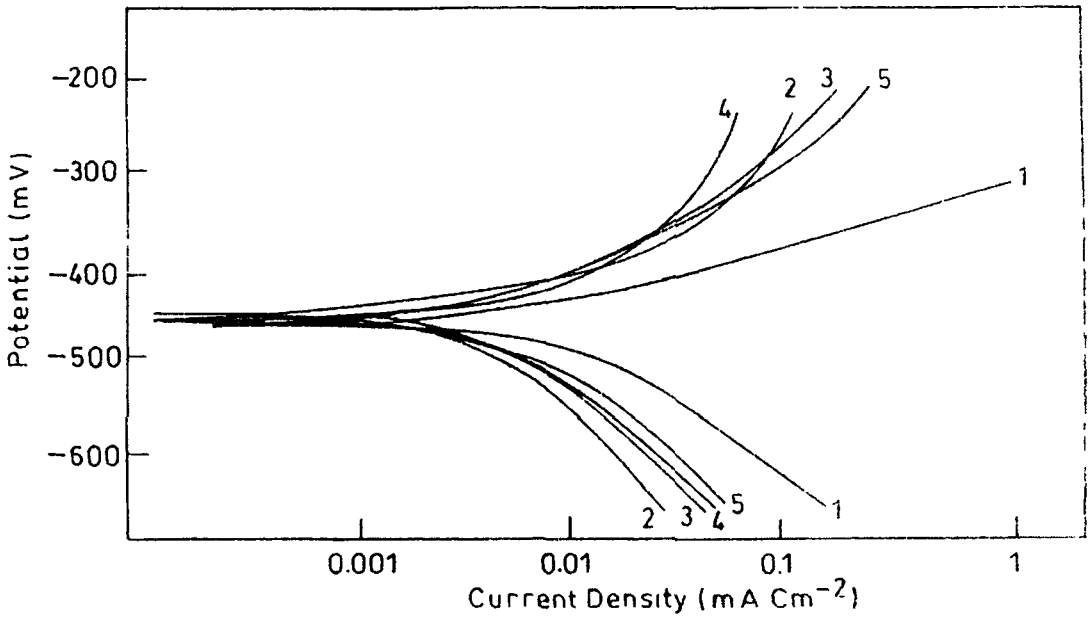

Fig 6.16. Potentiodynamic polarization curves of HI on mild steel (1) Blank (2) TX-100+HI (3) SDS+HI (4) CTAB+ (5) HI.
Reaction conditions[HCl]= 1.0 mol dm^{-3}, Temp =30°C.

REFERENCES

1. L. Shreir, *Corrosion*, 1 (1978) 16.

2. M. Stern and A. L. Geary, *J. Electrochem. Soc*, 104 (1957) 56.

3. M. Stern, *Corrosion*, 14 (1958) 440.

4. L. Gaiser and K. E. Heusle, *Electrochem. Acta*, 15 (1970) 161.

5. W. J. Lorenz, F. Hilberst, Y. Miyoshi and G. Eichkorn, Proc. 5th International Congress on Metallic Corrosion, Tokyo, Japan 1972 p.74.

6. H. H. Uhlig, *Corros. Sci*, 19 (1979) 777.

7. R. W. Revie, B. G. Baker and J. O'M. Bockris, 6th International Congress on Metallic Corrosion, Sydney. Australia 1975 p.1.

8. G. R. Chhatwal, "*Advanced Physical Chemistry*", Goel Publishing House, Meerut 1988 p. 101.

9. NACE, Inter. Bull, Houston (1992).

10. A.S. Khanna, News letter, NACE, India 4 (1997) 3.

11. F.N. Spellar, "*Corrosion: causes and prevention- An Engineering Problem*", Mc Graw Hill, New York 1935 p.8.

12. M.G. Fontana and N.D. Greene, "*Corrosion Engineering*", Mc Graw-Hill, New York 1967 p.43.

13. H.J.M Creigton and W.A. Kochler, "*Principles and Application of Electrochemistry*", Chapman & Hall, London 1943 p. 358.

14. A.S. Cushman, Scientific American supplement, 64 (1907) 151.

15. F. C. Burgess and S. G Engle, *Trans. Amer. Electrochem. Soc*, 9 (1903) 199.

16. W.H. Ailor, "*Engine Coolant Testing: State of the Art*", ASTM International 1980 p. 134.

17. G.W. Wrangler, "*An Introduction to Corrosion and Protection of metals*" Chapman and Hall, London 1985 p. 147.

18. G. L. Cherepakhova, A. V. Shreider and G. P. Charikova, *Chemical and Petroleum Engineering*, 6 (1970) 490.

19. J.H. Martin, "*Concise Encyclopedia of the Structure of Materials*", Elsevier 2006 p. 418.

20. D. R. Bush, J. C. Brown and K. R. Lewis, *Hydrocarbon Processing,* 2004 p. 73.

21. P. Marshall "*Austenitic stainless steels:- Microstructure and Mechanical Properties*", Springer 1984 p. 409.

22. K.J. Mcnaughton, "*Materials Engineering*" Reinhold Publishing Corporation 1992 p. 623.

23. D. Zeng, K. C. Yung and C. Xie, Scripta Materialia, 44 (2001) 2747.

24. V. G. D'yakov, A. V. Shreider and L. D. Zakharochkin, *Chemical and Petroleum Engineering*, 1 (1965) 587.

25. W.J. Neill, *Mater Perform* 19, (1980) 57.

26. P.A. Schweitzer, "*Corrosion- Resistant Lining and coating*", CRC Press 2001 p. 391.

27. E. Zcchech, C. Whelan and T.Mikolayick, "*Materials for Information Technology: Devices, Interconnects and Packaging*", Springer 2005 p. 366.

28. N. Hackermann and R.M. Hurd, 1st International Congress on Metallic Corrosion, Butterworths, London 1962 p.166.

29. K.S. Lee and D.H. Hwoejee, *Corros. Sci*, 13 (1969) 1375.

30. NACE-Glossary of Corrosion Terms, *Mat. Prot*, 4 (1965) 79.

31. D.M. Drazic, "*Modern Aspects of Electrochemistry*", Plenum Press, New York 1989, p. 69.

32. F. Mazza and N.D. Greena, Proc. 2nd Eur. Symp. on Corros. Inhi, Univ. of Ferrara, Ferrara, Italy 1965 p. 401.

33. R.H. Halusler, *"Corrosion Chemistry"*, ACS. Symp. Series, 89(1979) 262.

34. K. Juttener, *Workst. Und. Korros*, 31 (1980) 358.

35. G.W. Poling, *J.Electrochem.Soc,* 114 (1967) 1209.

36. G. L. Zucchini, F. Zucchi and G. Trabenelli, 3rd Eur. Symp. on Corros. Inhi, Ferrara, Italy 1971 p. 577.

37. U. R. Evans, "*Metallic Corrosion, Passivity and Protection*", Edward Arnold and Co, London 1948 p. 535.

38. J.G.N. Thomas and T.J. Nurse, *Br. Corros. J*, 2 (1967) 13.

39. Y.I Kuznetsor, "*Organic Inhibitors of Corrosion of Metals*", Springer 1996 p. 766.

40. M.A. Quraishi, M.A. Wajid Khan and M.Ajmal, *Anti –Corros. Meth. Mater*, 43 (1996) 5.

41. S.Muralidhran and S.V. K. Iyer, *Anti –Corros. Meth. Mater*, 44 (1997) 100.

42. N. Al- Andis and E. Khamis, *Corrosion. Prev. Control*, 42 (1995) 13.

43. B. Hammonite, *Corrosion*, 51 (1995) 41.

44. M.A. Quraishi, S.Muralidhran and S.V. K. Iyer, *Corrosi Sci*, 37 (1995) 1794.

45. M.A. Quraishi, M.A. Wajid Khan, M.Ajmal, S.Muralidhran and S.V. K. Iyer, *Br. Corros. J*, 32 (1997) 72.

46. M.M. Osman, E. Khamis and A. Michael, *Corrosion. Prev. Control*, 41 (1994) 34.

47. E. Stupnisek- Lisac and M. Metikos-Hukovic, *Br. Corros. J*, 28 (1993) 74.

48. S.L. Granes, *Corros Sci*, 33 (1992) 1439.

49. F.Zucchi and G.Trabanelli, Proc.7th European Symp. on Corros. Inhi, Univ of Ferrara, Ferrara, Italy1990 p.339.

50. G. Subramanian, K.Balasubramania and P. Sridhar, *Corros Sci*, 30, (1990) 1019.

51. S. Rangmani, S. Muralidharan, M. Ganesan and S.V. K. Iyer, *Indian J. Chem. Technol*, 1 (1994) 168.

52. S. Rangmani and S. Muralidharan, *J. Appl. Electrochem*, 24 (1994) 355.

53. S. Rangmani, T. Vasudevan and S.V.K. Iyer, *Indian J. Chem. Technol*, 31 (1993) 519.

54. K. Aramaki, T. Oya and S. Fuji, *Boshoki Gijutsu*, 31 (1961) 519.

55. N. Hackerman and R.M. Hurd, Proc. 1st Int. Cong. On Metallic Corrosion, London, United Kingdom 1960 p. 166.

56. O.L. Riggs and R.L. Every, *Corrosion*, 18 (1962) 262.

57. A. Raman and P. Labini, "*Reviews on Corrosion Inhibitiors Science & Technology*", Houston, NACE 1986 p. 20.

58. B.A. Abd –el-habey and E.Khamis, *Surf. Coat.Technol*, 28 (1986) 67.

59. M.A. Quraishi, D. Jamaal and R.N. Singh, *Corrosion*, 58 (2002) 201.

60. M.A. Quraishi, M.Ajmal, M.A. Wajid Khan and S.Muralidharan, *Port. Electrochim. Acta*, 13 (1995) 63.

61. M.A. Quraishi, M.Ajmal, M.A. Wajid Khan, S.Muralidhran and S.V.K. Iyer, *Anti–Corros Methods Mater*, 43 (1996) 5.

62. M.A. Quraishi, M.Ajmal, M.A. Wajid Khan, S.Muralidhran and S.V.K. Iyer, *J. Appl. Electrochem*, 26 (1996) 1253.

63. M.A. Quraishi, M.Ajmal, M.A. Wajid Khan, S.Muralidhran and S.V.K. Iyer, *Br. Corros. J*, 32 (1997) 72.

64. M.A. Quraishi, M.Ajmal, M.A. Wajid Khan, S.Muralidhran and S.V.K. Iyer, *Corrosion*, 53 (1997) 475.

65. E.G. Turbina and N.G. Klyuchnikov, *Uch. Zap. Mosl. Gos. Pedagog. Inst.*, 303 (1969) 50 [Chem. Abs. 77 (1972) 52712t].

66. N.G. Klyuchnikov and E.G. Turbina, *Uch. Zap. Mosl. Gos. Pedagog. Inst*, 340 (1974) 40 [Chem. Abs. 77 (1972) 65239u].

67. N.G. Klyuchnikov and G.L. Nemchninovas, *Inhibitory Korroz. Met*, 56 (1974) [Chem. Abs. 86 (1977) 175092j].

68. V.I. Komarov and S.A. Balezin, USSR Patent 141049. September 20th 1961 [Chem. Abs.56 (1962) 9830 c].

69. N.G. Klyuchnikov, *Uch. Zap. Mosl. Gos. Pedagog. Inst*, 340 (1971) 67 [Chem. Abs. 77 (1972) 29103z].

70. G.L. Nechaninova and N.G. Klyuchnikov, *Inhibitory Korroz. Met*, 117 (1972) [Chem. Abs. 84 (1976) 48408 a].

71. G.L. Nechaninova, N.G. Klyuchnikov and Izv. Vyssh.Ucheb. Zaved, *Khim. Tekhnol*, [Chem. Abs. 75 (1971) 8972].

72. R.H. Scott and H.B. Lockhart, (Celanese corp., USA) U.S. Patent 3, 770, 377, November 6th. 1973., [Chem. Abs. 80 (1974) 99352].

73. E.A. Braied and H.M. Winn, *Corrosion* 7(1951) 180.

74. W. Costsain and B.W.H. Terry, (Imperial Chemical Industries Ltd., England), Ger. Offen. 2, 147, 487, March 30th 1972., [Chem. Abs. 77 (1972) 82988e].

75. T. Kataoka and A. Tkada, (Nisin Oil Mills, Ltd., Japan), U.S. Patent 3,736,098. May 29th 1973; [Chem. Abs. 79 (1973) 4870].

76. T. Kataoka and A. Tkada, (Nisin Oil Mills, Ltd., Japan), Japan Patent 7415, 145. April 12th 1974 [Chem. Abs. 83 (1975) 193310].

77. J.M. Sykes, *Br. Corros. J*, 25 (1990)175.

78. M. Elachouri, *Corros. Sci*, 37 (1995) 381.

79. P.Chatterjee, M.K. Banerjee and K.P. Mukerjee, *Ind. J. Technol*, 29 (1991) 191.

80. F. Bentiss, M. Lagrenee and M. Traisnel, *Corros. Sci*, 40 (1998) 391.

81. A.B. Tadros and Abdenaby, *J. Electroanol Chem*, 246 (1988) 433.

82. F. Bentiss, M. Lagrenee and M. Traisnel, *Corros. Sci*, 41 (1999) 789.

83. R.J. Chin and K. Nobe, *J. Electroanol Chem*, 118 (1971) 545.

84. R. Agarwal and T.K.G. Namboodhiri, *J. Appl. Electrochem*, 22 (1992) 383.

85. N. Elkadar and K. Nobe, *Corrosion*, 32 (1976) 128.

86. J.O.M Bockris and A.K.N Readey, "*Modern Electrochemistry: An Introduction to an Interdisciplinary Area*", Springer 1970 p.1311.

87. E. Vuorinen, E. Kalman and W. Folke, *Surface Engineering* 20 (2004) 281.

88. S. U. M Khan, "*Surface Electrochemistry: A Molecular Level approach*", Springer 1993, p. 804.

89. R.S. Thornhill, *Ind. Eng. Chem*, 37 (1945) 706.

90. D. Talbot, "*Corrosion Science and Technology*", CRC Press, 1998 p.118.

91. R.E Kirk and D.F Othmer, *"Encyclopedia of Chemical Technology"*, Wiley 1979 p. 135.

92. W. Machu, *Trans. Electrochem. Soc*, 72 (1937) 333.

93. S. Q Deans Jr., R. Derby and G. T. Von Dem Burrche, *Mat Perform*, 20 (1981) 47.

94. B. Guo, *"Offshore pipelines"* , Elsevier 2005 p.199.

95. N. Hackermann and F. N. Finley, *J. Electrochem. Soc*, 107 (1960) 259.

96. N. Hackermann, Proc. 1st Eur, Symp. Corros. Inhib. Ferrara, Italy 1961 p. 9.

97. L. I. Antropov, *Corros. Sci*, 7 (1967) 607.

98. W. Machu, 1st. Eur. Symp. Corros. Inhib., Ferrara, Italy 1961 p. 183.

99. L. Horner, *Werkst Und. Korros*, 23 (1972) 466.

100. G. Trabanelli, F. Zucchi, G. Gullini and V. Carassiti, *Brit. Corros. J*, 4 (1969) 212.

101. T. P. Hoar and R. P. Khera, 1st Euro. Symp. Corros. Inhi. Univ. of Ferrara, Italy 1961 p. 73.

102. E. Blomgresens, J.O'M. Bockris and C. J. Jesch, *Z. Physik. Chem*, 65 (1961) 2000.

103. S.Q. Deans Jr, R. Derby and G.T. Von Dem Burrche, *Mat Perform*, 20 (1981) 47.

104. F. M. Donahue and K. Nobe, *J. Electorchem Soc*, 114 (1967) 1012.

105. E. J. Kelly, *J. Electrochem. Soc,* 115 (1968) 1111.

106. L. Cavallara, L. Felloni, F. Pulidori and G. Trbanelli, *Corrosion*, 18 (1962) 396.

107. B. M. W. Traprell, "*Chemisorption*", Butterworths Scientific Publication, London 1955 p 109.

108. M. Kutz, "*Handbook of Environmental Degaradation*" William Andrew Inc. 2005 p. 16.

109. W.L. Nelson, "*Petroleum Refinery Engineering*" Mc Graw Hill, New York 1941 p. 163.

110. D.R. Morris, L.P. Sampaleanu and D.N. Veysey, *J. Electrochem. Soc*, 127 (1980) 1228.

111. C. Leyens and M. Peterns, "*Titanium and Titanium alloys: Fundamental and application*" Wiley VCH 2003 p. 397.

112. S.T. Keera, *Anti–Corros Methods Mater,* 50 (2003) 280.

113. A.E. Dunstan, "*The Science of Petroleum*", Oxford University Press 1993 p. 189.

114. E.F. Roeber and H.C. Parmelee, "*Chemical and Metallurgical Engineering*", Mc Graw Hill, New York 1946 p. 136.

115. J.R. Crum, M.E. Adkins and W.G. Lipscomb, *Mat Perform*, 25 (1986) 27.

116. D.A. Hansen and R.B. Puyear, "*Material Selection for hydrocarbon and Chemical Plants*", CRC Press 1996 p. 154.

117. T. Kuppan, "*Heat Exchanger Design Handbook*", CRC Press 2000 p.735.

118. G.C. Moran and P. Labine, "*Corrosion Monitoring in Industrial Plants using Non destructive Testing and Electrochemical Methods*", ASTM International 1986 p. 32.

119. U.R. Evans and A.S. Winteratem, "*Metallic Corrosion, Passivity & Protection*" , E. Arnold & Co 1943 p. 340.

120. B.S. Wynor, A.G. Pattersons and D.A. Rothscheld, "*American Reference Books Annual*", Libaries Unlimited 1970 p. 611.

121. O.T. Zimmerman and I. Lavine, "*Industrial Research Service's Handbook of Material Trade Names*", Industrial Research Service 1953 p.60.

122. N. Hackermann and R.M. Hurd, 1st International Congress on Metallic Corrosion, Butterworths, London, 1962 p. 166.

123. K.S. Lee and D.H. Hwoejee, *Corros. Sci,* 13 (1969) 1375 [Chemical. Abstract. (1964) 72, 14978Y].

124. W. Machu, 3rd European symp Corrosion Inhibitors, Ferrara, Italy 1970 p. 107.

125. H.B. Walker, "*Reduce Fluid Catalytic Cracking (FCC) corrosion*", *Hydrocarbon processing*, 1984 p. 80.

126. S.L. Granes, B.M. Rosales, 10th International congress on metallic corrosion, Madras, India, 1987 p. 2733.

127. S. Hettvarchch, Y.W. Chan, R.B. Wilson and V.S. Agrawal, *Corros. Sci*, 45 (1989) 30.

128. G. Trabanelli and F.Zucchi, Proc 7th European Symposium on Corrosion Inhibitors Ferrara, Italy 1990 p. 339.

129. I.H. Omar and F.Zucchi, Proc 7th European Symposium on Corrosion Inhibitors Ferrara, Italy 1990 p. 321.

130. A. Jayaraman, R.C. Saxena, K.D. Neemla, "*The control of internal corrosion of petroleum pipelines by inhibitors*", Corrosion Prev. Control, 1991 p. 119.

131. M.J. Mehta, *"Chemical Engineering World"*, 27 (1992) 67.

132. S.L. Granes, B.M. Raosales, C. Orienda, J.O. Zerbino, *Corros. Sci*, 33 (1992) 1989.

133. S. Murlidharan, M.A. Quraishi and S.V.K. Iyer, *Protg. Electrochem Acta*, 11(1993) 225 .

134. R.D. Kane, S.M. Wilhelm, W.G. Ashbough and R.G. Taraborelli, "*Simulate Chemical Process Corrosion in the Laboratory*", Chemical Engineering Progress 1993 p. 65.

135. R.D. Keera, S. Eissa, A. Elha and A. R. Taman, *Research & Industry*, 39 (1994) 175.

136. M. Ajmal, A.S. Mideen, M.A. Quraishi, *Corros. Sci*, 36(1994) 274.

137. R.D. Kane and M.S. Cayard, "*Improve corrosion control in Refining Process"* Hydrocarbon processing 1995 p. 129.

138. M.A. Quraishi, M.A.W Khan and M. Ajmal, *Electrochem acta*, 11 (1995) 274.

139. R. Prasad, "*Petroleum Refining Technology*" 2000 p. 329.

140. V.S. Shastri, "*Corrosion Inhibitors Principles& Application*" John Wiley England p.677.

141. D.W. Alley and N.D. Coble, *Mater. Perform,* 45 (2003) 44.

142. L.J. Rokhehar, "*Corrosion in Refinery*", 11th National Congress on corrosion control Vadodra, India 2003 p. 29.

143. N. Raut and J. Patel, "*Corrosion of stripper overhead at Naptha – hydro-desulpherization plant*", 11th National Congress on corrosion control Vadodra, India 2003 p. 17.

144. M.A. Migahed, *Progr. Org. coat*, 54 (2005) 91.

145. A.S. Fouda, A.A. Al-Sarawy and E.E. El-Katori, *Desalination*, 201 (2006) 1.

146. M. A. Amin, S.S. Abd El-Rehim, E.E.F. El-Sherbini and R. S. Bayoumi, *Electrochim. Acta*, 52 (2007) 3588.

147. C.D. Danlate, A.M. Mirajkar and K.M. Hosamani, *J Oil Tech Assoc India*, 21 (1984) 27.

148. M. Iqbal, M H Kittur and C S Mahajanshetti, *J Oil Tech Assoc India*, 16 (1984) 49.

149. K. Hofmann, "*Imidazolines & its derivatives – Part 1: The chemistry of heterocyclic compound*", Interscience Publishers, New york 1953 p. 213.

150. S.N. Dubey and Beena Kaushik, *Ind. J. Chem*, 24 (B) (1985) 950.

151. M.S. Chande, R.S. Jagtap and R.N. Sharma, *Ind. J. Chem*, 34 (B) (1995) 924.

152. Standard Practice for Laboratory Immersion Corrosion Testing of Metals, Annual Book of Standards, ASTM 1990, 3.02, G 31-72.

153. Metal Corrosion, Erosion and Wear, Annual Book of ASTM Standards, ASTM 1987, 03-02, G1-72.

154. Standard Practice for conducting potentiodynamic polarization resistance measurements, Annual Book of Standards, ASTM 1991, G 59 -91.

155. Standard Practice for Calculation of Corrosion Rate and related Information from Electrochemical Measurements, Annual Book of Standards, ASTM 1994, 3.02, G 102-89.

156. Basics of AC Impedance Measurements, EG & G Princeton Applied Research, Application Note: AC-1.

157. H Ashassi-Sorkhabi, B Shaabani & D Seifzadeh, *Electrochim. Acta*, 50 (2005) 3446.

158. M .A. Quraishi and S Khan, *Ind.J. Chem. Technol*, 12 (2005) 576.

159. C. B. Breslin and W.M. Carrol, *Corros. Sci*, 34 (1993) 327.

160. M.G. A. Khedr and M. S. Lashien, *Corros. Sci*, 33 (1992) 137.

161. M. Schorr and J. Yahalom, *Corros. Sci*, 12 (1972) 876.

162. L. J. Jha, Ph.D Thesis – Delhi University, Delhi, India, 1990.

163. S.S. Abd El Rehim, *Mater Chem Phys*, 70 (2001) 268.

164. O.K.Orubite and N.C. Oforka, *J. Appl. Sci. Environ*, 8 (2004) 57.

165. P.W. Atkins, "*Chemisorbed and Physisorbed Species- A Textbook of Physical Chemistry*", University Press, Oxford 1980 p. 936.

166. F Hanna, G M Sherbini and Y Brakat, *Brit Corros J*, 24 (1989) 269.

167. B M Badran, A A Abdel Fattah and A A Abdul Azim, *Corros. Sci,* 22 (1982) 513.

168. B M Badran, A A Abdel Fattah and A A Abdul Azim , *Corros. Sci*, 22 (1982) 525.

169. S.S. Abd El Rehim, M.A.M. Ibrahim and K.F. Khalid, *J. Appl. Electrochem*, 29 (1999) 593.

170. P. Chatterjee, M.K. Banerjee and K.P. Mukherjee, *Indian J. Technol*, 29 (1991) 191.

171. S. Rengamani, S.Muralidharan, M. Anbu Kulamdainathan and S.Venkatakrishna Iyer, *J. Appl. Electrochem,* 24 (1994) 355.

172. G.K. Gomma and M.H. Wahdan, *Bull. Chem. Soc. Jpn*, 67 (1994) 2621.

173. A. El-Sayed, *J. Appl. Electrochem*, 27 (1992) 193.

174. A.V. Radushev, A.B. Shein, R.G. Aitov, V.U. Gusev, N.E. Petina, G.I. Popov and N.B. Tarasova, *Protection of Metals*, 28 (1992) 667.

175. E.S. Lower, *Corrosion. Prev. Control*, 37 (1990) 121.

176. G.Schmitt, *Br.Corros.J,* 19 (1984) 165.

177. L. Larabi, Y. Harek, O. Benali and S. Ghalem, *Prog. Organ. Coat*, 54 (2005) 256.

178. B.I. Ita and O.E. Offiong, *Mater. Chem. Phys*, 48 (1997) 164.

179. A.A. El-Shafei, *Mater. Chem. Phys,* 70 (2001) 175.

180. M. A. Quaraishi, D.Jamal and M. T. Saeed, *J. Am. Oil. Chem.Soc*, 77 (2000) 265.

181. M. A. Quaraishi and D. Jamal, *Mater. Chem. Phys,* 78 (2003) 608.

182. B.H. Loo, Y.G. Lee and A.El- Hage, Proc. 9thInt. Conf. on Raman Spectroscopy, Tokyo.

183. M. A. Quaraishi and F.A. Ansari, *J. Appl. Electrochem*, 36 (2006) 309.

184. M. A. Quraishi, J. Rawat and M. Ajmal, *Corrosion* , 54 (1996) 99.

185. I.N. Putilova, S.A. Balzin and U.P. Branik, "Mettalic corrosion inhibitors", Pergamon Press, New York 1960 p. 31.

186. F. Bentiss, M.Lebrini and M.Lagrenee, *Corros. Sci,* 47 (2005) 2915.

187. S.S. Abd El Rehim, M.A.M. Ibrahim and K.F. Khalid, *Mater. Chem. Phys,* 70 (2001) 268.

188. A. Yurt, A. Balaban, S.U. Kandemir, G. Bereket and B. Erk, *Mater. Chem. Phys,* 85 (2004) 420.

189. M. K. Gomma and M.H. Wahdan, *Mater. Chem. Phys,* 39 (1995) 209.

190. M. Schorr and J Yahalom, *Corros. Sci*, 12 (1972) 876.

191. G. K. Gomma and M.H. Wahdan, *Ind. J. Chem. Technol,* 2 (1995) 107.

192. S. Brinic, Z. Grubac, R. Babic and M. Metikos-Hukovic, 8th Euro. Symposium on Corrosion Inhibitors, Ferrara, Italy 1995 p. 197.

193. M.A. Quraishi and S. Khan, *J. Appl.Electchem*, 36 (2006) 539.

194. M.A. Quraishi and F.A. Ansari, *J. Appl.Electchem*, 36 (2006) 309.

195. K. Juttner, *Electrochim. Acta*, 35 (1990) 1501.

196. S.L. Li, Y.G. Wang, S.H. Chen, R. Yu, S.B. Lei, H.Y. Ma and D.X. Liu, *Corros.Sci,* 41 (1999) 1769.

197. N.C. Subramaniyam, and S. Mayanna, *Corros.Sci,* 25 (1985) 163.

198. H.L. Wang, H.B. Fan and J.S. Zheng, *Mater. Chem. Phys,* 77 (2002) 655.

199. M. A. Quraishi, A.S. Mideen, M.A.W. Khan, and M. Ajmal, *Ind. J. Chem. Technol*, 1 (1994) 329.

200. M. A. Quraishi, N. Saxena and D. Jamal, *Ind.J. Chem. Technol,* 11 (2005) 220.

201. M.A. Quraishi and F.A. Ansari, *J. Am. Oil. Chem.Soc,* 80 (2003) 3.

202. S.S. Abd El Rehim, M.A.M. Ibrahim, K.F. Khalid, *J. Appl. Electrochem*, 29 (1999) 593.

203. A. El-Sayed, *J. Appl. Electrochem*, 27 (1997) 193.

204. A.R. Kartritzky, "*Advances in Hetrocyclic Chemistry*", Elsevier (2005) 84.

205. D.Bajpai and V.K. Tyagi, *J. Oleo. Sci*, 55 (2006) 319.

206. S. Ramachandran, B. Tsai, M. Blanco, H. Chen, Y. Tang, and W.A.Goddard, *Langmuir*, 12 (1996) 6419.

207. M. Joseph, J. Hodge and D. Klenerman, *Faraday Discuss,* 94 (1992) 273.

208. Y. Abbound, A. Abouriche, M.Berrada, M. Charrout, A. Cherquaue, A. Bemamara and D. Takky, *Appl. Surf. Sci,* 252 (2006) 8178.

209. D.Wang, S.Li, Y. Ying, M.Win, H.Xiao and Z. Chen, *Corros. Sci,* 41 (1999) 1911.

210. J.Zhang. G.Yang and W. Goa, *Cailiao Baohu, 34* (2001) 13.

211. D. Ghiran, I. Schwartz and I. Simiti, *Farmacia,* 22 (1974) 141.

212. J.J. Piala and H.L. Yale, U.S. Patent, 3141022 (1964).

213. V. Otieno- Alego, N. Huyuh, T. Notoya, S.E. Bottle and D.P. Schweinberg, *Corros. Sci,* 41 (1999) 685.

214. R. Gasparac, E. Stupnisek- Lisac, C.R. Martin, *Euro. Fed. Corros. Publ,* 2000 p. 20.

215. K. Wippermann, J.W. Schultze, R. Kessel and J. Penniger, *Corros. Sci,* 32 (1991) 205.

216. S. Vishwanathan and N.S. Rawat, *Ind. J. Technol,* 31 (1993) 796.

217. S. Muralidharan, M.A. Quraishi and S.V. K. Iyer, *Corros. Sci,* 37 (1995) 1739.

218. A.M.S. Abdennaby, A.I. Abdulhadi, S.T. Abu-Orabi, H. Saricimen, *Corros. Sci,* 38 (1996) 1791.

219. A.M.S. Abdennaby, A.I. Abdulhadi, S.T. Abu-Orabi, H. Saricimen, *Anti-Corros Methods Mater,* 45 (1998) 103.

220. A. Kumar, S.P. Brothakur and H.C. Dhawan, Bull. Electrochem, 15 (1999) 63.

221. M.A. Quraishi, S. Muralidharan and S.V. K. Iyer, *Anti-Corros Methods Mater,* 47 (2000) 354.

222. B. Mernari, L.El Kadi and S.Kertit, *Bull. Electrochem,* 15 (1999) 63.

223. H.L. Wang, H.B. Fan and J.S. Zheng, *Mater. Chem. Phys,* 77 (2002) 655.

224. A.H. Abdel Rahman, *Corrosion,* 47 (1991) 424.

225. S. da Costa, S. Agostinho, H. Chagas, J.C. Rubin, *Corrosion,* 43 (1987) 149.

226. K. Aramaki, T. Kiuchi, T. Sumiyoshi, H. Nishihara, *Corros. Sci,* 32 (1991) 593.

227. M. A. Quraishi and D. Jamal, *J Am Oil Chem Soc*, 77 (2000) 1107.

228. M. A. Quraishi and D. Jamal, *Anti-Corros Methods Mater*, 47 (2000) 77.

229. M. A. Quraishi and D. Jamal, *Anti-Corros Methods Mater*, 47 (2000) 233.

230. M. A. Quraishi and R. Sardar, *Ind. J. Chem. Technol*, 78 (2003) 425.

231. F. Bentiss, M. Traisnel, L. Gengembre, M. Lagrenée, *Appl. Surf. Sci,* 161 (2000) 194.

232. S. El Hajjaji, A. Lgamri, D. Aziane, A. Guenbour, E.M. Essassi, M. Akssira, A. Ben Bachir, *Progr. Org. Coat*, 38 (2000) 207.

233. R.Sardar, Ph.D Thesis – Aligarh Muslim University, Aligarh, India 2004.

234. L. Niu, C.N. Cao, H.C. Lin and G.L. Song, *Corros. Sci,* 407 (1998) 109.

235. B. Mernari, H.El. Attari, M. Traisnel, F. Bentiss and M. Lagrenée, *Corros. Sci,* 40 (1998) 391.

236. M. A. Quraishi and D. Jamal, *J. Appl.Electchem*, 32 (2002) 425.

237. F. Bentiss, M. Traisnel, L. Gengembre, M. Lagrenée, *Corros. Sci,* 34 (1999) 310.

238. M.I. Rosen, "Surfactants and Interfacial Phenomena", Wiley, New York 1989.

239. T.F. Tadros, "Surfactants", Academic Press, New York 1984.

240. D.W. Fuerstenau, *J.Phys.Chem,* 60 (1956) 981.

241. P.Somasundaran, T.W. Healy and D.W. Fuerstenau, *J.Phys.Chem,* 68 (1964) 3562.

242. J. H. Harwell, I.C. Haskins, R.S. Schecter and W.H. Wad, *Langmuir,* 1 (1985) 251.

243. A. Frignani, M. Tassinari, L. Meszaros and G. Trabanelli, *Corros. Sci,* 32 (1991) 903.

244. A. Frignani, C. Monticelli, G. Bassinari and G. Trabanelli, Proc 6th Euro. Symp. Corros. Inib, Ann. Univ. Ferrara, N.S. Sez. V, Suppl no 8, Ferrara, Italy 1985 p.1519.

245. N. Hajjaji, I.Ricco, A.Srhiri, A.Lattes, M.Soufiaoui and A.B. Bachir, *Corrosion*, 49 (1993) 326.

246. M.El Achouri, M.S. Hajji, S.Kertit, E.M. Essassi, M.Salem and R.Courdert, *Corros. Sci,* 37 (1995) 381.

247. M.El Achouri, M.S. Hajji, M.Salem, S.Kertit, J.Aride, R.Courdert, E.M. Essassi, *Corrosion,* 52 (1996) 103.

248. A. Frignani, G. Trabanelli,F.Zucchi, M.Zucchini, SEIC 5 Univ. Ferrara N.S. Sez, V. Suppl no 7, Ferrara, Italy 1980 p.1185.

249. V. Branzoi, F.Branzoi, E.Trimbitasu, M.Stanciu and C.Anghel, *Sci. Bull. Politechnica,* 62 (2000) 15.

250. W. Wang, M.L. Free and D. Horsup, *Metallurgical and Materials Transactions*, 36 (2005) 335.

251. W. L. Wang and M.L. Free, *Anti-Corr. Method Mater*, 50 (2003)186.

252. A.C. Zettlemoyer, *J.Colloid Interface Sci,* 28 (1968) 343.

253. D.W. Fuerstenau, *J.Phys. Chem*, 60 (1956) 981.

254. M.A. Mighad, E.M.S. Azzam, A.M.A. Sabagh, *Mater. Chem. Phys*, 85 (2004) 273.

Indian Journal of Chemical Technology
Vol. 11, March 2005, pp. 220-224

Inhibition of mild steel corrosion by oleochemical based hydrazides

M A Quraishi*, N Saxena & D Jamal

Corrosion Research Laboratory, Department of Applied Chemistry,
Faculty of Engineering & Technology, Aligarh Muslim University, Aligarh 202 002, India

Received 26 May 2004; revised received 22 November 2004; accepted 17 December 2004

Selected hydrazides of fatty acids with C_9–C_{17} carbon atoms have been synthesized and evaluated as corrosion inhibitors of mild steel (MS) in hydrochloric acid (HCl) solutions by weight loss and potentiodynamic polarization methods. The adsorption of all the hydrazides on mild steel surface in the acid solution has been found to obey Langmuir's adsorption isotherm. The potentiodynamic polarization studies revealed that all compounds block the corrosion reactions. Inhibition efficiency (IE) of these compounds has been found to vary with the concentration of the compound, solution temperature, immersion time and concentration of the acid solution. The values of activation energy (E_a) and free energy of adsorption (ΔG_{ads}) have been calculated to investigate the mechanism of the corrosion inhibition.

Keywords: Corrosion inhibition, oleochemical, hydrazines, mild steel, polarization

IPC Code: C23F 11/00; C07C 243/00

The use of corrosion inhibitors has increased considerably in recent years as awareness of corrosion has expanded. Organic compounds are widely used in various industries as corrosion inhibitors in acidic environments[1-3]. Acid inhibitors find wide applications in the industrial field as a component in pretreatment composition, in cleaning solution for industrial equipments and in acidization of oil wells.

A perusal of literature reveals corrosion inhibitors derived from fatty acid constitute an important and potential class of corrosion inhibitors. However, very little work has been done on fatty acid derivatives as corrosion inhibitors[4-6].

In continuation of the earlier work on the development of oleochemicals as acid corrosion inhibitors[7-13], the authors have studied the corrosion inhibiting behaviour of fatty acid hydrazides, namely decanohydrazide (DH), dodecanohydrazide (DDH), hexadecanohydrazide (HDH) and octadecanohydrazide (ODH) on the corrosion of MS in HCl solutions.

*For correspondence
(E-mail: maquraishi@rediffmail.com; Fax: 0091+571+2700528)

Experimental Procedure

Inhibitors

The inhibitors were synthesized in the laboratory following the procedure described earlier[14] and compounds were characterized through their spectral data and their purity was confirmed by thin layer chromatography (TLC). Name, structural formulas, melting points and molecular weight of the condensation products are given in Table 1.

Electrolyte

Analytical grade hydrochloric acid (Merck) and doubled distilled water were used for preparing test solutions for all the experiments. All the experiments were carried out, in 1 N acid solutions.

Specimens

The mild steel samples having composition, (Wt %): C, 0.14; Mn, 0.35; Si, 0.17; S, 0.025; P, 0.03% and balance Fe have been used for the experiment.

Weight loss studies

The mild steel sample of size 2.0 × 2.0 × 0.025 cm were used for weight loss measurement studies. Weight loss measurement studies were carried out at various temperatures ranging from 30 to 60 °C for various immersion times from 3 to 24 h. The experiments were performed as per ASTM method[15].

Table 1 — Name and molecular structures of the compounds used

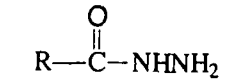

1. R= $CH_3(CH_2)_8$ (Decanohydrazide, DH); mol. wt =186.27; m p, 92-95 °C
2. R= $CH_3(CH_2)_{10}$ (Dodecanohydrazide, DDH); mol. wt=214.32; m p, 113-14 °C
3. R= $CH_3(CH_2)_{14}$ (Hexadecanohydrazide, HDH); mol. wt=270.43; m p, 78-79 °C
4. R= $CH_3(CH_2)_{16}$ (Octadecanohydrazide, ODH); mol. wt=298.48; m p 81-82 °C

The inhibition efficiency (%) of the inhibitors was calculated by using the following equation:

$$IE = \frac{CR_o - CR_i}{CR_o} \times 100$$

where

CR_o = Corrosion rate of blank hydrochloric acid.

CR_i = Corrosion rate after adding inhibitors.

Electrochemical polarization measurement

For potentiodynamic polarization studies, mild steel strips of same composition, coated with commercially available lacquer with an exposed area of 1.0 cm^2 were used and the experiments were carried out at temperature (30 ± 1 °C). Equilibrium time leading to steady state of the specimens was 30 min. Sweep rate in potentiodynamic experiment was 1mV/sec. Potentiodynamic polarization studies were carried out using an EG & G Princeton Applied research (PAR) potentiostat/galvanostat (model 173), a universal programmer (model 175) and a X-Y recorder (model RE0089). A platinum foil was used as auxiliary electrode and a saturated calomel electrode (SCE) was used as reference electrode. Corrosion rate (CR) was calculated using the following formula[16]:

$$CR = \frac{0.13 \times I_{corr} \times EW}{D}$$

where,

I_{corr} = Corrosion current density in mA/cm^2.

EW = Equivalent weight of the metal in g/eq.

D = Density of the metal in g/cm^2.

Table 2 — Corrosion parameters for mild steel in 1 N HCl in absence and presence of different concentrations of various inhibitors from weight loss measurement at 30 °C for 3 h

Inhibitor conc. (ppm)	Weight loss (mg)	IE (%)	CR mean (mmpy)	SD
HCl	60.0	-	22.35	0.0
DDH				
100	10.7	82.1	3.90	0.43
200	9.7	83.7	3.55	0.26
300	8.3	86.1	2.90	0.06
400	6.9	88.5	2.46	0.28
500	6.4	89.3	2.34	0.34
DH				
100	20.3	66.2	7.44	2.49
200	15.3	74.5	5.66	0.35
300	11.7	80.5	4.24	0.35
400	11.2	81.3	3.99	0.48
500	9.6	84.0	3.46	0.74
HDH				
100	26.2	56.3	9.64	0.80
200	22.8	62.0	8.46	0.21
300	20.8	65.3	7.63	0.20
400	20.2	66.3	7.47	0.28
500	19.2	68.0	7.00	0.52
ODH				
100	27.3	54.5	9.95	0.73
200	24.0	60.0	8.84	0.17
300	21.9	63.5	7.99	0.25
400	21.6	64.0	7.95	0.27
500	21.0	65.0	7.74	0.37

Results and Discussion

Weight loss studies

The values of percentage inhibition efficiency (%IE) and corrosion rate (CR) obtained from weight loss method at different concentrations of inhibitors at 30 °C are summarized in Table 2. It has been found that all these compounds inhibit the corrosion of mild

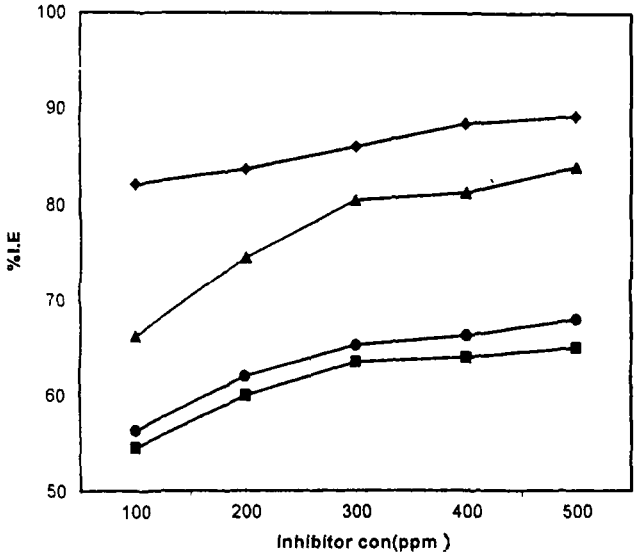

Fig 1 — Variation of inhibition efficiency with inhibitor concentration for 100-500 ppm concentration of inhibitors (♦-DDH; ▲-DH; ●-HDH; ■-ODH)

steel in 1 N HCl solution, at all concentrations used in this study i.e., 100-500 ppm. It has also been observed that the inhibition efficiency for all these compounds increased with the increase in concentrations (Fig. 1).

The variation of IE with solution temperature is shown in Fig. 2. It can be seen that IE for all of the compounds cause a significant increase with an increase in temperature from 30 to 40 °C. No significant change in IE has been observed for DH and DDH with the increase of temperature beyond 40-60 °C indicating that the inhibitive film formed on the metal surface is protective in nature at higher temperatures. HDH and ODH have been found to show decreasing IE trend for higher temperatures. The decrease in the IE for HDH and ODH may be attributed to the decomposition of the hydrophobic long carbon chain at higher temperatures.

The variation of inhibition efficiency of all the four hydrazides with the immersion time is shown in Fig. 3. It is observed that all the tested hydrazides show increase in the inhibition efficiency with the increase of immersion time from 3 to 24 h. This shows the persistency of the adsorbed fatty acid hydrazides over a longer test period.

From Fig. 4, it is clear that IE increases with increase in acid concentration up to 3 N HCl for all the hydrazides tested. Further increase in acid concentration up to 5 N HCl causes decreased IE for all the hydrazides except for DH. DH having C_9 has

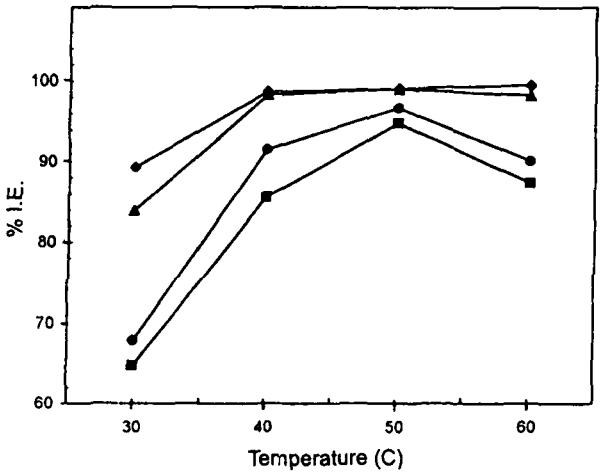

Fig. 2 — Variation of inhibition efficiency with solution temperature in 1 N HCl for 500 ppm concentration of inhibitors (♦-DDH; ▲-DH; ●-HDH; ■-ODH)

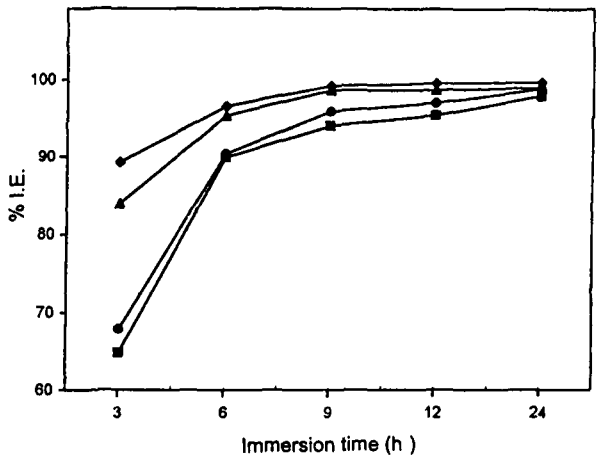

Fig. 3 — Variation of inhibition efficiency with immersion time in 1 N HCl for 500 ppm concentration of inhibitors (♦-DDH; ▲-DH; ●-HDH; ■-ODH)

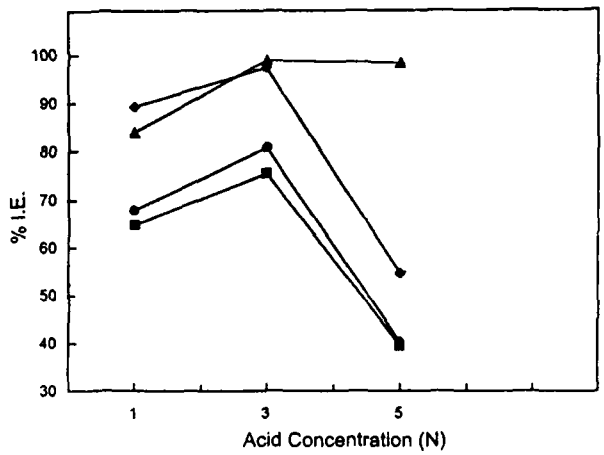

Fig. 4 — Variation of inhibition efficiency with acid concentration for 500 ppm concentration of inhibitors (♦-DDH; ▲-DH; ●-HDH; ■-ODH)

shown almost no change in IE with the increase in acid concentration from 3 N to 5 N HCl. The decrease in IE on increasing acid concentration beyond 3 N is due to increased aggressiveness of the acid[17].

Application of adsorption isotherm

In order to understand the mechanism of corrosion inhibition, the adsorption behaviour of the organic adsorbate on the metal surface must be known. The degree of surface coverage (θ) for different concentration of inhibitors in 1 N HCl at 30 °C for 3 h of immersion time has been evaluated from weight loss values. The data were tested graphically by fitting to various isotherms. A straight line was obtained on plotting log (θ/1-θ) verses log *C* (Fig. 5) suggesting, that, the adsorption of the compounds from HCl on mild steel surface follows Langmuir's adsorption isotherm.

Inhibition of corrosion of mild steel in the acidic solutions by the oleochemical-based hydrazides can be explained on the basis of molecular adsorption. It is apparent from the molecular structures that these compounds are able to get adsorbed on the metal surface through π-electrons of aromatic ring and lone pair of electrons of N- and O- atoms, and as a protonated species like amines[18]. The presence of long hydrophobic chain also plays a role in IE by preventing acid solution away from metal surface. Among the compounds investigated in the present study, the order of IE has been found as follows:

DDH > DH > HDH > ODH

(C_{11}) (C_9) (C_{15}) (C_{17})

It has been observed that IE of the tested hydrazides increased with the increase in chain length up to C_{11}, the IE of DDH is greater than DH but on further increasing carbon atoms more IE decreases due to increase in stearic hindrance, which lowers IE of HDH and ODH[19].

The values of activation energy (E_a) obtained from Arrhenius equation[20,21] and free energy of adsorption (ΔG_{ads}) calculated using the following relations are given in Table 3.

$$\Delta G_{ads} = -RT \ln (55.5\ K)$$

and K is given by:

$$K = \theta / C (1 - \theta)$$

where θ is degree of coverage on the metal surface, C is concentration of inhibitor in mole/L, K is equilibrium constant, R is a constant and T is temperature. It is found that the ΔG_{ads} value is less than -40 k J/mol (-9.56 k Cal/mol) indicating that the tested hydrazides of fatty acids are physically adsorbed on the metal surface[22]. The low and negative value of ΔG_{ads} indicated the spontaneous adsorption of inhibitor on the surface of mild steel[23]. It was also found that value of activation energy of the inhibited systems were lower than that of uninhibited system. Putilova[24] has indicated that this type of inhibitor is effective at higher temperatures.

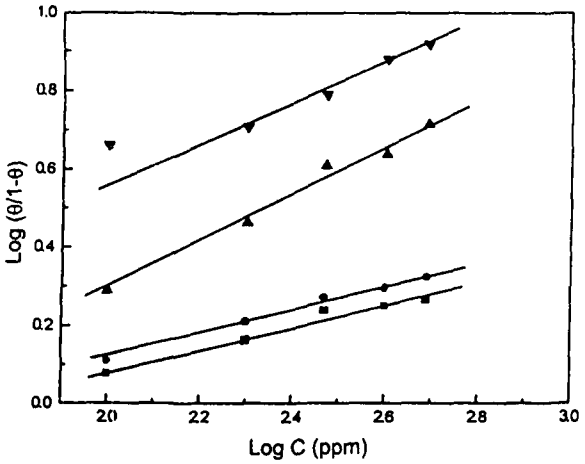

Fig. 5 — Langmuir s adsorption isotherm plots for the adsorption of various inhibitors in 1 N HCl on the surface of mild steel (▼-DDH; ▲-DH; ●-HDH; ■-ODH)

Table 3 — Activation energy (E_a) and free energy (ΔG_{ads}) for mild steel in absence and presence of maximal concentration of the inhibitor

Inhibitor conc. (ppm)	E_a (kJ.mol^{-1})	ΔG_{ads} (kJ.mol^{-1})			
		30 °C	40 °C	50 °C	60 °C
HCl	52.4	-	-	-	-
DDH	86.3	30.7	37.5	37.9	39.9
DH	74.3	29.5	36.7	39.9	39.1
HDH	74.1	26.9	30.8	34.8	33.2
ODH	66.9	27.2	32.4	36.1	32.9

Potentiodynamic polarization studies

Various corrosion parameters such as E_{corr}, I_{corr}, IE and CR obtained from Fig. 6, by Tafel extrapolation method are given in Table 4. It is observed that presence of the hydrazides decrease I_{corr} values. Maximum decrease in I_{corr} was observed in case of DDH. The trend of the IE was found to be same as that of weight loss study. E_{corr} values do not show any

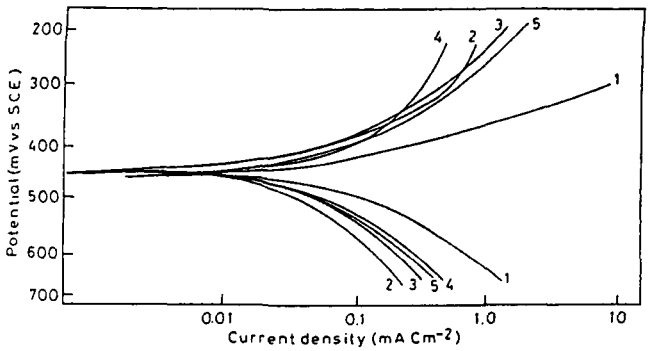

Fig. 6 — Potentiodynamic polarization curves of mild steel in 1 N HCl containing 500 ppm concentrations of various hydrazides (1) Blank (2) DDH (3) DH (4) ODH (5) HDH

Table 4 — Electrochemical polarization parameters for the corrosion of mild steel in HCl containing maximal concentration of various inhibitors at 30 °C

Inhibitor conc. (ppm)	E_{corr} (mV)	I_{corr} (mA cm^{-2})	IE (%)	CR (mmpy)
HCl	-458	0.36	-	6.65
DDH	-454	0.08	77.8	1.48
DH	-452	0.11	69.4	2.03
HDH	-456	0.13	63.9	2.40
ODH	-456	0.16	55.5	2.95

significant change in presence of all the hydrazides in the acid solution suggesting that all these hydrazides are mixed type inhibitors (*i.e.*, they retard the corrosion reaction by blocking both anodic and cathodic sites of the metal).

Conclusion

(i) The acid hydrazides showed good performance as corrosion inhibitors in hydrochloric acid media.

(ii) All of the four acid hydrazides inhibited corrosion by adsorption mechanism and the adsorption of these compounds from acid solution followed Langmuir's adsorption isotherm.

(iii) All the compounds examined acted as mixed inhibitors.

References

1 Abd-El-Nabey B A, Khamis E, Ramadan M S & El-Gindy A, *Corrosion*, 52 (1996) 671.

2 Al-Andis N, Khamis E, Al-Mayouf A & Aboul-Enicm A, *Corros Prev Control*, 42 (1995) 13.

3 Raman A & Labine P, *Reviews on Corros Inhib Sci Tech NACE International Houston*, 2 (1996) 1.

4 Hanna F, Sherbini G M & Brakat Y, *Brit Corros J*, 24 (1989) 269.

5 Badran B M, Abdel Fattah A A & Abdul Azim A A, *Corros Sci*, 22 (1982) 513.

6 Badran B M, Abdel Fattah A A & Abdul Azim A A, *Corros Sci*, 22 (1982) 525.

7 Qurashi M A, Jamal D & Sardar R, *Mat Chem Phy*, 71 (2001) 313.

8 Quraishi M A, Jamal D & Saeed M A, *J Am Oil Chem Soc*, 77 (3) (2000) 265.

9 Quraishi M A & Jamal D, *J Am Oil Chem Soc*, 77 (10) (2000) 1107.

10 Quraishi M A & Jamal D, *Mat Chem Phys*, 71 (2) (2001) 205.

11 Ajmal M, Jamal D & Quraishi M A, *Anti-Corros Meth Mater*, 47(2) (2000) 77.

12 Quraishi M A, Jamal D & Singh R N, *Corrosion*, 56 (2) (2002) 201.

13 Quraishi M A & Jamal D, *J Applied Electrochem*, (Ref. No. UK 161-01).

14 Iqbal M, Kittur M H & Mahajanshetti C S, *J Oil Tech Assoc India*, 16 (1984) 49.

15 ASTM, *Standard Practice for Laboratory Immersion Corrosion Testing of Metals*, Annual Book of Standards, G 31-72, 3.02 (1990).

16 ASTM, *Standard Practice for Calculation of Corrosion Rate and related Information from Electrochemical Measurements*, Annual Book of Standards, G 102-89, 3.02 (1994).

17 Quraishi M A, Rawat J & Ajmal M, *Corrosion*, 54 (1996) 99.

18 Quraishi M A, Ahmad S & Ansari M Q, *Brit Corros J*, 32 (1997) 297.

19 Lal P, Tan T C & Lee J Y, *Corrosion*, 53 (1997) 186.

20 Vashi R T & Champaneri V A, *Indian J Chem Technol*, 4 (1997) 180.

21 Schorr M & Yahalom J, *Corros Sci*, 12 (1972) 867.

22 Brinic S, Grubac Z, Babic R & Metikos-Hukovic M, *8th Eur Sump Corros Inhib Ferrara*, Italy, 1 (1995) 197.

23 Gomma G K & Wahdan M H, *Indian J Chem Technol*, 2 (1995) 107.

24 Putilova I N, Balezin S A & Baranik U P, *Metallic Corrosion Inhibitors* (Pergamon Press, New York), 1960, 31.

ЗАЩИТА МЕТАЛЛОВ, 2008, том 44, № 1, с 1–8

ФИЗИКО-ХИМИЧЕСКИЕ ПРОБЛЕМЫ ЗАЩИТЫ МАТЕРИАЛОВ

УДК 541.183;147

INHIBITION of MILD STEEL CORROSION in PRESENCE of FATTY ACID IMIDAZOLINES in HYDROCHLORIC ACID

© 2007 г. M. A. Quraishi, M. Z. A. Rafiquee, Nidhi Saxena*, Sadaf Khan

Department of Applied Chemistry, Corrosion Research Laboratory, Faculty of Engineering & Technology, Aligarh Muslim University. Aligarh-202 002, India.

E-mail: nidhisaxena10@rediffmail.com

Fax No. 0091 + 571 + 2504361

Поступила в редакцию 11.12.06

The corrosive behavior of mild steel in 1M HCl solutions containing selected imidazolines of fatty acids with C_7–C_{17} was investigated using weight loss method, potentiodynamic polarization technique and scanning electron microscopy. The results obtained revealed that all the studied imidazolines are effective in reducing corrosion of mild steel in HCl media. The adsorption of the inhibitors on the mild steel surface obeys Langmuir's adsorption isotherm. The thermodynamic parameters of adsorption deduced reveal a strong interaction and spontaneous adsorption of inhibitors on the mild steel surface. The influence of inhibitor concentration, solution temperature, immersion time and acid concentration on the corrosion of mild steel has also been investigated. Scanning electron microscopy(SEM) of mild steels samples is performed to show adsorption of inhibitors on metal surface. Potentiodynamic polarization data showed that the compounds studied are mixed type inhibitors in the acid solution.

PACS:

INTRODUCTION

Metals are exposed to action of acids in many industrial and commercial applications. Many methods are adopted to prevent corrosion but the simple & cost effective method is the use of organic corrosion inhibitors. While developing corrosion inhibitor for metal and its alloys in corrosive medium, it is of important to know mechanism of their adsorption on metal surface [1–4]. The polar group of inhibitor is frequently regarded as the reaction centre for the adsorption process establishment, since the adsorption bond strength is determined by the electron density and polarizability of the functional group [5]. Organic inhibitors have been employed in several industries: during the pickling of metals, cleaning of boilers, oil and gas wells acidizing, acid descaling, in crude distillation towers in refineries to protect overhead condensers, coolers, reflux drains and associated piping from excessive corrosion [6–7]. In continuation of our effort [8–19], in development of corrosion inhibitors for metals, the authors have synthesized a few derivatives such as 2-Undecane 1-3 Imidazoline(UDI), 2-Nonayl 1-3 Imidazoline(NI), 2-Pentadecyl 1-3 Imidazoline(PD), 2-Heptadecyl 1-3 Imidazoline(HDI), 2-Heptayl 1-3 Imidazoline(HI) has been studied and their inhibitive action on corrosion of mild steel in hydrochloric acid are reported here.

EXPERIMENTAL

Material Preparation

AR grade hydrochloric acid (MERCK) and double distilled water were used for preparing test solutions for all the experiments. The inhibitors were synthesized in the laboratory following the procedure described earlier [20] and compounds were characterized through their IR and NMR spectral data and their purity was confirmed by thin layer chromatography (TLC). Name, structural formulas, melting points and molecular weight of the inhibitors are given in Table 1.

Weight Loss Determination

Experiments were performed with cold rolled mild steel strips of size 2.0 cm × 2.5 cm × 0.2 cm having composition, (wt%): 0.14% C, 0.35% Mn, 0.17% Si, 0.025% S, 0.03% P and remaining iron Fe as per standard methods [21].The specimens were degreased using acetone and finally dried. The cleaned specimens were weighed before and after the experiments. Weight loss studies were carried out at various temperatures ranging from 30 to 60°C and for various immersion times from 3 to 24 hours. The aggressive solutions used were made of AR grade 35% HCl using appropriate concentrations of acid in double distilled water. The concentration range of inhibitor employed was 100 to 500 ppm in the hydrochloric acid. The inhibition efficiency (%) of the inhibitors was calculated by using the following equation:

$$IE = \frac{CR_0 - CR_i}{CR_0} \times 100.$$

Table 1. Name and molecular structures of the compounds used

S No	Strucure	Designation and abbreviation
1	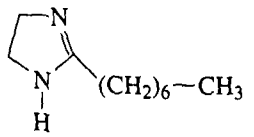	2-Heptayl 1-3 imidazoline (HI)
2	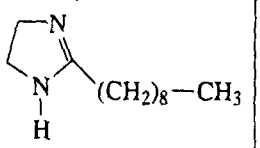	2-Nonayl-1,3-imidazoline (NI)
3	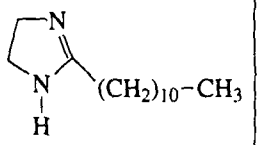	2-Undecyl-1,3-imidazoline (UDI)
4	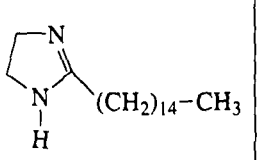	2-Pentadecyl-1,3- imidazoline (PDI)
5	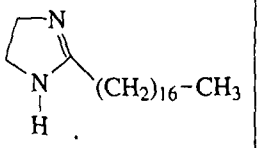	2-Heptadecyl-1,3-imidazoline (HDI)

Where IE – inibition efficiency, CR_0 – corrosion rate of blank hydrochloric acid, CR_i – corrosion rate after adding inhibitors.

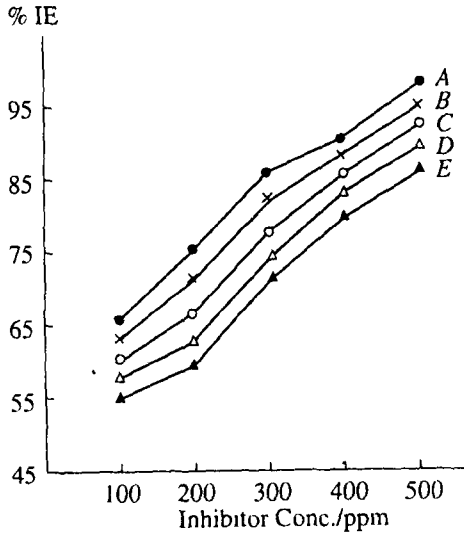

Fig. 1. Variation of inhibition efficiency (*IE*) with inhibitor concentration for 10–100 ppm concentration of inhibitors (●, UDI, x. NI, ○, PDI, , △ HDI, ▲, HI)

Potentiodynamic polarization studies

The potentiodynamic polarization studies of mild steel strips of composition, (wt%): 0.14% C, 0.35% Mn, 0.17% Si, 0.025% S, 0.03% P and remaining iron Fe as per standard methods and was coated with commercially available lacquer as per standard methods with exposed area of 1.0 cm^2 were used and all the experiments were carried out at temperature (30 ± 1°C). Equilibrium time leading to steady state of the specimens was 30 minutes. Sweep rate in potentiodynamic experiment was 1mV/sec. Potentiodynamic polarization studies were carried out using an EG & G Princeton Applied research (PAR) potentiostat/galvanostat (model 173), a universal programmer (model 175) and a X-Y recorder (model RE0089). A platinum foil was used as auxiliary electrode and a saturated calomel electrode (SCE) was used as reference electrode and mild steel was used as working electrode.

Electrochemical Impedance Studies

Impedance measurements were performed in mild steel in 1 M HCl in absence and presence of 100, 300 and 500 ppm of UDI in the frequency range 5 Hz–100 kHz. A time interval of few mintues was given for open circuit potential (o. c. p) to reach a steady value. All the measurements were carried out using Zahner IM-6 electrochemical workstation at 30° ± 2°C.

Scanning Electron Microscopy

Scanning electron microscope (SEM) Model No 435 VP LEO, was used to study the morphology of corroded surface in presence and absence of inhibitors. The specimens were thoroughly washed with double distilled water before putting on the slide. The photographs have been taken from that portion of specimen from where better information was obtained. They were photographed at 3000 μ magnification. To understand the morphology of the steel surface in absence and presence of inhibitors, the following cases have been examined: polished mild steel specimen, mild steel specimen dipped in 1N HCl, mild steel specimens dipped in 1N HCl containing 500ppm concentration of UDI.

RESULTS AND DISCUSSION

Weight loss studies

The values of percentage inhibition efficiency (%IE) and corrosion rate (*CR*) obtained from weight loss method at different concentrations at 30°C are summarized in Table 2. It has been found that all of these compounds inhibit the corrosion of mild steel in HCl solution, at all concentrations used in this study i.e., 100 ppm–500 ppm. It has also been observed that the inhibition efficiency of these compounds increases with the increase in concentration of inhibitor as shown in Fig. 1.

The variation of inhibition efficiency (*IE*) with solution temperature is depicted in Fig. 2. It can be seen that *IE* for all inhibitors such as UDI, PDI & HDI do not cause

any significant change with an increase in temperature from 30°C to 60°C indicating that the inhibitive film formed on the metal surface is protective in nature at higher temperatures while in case of *NI & HI* Inhibition efficiency (*IE*) increases with the increase in temperature.

The variation of inhibition efficiency in all fatty acids imidazolines with immersion time is shown in Fig. 3. It is observed that no significant change in *IE* occurred with the increase in immersion time from 3h to 24h. This shows the persistency of the adsorbed fatty acid imidazolines over a longer test period.

From Fig. 4, it is clear that the change in acid concentration does not cause any significant change in inhibition efficiency of all the compounds studied thereby suggesting that all the compounds are effective inhibitors in acid solution of different concentrations.

Application of the principles of chemical kinetics to the results

Adsorption Isotherm studies

The degree of surface coverage (θ) for different concentration of inhibitors in 1N HCl at 30°C for 3 hour of immersion time has been evaluated from weight loss values. The data were tested graphically by fitting to various isotherms. A straight line was obtained on plotting $\log\theta/(1-\theta)$ versus log C as shown in Fig. 5, suggesting that the adsorption of these compounds in HCl on mild steel surface follows Langmuir's adsorption isotherm.

A plot of $\log\theta/(1-\theta)$ versus 1/T is given in Fig. 6, the plot gives the values for calculating heat of adsorption (Q) with a slope (–Q/2.303R). The values for the heat of adsorption are depicted in Table 3. The lower values of heat of adsorption for these inhibitors shows physical nature of adsorption [22].

It has been reported by a number of authors [23–25] that in acid solution, the logarithm of the corrosion rate is a linear function with 1/T (Arrhenius equation):

$$\log(RATE) = \frac{-E_a^0}{2.303RT} + A,$$

where, E_a^0 is apparent effective activation energy, R is general gas constant and A is Arrhenius preexponential factor. A plot of log (corrosion rate) versus 1/T gave straight line as shown in Fig. 7. The values of activation energy (E_a^0) obtained from the slope of the lines are given in Table 3. An alternative formula of the Arrhenius equation for the transition state is :

$$RATE = \frac{RT}{Nh}\exp\left(\frac{\Delta S^0}{R}\right)\exp\left(-\frac{\Delta H^0}{RT}\right),$$

where, h is the plank' s constant, N the Avogadro' s number, ΔS° the entropy of activation, and ΔH° the enthalpy of activation. A plot of log (rate/T) versus 1/T give a straight line (Fig. 8) with a slope of (–ΔH°/2.303 R) and an intercept of [(log(R/Nh) + (ΔS°/2.303 R)], from which the values of ΔS° and ΔH° were determined and are listed in Table 3. The data show that the thermodynamic activation function (E_a^0) for inhibited system are lower than those in the free acid solution indicating that all inhibitors exhibit high efficiency at elevated temperature [26].

Table 2. Corrosion parameters for mild steel in 1N HCl in absence and presence of different concentrations of various inhibitors from weight loss measurement at 30°C for 3 h

Concentration (ppm)	Weightloss (mg)	I.E (%)	C.R (mmpy)
HCl	68.12	–	25.31
UDI			
100	23.6	65.23	8.80
200	16.7	75.21	6.29
300	9.9	85.32	3.71
400	6.3	90.61	2.37
500	1.1	98.31	0.42
NI			
100	24.8	63.57	9.22
200	19.6	71.12	7.30
300	12.0	82.27	4.48
400	8.1	88.10	3.01
500	2.7	96.03	1 00
PDI			
100	27.1	60.10	10.09
200	22.4	67.04	8.34
300	14.7	78.31	5.48
400	10.0	85.22	3.74
500	4.0	93.99	1.52
HDI			
100	27.9	59.01	10.37
200	24.9	63.41	9.26
300	16.8	75.20	6.27
400	10.3	84.81	3.84
500	6.0	90.88	2.30
HI			
100	29.9	56.10	11.11
200	27.1	60.09	10.10
300	18.7	72.50	6.96
400	12.3	81.93	4.57
500	9.6	85.80	3.59

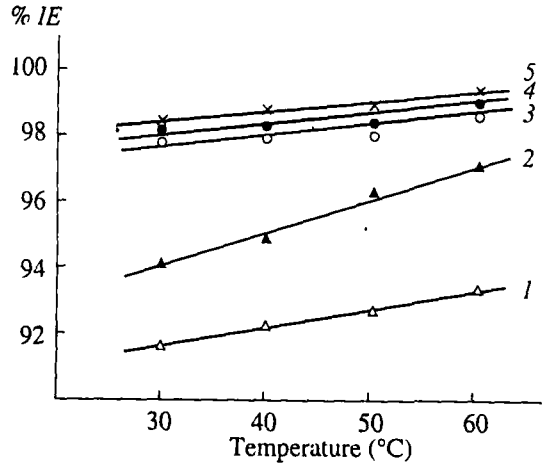

Fig. 2. Variation of inhibition efficiency (*IE*) with solution temperature in 1N hydrochloric acid for 500 ppm concentration of inhibitors (×, UDI; ●, NI; ○, PDI; ▲, HDI; △, HI).

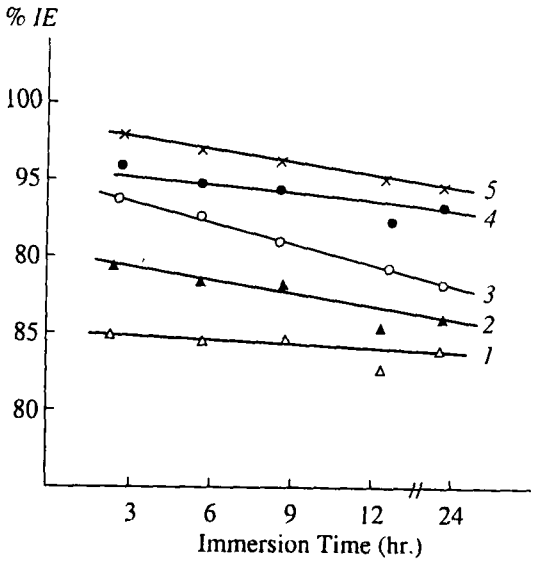

Fig. 3. Variation of inhibition efficiency (*IE*) with immersion time in 1N hydrochloric acid for 500 ppm concentration of inhibitors (×, UDI; ●, NI; ○, PDI; ▲, HDI; △, HI).

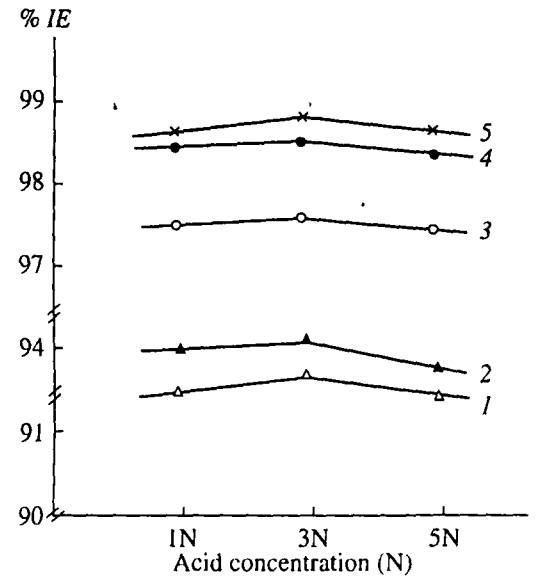

Fig. 4. Variation of inhibition efficiency (*IE*) with acid concentration in 1N hydrochloric acid for 500 ppm concentration of inhibitors (×, UDI; ●, NI; ○, PDI; ▲, HDI; △, HI).

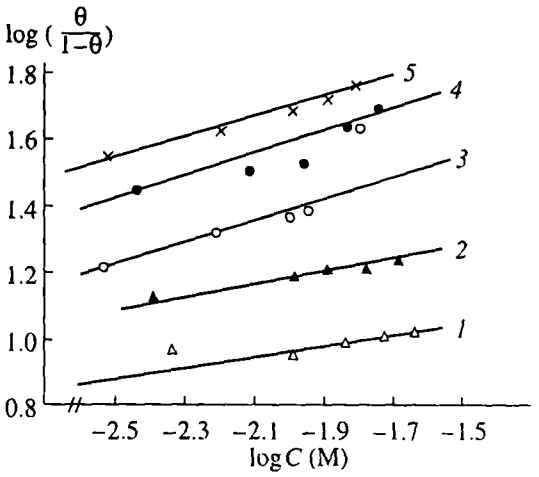

Fig. 5. Langmuirs adsorption isotherm plots for the adsorption of various inhibitors in 1N hydrochloric acid on the surface of mild steel (×, UDI; ●, NI; ○, PDI; ▲, HDI; △, HI).

The value of ΔH° for all the inhibitors are lower than those in the free acid solution indicating less energy barrier for the reaction in presence of the inhibitor is attained. The entropy of activation ΔS° in the absence and presence of the inhibitors are large and negative. This indicates that the activated complex in the rate determining step represents an association rather than a dissociation step, meaning that a decrease in disorderness takes place on going from reactants to the activated complex [27]. Free energy of adsorption (ΔG_{ads}) was calculated by using the following equations [28] and the values are given in Table 3.

$$\Delta G_{ads} = -RT\ln(55.5K),$$

and K is given by:

$$K = \frac{\theta}{C(1-\theta)},$$

where θ is degree of coverage on the metal surface, C is concentration of inhibitor in mole/l, K is equilibrium constant, R is gas constant and T is temperature. It has been found that the values of ΔG_{ads} is less than –40 k J/mol (–9.56 k Cal/mol) indicating that the imidazolines are physically adsorbed on the metal surface [29].The negative value of ΔG_{ads} indicates the spontaneous adsorption of inhibitor on the surface of mild steel [30]. It was also

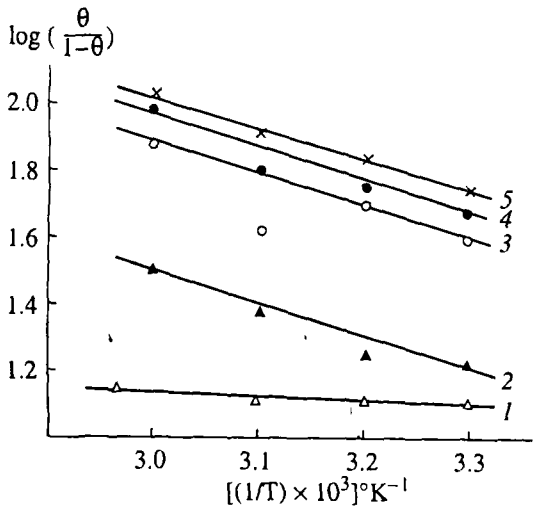

Fig. 6. Adsorption isotherm plot for log(θ/1 − θ) versus 1/T (×, UDI; ●, NI; ○, PDI; ▲, HDI; △, HI.

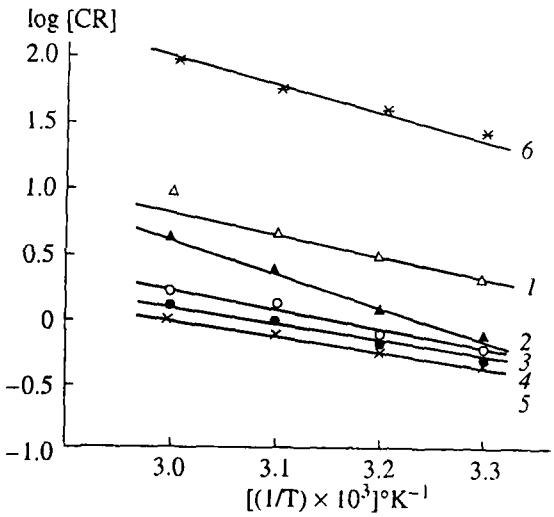

Fig. 7. Adsorption isotherm plot for log(CR) versus 1/T (×, UDI; ●, NI; ○, PDI; ▲, HDI; △, HI; *, Blank).

found that the value of activation energy of the inhibited systems were lower than that of uninhibited system. Putilova [26] has reported that this type of inhibitor is effective at higher temperatures.

The plot of log (weight loss) vs immersion time. gave a straight line as shown in Fig. 9 indicating that the reaction is first order. The value of the rate constant was calculated using the first order rate law [31].

$$k = \frac{2.303}{t}\log\left(\frac{A_0}{A}\right),$$

where A_0 is the intial mass of the metal and A is the mass corresponding to time t. The half life ($t_{1/2}$) values were calculated using equation [32].

$$t_{1/2} = 0.693/k.$$

The value of the rate constant and half life ($t_{1/2}$) obtained from above equation are summarized in Table 4.

Table 3. Thermodynamic activation parameters for mild steel in 1 HCl in absence and presence of inhibitors of 500 ppm concentration

Concentration 500 ppm	E_a KJ mol^{-1}	ΔH KJ mol^{-1}	ΔS J mol/K^{-1}	ΔG_{ad} KJ mol^{-1}	−Q KJ mol^{-1}
Blank	47.59	50.23	159.31	–	–
UDI	23.71	26.35	203.73	38.41	23.66
NI	24.76	27.40	202.20	37.12	23.04
PDI	23.77	32.42	198.75	36.25	18.08
HDI	29.75	32.39	192.43	35.81	18.62
HI	30.73	43.37	186.19	32.10	7.40

Half life ($t_{1/2}$) values were found to be constant at different immersion times. The constant values of rate constant further confirmed that corrosion of mild steel in I N HCl in presence of different inhibitors follows first order kinetics [33].

Potentiodynamic Polarization Studies

The corrosion parameters such as E_{corr}, I_{corr}, IE and CR obtained from Fig. 10 are given in Table 5. It is observed that the presence of the imidazolines decreases I_{corr}, values. Maximum decrease in I_{corr}, was observed in case of UDI. The trend of the IE was found to be same as that of weight loss study. E_{corr} values do not show any significant change in presence of all the imidazolines in the acid solution suggesting that all these compounds are mixed type inhibitors (i.e., they retard the corrosion reaction by blocking both anodic and cathodic sites of the metal).

Table 4. First order rate constant and half life values in hours (h) for the corrosion of mild steel in 1N HCl in absence and presence of inhibitors of 500 ppm at 30°

System	K × 10^{-3} h^{-1}	$t_{1/2}$, h
1N HCl	32.79 ± 0.141	21.15
UDI	3.83 ± 0.221	180.93
NI	5.41 ± 0.201	128.00
PDI	10.78 ± 0.187	64.28
HDI	11.95 ± 0.156	57.99
HI	14.83 ± 0.134	49.89

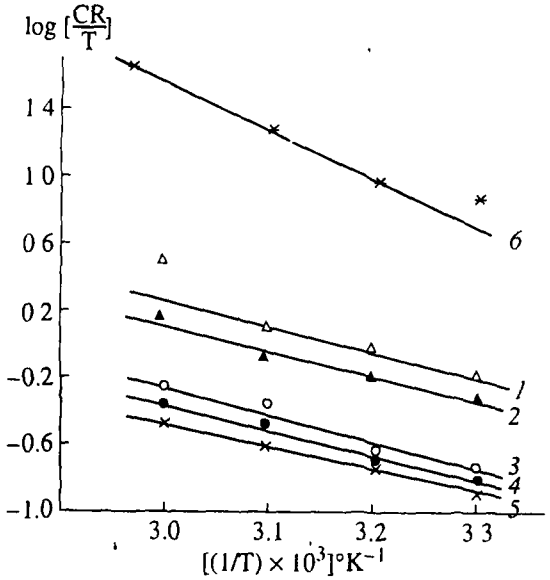

Fig. 8. Adsorption isotherm plot for log(CR/T) versus 1/T (×, UDI, ●, NI, ○, PDI, ▲, HDI, △, HI, *, Blank)

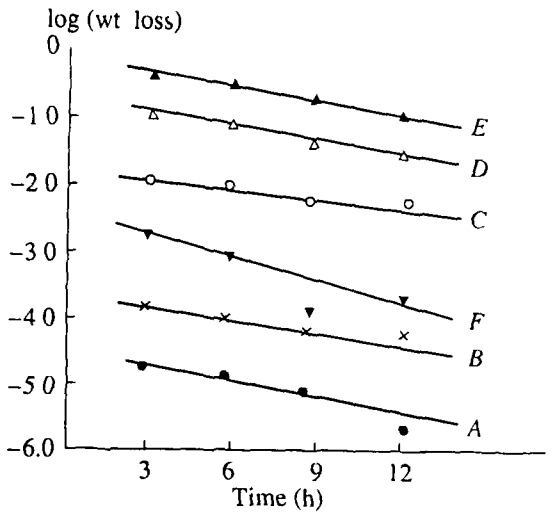

Fig. 9. Plot of Log (weight loss) vs Immersion time (●, UDI, ×, NI, ○, PDI, ▲, HDI, △, HI, ▼, Blank)

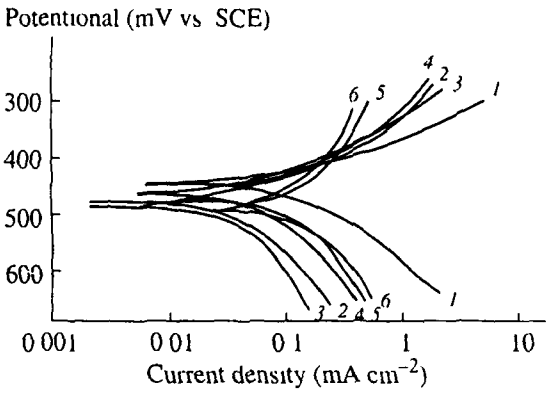

Fig. 10. Potentiodynamic polarization curves of mild steel in 1N hydrochloric acid containing 100 ppm concentrations of various Imidazolines (*1*) Blank (2) NI (*3*) UDI (*4*) PDI (*5*) HDI (*6*) HI

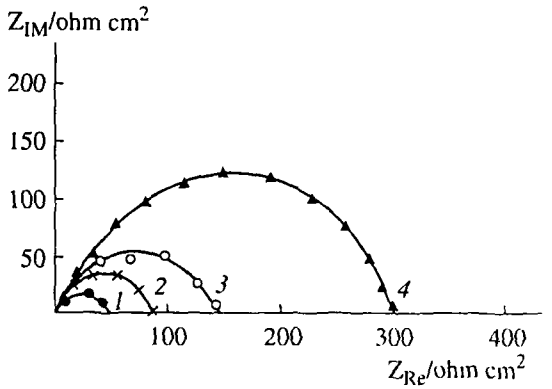

Fig. 11. Nyquist plot of mild steel in 1M hydrochloric acid in the absence and presence of 100, 300 and 500 ppm of UDI (*1*) Blank (2) 100 ppm UDI (*3*) 300 ppm UDI (4) 500 ppm UDI

Electrochemical Impedance Studies

Table 6 includes the results of impedance studies and Figure 11 shows Nyquist plots in the absence and presence of 100, 300 and 500 ppm of UDI. The Nyquist plots are not perfect semicircles and this difference has been attributed to frequency dispersion [34]. The values of Rt and Cdl were calculated from Nyquist plots as described elsewhere [35]. The percentage IE was calculated using equation [36]

$$\%IE = \frac{(1/RTo) - (1/RTi)}{(1/RTo)} \times 100,$$

where *Rto* and *Rti* are charge transfer resistance without and with inhibitor, respectively and are given in Table 6. *Rt* values increases with increase in inhibitor concentration (UDI) and this in turn leads to an increase in inhibition efficiency. The addition of UDI to 1M HCl lowers the Cdl values, which shows that the inhibition can be attributed to surface adsorption of the inhibitor [37].

Scanning electron microscopy

It is seen in Fig. 12 that the surface of mild steel immersed in inhibited solution is smoother than that in 1N HCl alone. These observations suggest that inhibitors form protective layer on the metal surface and prevent attack of acid on metal surface.

Table 5. Electrochemical polarization parameters for the corrosion of mild steel in 1N HCl containing 500 ppm inhibitors at 30°

Concentration ppm	E_{corr}, mV	I_{corr}, mAcm^{-2}	IE, %
HCl	–461	0.360	–
UDI	–480	0.033	90.83
NI	–476	0.037	89.72
PDI	–466	0.085	76.38
HDI	–479	0.120	66.66
HI	–493	0.150	58.33

Table 6. Electrochemical impedance parameters for mild steel in 1M HCl containing different concentrations of UDI at 30°C

Concentration ppm	R_t, ohm cm^2	C_{dl}, μF cm^{-2}	IE, %
1M HCl	36.02	1511.50	–
UDI			
100	86.95	946.84	58.48
300	141.30	776.92	74.45
500	304.34	315.22	88.13

Mechanism of corrosion inhibition

Inhibition of corrosion of mild steel in the acidic solutions by the fatty acid imidazolines can be explained on the basis of molecular adsorption. It is apparent from the molecular structures that these compounds are able to get adsorbed on the metal surface through π-electrons of aromatic ring and lone pair of electrons of N, O and S atoms [38]. The presence of long hydrophobic chain also plays a role in IE by keeping acid solution away from metal surface. Among the compounds investigated in the present study, the order of IE has been found as follows:-

$$UDI > NI > PDI > HDI > HI$$

$$(C_{11}) (C_9) (C_{15}) (C_{17}) (C_7)$$

It has been observed that IE of the tested imidazolines increased with the increase in chain length up to C_{11}. A further increase in chain length up to $C_{17}7$ has been found to decrease the IE.

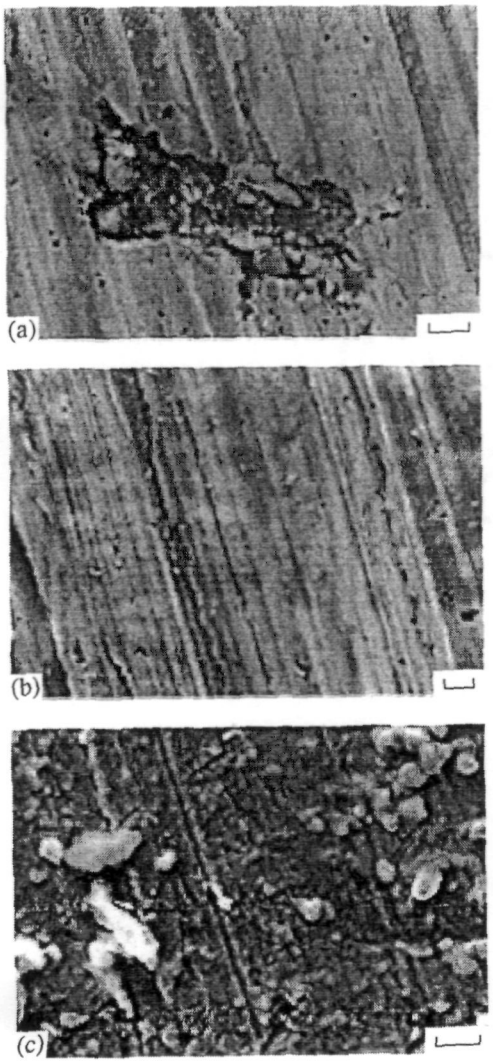

Fig. 12. Scanning electron micrographs for mild steel surface in absence and presence of inhibitors (a) mild steel in *1N HCl* (b) *polished mild steel and* (c) *mild steel in* presence of UDI.

CONCLUSIONS

The fatty acid imidazolines shows good performance as corrosion inhibitors in hydrochloric acid media.

All of the tested imidazolines inhibit corrosion by adsorption mechanism and the adsorption of these compounds from acid solution follow Langmuir's adsorption isotherm.

The Inhibition effiency increases with increasing inhibitor concentration, Inhibition effiency however did not change significantly with an increase in temperature and immersion time.

The lower values of Heat of adsorption (Q) for these inhibitors shows physical nature of adsorption and lower values of ΔG_{ads} indicates that the inhibitors are physically adsorbed on the metal surface and negative value of ΔG_{ads} indicates the spontaneous adsorption of inhibitor on the surface of mild steel.

Lower values of thermodynamic activation function (E_a^0) for inhibited system than those in the free acid solution indicating that all inhibitors exhibit high efficiency at elevated temperature.

The value of $\Delta H°$ is low for all the inhibitors indicating less energy barrier for the reaction in presence of the inhibitor is attained.

The entropy of activation $\Delta S°$ in the absence and presence of the inhibitors are large and negative. This indicates

that the activated complex in the rate determining step represents an association rather than a dissociation step

All the compounds examined acted as mixed inhibitors in HCl

Scanning electron microscopy studies shows that inhibitors prevent corrosion by adsorption on the metal surface thus preventing attack of acid

REFERENCES

1 *Hackerman N , Mackrides A C* / Ind Eng Chem 1954 V 46 P 523

2 *Makrides A C Hackerman N* / J Phys Chem 1955 V 59 P 707

3 *Ateya B G El Anadouli B E , El Nizamy F M A* / Bull Chem Soc Jpn 1981 V 54 P 3157

4 *Bhajiwala H M , Vashi R T* / Bull Electrochem 2001 vol 17, p 441

5 *Giacomelli F C , Giacomelli C , Amadori M F et al* / Mater Chem Phys 2004 V 33 P 124

6 *Hafsten R J Walston K R* / Proc API 1955 V 35 P 80

7 *Baumann C , Scherrer C* / Mater Perf 1979 V 18 P 51

8 *Quraishi M A , Khan M A W , Ajmal M* / Prog Electrochem Acta 1995 V 13 P 63

9 *Muralidharan S Quraishi M A Iyer S V K* / Corros Sci 1995 V 37 P 1739

10 *Quraishi M A Khan M A W Ajmal M* / Anti Corros Methods Mater 1996 V 43 P 5

11 *Quraishi M A Khan M A W , Ajmal M* / Br Corros J 1997 V 32 P 72

12 *Quraishi M A Jamal D* / Anti-Corros Methods Mater 2000 V 47 P 233

13 *Quraishi M A Jamal D* / Corrosion 2000 V 56 P 156

14 *Quraishi M A Jamal D* / Corrosion 2000 V 56 P 983

15 *Quraishi M A , Jamal D , Saeed M T* / J Am Oil Chem Soc 2000 V 77 P 265

16 *Quraishi M A Jamal D* / J Am Oil Chem Soc 2000 V 77 P 1107

17 *Quraishi M A , Jamal D* / Anti-Corros Methods Mater 2000 V 47 P 77

18 *Quraishi M A Jamal D Singh R* / Corrosion 2002 V 58 P 201

19 *Quraishi M A , Ansari F* / J Am Oil Chem Soc 2003 V 80 P 7

20 *K Hofmann* Imidazolines & its derivatives – Part I The chemistry of heterocyclic compound New York Inter science Publishers, 1953 P 213

21 ASTM, Metal Corrosion, Erosion and Wear Annual Book of ASTM Standards 1987 0 3 02 G1–72

22 *Jha L J Ph* D Thesis "Studies of the Adsorption of amide derivative during acid during acid corrosion of pure iron & its characterization Delhi Delhi University, 1990 111 pp

23 *Christopher M A B , Isabel A R G Jenny P S M* / Corros Sci 1994 V 36 P 15

24 *Breslin C B Carrol W M* / Corros Sci 1993 V 34 P 327

25 *Khedr M G A , Lashien M S* / Corros Sci 1992 V 33 P 137

26 *Putilova I N , Balzin S A Branik U P* Mettalic corrosion inhibitors New York Pergamon Press, 1960 P 31

27 *Gomma M K Wahdan M H* / Mater Chem Phys 1995 V 39 P 209

28 *Schorr M , Yahalom J* / Corros Sci 1972 V 12 P 867

29 *Brinic S et al* // 8th Euro Symp Corros Inhib Ferrara Italy, V 1 P 197

30 *Gomma G K , Wahdan M H* / Ind J Chem Technol 1995 V 2 P 107

31 *Orubite O K , Oforka N C* / J Appl Sci Environ 2004 V 8 P 57

32 *Atkins P W* Chemisorbed and Physisorbed Species A Textbook of Physical Chemistry Oxford University Press, 1980 P 936

33 *Quraishi M A Khan S* / J Appl Electrochem 2006 V 36 P 539

34 *Juttner K* / Electrochim Acta 1990 V 35 P 1501

35 *Ashassi-Sorkhabi H Shaabani B Seifzadeh D* / Electrochim Acta 2005 V 50 P 3446

36 *Li S L , Wang Y G , Chen S H et al* / Corros Sci 1999 V 41 N 6 P 1769

37 *Subramaniyam N C , Mayanna S* / Corros Sci 1985 V 25 P 163

38 *Quraishi M A et al* / Ind J Chem Technol 1994 V 1 P 329

SPELL 1 elecron, 2 Strucure, 3 inibition, 4 mintues, 5 intial, 6 Mettalic

Indian Journal of Chemical Technology
Vol. 14, October 2007, pp.

Some fatty acid oxadiazoles for corrosion inhibition of mild steel in HCl

M Z A Rafiquee, Nidhi Saxena*, Sadaf Khan & M A Quraishi

Corrosion Research Laboratory, Department of Applied Chemistry,

Faculty of Engineering & Technology, Aligarh Muslim University, Aligarh 202 002, India

Email*: nidhisaxena01@gmail.com

Received 3 April 2007; revised received 7 September 2007; accepted 12 September

Inhibition effect of some fatty acid oxadiazoles on the corrosion of mild steel (MS) in aqueous solution containing 1 N HCl was investigated by weight loss, potentiodynamic polarization technique, electrochemical impedance spectroscopy and scanning electron microscopy. The adsorption of these compounds was found to obey Langmuir adsorption isotherm. Various thermodynamic parameters were calculated to investigate the mechanism of corrosion inhibition. The effect of inhibitor concentration, solution temperature, immersion time and acid concentration on the corrosion of mild steel has also been investigated by weight loss technique. Scanning electron microscopy (SEM) is used to examine the surface morphology of the mild steel samples both in absence and presence of inhibitor at optimum concentration. Potentiodynamic polarization data showed that the compounds studied are cathodic type inhibitors in the acid solution. Electrochemical impedance spectroscopy was also used to investigate the mechanism of the corrosion inhibition.

Keywords: Mild steel, Oxadiazoles, Potentiodynamic polarization, Electrochemical impedance spectroscopy (EIS), Scanning Electron microscopy (SEM)

IPC Code(s): C23F11/00

Mild steel is an industrially important material used in the fabrication of reaction vessels, storage tanks which either manufacture or use hydrochloric acid as reactant. It is corroded by many agents, of which aqueous acids are the most dangerous. The protection of steel from corrosion is the need of hour. Various methods are adopted to prevent corrosion but the use of inhibitors is one of the most practical methods for protection against corrosion, especially in acidic media. Fatty acid inhibitors constitute an important class of corrosion inhibitors[1-3]. Azoles are found to be excellent corrosion inhibitors for steel[4-9]. In continuation of previous work on development of fatty acid derivatives as corrosion inhibitors[10-13], the inhibitory effect of aliphatic and aromatic oxadiazoles namely 2-decane-5-mercapto-1-oxa-3,4-diazole (UMOD), 2-pentadecane-5-mercapto-1-oxa-3,4-diazole (PMOD), 2-aminophenyl-5-mercapto-1-oxa-3,4-diazole (AMOD) and 2-nitrophenyl-5-mercapto-1-oxa-3,4-diazole (NMOD) on the corrosion of mild steel in hydrochloric acid have been studied.

Experimental Procedure

Inhibitors

The inhibitors were synthesized in the laboratory following the procedure described earlier[14] and characterized through their spectral data (FTIR) and their purity was confirmed by thin layer chromatography (TLC). Name and structural formulas of the inhibitors are given in Table 1.

Electrolyte

Hydrochloric acid (MERCK) of AR grade was used to prepare solution of appropriate concentrations using double distilled water. All the experiments were done in 1 N acid solution.

Specimens

Cold rolled mild steel strips having composition[15], (wt%): 0.14%C, 0.35% Mn, 0.17%Si, 0.025%S, 0.03%P and balance iron Fe were used.

Weight loss studies

Mild steel coupons of size 2.0 x 2.5 x 0.2 cm were degreased using acetone and finally dried. The cleaned specimens were weighed before and after the experiments. The concentration range of inhibitor employed in experiments was 100 to 500 ppm in 1 N HCl and maximum inhibition efficiency is attained at 500 ppm. Weight loss measurements were conducted in 1 N HCl for various immersion time (3 to 24 h) and at various temperatures ranging from 30 to 60 °C as per ASTM method[16].

Electrochemical polarization measurement

Potentiodynamic polarization studies were carried out using an EG & G Princeton Applied Research (PAR) potentiostat/galvanostat (model 173), a universal programmer (model 175) and an X-Y recorder (model RE0089). A platinum foil was used as auxiliary electrode and a saturated calomel electrode (SCE) was used as reference electrode and mild steel was used as working electrode. All the experiments were carried out at temperature (30±1°C). Equilibrium time leading to steady state of the specimens was 30 min. Sweep rate in potentiodynamic experiments was 1 mV/s.

Electrochemical impedance studies

Electrochemical impedance spectroscopy (EIS) measurements were performed on mild steel in 1 N HCl in absence and presence of 100, 300 and 500 ppm of DMOD in the frequency range 5 Hz- 100 kHz. A time interval of few minutes was required for open circuit potential (o.k.) to reach a steady value. All the measurements were carried out using Zahner IM-6 electrochemical workstation at 30 ± 2°C.

Scanning electron microscopy

Scanning electron microscope (SEM) Model No 435 VP LEO was used to study the morphology of corroded surface in presence and absence of inhibitors. The specimens were thoroughly washed with double distilled water before putting on the slide. The photographs were taken of that portion of specimen from where better information was obtained. They were photographed at 3000μ magnification. To understand the morphology of the steel surface in absence and presence of inhibitors, the following cases have been examined.

(i) Polished mild steel specimen

(ii) Mild steel specimen dipped in 1 N HCl

(iii) Mild steel specimens dipped in 1 N HCl containing 500 ppm concentration of UMOD.

Results and Discussion

Weight loss studies

The values of percentage inhibition efficiency (%IE) and corrosion rate (CR) obtained from weight loss method at different concentrations of inhibitors at 30°C is shown in Fig. 1. It has been found that all compounds inhibit the corrosion of mild steel in HCl solution, at all concentrations (100 – 500 ppm) used in this study. It has also been observed that the inhibition efficiency for all of these compounds increases with the increase in concentration up to 500 ppm.

Figure 2 shows the variation of inhibition efficiency with solution temperature. Inhibition efficiency (IE) for all studied inhibitors first increases on increasing temperature from 30 to 40°C and then decreases with further increase in temperature upto 60°C indicating the desorption of the inhibitor molecules from metal surface occur at higher temperatures[17].

The influence of immersion time on inhibition efficiency for all four fatty acids oxadiazoles is presented in Figure 3. It is observed that inhibition efficiency (IE) decreases with increase in immersion time from 3 to 24 h which shows the non persistency of the adsorbed fatty acid oxadiazoles over a longer test period. Figure 4 depicts the effect of acid concentration on inhibition efficiency. It is clear that the change in acid concentration (1 to 5 N) does not cause any significant change in inhibition efficiency of all the compounds studied thereby suggesting that all the compounds are effective inhibitors in acid solution of different concentrations.

Adsorption isotherm studies

The degree of surface coverage (θ) for different concentration of inhibitors in 1 N HCl at 30°C for 3 h of immersion time has been evaluated from weight loss values. The data were tested graphically by fitting to various isotherms. A straight line was obtained on plotting log (θ/1-θ) versus log C (Fig. 5) suggesting that the adsorption of the compounds on mild steel surface in HCl follows Langmuir's adsorption isotherm.

A plot of log θ/1-θ versus 1/T is given in Fig. 6. Slope of the plot (-Q/2.303R) gives the values for calculating heat of adsorption (Q) and are depicted in Table 2. Since the values of heat of adsorption for all the inhibitors are less than (-40 KJ mol^{-1}), hence showing physical adsorption of inhibitors on metal surface[18].

It has been reported by some authors [19-21] that in acid solution, the logarithm of the corrosion rate is a linear function of 1/T (Arrhenius equation):

$$\text{Log (Rate)} = \frac{-E_a^0}{2.303RT} + A$$

where, E^{o}_{a} is the apparent effective activation energy, R is the general gas constant and A the Arrhenius pre exponential factor. A plot of log of corrosion rate obtained by weight loss measurement versus 1/T gave straight line as shown in Fig. 7. The values of activation energy (E^{o}_{a}) obtained from the slope of the lines are given in Table 2. An alternative formula of the Arrhenius equation is the transition state equation:

$$\text{Rate} = \frac{RT}{Nh}\exp\left(\frac{\Delta S^{0}}{R}\right)\exp\left(-\frac{\Delta H^{0}}{RT}\right)$$

where, h is the plank's constant, N is the Avogadro's number, ΔS^{o} is the entropy of activation and ΔH^{o} is the enthalpy of activation. A plot of log (rate/T) versus 1/T should give a straight line (Fig. 8) with a slope of ($-\Delta H^{o}$ /2.303 R) and an intercept of [(log (R/ Nh) + (ΔS^{o}/ 2.303 R)], from which the values of ΔS^{o} and ΔH^{o} were calculated and listed in Table 2.

The data shows that activation energy (E^{o}_{a}) values for inhibited system are higher than those of uninhibited system except NMOD and are more effective at room temperature. The E^{o}_{a} value for NMOD is less than those in free acid indicating that inhibitor exhibit high efficiency at elevated temperature[22]. The values of ΔH^{o} for all inhibitors are higher indicating more energy barrier for the reaction in presence of inhibitor is attained[23]. The entropy of activation ΔS^{o} in the absence and presence of the inhibitors are large and negative. This indicates that the activated complex in the rate determining step represents an association rather than a dissociation step, meaning that a decrease in disorderness takes place during transformation from reactants to the activated complex[24]. Free energy of adsorption (ΔG_{ads}) calculated using the following equations [25] are given in Table 3.

$$\Delta G_{ads} = - RT \ln (55.5\, K)$$

and K is given by:

$$K = \theta/C\,(1-\theta)$$

where θ is degree of coverage on the metal surface, C is concentration of inhibitor in mole/L, K is equilibrium constant, R is a constant and T is temperature. The low and negative value of ΔG_{ads} indicated the spontaneous adsorption of inhibitor on the surface of mild steel[26]. ΔG_{ads} values are less than -40 KJ/mol (-9.56 k Cal/mol), which shows physical adsorbtion of oxadiazoles on the metal surface[27].

The plot of log (weight loss) versus immersion time depicted in Fig. 9, gave a straight line indicating that the reaction is first order reaction. The value of the rate constant was calculated using the first order rate law[28]

$$k = \frac{2.303}{t}\log\frac{A_0}{A}$$

where A_o is the intial mass of the metal and A is the mass corresponding to time t. The half life ($t_{1/2}$) values were calculated using equation[29].

$$t_{1/2} = \frac{0.693}{k}$$

and weight loss is expressed in grams.

The values of the rate constant and half life ($t_{1/2}$) obtained from above equation are summarized in Table 3. Half life ($t_{1/2}$) values were found to be constant at different immersion times. The constant values of rate constant further confirmed that corrosion of mild steel in 1 N HCl in presence of different inhibitors follows first order kinetics[30].

Potentiodynamic polarization studies

Various corrosion parameters such as E_{corr}, I_{corr}, IE and CR obtained from Fig. 10 are given in Table 4. It is observed that presence of the oxadiazoles decreases I_{corr} values. Maximum decrease in I_{corr} was observed in case of UMOD. The trend of the IE was founds to be same as that of weight loss study. E_{cor} values do not show any significant change in presence of all the oxadiazoles in the acid solution suggesting that all these oxadiazoles are cathodic type inhibitors (i.e., they retard the corrosion reaction by blocking cathodic sites of the metal)[31].

Electrochemical impedance studies

Table 6 includes the results of impedance studies and Fig. 11 shows Nyquist plots in the absence and presence of 100, 300 and 500 ppm of UMOD. The values of R_t and C_{dl} were calculated from Nyquist plots as described elsewhere[32]. The percentage IE was calculated using equation[33].

$$\%\ \text{I. E.} = \frac{1/R_{t_o} - 1/R_{t_i}}{1/R_{t_o}} \times 100$$

where R_{to} and R_{ti} are charge transfer resistance without and with inhibitor, respectively and are given in Table 5. The Nyquist plots (Fig. 11) contain depressed semi-circles with the center under the real axis, whose size increase with the increase in UMOD concentration, indicating a charge transfer process mainly controlling the corrosion of mild steel. Such behaviour is characteristic for solid electrodes and often referred to frequency dispersion[34], attributed to roughness and other inhomogeneities of the solid surface, adsorption of inhibitors[35], and formation of layers[36,37]. It is clear that the charge transfer resistance of mild steel in uninhibited HCl solution has significantly changed after the addition of UMOD in the corrosive solution. This means that the impedance of inhibited substrate increases with increasing DMOD concentration and consequently the inhibition efficiency increases.

The C_{dl} value decreases due to the increase in the thickness of the electrical double layer, suggesting that the UMOD function by adsorption at the metal/solution interface. Thus, the change in C_{dl} values was caused due to the gradual replacement of water molecules by the adsorption of the UMOD molecules on the metal surface, thus decreasing the extent of the metal dissolution[38].

Scanning electron microscopy

It is evident from Figure 12 that the surface of mild steel immersed in inhibited solution is smoother than that in 1N HCl alone. These observations suggest that inhibitors form protective layer on the metal surface, which prevent attack of acid on metal surface.

Mechanism of corrosion inhibition

Inhibition of corrosion of mild steel in the acidic solutions by the fatty acid oxadiazoles can be explained on the basis of molecular adsorption. In acidic solutions these compounds exist as protonated species. These protonated species may adsorb on the cathodic sites of the mild steel and decrease the evolution of hydrogen. It is apparent from the molecular structures that these compounds are able to get adsorbed on the metal surface through π-electrons of aromatic ring and lone pair of electrons of N, O and S atoms[39]. Among the compounds investigated in the present study, the order of IE has been found as follows,

UMOD > PMOD > AMOD > NMOD

In case of aliphatic oxadiazoles the presence of long hydrophobic chain plays an important role in increasing inhibition efficiency by keeping acid solution away from metal surface[40]. Inhibition efficiency of the tested aliphatic oxadiazoles increased with the increase in chain length up to C_{11} (UMOD) however further increase in chain length (C_{15}), as in case of PMOD, decreases the inhibition efficiency due to increase in stearic hindrance[41]. However, in case of aromatic oxadiazoles (AMOD and NMOD) orientation of substituted groups, prevent their flat orientation on the metal surface causing less adsorption and thereby exhibit less inhibition efficiency as compared to aliphatic oxadiazoles[42]. Presence of electron donating (NH_2) group in AMOD increases density of electron in the ring which facilitates stronger adsorption of AMOD on the mild steel surface that leads to higher inhibition efficiency of AMOD than NMOD.

Conclusions

(i) All fatty acid oxadiazoles exhibit good performance as corrosion inhibitors in hydrochloric acid media.

(ii) All of the studied oxadiazoles inhibit corrosion by adsorption mechanism and the adsorption of these compounds from acid solution follow Langmuir's adsorption isotherm.

(iii) All the compounds examined acted as cathodic inhibitors in HCl.

(iv) SEM photographs of mild steel exposed to 1 N HCl in presence of UMOD show smooth surface as compared to mild steel exposed to 1 N HCl alone.

(v) EIS studies show that addition of increasing concentration of UMOD decreases Cdl values and increases Rt values and inhibition efficiency.

References

1 Abd-El-Nabey B A, Khamis E, Ramadan S M & El-Gindy A, *Corrosion*, 52 (1996) 671

2 Raman A & Labine P, *Reviews on Corros Inhib Sci Tech* NACE International Houston, 2 (1996) 1

3 Schmidt G, *Brit Corros J* 19 (1984) 99

4 Quraishi M A, Khan M A W & Ajmal M, *Anti-Corros Methods Mater*, 43 (1996) 5.

5 Muralidharan S & Iyer S V K, *Anti-Corros Methods Mater*, 44 (1997) 100

6 Al-Andis N, Khamis E, Al-Mayouf A & Aboul-Enein A, *Corros Prev Control*, 42 (1995) 13.

7 Hammouti B, Aouniti A, Taleb M, Brighli M & Kertit S, *Corrosion*, 51 (1995) 411

8 Quraishi M A & Jamal D, *Mater Chem Phys*, 71 (2001) 202

9 Quraishi M A & Jamal D, *Corrosion*, 56 (2000) 983

10 Quraishi M A & Jamal D & Saeed M T, *J Am Oil Chem Soc*, 77 (2000) 265

11 Quraishi M A & Jamal D, *J Am Oil Chem Soc*, 77 (2000) 1107

12 Quraishi M A & Jamal D. *Anti-Corros Methods Mater* 47 (2000) 77

13 Quraishi M A & Jamal D. *Anti-Corros Methods Mater*. 47 (2000) 233

14 Chande M S, Jagtap R S & Sharma R N, *Indian J Chem*, 34B (1995) 924

15 ASTM, *Metal Corrosion, Erosion and Wear*, Annual Book of ASTM Standards, G1-72, 0 3 02 (1987)

16 ASTM, Standard *Practice for Laboratory Immersion Corrosion Testing of Metals*, Annual Book of Standards, G 31-72, 3 02 (1990)

17 Loo B H, Lee Y G & El-Hage A, *Proc 9th Int conf on Raman Spectroscopy, Tokyo*

18 Lakhan Jee Jha, *Ph D Thesis*, Delhi University, Delhi, India, 1990

19 Quraishi M A & Khan S, *Indian J Chem Technol* 12 (2005) 576

20 Breslin C B & Carrol W M, *Corros Sci*, 34 (1993) 327

21 Khedr M G A & Lashien M S, *Corros* Sci. 33 (1992) 137

22 Putilova I N Balzin S A & Branik U P, *Metallic Corrosion Inhibitors* (Pergamon Press, New York), 1960, 31

23 Sayed S A R, Hamdy H H & Mohammed A A, *Mater Chem Phys*, 70 (2001) 64

24 Gomma G K & Wahdan M H, *Mater Chem Phys*, 39 (1995) 209

25 Schorr M & Yahalom J, *Corros* Sci, 12 (1972) 876

26 Gomma G K & Wahdan M H, *Indian J Chem Technol* 2 (1995) 107

27 Brinic S, Grubac Z, Babic R & Metikos-Hukovic M, *8th Eur Symp Corros Inhibitors, Ferrara*, Italy, 1 (1995) 197

28 Orubite O K & Oforka N C, *J Appl Sci Environ*, 8 (2004) 57

29 Atkins P W, *Chemisorbed and Physisorbed Species, A Textbook of Physical Chemistry* (University Press, Oxford), 1980, 936

30 Quraishi M A & Khan S, *J Appl Electchem*, 36 (2006) 539

31 Quraishi M A & Ansari F A, *J Appl Electchem* 36 (2006) 309

32 Ashassi-Sorkhabi H, Shaabani B & Seifzadeh D, *Electrochim Acta*, 50 (2005) 3446

33 Li S L Wang Y G, Chen S H, Yu R, Lei S B, Ma H Y & Liu D X, *Corros Sci*, 41 (1999) 1769

34 Juttner K, *Electrochim Acta* 35 (1990) 1501

35 Bentiss F, Traisnel M, Gengembre L & Lagrenee M, *Appl Surf Sci*, 152 (1999) 237

36 Bentiss F, Traisnel M, Gengembre L & Lagrenee M *Br Corros J*, 35 (2000) 315

37 Veleva S, Popova A & S Raicheva, *Proc 7th Eur Corros Inhibitors, Ferrara* (1990) 149

38 McCafferty E & Hackerman N, *J Electrochem Soc* 119 (1972) 146

39 Quraishi M A, Mideen A S, Khan M A W & Ajmal M *Indian J Chem Technol*, 1 (1994) 329

40 Quraishi M A, Saxena N & Jamal D, *Indian J Chem Technol* 11 (2005) 220

41 Lal P, Tan T C & Lee J Y, *Corrosion*, 53 (1997) 186

42 Quraishi M A, Sardar R & Jamal D *Mater Chem Phys* 71 (2001) 309

Table 2 — Thermodynamic activation parameters for mild steel in 1 N HCl in absence and presence of inhibitors of 500 ppm concentration

Inhibitors (500 ppm)	E_a KJ mol^{-1}	ΔH KJ mol^{-1}	$-\Delta S$ J mol/K^{-1}	$-\Delta G_{ads}$ KJ mol^{-1}	Q KJ mol^{-1}
1 N HCl	50 10	47 41	202 20	-	-
UMOD	55 04	80 03	220 58	34 90	30 43
PMOD	52 13	87 85	217 52	33 71	23 36
AMOD	51 12	101 41	215 98	30 24	18 02
NMOD	48 08	103 50	210 24	29 30	14 35

Table 3 — First order rate constant and Half-life values in hours (h) for the corrosion of mild steel in 1 N HCl in absence and presence of inhibitors of 500 ppm concentration at 30 C

System	$K \times 10^{-1}$	$t_{1/2}$ (h)
1 N HCl	32 79 ± 0 141	21 13
UMOD	2 09 ± 0 112	134 48
PMOD	5 80 ± 0 145	119 47
AMOD	6 62 ± 0 194	104 74
NMOD	8 20 ± 0 212	84 44

Table 4 — Electrochemical polarization parameters for the corrosion of mild steel in 1 N HCl containing 500 ppm inhibitors at 30°C

Inhibitor conc (ppm)	E_{corr} (mV)	I_{corr} (mA cm^{-2})	IE (%)
1 N HCl	-507	0 360	-
UMOD	-552	0 027	92 50
PMOD	-533	0 031	91 38
AMOD	-526	0 036	89 85
NM0D	-517	0 045	87 52

Table 5 — Electrochemical impedance parameters for mild steel in 1N HCl containing different concentrations of UMOD at 30°C

Inhibitor conc (ppm)	R_t (ohm cm^2)	C_{dl} (μF cm^{-2})	IE (%)
1 N HCl	36	1511 50	-
UMOD 100	139 13	769 72	74 11
300	167 64	708 96	78 52
500	243 47	501 87	85 15

CAPTION FOR FIGURES

Fig 1 — Variation of inhibition efficiency with inhibitor concentration for 100-500 ppm concentration of inhibitors (•,UMOD, x, PMOD , o, AMOD Δ, NMOD)

Fig 2 — Variation of inhibition efficiency with solution temperature in 1 N HCl for 500 ppm concentration of inhibitors (•,UMOD, x PMOD , o, AMOD, Δ NMOD)

Fig 3 — Variation of inhibition efficiency with immersion time in 1 N HCl for 500 ppm concentration of inhibitors (• UMOD x PMOD, o AMOD Δ NMOD)

Fig 4 — Variation of inhibition efficiency with acid concentration in 1 N HCl for 500 ppm concentration of inhibitors (•,UMOD, x, PMOD , o, AMOD, Δ, NMOD)

Fig 5 — Langmuir's adsorption isotherm plots for the adsorption of various inhibitors in 1 N HCl on the surface of mild steel (•,UMOD, x, PMOD , o, AMOD, Δ, NMOD)

Fig 6 — Adsorption isotherm plot for log (θ/1- θ) versus 1/7 (•,UMOD, x, PMOD , o, AMOD, Δ, NMOD)

Fig 7 — Adsorption isotherm plot for log (CR) versus 1 /T (▲,UMOD, x, PMOD , o, AMOD, Δ, NMOD •, Blank)

Fig 8 — Adsorption isotherm plot for log (CR/T) versus 1 /T (▲,UMOD, x, PMOD , o, AMOD, Δ NMOD, • Blank)

Fig 9 — Plot of Log (weight loss) versus immersion time (•,UMOD, x, PMOD , o, AMOD, Δ NMOD, ▲, Blank)

Fig 10 — Potentiodynamic polarization curves of mild steel in 1 N HCl containing 500 ppm concentrations of various oxadiazoles (1) Blank (2) NMOD (3) AMOD (4) PMOD (5) UMOD

Fig 11 — Nyquist plot of mild steel in 1 N HCl in the absence and presence of 100, 300 and 500 ppm of UMOD (1) Blank (2) 100 ppm (3) 300 ppm (4) 500 ppm

Fig 12 — Scanning electron micrographs for mild steel surface in absence and presence of inhibitors (a) mild steel in 1 N HCl (b) polished mild steel and (c) mild steel in presence of UMOD

Table 1 — Name and molecular structures of the compounds used

S No	Strucures	Designation and abbreviation
1	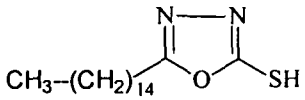	2-Pentadecane–5-mercapto-1-oxa-3.4-diazole (PMOD)
2	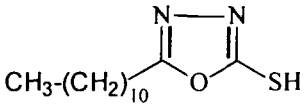	2-Undecane-5-mercapto-1-oxa-3.4- diazole (UMOD)
3	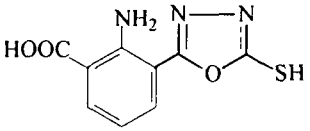	2-Aminophenyl-5-mercapto-1-oxa-3.4-diazole (AMOD)
4	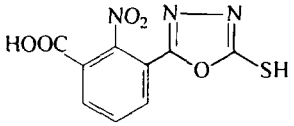	2-Nitrophenyl-5-mercapto-1-oxa-3.4-diazole (NMOD)

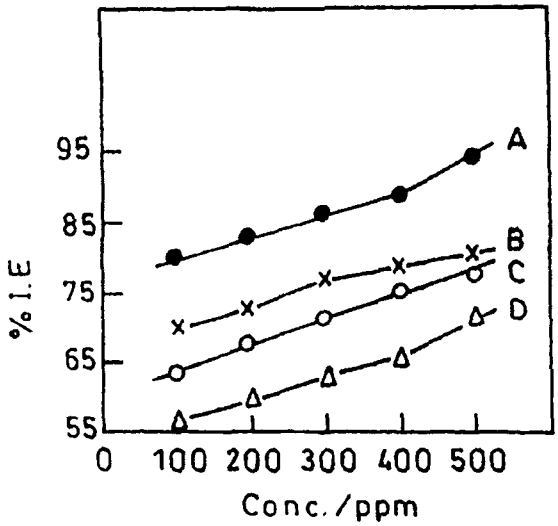
95
85
75
65
55
% I.E
0 100 200 300 400 500
Conc./ppm
A
B
C
D

FIG 1

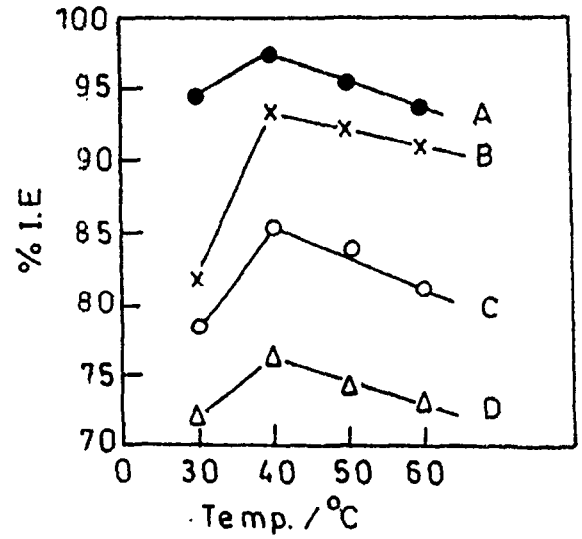
100
95
90
85
80
75
70
% I.E
0 30 40 50 60
Temp./°C
A
B
C
D

FIG 2

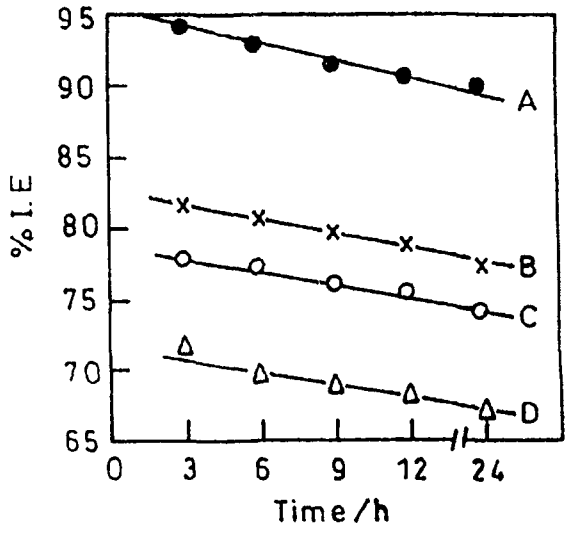
95
90
85
80
75
70
65
% I.E
A
B
C
D
0
3
6
9
12
24
Time /h

FIG 3

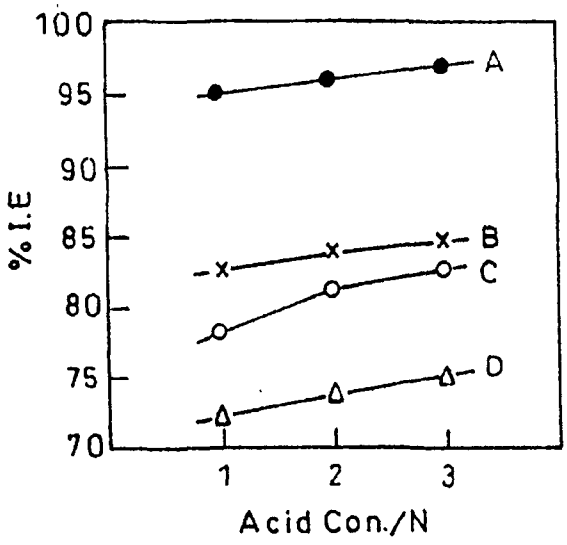
100
95
90
85
80
75
70
% I.E
A
B
C
D
1
2
3
Acid Con./N

FIG 4

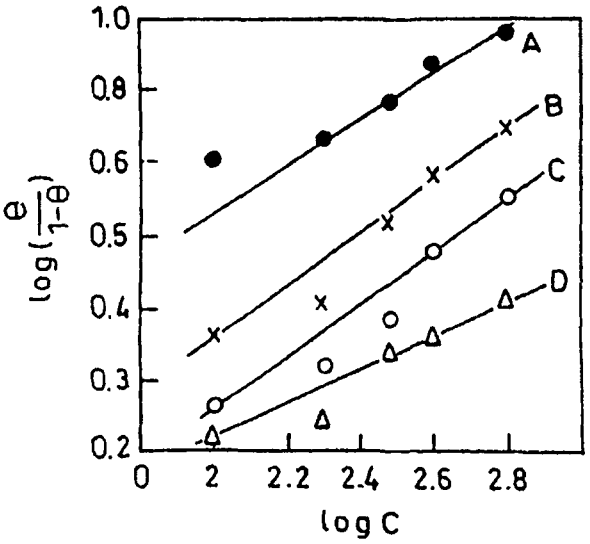
1.0
0.8
0.6
0.5
0.4
0.3
0.2
0
2
2.2
2.4
2.6
2.8
log C
log (θ/1-θ)
A
B
C
D

FIG 5

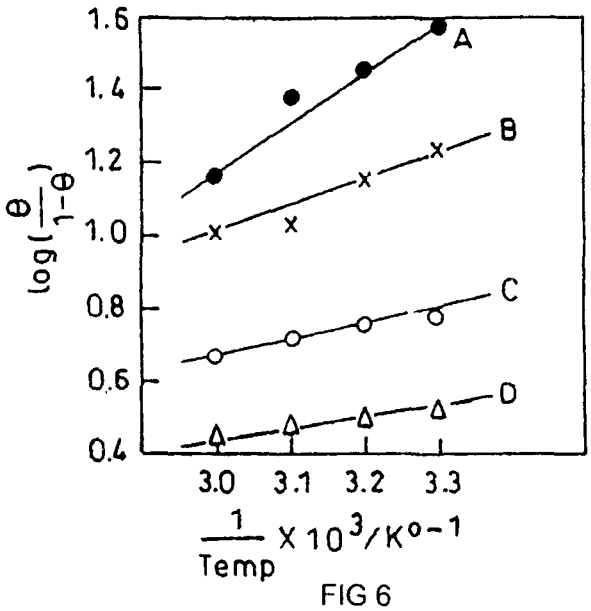
1.6
1.4
1.2
1.0
0.8
0.6
0.4
3.0
3.1
3.2
3.3
1/Temp X 10³/K°-1
log (θ/1-θ)
A
B
C
D

FIG 6

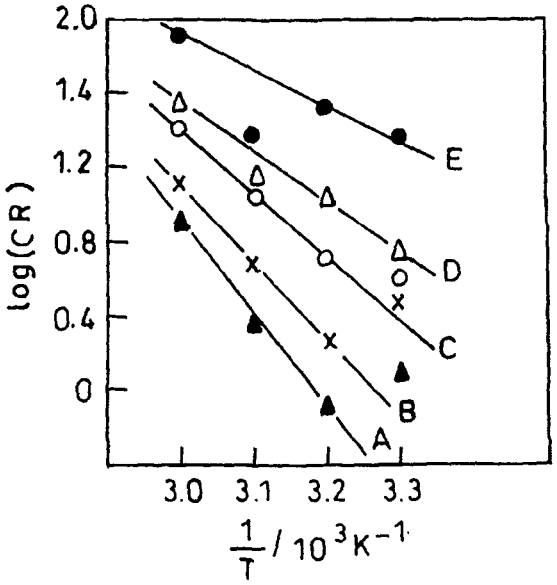
2.0
1.4
1.2
0.8
0.4
0
log(CR)
E
D
C
B
A
3.0
3.1
3.2
3.3
1/T / 10^3 K^-1

FIG 7

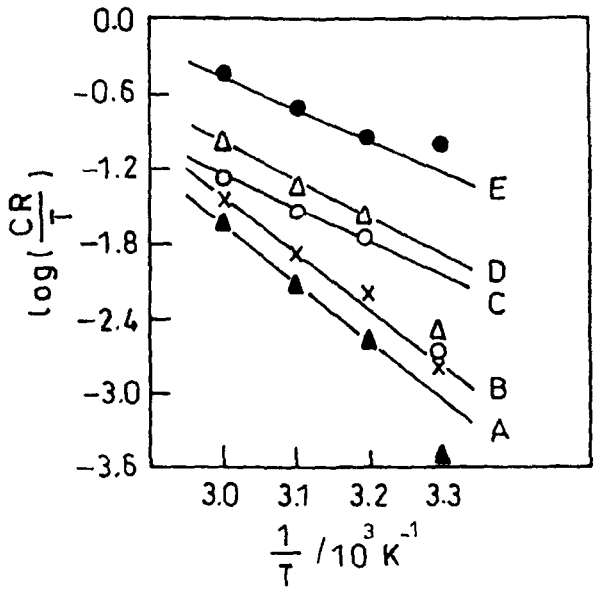
0.0
-0.6
-1.2
-1.8
-2.4
-3.0
-3.6
log(CR/T)
E
D
C
B
A
3.0
3.1
3.2
3.3
1/T /10^3 K^-1

FIG. 8

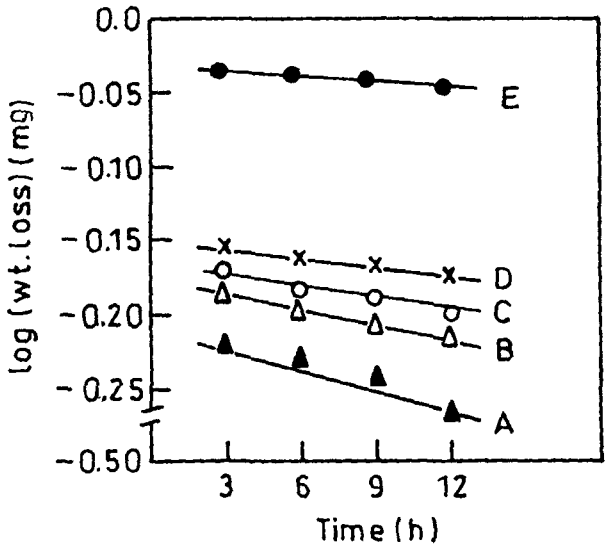
0.0
-0.05
-0.10
-0.15
-0.20
-0.25
-0.50
log (wt.loss) (mg)
E
D
C
B
A
3
6
9
12
Time (h)

FIG 9

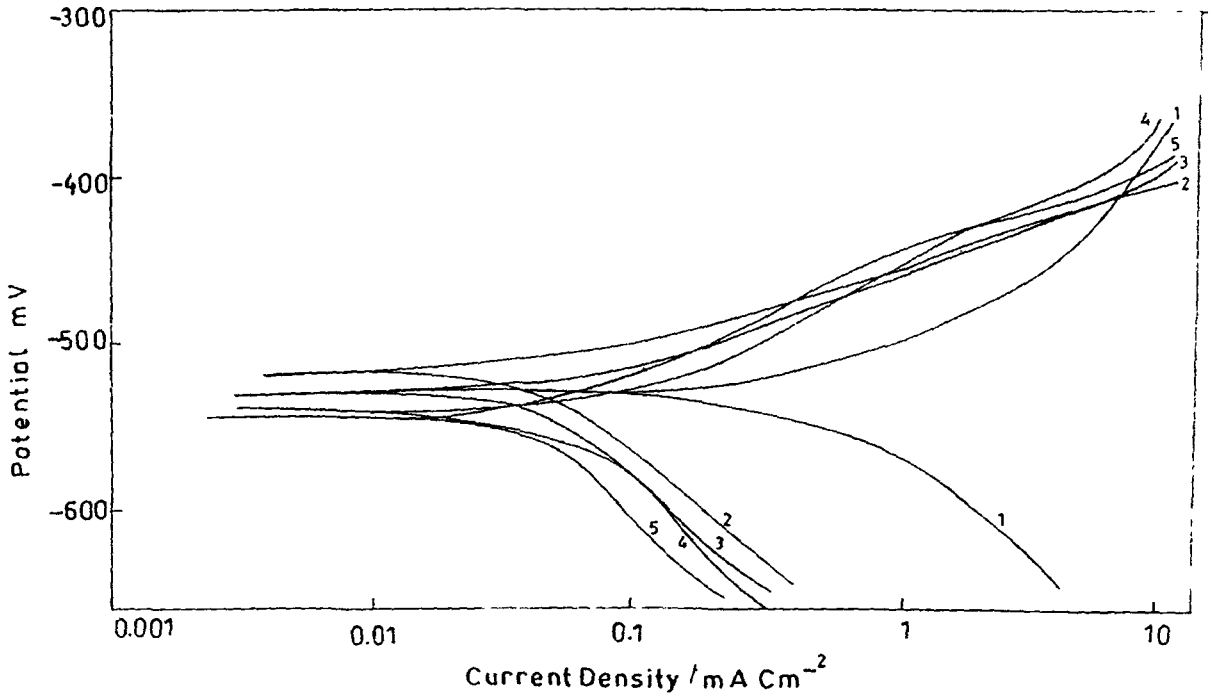
-300
-400
-500
-600
Potential mV
0.001
0.01
0.1
1
10
Current Density / mA Cm^{-2}

FIG 10

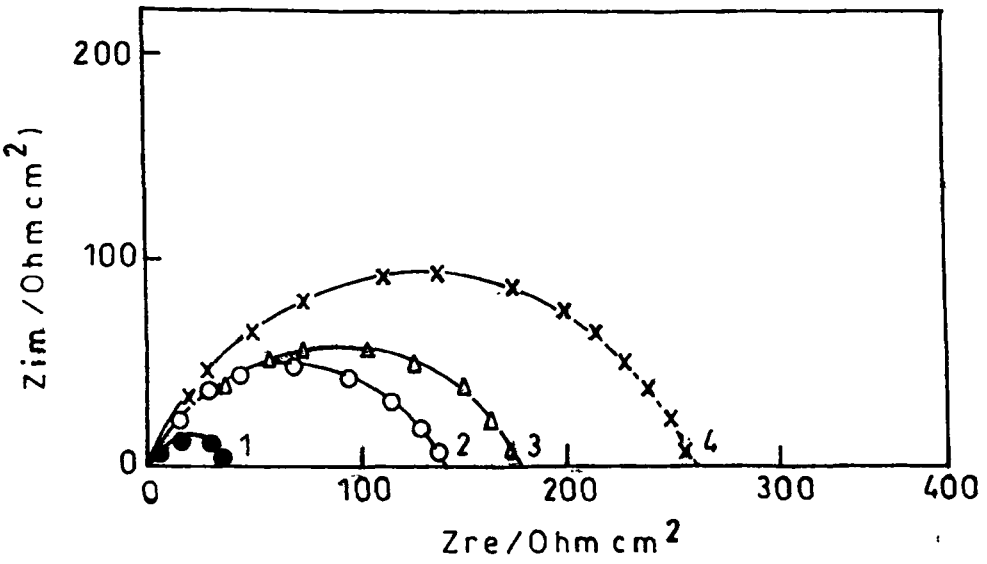

Fig 11

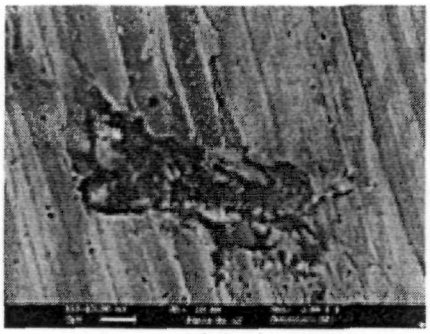

(a)

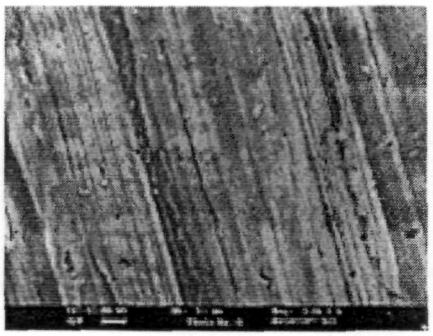

(b)

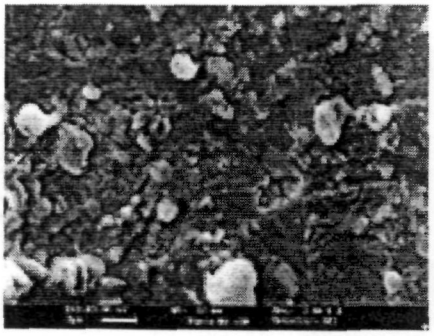

(c)

Fig 12

+Model
MAC-12089; No. of Pages 6

Available online at www.sciencedirect.com
ScienceDirect
Materials Chemistry and Physics xxx (2007) xxx–xxx
MATERIALS CHEMISTRY AND PHYSICS
www.elsevier.com/locate/matchemphys

Influence of surfactants on the corrosion inhibition behaviour of 2-aminophenyl-5-mercapto-1-oxa-3,4-diazole (AMOD) on mild steel

M.Z.A. Rafiquee[a,*], Nidhi Saxena[a], Sadaf Khan[a], M.A. Quraishi[b]

[a] *Department of Applied Chemistry, Corrosion Research Laboratory, Faculty of Engineering & Technology, Aligarh Muslim University, Aligarh 202002, India*

[b] *Department of Applied Chemistry, IT-BHU Banaras Hindu University, India*

Received 26 February 2007, received in revised form 22 August 2007; accepted 25 August 2007

Abstract

The corrosion inhibition characteristics of 2-aminophenyl-5-mercapto-1-oxa-3,4-diazole (AMOD) on mild steel in HCl solution have been studied by weight loss studies and potentiodynamic polarization. AMOD is a good corrosion inhibitor in HCl solution and its inhibition efficiency is increased markedly in presence of surfactants (SDS, CTAB, TX-100). TX-100 is found to be most effective among the tested surfactants. Weight loss measurements showed that the inhibition efficiency increased with the increasing surfactant concentration and attained a maximum value around 0.2 mol dm^{-3}. In presence of surfactant, the adsorption of AMOD on the mild steel surface obeyed Langmuir's adsorption isotherm. The influence of inhibitor concentration, solution temperature, and acid concentration on the corrosion rate of mild steel has also been investigated. The deduced thermodynamic parameters for adsorption reveal a strong interaction between the inhibitor and mild steel surface. The negative values of G_{ads} indicate the spontaneous adsorption of inhibitors on the mild steel surface. Potentiodynamic polarization studies show that these surfactants are mixed-type inhibitors.

Keywords: Adsorption; Corrosion; Electrochemical technique; Metals

1. Introduction

Surfactants [1,2] also called detergents are amphiphile that contain polar or ionic head group and apolar residues. In the water or similarly strongly hydrogen-bonded solvents, they self-associate at concentrations above the critical micellar concentration (cmc) to form association colloids called micelles. Micelles have interfacial regions containing ionic or polar headgroups. This polar or ionic headgroups plays an important role in the adsorption [3,4] of surfactants onto the solid surfaces and thereby inhibit corrosion by blocking the surface of metal. Surfactant adsorption may occur due to electrostatic interaction, van der Waals interaction, hydrogen bonding and/or solvation and desolvation of adsorbate and adsorbent species [5]. Studies in surfactant media have demonstrated a marked inhibiting effect on corrosion [6–8]. The best efficiency appears to be at concentrations in the region of cmc. Depending upon the concentration of the surfactant, the adsorption may occur as an individual molecule or as surfactant aggregates of various types.

Surfactant adsorption to the metallic surface is below monolayer level at concentrations below cmc. At concentrations above cmc, adsorption of surfactant can consists of multiple layers of physically adsorbed surfactant molecules. In the present study we have investigated the effect of anionic sodium dodecylsulfate (SDS), cationic cetyltrimethylammonium bromide (CTAB), and non-ionic Triton-X-100 (TX-100) surfactants on the corrosion efficiency of 2-aminophenyl-5-mercapto-1-oxa-3,4-diazole (AMOD) by weight loss measurements and potentiodynamic measurement studies.

2. Experimental

2.1. Material preparation

The inhibitor (2-aminophenyl-5-mercapto-1-oxa-3,4-diazole, AMOD) was synthesized in the laboratory following the procedure described earlier [9]. The mild steel samples having composition (wt%): 0.14% C, 0.35% Mn, 0.17% Si, 0.025% S, 0.03% P and balance Fe have been used for the experiment. CTAB (CDH, India), SDS (BDH, India) and TX-100 (Himedia, India) were used as

* Corresponding author. Tel.: +91 571 2700920x3000; fax: +91 571 2700528.
E-mail address: drrafiquee@gmail.com (M.Z.A. Rafiquee)

0254-0584/$ – see front matter © 2007 Elsevier B.V. All rights reserved
doi:10.1016/j.matchemphys.2007.08.022

received. All the other chemicals used were of reagent grade. The stock solutions of HCl and surfactants were prepared using double distilled water.

2.2. Weight loss measurements

Weight loss measurements were conducted on the mild steel of size (surface area 2 cm × 2 cm and thickness 2.5 mm) in 1 mol dm^{-3} HCl in varying concentration ranges of surfactants in the absence and presence of inhibitor. Mild steel samples were polished with Emery Polishing paper III Grade 1/0 Plus and then degreased using acetone and was finally dried. The cleaned specimens were weighed before and after the experiments. The experiments were performed as per ASTM method described previously [10]. The inhibition efficiency (IE) was calculated by using the following equation:

$$IE = \frac{CR_{o,wl} - CR_{i,wl}}{CR_{o,wl}} \times 100 \quad (1)$$

where $CR_{o,wl}$ is the corrosion rate in blank hydrochloric acid determined by weight loss method; $CR_{i,wl}$ is the corrosion rate in presence of surfactant with and without inhibitor determined by weight loss method.

2.3. Potentiodynamic polarization studies

Potentiodynamic polarization studies were carried out using an EG&G Princeton Applied research (PAR) potentiostat/galvanostat (model 173), a universal programmer (model 175) and a X-Y recorder (model RE0089). A platinum foil was used as auxiliary electrode. A saturated calomel electrode (SCE) and mild steel were used as reference and working electrodes, respectively. All the studies were carried out at temperature (30 ± 1 C). Equilibrium time leading to steady state of the specimens was 30 min. Sweep rate in potentiodynamic experiment was 1 mV s^{-1}. The inhibition efficiency (IE) was calculated by using the following relationship [11]:

$$CR_{corr} = \frac{0.13 I_{corr} EW}{D} \quad (2)$$

$$IE = \frac{CR_{o,corr} - CR_{i,corr}}{CR_{o,corr}} \times 100 \quad (3)$$

where CR_{corr} is the corrosion rate determined by measuring I_{corr}; $CR_{o,corr}$ the corrosion rate in blank hydrochloric acid; $CR_{i,corr}$ the corrosion rate in presence of surfactant with and without inhibitor; EW the equivalent weight of iron; D the density of iron; I_{corr} is the corrosion current density.

3. Results

3.1. Weight loss measurements

Tables 1–3 show the dependence of inhibition efficiency (IE) on varying concentrations of surfactants of cationic CTAB, anionic SDS and non-ionic TX-100, respectively, in the range from 1×10^{-2} mol dm^{-3} to 5×10^{-1} mol dm^{-3} in the absence and presence of 500 ppm AMOD. These surfactants alone displayed good IE and the presence of AMOD has further enhanced the IE appreciably as shown in Fig. 1. The IE first increased with increase in [surfactant], giving a maxima at concentration 0.2 mol dm^{-3} and, thereafter, a decrease in IE was observed on further increasing the [surfactant].

The dependence of IE on variation in concentration of acid (0.01–5.0 mol dm^{-3}) at fixed concentrations of surfactant (0.2 mol dm^{-3}) and AMOD (500 ppm) at 30 °C are depicted in Fig. 2. The IE decreased with the increase in acid concentration. It may be due to the greater aggressiveness of acid solutions at higher concentration.

A very small change in IE was observed (Fig. 3) on varying the temperature from 30 °C to 60 °C. The concentration of surfactant was kept constant at 0.2 mol dm^{-3} in presence of 500 ppm AMOD and 1.0 mol dm^{-3} HCl. These studies demon-

Table 1
Variation of corrosion parameters on [CTAB] for mild steel in 1 mol dm^{-3} HCl in the absence and presence of AMOD at 30 C for 3 h

[CTAB] (mol dm^{-3})	In absence of AMOD			In presence of AMOD		
	Weight loss (mg)	IE (%)	CR (mmpy)	Weight loss (mg)	IE (%)	CR (mmpy)
0.0	62.4	–	23.20	11.3	81.85	4.21
0.01	31.0	50.09	11.62	9.1	85.43	3.38
0.05	28.8	54.17	10.69	8.6	86.12	3.20
0.075	29.7	54.89	11.03	7.4	88.14	2.74
0.10	24.7	60.16	9.20	5.2	91.66	1.93
0.20	23.9	61.57	8.91	4.1	93.43	1.52
0.30	24.7	60.31	9.20	6.2	90.05	2.30
0.50	26.0	58.24	9.68	10.9	82.49	4 06

Table 2
Variation of corrosion parameters on [SDS] for mild steel in 1 mol dm^{-3} HCl in the absence and presence of AMOD at 30 C for 3 h

[SDS] (mol dm^{-3})	In absence of AMOD			In presence of AMOD		
	Weight loss (mg)	IE (%)	CR (mmpy)	Weight loss (mg)	IE (%)	CR (mmpy)
0.0	62.4	–	23.20	11.3	81.85	4 21
0.01	29.8	52.07	11.08	8 8	85.87	3 27
0.05	27.9	55 14	10.37	7 1	88.66	2 63
0.075	26.3	57.64	9.79	6 8	89.11	2.52
0.10	23.8	61.62	8.87	4 3	91.03	2.08
0.20	22.2	64 31	8.25	2.5	95.99	0.92
0.30	23.3	62.47	8.67	4.5	92.74	1.67
0.50	24.6	60.49	9.13	9.6	84.61	3.57

Please cite this article in press as: M.Z.A. Rafiquee, et al., Influence of surfactants on the corrosion inhibition behaviour of 2-aminophenyl-5-mercapto-1,oxa-3,4-diazole (AMOD) on mild steel, Mater. Chem. Phys. (2007), doi:10.1016/j.matchemphys.2007.08.022

Table 3
Variation of corrosion parameters on [TX-100] for mild steel in 1 mol dm^{-3} HCl in the absence and presence of AMOD at 30 C for 3 h

[TX-100] (mol dm^{-3})	In absence of AMOD			In presence of AMOD		
	Weight loss (mg)	IE (%)	CR (mmpy)	Weight loss (mg)	IE (%)	CR (mmpy)
0 0	62.4	–	23.20	11.3	81.85	4 21
0.01	23.9	61.45	8.91	7.2	88.47	2 67
0.05	22.3	63.48	8.91	6.1	90.15	2 28
0.075	20.4	67.52	8.44	5.8	90.65	2 16
0.10	16.0	73.12	7.50	2.6	95.67	1 04
0.20	15.0	75 82	6.21	1.4	97.63	0 54
0.30	15.8	74.54	5.59	1.7	97.27	0 63
0.50	17.7	71 43	6.60	4.8	92 15	1 82

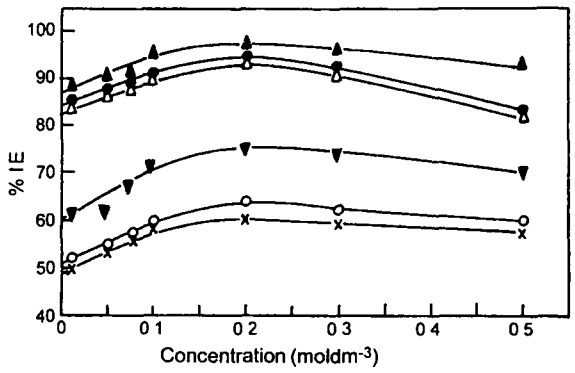

Fig. 1 Variation of inhibition efficiency on [surfactant] in absence and presence of AMOD (×, CTAB; ○, SDS; ▼, TX-100; △, CTAB + AMOD; ●, SDS + AMOD; ▲, TX-100 + AMOD).

strate that AMOD in presence of surfactant acts as more effective inhibitor at different temperatures up to 60 °C.

Surface coverage (θ) was calculated by using following relationship:

$$\theta = \frac{CR_{o,wl} - CR_{i,wl}}{CR_{o,wl}} \quad (4)$$

The surface coverage (θ) at different concentrations of surfactant in the range from 1×10^{-2} mol dm^{-3} to 5×10^{-1} mol dm^{-3} in the presence of 500 ppm AMOD has been evaluated by weight loss method. The temperature was kept constant at 30 °C and the immersion time was 3 h in 1.0 mol dm^{-3} HCl. The data was tested graphically by fitting to various isotherms. A straight line was obtained on plotting $\log\theta/(1-\theta)$ versus $\log C$ (concentration of surfactants in mol dm^{-3}) as shown in Fig. 4 which suggests that the adsorption of AMOD in presence of surfactant on mild steel follows Langmuir's adsorption isotherm. The adsorption of AMOD on mild steel surface is enhanced in presence of all the tested surfactants. This may be due to the ionic or hydrophobic interaction between the surfactant molecules and AMOD.

In order to evaluate the heat of adsorption (Q_d) and to determine the nature of adsorption, logarithm of $\theta/(1-\theta)$ was plotted against $1/T$, where T is solution temperature (Fig. 5). The heat of adsorption (Q_d) was calculated from the slope ($-Q_d/2.303R$) of the plot and its values are listed in Table 4.

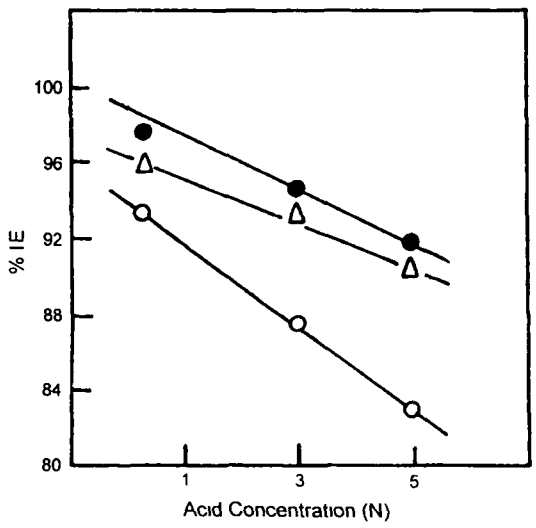

Fig 2. Variation of inhibition efficiency on [hydrochloric acid] (●, TX-100 + AMOD, △, SDS + AMOD; ○, CTAB + AMOD)

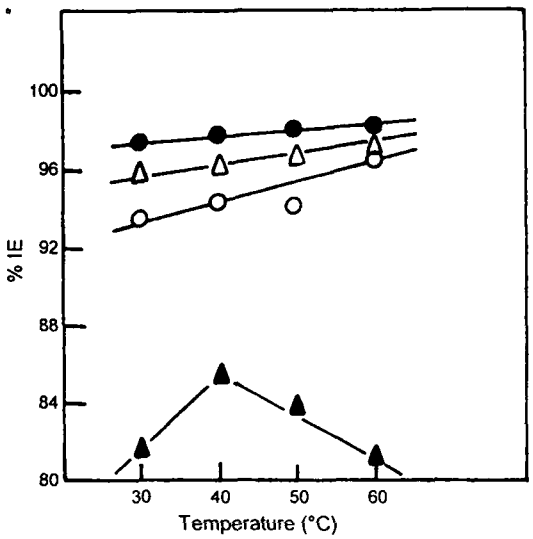

Fig 3 Variation of inhibition efficiency on temperature in 1 mol dm^{-3} HCl (●, TX-100 + AMOD; △, SDS + AMOD, ○, CTAB + AMOD, ▲, AMOD)

Please cite this article in press as: M.Z.A. Rafiquee, et al., Influence of surfactants on the corrosion inhibition behaviour of 2-aminophenyl 5-mercapto-1-oxa-3,4-diazole (AMOD) on mild steel, Mater. Chem. Phys. (2007), doi:10.1016/j.matchemphys.2007.08.022

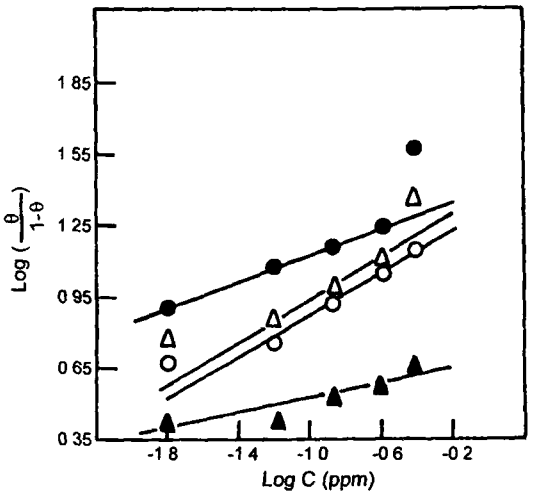

Fig 4 Langmuir's adsorption isotherm plots for the adsorption of surfactants in presence of AMOD in 1 mol dm^{-3} HCl on the surface of mild steel (●, TX 100 + AMOD, △, SDS + AMOD, ○, CTAB + AMOD, ▲, AMOD)

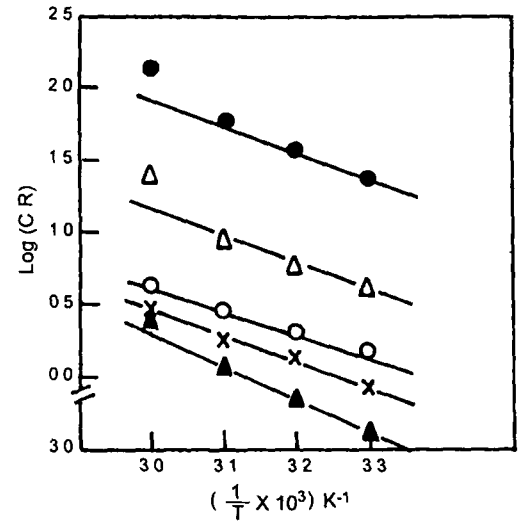

Fig 5 Arrhenius plot for log(θ/1 − θ) vs 1/T (▲, TX 100 + AMOD, × SDS + AMOD, ○, CTAB + AMOD, △, AMOD)

An alternative formula of the Arrhenius equation for rate in transition state is given by

$$\text{rate} = \frac{RT}{Nh}\exp\left(\frac{\Delta S}{R}\right)\exp\left(-\frac{\Delta H}{RT}\right) \quad (5)$$

where h is the Plank's constant, N the Avogadro's number, R is the gas constant, ΔS the entropy of activation, and ΔH the enthalpy of activation A plot of log(CR/T) versus 1/T in presence of surfactant and AMOD gave a straight line (Fig 6) with slope of ($-\Delta H/2\,303R$) and an intercept of [(log(R/Nh) + ($\Delta S/2\,303R$)] The values of ΔS was obtained from the intercept and ΔH was evaluated from the slope and are presented in Table 2 The values of enthalpies were found to be lower in presence of surfactants However, ΔS values were found to be higher in presence of surfactants than those found in free acid solution Free energy of adsorption (ΔG_{ads}) was calculated by using the following equations [12] and its values are given in Table 2

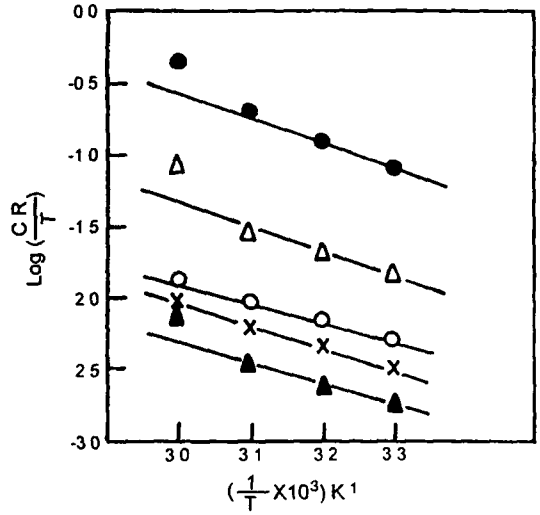

Fig 6 Arrhenius plot for log(CR/T) versus 1/T (▲ TX 100 + AMOD × SDS + AMOD, ○, CTAB + AMOD, △ AMOD, ● blank)

$$\Delta G_{ads} = -RT\ln(55\,5K) \quad (6)$$

where K is equilibrium constant and is given by

$$K = \frac{\theta}{C(1-\theta)} \quad (7)$$

where θ is degree of surface coverage of the metal surface, C the concentration of surfactants in mol dm^{-3}, R gas constant and T is the solution temperature ΔG_{ads} values calculated for all surfactants in presence of AMOD is found to be negative and the absolute values were less than −40 kJ mol^{-1} (i e −9 56 kcal mol^{-1})

Table 4
The thermodynamic activation parameters for the corrosion of mild steel in the absence and presence of surfactants and AMOD

[Inhibitor] (ppm)	[Surfactant] (mol dm^{-3})	ΔH (kJ mol^{-1})	$-\Delta S$ (J K^{-1} mol^{-1})	$-\Delta G_{ads}$ (kJ mol^{-1})	$-Q_d$ (kJ mol^{-1})
0 0	0 0	47 41	205 24	–	–
500	0 0	101 41	215 98	30 24	18 02
500	0 2 (CTAB)	29 90	231 86	34 90	30 43
500	0 2 (SDS)	29 16	234 16	33 71	23 36
500	0 2(TX 100)	40 74	238 18	29 30	14 35

Please cite this article in press as: M.Z.A. Rafiquee et al., Influence of surfactants on the corrosion inhibition behaviour of 2-aminophenyl-5-mercapto-1-oxa-3,4-diazole (AMOD) on mild steel, Mater. Chem. Phys. (2007), doi:10.1016/j.matchemphys.2007.08.022

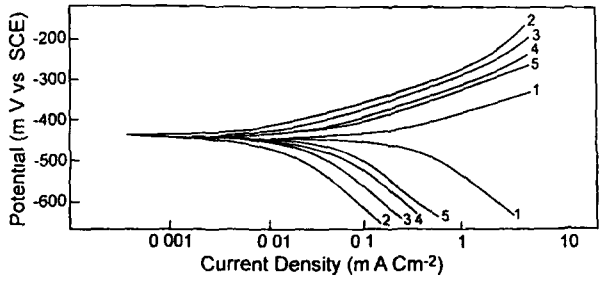

Fig. 7. Potentiodynamic polarization curves of mild steel in 1 mol dm^{-3} HCl: (1) blank; (2) TX-100 + AMOD; (3) SDS + AMOD; (4) CTAB + AMOD; (5) AMOD.

Table 5
Values of E_{corr}, I_{corr} and IE for the corrosion of mild steel under varying conditions of solution composition at 30 C

Solution composition	$-E_{corr}$ (mV)	I_{corr} (mA cm^{-2})	IE (%)
HCl	507	0.360	–
HCl + AMOD	526	0.036	89 85
HCl + AMOD + CTAB	521	0 032	90 87
HCl + AMOD + SDS	519	0.021	94 12
HCl + AMOD + TX-100	514	0.012	96.53

3.2. Potentiodynamic polarization studies

The polarization behaviour of mild steel in 1 mol dm^{-3} HCl containing 0.2 mol dm^{-3} surfactant (SDS, CTAB, TX-100) and 500 ppm AMOD at 30 °C were recorded and are shown in Fig. 7. Electrochemical parameters such as corrosion current density (I_{corr}), corrosion potential (E_{corr}), and percentage inhibition efficiency (%IE) were calculated from Tafel plots and their values are given in Table 5. The IE was calculated from the Tafel plots by using Eqs. (2) and (3).

4. Discussion

4.1. Weight loss measurements

The increased IE in the presence of surfactant (Fig. 1) may be attributed to the adsorption of surfactants [13,14] and AMOD to the mild steel surfaces. The anionic surfactant (SDS) tends to adsorb on the surface due to electrostatic interactions through the head groups. The surface adsorption of CTAB may take place via hydrogen bonding or other attractive dispersion forces. The adsorption of non-ionic surfactant, i.e. TX-100 involves hydrogen bonding between surface hydrogen atoms and proton acceptors in polar group and the hydrophobic bonding between the surface and the hydrocarbon tails. The increase in [surfactant] leads to the association of the adsorbed surfactant into aggregates to form monolayer coverage called hemimicelles. The surfactants are effective even at their low concentrations. At low concentrations, the surfactant monomers are adsorbed as individual ions/molecules without mutual interactions.

At higher concentrations, tail–tail interactions of surfactants may begin to cause association of the adsorbed surfactants aggregates into an additional coverage beyond the monolayer, i.e. admicelles or bilayer formation. The surfactant monomers headgroups of the first layer faces the surface while those of the second layer face the bulk solution. Thus the increase in concentration of surfactant solutions increases the surface coverage from coverage at lower [surfactant] to bilayer coverage at higher [surfactant]. The addition of AMOD to the surfactant solution further increases the IE as illustrated by Fig. 1. AMOD is poorly soluble in water and it exists in the protonated form in acidic solution. The non-ionic surfactants, TX-100 and anionic SDS bind with AMOD through electrostatic interaction [15]. Thus TX-100 and SDS help AMOD to adsorb at the surface more firmly and, therefore, display higher IE. The IE in CTAB is still higher but lower as compared to TX-100 and SDS. It may be due to the adsorption of AMOD to the surface by binding with CTAB as co-ions or through hydrophobic interactions. The adsorption of AMOD along with surfactant results in the enhancement of the corrosion inhibition behaviour of AMOD.

From Fig. 2, it is clear that IE decreases with increase in acid concentration from 1.0 mol dm^{-3} to 5.0 mol dm^{-3} HCl for all the three surfactants (SDS, CTAB, TX-100) in presence of AMOD. The decrease in IE on increasing acid concentration is due to increased aggressiveness of the acid solutions [16]. The variation of IE with solution temperature is shown in Fig. 3. The small variation in IE with the increase in temperature from 30 °C to 60 °C demonstrates that the inhibitive film formed on the metal surface is protective in nature in this temperature range. A straight line was obtained on plotting $\log(\theta/1-\theta)$ versus $\log C$ as shown in Fig. 4 suggesting that the adsorption of AMOD in the presence of surfactants on mild steel surface follows Langmuir's adsorption isotherm.

The values of the heat of adsorption (Q_d) calculated from slope ($-Q_d/2.303R$) of the plot $\log\theta/(1-\theta)$ versus $1/T$ (Fig. 5) are presented in Table 4. The values of heat of adsorption for SDS, CTAB and TX-100 in presence of AMOD show the physical nature of adsorption [17].

From the plot of $\log(CR/T)$ versus $1/T$ (Fig. 6), the values of ΔH and ΔS were deduced. The slope ($-\Delta H/2.303R$) and intercept [$(\log(R/Nh)+(\Delta S/2.303R)$] gave the values of ΔH and ΔS, respectively. The lower values of ΔH for surfactants in presence of AMOD indicate less energy barrier for the reaction in presence of surfactants [18]. The entropy of activation ΔS in the absence and presence of the surfactants along with AMOD are negative and large. This indicates that the activated complex in the rate-determining step represents an association rather than a dissociation step, meaning that a more decrease in disorderness takes place during transformation from reactants to the activated complex [19]. The absolute values of ΔG_{ads} calculated for all surfactants in presence of AMOD are found to be less than -40 kJ mol^{-1} (-9.56 kcal mol^{-1}) suggesting that all surfactants are physically adsorbed on the metal surface [20]. The low and negative values of ΔG_{ads} indicate the spontaneous nature of adsorption of surfactants on the surface of mild steel [21].

Please cite this article in press as: M.Z.A. Rafiquee, et al., Influence of surfactants on the corrosion inhibition behaviour of 2-aminophenyl-5-mercapto-1-oxa-3,4-diazole (AMOD) on mild steel, Mater. Chem. Phys. (2007), doi:10.1016/j.matchemphys.2007.08.022

4.2. Potentiodynamic polarization studies

Various corrosion parameters such as E_{corr}, I_{corr}, IE and CR were obtained from Fig. 7 and are given in Table 5. It is observed that the presence of surfactant decreases I_{corr}, values. Maximum decrease in I_{corr} was observed for TX-100 indicating that TX-100 is most effective surfactant among the tested surfactants. E_{corr} values do not vary significantly in presence of surfactant suggesting that they are of mixed-type inhibitors (i.e. they retard the corrosion reaction by blocking both anodic and cathodic sites of the metal) [22].

5. Conclusions

1. SDS, CTAB and TX-100 in presence of AMOD showed good performance as corrosion inhibitor in hydrochloric acid media.
2. All of the three tested surfactants inhibited corrosion by adsorption mechanism and the adsorption of these compounds from acid solution followed Langmuir's adsorption isotherm.
3. The examined surfactants acted as mixed inhibitors.

Acknowledgement

The authors are thankful to the Chairman, Department of Applied Chemistry, Aligarh Muslim University, Aligarh for the facilities provided during the research work.

References

[1] M.I. Rosen, Surfactants and Interfacial Phenomena, 2nd ed., Wiley, New York, 1989.
[2] Th.F. Tadros, Surfactants, Academic Press, New York, 1984
[3] D.W. Fuerstenau, J. Phys. Chem. 60 (1956) 981.
[4] P. Somasundaran, T.W. Healy, D.W. Fuerstenau, J. Phys Chem 68 (1964) 3562.
[5] J.H. Harwell, I.C. Haskins, R.S. Schecter, W.H. Wad, Langmuir 1 (1985) 251.
[6] W.A. Monika, A. Siddique, Dubey, Prog. Electrochem Acta 23 (2005) 445
[7] M.L. Free, Corros. Sci. 44 (2002) 2865.
[8] Z.A. Hamid, T.Y. Soror, H.A. El-Dahan, A.M.A. Omar, Anti-Corros Meth Mat. 45 (1998) 306.
[9] M.S. Chande, R.S. Jagtap, R.N. Sharma, Ind. J. Chem 34(B) (1995) 924
[10] ASTM G 31-72, Annual Book of Standards, ASTM, 1990, p 3 02
[11] M.A. Quraishi, S. Khan, J. Appl. Electrochem. 36 (2006) 539
[12] J.M. Cases, F. Villieras, Langmuir 8 (1992) 1251
[13] Y. Gao, J. Du, T. Gu, J. Chem Soc , Faraday Trans. 83 (1987) 2671
[14] R. Sharma, Surfactant Adsorption and Surface Solubilization, American Chemical Society, Washington, 1995.
[15] M.A. Mighad, E.M.S. Azzam, A M.A. Sabagh, Mater Chem Phys. 85 (2004) 273.
[16] M.A. Quraishi, J. Rawat, M. Ajmal, Corrosion 54 (1998) 996
[17] L.J. Jha, Ph.D. Thesis, Faculty of Science, Delhi University, Delhi. 1990
[18] S.A.R. Sayed, H.H. Hamdy, A.A Mohammed, Mater Chem Phys 70 (2001) 64.
[19] G.K. Gomma, M.H. Wahdan, Mater Chem Phys 39 (1995) 209
[20] S. Brinic, Z. Grubac, R. Babic, M. Metikos-Hukovic, Proceedings of the 8th European Symposium on Corrosion Inhibitors, Ferrara, Italy, 1995, p 197.
[21] G.K. Gomma, M.H. Wahdan, Ind. J. Chem Technol. 2 (1995) 107
[22] M.A. Quraishi, F.A. Ansari, J. Appl. Electrochem 36 (2006) 309

Please cite this article in press as: M.Z.A. Rafiquee, et al., Influence of surfactants on the corrosion inhibition behaviour of 2-aminophenyl-5-mercapto-1-oxa-3,4-diazole (AMOD) on mild steel, Mater. Chem. Phys. (2007), doi:10.1016/j.matchemphys.2007.08.022

J Appl Electrochem
DOI 10.1007/s10800-007-9379-0

ORIGINAL PAPER

Corrosion inhibition of aluminium in acid solutions by some imidazoline derivatives

M. A. Quraishi · M. Z. A. Rafiquee · Sadaf Khan · Nidhi Saxena

Received: 31 January 2007 / Revised: 5 July 2007 / Accepted: 13 July 2007

Abstract 2-Pentadecyl-1,3-imidazoline (PDI), 2-Undecyl-1,3-imidazoline (UDI), 2-Heptadecyl-1,3-imidazoline (HDI), 2-Nonyl-1,3-imidazoline (NI) were synthesized and characterized by FT-IR and NMR Studies. The corrosion inhibition properties of these compounds on aluminium in 1 M HCl and 0.5 M H_2SO_4 were investigated by weight loss, potentiodynamic polarization, electrochemical impedance and scanning electron microscopic techniques. The weight loss study showed that the inhibition efficiency increases with increase in the concentration of the inhibitor and was found to be inversely related to time and temperature while it shows no significant change with increase in acid concentration. The effectiveness of these inhibitors were in the order of UDI > NI > PDI > HDI .The values of activation energy, free energy of adsorption, heat of adsorption, enthalpy of activation and entropy of activation were also calculated to elaborate the mechanism of corrosion inhibition. The adsorption of these compounds on aluminium surface follows the Langmuir adsorption isotherm. The potentiodynamic polarization data show that the compounds studied are mixed type inhibitors. Electrochemical impedance was used to investigate the mechanism of corrosion inhibition. The surface characteristics of inhibited and uninhibited metal samples were investigated by scanning electron microscopy (SEM).

M. A. Quraishi
Department of Applied Chemistry, Institute of Technology, Banaras Hindu University, Varanasi 221 005, India

M. Z. A. Rafiquee · S. Khan (✉) · N. Saxena
Corrosion Research Laboratory, Department of Applied Chemistry, Faculty of Engineering and Technology, Aligarh Muslim University, Aligarh 20 2002, India
e-mail: sadaf_khan5@rediffmail.com

Keywords Corrosion inhibitors · Aluminum · Scanning electron microscopy · Potentiodynamic polarization · Electrochemical impedance

1 Introduction

Aluminium has a great economic and industrial importance owing to its low cost, light weight and high thermal and electrical conductivity. An important feature of aluminium is its corrosion resistance due to the formation of a protective film on its surface upon exposure to the atmosphere or aqueous solutions [1–3]. Hydrochloric and sulphuric acid solutions are used for pickling of aluminium or for its chemical or electrochemical etching. It is very important to add a corrosion inhibitor to decrease the rate of aluminium dissolution in such solutions. The corrosion inhibition of aluminium in acid medium has been reported recently by using hydrazone [4], anionic surfactants [5] and amino acid [6] as inhibitors.

Imidazoline compounds are reported to show corrosion resistant behaviour on copper [7, 8] and mild steel [9]. However no substantial information is available on aluminium in acid medium by imidazoline derivatives as corrosion inhibitors. Thus, it was thought worthwhile to study the corrosion inhibition behaviour of newly synthesized imidazoline derivatives namely, 2-Nonyl-1,3-imidazoline (NI), 2-Undecyl-1,3-imidazoline (UDI), 2-Pentadecyl-1,3-imidazoline (PDI), 2-Heptadecyl-1,3-imidazoline (HDI) on aluminium in acidic medium. These compounds were derived from the respective fatty acids viz., capric, lauric, palmitic and stearic acid, with a view to establish their corrosion inhibition efficiencies along with the mechanism involved in their adsorption phenomenon.

Journal 10800 | Dispatch 21-7-2007 | Pages 10
Article No 9379 | LE | TYPESET
MS Code JACH K019-07 | CP | DISK

2 Experimental details

Cold rolled aluminium strips of size 2 cm × 2.5 cm × 0.025 cm were used for weight loss measurements. For potentiodynamic polarization studies, aluminium strips coated with lacquer with an exposed area of 1 cm^2 were used. Electrodes were polished with emery papers of 1/0,2/0,3/0 and 4/0 grade and degreased with trichloroethylene. HCl and H_2SO_4 (MERCK) used for preparing solutions were of AR grade. Double distilled water was used to prepare solutions of 1 M HCl and 0.5 M H_2S0_4. The fatty acid imidazolines were synthesized as described by Hofmann [10] and the purity of the compounds was checked by TLC. The molecular structures and other details of these compounds are given in Table 1.

2.1 Synthesis of imidazoline derivatives

An appropriate amount of respective fatty acid (0.1 M) was dissolved in 50 ml absolute alcohol and treated with thionyl chloride (0.1 M). The mixture was refluxed for 3 h. The reaction product was then treated with ethylene diamine (6 ml) and was further refluxed for another 4 h. After the completion of the reaction, the solution was filtered, washed with water, dried and then crystallized in ethanol (Scheme 1).

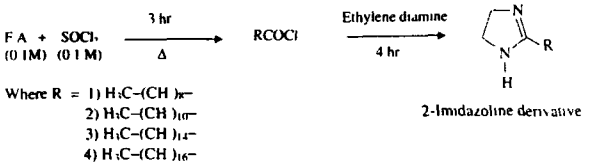

Scheme 1

2.2 FT-IR spectroscopy

FT-IR spectra of imidazoline derivative were obtained in KBr with Fourier transform spectrometer (Interspec 2020, UK), for the detection of various functional groups present in these inhibitors. FT-IR values are given in cm^{-1}.

2.3 NMR spectroscopy

^{1}H-NMR spectra run in $CDCl_3$ on a Bruker spectrospin 300 mHz spectrometer with TMS (Me_4Si) as the internal standard and its values are given in ppm (δ). The chemical shift was recorded relative to TMS assigned at zero. NMR helps in analyzing the type of protons attached to different groups of the inhibitors used.

Table 1 Name, structure and molecular weights of the compounds used

S.No	Structure	Name and abbreviation	Relative mol weight
1	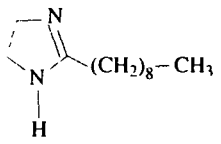	2-Nonyl-1,3-imidazoline (NI)	248
2	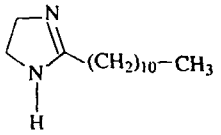	2-Undecyl-1,3-imidazoline (UDI)	276
3	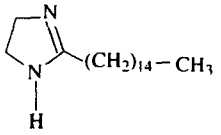	2-Pentadecyl-1,3-imidazoline (PDI)	332
4	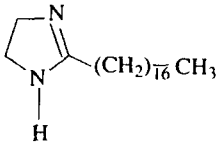	2-Heptadecyl-1,3-imidazoline (HDI)	360

Journal 10800 | Dispatch 21-7-2007 | Pages 10
Article No 9379 | LE | TYPESET
MS Code JACH K019-07 | CP | DISK

2.4 Weight loss

A number of experiments were performed with varying concentrations of imidazoline derivatives for the weight loss of aluminium as per the ASTM method described previously [11]. The inhibition efficiency of these inhibitors was calculated using the following Equation:

$$IE = \frac{CR_o - CR_i}{CR_o} \times 100 \quad (1)$$

where

CR_o = Corrosion rate in blank hydrochloric and sulphuric acid

CR_i = Corrosion rate after adding inhibitors.

2.5 Potentiodynamic polarization

Potentiodynamic polarization studies were carried out using an EG and G Princeton Applied research (PAR) potentiostat/galvanostat (model 173), a universal programmer (model 175) and a X-Y recorder (model RE0089). A platinum foil was used as auxiliary electrode and a saturated calomel electrode (SCE) as reference for the potentiodynamic polarization studies. The CR was calculated using the equation [12],

$$CR = \frac{0.13 \times I_{corr} \times EW}{D} \quad (2)$$

where,

I_{corr} = Corrosion current density in $\mu A\ cm^{-2}$.

EW = Equivalent weight of the metal in gram.

D = Density of the metal in gcm^{-3}.

2.6 Electrochemical impedance studies

The electrical equivalent circuit for the system is shown in Fig. 1.

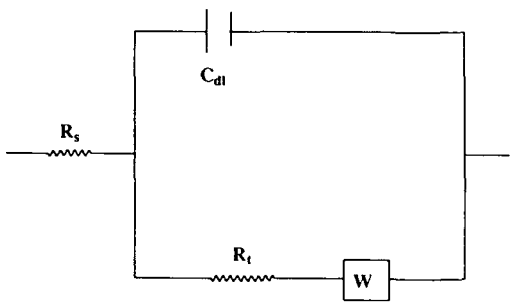

Fig. 1 Electrical equivalent circuit for the system (R_s = solution resistance, R_t = charge transfer resistance, C_{dl} = double layer capacitance, W = Warburg impedance)

The values of R_t and C_{dl} were obtained using Nyquist plots [13]. The %IE was calculated using the equation [14]:

$$IE\ \% = \frac{1/R_o - 1/R_t}{1/R_{to}} \times 100 \quad (3)$$

where R_t and R_{to} are the charge transfer resistance with and without inhibitor, respectively.

The impedance diagrams are not perfect semicircles and this difference has been attributed to frequency dispersion [15]. All the measurements were carried out using a Zahner IM-6 electrochemical workstation at 30 ± 2 °C, in the frequency range 5–100 kHz at E_{corr} for aluminium in 1 M HCl at different inhibitor concentration.

2.7 Scanning electron microscopy

A scanning electron microscope (SEM) [Model No 435 VP LEO] was used to study the morphology of the corroded surface in the presence and absence of inhibitors. The specimens were thoroughly washed with double distilled water before examination. To understand the morphology of the aluminium surface in the absence and presence of inhibitors, the following cases were examined.

(i) Polished aluminium specimen
(ii) Aluminium specimen dipped in 1 M HCl
(iii) Aluminium specimen dipped in 1 M HCl containing 500 ppm of UDI inhibitor.

3 Results and discussion

The structure elucidation was established by the results obtained from IR and NMR studies as under:

3.1 FT-IR spectroscopy

The FT-IR spectroscopic study was used to investigate the purity of the synthesized compound. The results are listed below:

(i) NI—IR (KBr): 1648 (C=N), 1352 (C–N), 2924 (C–H), 3146 (N–H), 1172 (CH_3) cm^{-1}.
(ii) UDI—IR (KBr) 1647 (C=N), 1323 (C–N), 2852 (C–H), 3257 (N–H), 1166 (CH_3) cm^{-1}.
(iii) PDI,—IR (KBr): 1640(C=N), 1463 (C–N), 2845 (C–H), 3290 (N–H), 1164 (CH_3) cm^{-1}.
(iv) HDI IR (KBr): 1665 (C=N), 1372 (C–N), 2845 (C–H), 2921 (N–H), 1250 (CH_3) cm^{-1}.

3.2 NMR spectroscopy

NMR spectral data ($\delta CDCl_3$)

UDI—7.350 (1H, NH), 1.936 (20H $(CH_2)_{10}$), 1.253 (3H, CH_3), 2.006 (4H, $(CH_2)_2$)

Journal 10800 | Dispatch 21-7-2007 | Pages 10
Article No 9379 | LE | TYPESET
MS Code JACH K019-07 | CP | DISK

3.3 Weight loss

The imidazoline compounds inhibited corrosion rate of aluminium in both 1 M HCl and 0.5 M H_2SO_4 at all concentrations under study. Inhibition efficiency increases with increase in inhibitor concentration from 25 to 700 ppm (Figs. 2a and 3a). The maximum inhibition efficiency was achieved at 500 ppm and a further increase in inhibitor concentration caused no appreciable change in performance. The effect of immersion time on inhibition efficiency is shown in Figs. 2b and 3b. All the tested imidazoline show a decrease in inhibition efficiency with increase in immersion time from 2 to 24 h. This indicates de-sorption of the fatty acid imidazoline over a longer test period and may be attributed to various other factors such as increase in cathodic reaction or increase in ferrous ion concentration [16]. The influence of solution temperature on inhibition efficiency is shown in Figs. 2c and 3c. The inhibition efficiency for all the imidazolines decreases with increase in temperature from 30 to 60°C. The decrease in inhibition efficiency with rise in temperature may be attributed to desorption of inhibitor molecules at higher temperatures. From Figs. 2d and 3d, it is evident that increase in acid concentration from 1 to 3 M HCl and 0.5 to 1.5 M H_2SO_4 did not cause significant change in the e_{IE} values, thereby suggesting that all the compounds are effective corrosion inhibitors in acid solutions over this concentration range [17].

The degree of surface coverage (θ) for different inhibitor concentrations in 1 M HCl and 0.5 M H_2SO_4 at 30°C after 2-h immersion time was evaluated from weight loss values. The data were tested graphically by fitting to various isotherms. A plot of log (θ/1-θ) versus 1/T is shown in Figs. 4a and 5a. The heats of adsorption (Q) was calculated from the slope (–Q/2.303R) of the plot and are given in Table 2. The values of heat of adsorption (<–40 kJ mol^{-1}) suggest physical adsorption [18].

A number of authors [19–21] have reported that, in acid solution, the logarithm of the corrosion rate is a linear function of 1/T (Arrhenius equation):

$$\log (\text{Rate}) = \frac{-E_a^o}{2.303RT} + A \qquad (4)$$

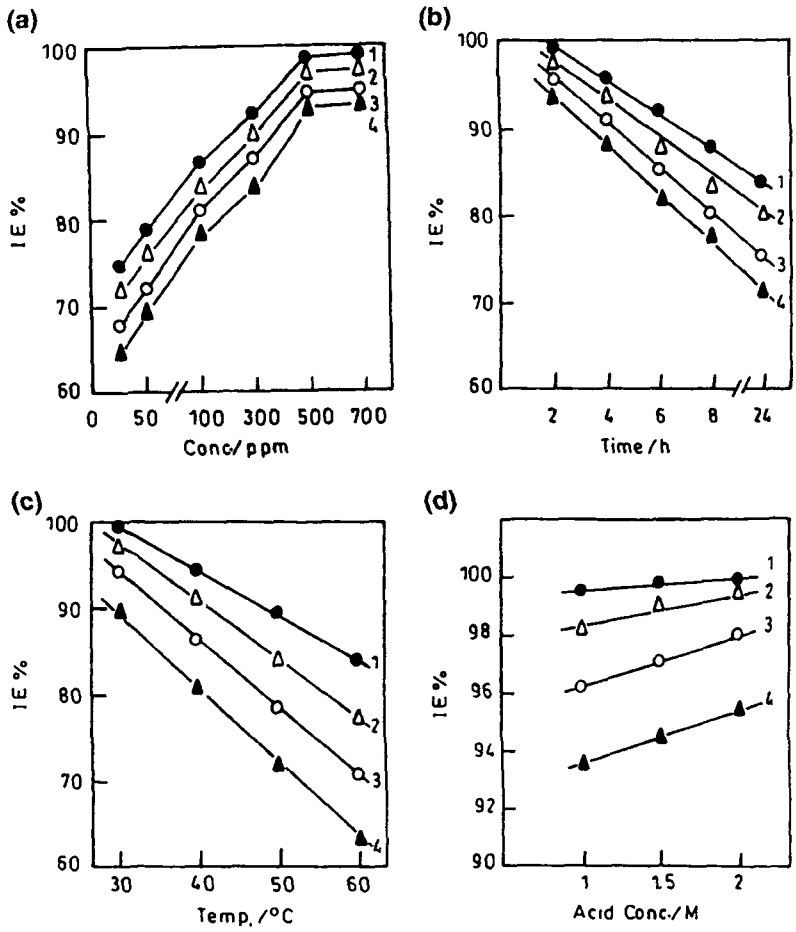

Fig. 2 Variation of inhibition efficiency with (a) inhibitor concentration, (b) immersion time, (c) solution temperature, (d) acid concentration in 1 M HCl (1 UDI, 2 NI; 3 PDI, 4 HDI)

Journal 10800 Dispatch 21-7-2007 Pages 10
Article No 9372 LE TYPESET
MS Code JACH K019-07 CP DISK

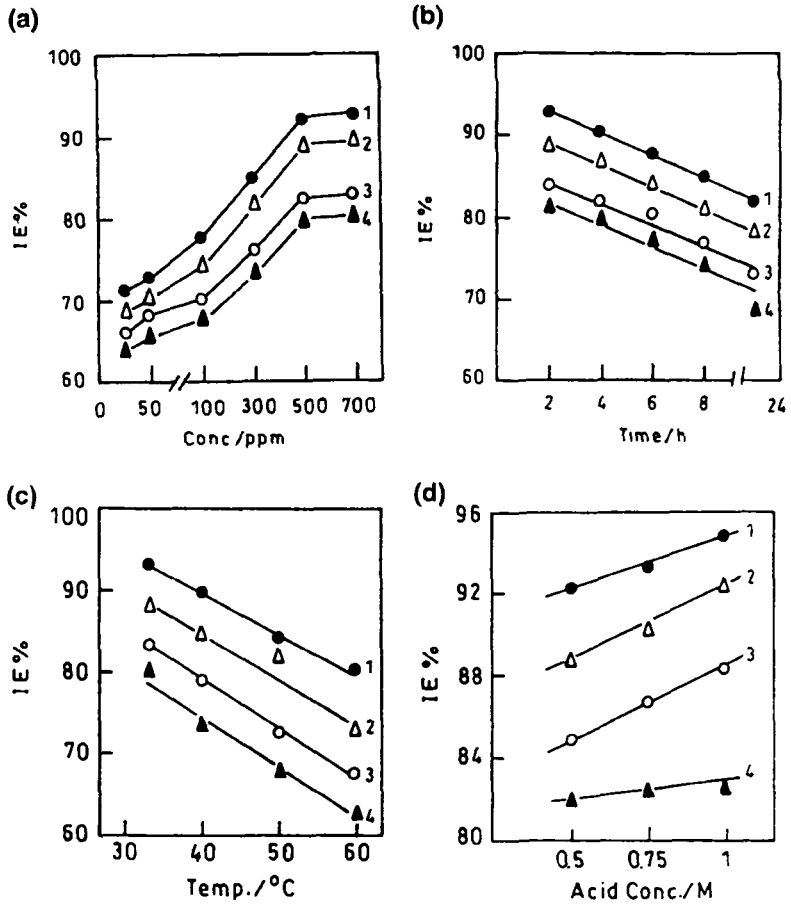

Fig. 3 Variation of inhibition efficiency with (a) inhibitor concentration, (b) immersion time, (c) solution temperature, (d) acid concentration in 0.5 M H_2SO_4 (1: UDI; 2: NI; 3: PDI; 4. HDI)

where, E^{o}_{a} is the apparent effective activation energy, R is the gas constant and A is the Arrhenius pre exponential factor. Plots of logarithm of corrosion rate obtained by weight loss measurement versus 1/T gave straight lines as shown in Figs. 4b and 5b.

The thermodynamic parameters (Table 2) show that the values of the activation energy $E^{o}_{a}$is higher for inhibited system as compared to the uninhibited system (Blank). The inhibition efficiency follows the order: UDI > NI > PDI > HDI. From the values of thermodynamic parameters, it is observed that the inhibitors are effective at lower temperatures [22].

An alternative formula for the Arrhenius equation is the transition state equation:

$$\text{Rate} = \frac{RT}{Nh}\exp\left(\frac{\Delta S^{o}}{R}\right)\exp\left(-\frac{\Delta H^{o}}{RT}\right) \quad (5)$$

where, h is the Plank constant, N is the Avogadro number, ΔS^{o} is standard entropy change and ΔH^{o} is the standard enthalpy change. A plot of log (CR/T) versus 1/T gave a straight line, (Figs. 4c and 5c) with a slope of $(-\Delta H^{o}/2.303 R)$ and an intercept of $[(\log (R/Nh) + (\Delta S^{o}/2.303 R)]$, from which the values of ΔS^{o} and ΔH^{o} were calculated. The values of standard enthalpy change, ΔH^{o} (Table 2) follow the order UDI > NI > PDI > HDI for various imidazoline inhibitors [22]. The entropy change, ΔS^{o} in the absence and presence of inhibitors is large and negative indicating that the activated complex in the rate determining step represents an association rather than a dissociation step. Thus a greater degree of orderliness appears during its transformation from reactant to activated complex [23].

The free energy of adsorption (ΔG_{ads}), was calculated by using the following equations [24] and the values are given in Table 2.

$$\Delta G_{ads} = -RT \ln (55.5 K) \quad (6)$$

where the equilibrium constant is

$$K = \theta / C (1 - \theta) \quad (7)$$

where θ is degree of coverage and C is inhibitor concentration in mol l^{-1}. The low and negative value of ΔG_{ads} indicate spontaneous physical adsorption [25].

Journal 10800 | Dispatch 21-7-2007 | Pages 10
Article No 9379 | LE | TYPESET
MS Code JACH K019-07 | CP | DISK

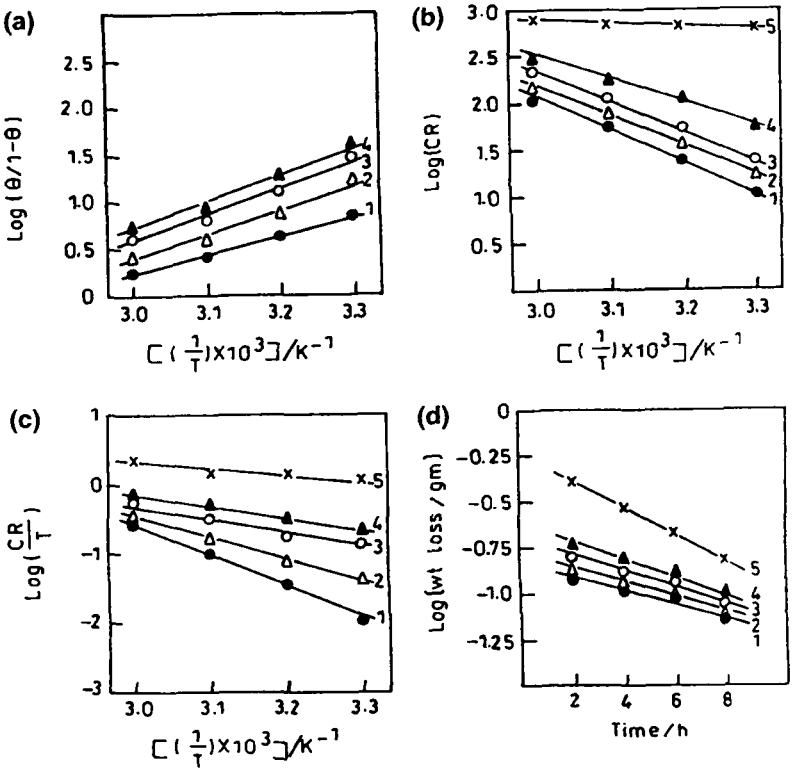

Fig. 4 Plots of (**a**) log (*θ*/1–*θ*) vs. 1/T; (**b**) log (CR) vs. 1/T; (**c**) log (CR/T) vs. 1/T; and (**d**) log (weight loss) versus immersion time in 1 M HCl (1: UDI; 2: NI; 3: PDI; 4: HDI; 5: Blank)

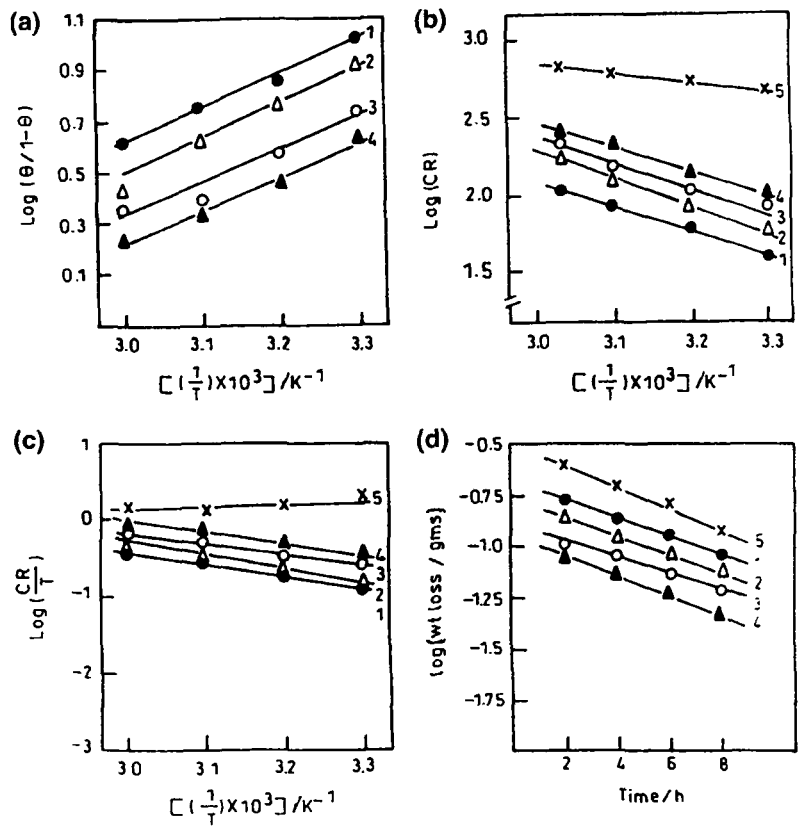

Fig. 5 Plots of (**a**) log (*θ*/1–*θ*) vs. 1/T; (**b**) log (CR) vs. 1/T; (**c**) log (CR/T) vs. 1/T; and (**d**) log (weight loss) vs. immersion time in 0.5 M H_2SO_4 (1: UDI; 2: NI; 3: PDI; 4: HDI; 5:Blank)

Journal 10800 Dispatch 21-7-2007 Pages 10
Article No 9379 LE TYPESET
MS Code JACH K019-07 CP DISK

Table 2 Thermodynamic activation parameters for dissolution of aluminium in 1 M HCl and 0 5 M H_2SO_4 in absence and presence of 500 ppm inhibitor

System	E_a (kJ mol^{-1})	ΔH (kJ mol^{-1})	$-\Delta S$ (J mol^{-1}K^{-1})	$-\Delta G_{ads}$ (kJ mol^{-1})	$-Q$ (kJ mol^{-1})
1 M HCl	9 57	22 34	189 94	–	–
UDI	67 02	76 58	210 70	35 18	38 29
NI	60 03	60 63	207 17	33 12	35 10
PDI	57 44	31 91	205 26	32 59	31 90
HDI	47 86	25 53	199 51	31 52	28 72
0 5 M H_2SO_4	12 76	9 57	194 7	–	–
UDI	25 53	31 91	207 17	32 32	26 17
NI	31 89	28 72	204 94	31 20	25 53
PDI	35 10	22 33	198 56	30 89	24 25
HDI	25 53	19 15	201 43	30 48	22 97

The rate of dissolution of metal in the presence and absence of inhibitors in acidic solution was studied by observing the weight loss at various times The reaction was followed up to 90% of the dissolution of the metal A straight-line plot (Figs 4d and 5d) was obtained for log (weight loss) versus immersion time indicating that dissolution follows first order kinetics

The values of the rate constant were calculated using the following first order rate law [26]

$$k = \frac{2\,303}{t} \log \frac{[A_o]}{[A]} \quad (8)$$

where $[A_o]$ is the initial mass of the metal and [A] is the mass corresponding to time t The half-life ($t_{1/2}$) value was calculated [27] using the following relationship

$$t_{1/2} = 0\,693/k \quad (9)$$

The values of rate constants and half-life periods obtained are summarized in Table 3 The value of rate constant (k) was found to be higher in the case of inhibited metal samples than few uninhibited samples The corrosion rate is higher in the absence of inhibitors than with inhibited aluminium samples Half-life values provide information regarding the rate of dissolution of coated and uncoated samples The half-life periods in the presence of various inhibitors are in the order UDI > NI > PDI > HDI The blank sample has the lowest $t_{1/2}$ value

Table 3 The values of first order rate constant and half life period for the dissolution of aluminium

System	10^2 k (h^{-1})	$t_{1/2}$ (h)
1 M HCl	18 690 ± 0 227	3 06
UDI	0 641 ± 0 089	108 11
NI	0 789 ± 0 104	87 84
PDI	1 660 ± 0 021	41 75
HDI	2 702 ± 0 038	25 64
0 5 M H_2SO_4	14 7 ± 0 184	4 71
UDI	1 156 + 0 013	59 95
NI	1 659 ± 0 019	41 77
PDI	2 060 ± 0 024	33 64
HDI	2 370 ± 0 282	29 24

Reaction condition [inhibitor] = 500 ppm, Temperature = 30 °C

3 4 Application of adsorption isotherm

The mechanism of corrosion inhibition may be explained on the basis of adsorption of imidazoline compounds [28] The degrees of surface coverage (θ) for different inhibitor concentrations were evaluated from weight-loss data Data were tested graphically by fitting to various isotherms A plot of log [$\theta/(1-\theta)$] vs log C shows a straight line (Fig 6a, b) indicating that adsorption in both the acids follows the Langmuir isotherm

$$\theta/(1-\theta) = k\,C \exp(-G_{ads}/RT) \quad (10)$$

where G_{ads} is the free energy of adsorption and C is the inhibitor concentration

3 5 Potentiodynamic polarization studies

The cathodic and anodic polarization curves of aluminium in 1 M HCl and 0 5 M H_2SO_4 in the absence and presence of different inhibitors at 500-ppm concentration at 28 ± 2°C are shown in (Fig 7a and b) Electrochemical parameters such as corrosion current density (I_{corr}), corrosion potential (E_{corr}), Tafel constants, b_a and b_c, and % inhibition efficiency were calculated from Tafel plots and are given in Table 4 It is observed that the presence of inhibitor lowers I_{corr} Maximum decrease in I_{corr} values was observed for UDI indicating that this is the most effective corrosion inhibitor among the studied imidazoline compounds, a trend obtained in conformity with weight loss data It is also observed from Table 4 that E_{corr} values and Tafel slope constants b_a and b_c do not change significantly

Journal 10800 Dispatch 21 7 2007 Page 10
Article No 9379 LE TYPESET
MS Code JACH K019-07 CP DISK

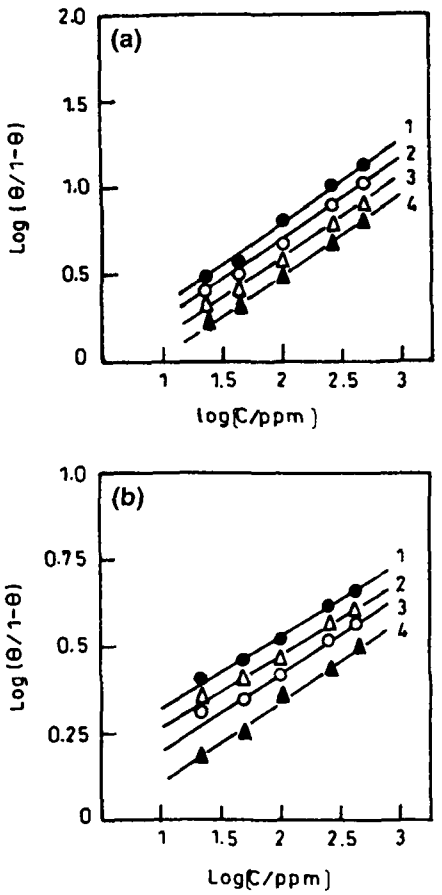

Fig. 6 Langmuir's adsorption isotherm plots for log [*0*/(1–*0*)] versus log C for the adsorption of various inhibitors on the surface of aluminium in (**a**) 1 M HCl (**b**) 0.5M H_2SO_4 (1: UDI; 2: NI; 3: PDI; 4: HDI)

in inhibited solution as compared to uninhibited solution. The imidazoline derivatives do not shift the E_{corr} values significantly, suggesting that they behave as mixed type inhibitors [29].

3.6 Electrochemical impedance study

The Impedance diagram obtained for aluminium in 1 M HCl is shown in Fig. 8 and the values of R_t, $C_{dl}$and %IE are given in Table 5. Values of R_t increases with increase in inhibitor concentration and this is, in turn, leads to an increase in the I.E [30]. A decrease in C_{dl} was observed with addition of 1 M HCl, suggesting that inhibition can be attributed to surface adsorption [31].

3.7 Scanning electron microscopy

Scanning electron microscopy of the metal samples of inhibited and uninhibited metal samples is presented in Fig. 9. The SEM study shows that the inhibited metal surface is found smoother than the uninhibited surface.

3.8 Mechanism of corrosion inhibition

In acidic solutions imidazoline compounds exist in protonated form. These protonated species are adsorbed on the cathodic sites through the π-electrons and lone pair electrons of nitrogen atoms of the imidazoline ring [28]. The observed order of e_{IE} (UDI > NI > PDI > HDI) can be explained on the basis of the nature of binding of the imidazoline ring to the metal surface and the length of the alkyl chain.

The binding of the imidazole ring to the metal surface can be presented by the diagram of Fig. 10. With the increase in chain length of the alkyl group (i.e. molecular weight), the number of imidazoline rings decreases in 500 ppm inhibitor concentration and therefore, e_{IE} decreases. The decrease in e_{IE} of NI may be due to its being least hydrophobic among the tested imidazolines and having less tendency to adsorb.

Therefore, UDI having (C_{11}) in its alkyl group has the highest adsorption to the metal surface. However the lower adsorption of PDI (C_{15}) and HDI (C_{17}) seems to be due to steric hindrance posed by the bulky alkyl groups in their adsorption phenomenon [32].

4 Conclusions

(1) The fatty acid imidazolines showed very good corrosion inhibiting behaviour for aluminium in both 1 M HCl and 0.5 M H_2SO_4 and follow the order UDI> NI > PDI > HDI.

(2) In weight loss studies, the e_{IE} of all imidazoline derivatives increase with increases in inhibitor concentration, whereas it decreases with increase in immersion time and temperature and shows no significant change with increase in acid concentration.

(3) Inhibition of aluminium surfaces in acid solutions is characterized by an adsorption mechanism which follows the Langmuir isotherm.

(4) All the compound studied behave as mixed-type inhibitors in both 1 M HCl and 0.5 M H_2SO_4.

(5) The Electrochemical study shows that the application of UDI, NI, PDI, HDI as inhibitors significantly increases R_t values and decreases C_{dl} values in 1 M HCl, suggesting that corrosion inhibition takes place by adsorption.

(6) Scanning Electron Microscopy shows a smoother surface for inhibited metal samples than uninhibited samples due to the formation of film like deposits on the inhibited surfaces.

Journal 10800 Dispatch 21-7-2007 Pages 10
Article No 9379 LE TYPESET
MS Code JACH K019-07 CP DISK

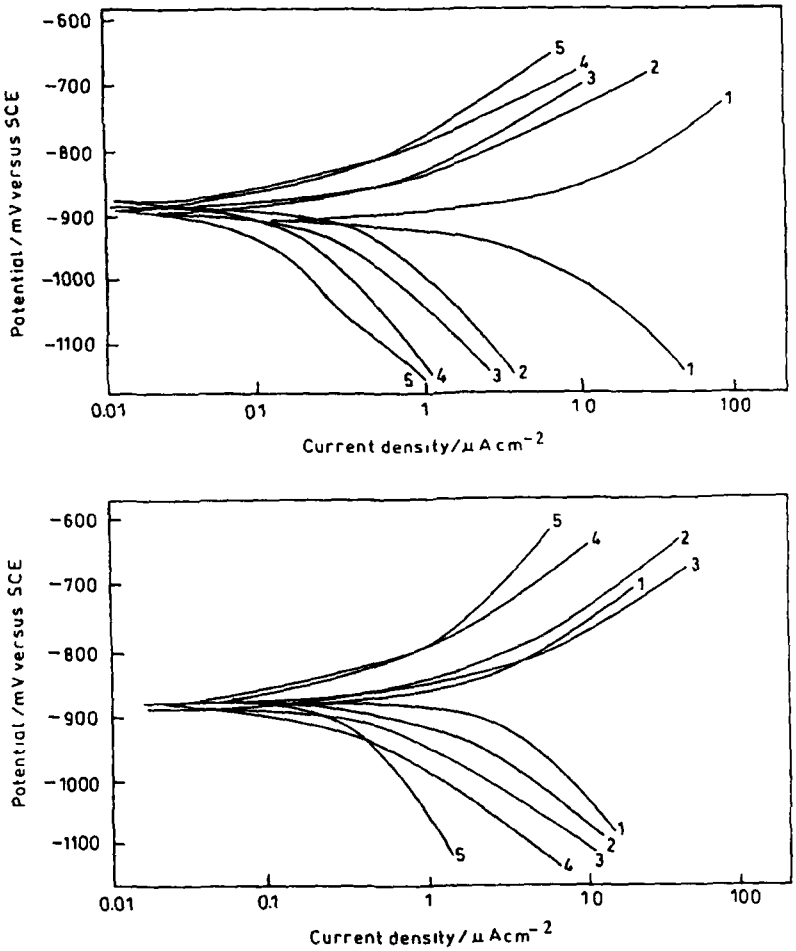

Fig. 7 Potentiodynamic polarization curves for aluminium containing 500-ppm imidazolines in (a) 1 M HCl (b) 0.5 M H_2SO_4 (1: Blank; 2: HDI; 3: PDI; 4: NI; 5: UDI)

Table 4 Electrochemical polarization parameters for the corrosion of aluminium in 1 M HCl and 0.5 M H_2SO_4 containing 500-ppm inhibitors at 30 °C

System	E_{corr} (mV)	I_{corr} (mA cm^{-2})	e_{IE} (%)	b_a (mV dec^{-1})	b_c (mV dec^{-1})
1 M HCl					
Blank	-902	4.490	-	68	174
UDI 500	-898	0.089	98.02	60	170
NI 500	-893	0.106	97.63	54	126
PDI 500	-890	0.184	93.91	56	114
HDI 500	-888	0.303	93.25	50	100
0.5 M H_2SO_4					
Blank	-890	4.160	-	56	120
UDI 500	-884	0.320	92.30	50	84
NI 500	-879	0.479	88.47	40	110
PDI 500	-880	0.681	83.63	54	94
HDI 500	-875	0.826	80.15	54	134

Journal 10800 | Dispatch 21-7-2007 | Pages 10
Article No 9379 | LE | TYPESET
MS Code JACH K019-07 | CP | DISK

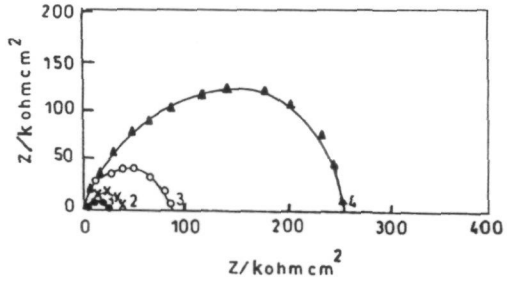

Fig. 8 Electrochemical impedance diagram (Nyquist plot) for aluminium in 1 M HCl in the absence and presence of UDI at different concentrations (1:Blank; 2: 25 ppm; 3: 100 ppm; 4: 500 ppm)

Table 5 Electrochemical impedance parameters for the corrosion of aluminium in 1 M HCl containing different concentrations of UDI at 30 °C

System	R_t (kΩ cm^2)	C_{dl} (F cm^{-2})	e_{IE} (%)
1 M HCl	16.23	4.51	–
UDI			
25	18.36	3.52	70.19
100	93.65	0.74	82.67
500	247.03	0.29	93.43

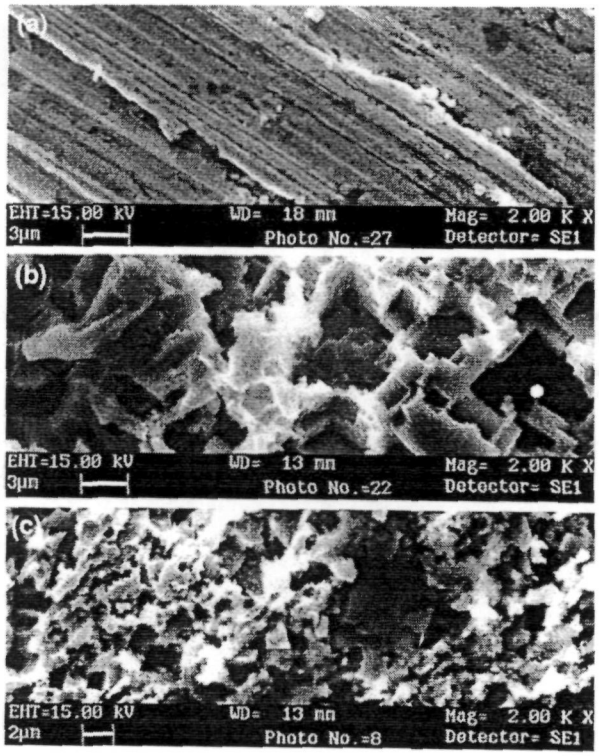

Fig. 9 Scanning electron micrographs of Polished aluminium (**b**) After dipping aluminium in 1 M HCl for 2 h (**c**) After dipping aluminium in 1 M HCl for 2 h containing 500 ppm UDI

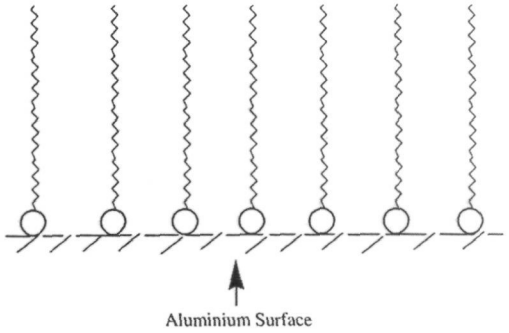

Fig. 10

References

1. Brett CM (1992) Corros Sci 33:203
2. Beck TR (1998) Electrochim Acta 33:1321
3. Hunkeler F, Frankel GS, Bohni H (1987) Corrosion 43:189
4. Ahmed Awad I, El-Asklany AH, Fouda AS (1985) J Indian Chem Soc 22:367
5. Tianpei Z, Guannan M (1999) Corros Sci 41:1937
6. Fouda AS, El-Semongy MM (1982) J Ind Chem Soc 19:89
7. Gasparac R, Martin CR, Stupnisek-Lisac E (2000) J Electrochem Soc 147:548
8. Zhang DQ, Gao LX, Zhu GD (2004) Corros Sci 46:3031
9. Muralidharan S, Iyer SVK (1997) Anti Corros Met Mat 44:100
10. Hoffmann K (1953) Imidazole and its derivatives –Part-I. The chemistry of heterocyclic compounds, Interscience publishers, Inc., New York, p 213
11. ASTM (1994) Standard practice for calculation of corrosion rate and related information from electrochemical measurements, annual book of standards, G 102-89
12. Schmidt G (1984) Br Corros J 19:99
13. Hirozawa ST (1995) Proc. 8th Eur. Symp Corros Inhi Ann Univ, Ferrara, Italy, 1:25
14. Ashassi-Sorkhabi H, Shaabani B, Seifzadeh D, (2005) Electrochim Acta 50:3446
15. Juttner K (1990) Electrochim Acta 35:1501
16. Quraishi MA, Rawat J (2001) Corrosion 19:273
17. Quraishi MA, Sardar R (2001) Corrosion 58:103
18. Jha LJ (1990) Studies of the adsorption of amide derivative during acid corrosion of pure iron & its characterization, PhD thesis, University of Delhi, p 111
19. Breslin CB, Carrol WM (1993) Corros Sci 34:327
20. Khedr MGA, Lashien MS (1992) Corros Sci 33:137
21. Rehim SSA, Hassan HH, Amin MA (2001) Mater Chem Phys 70:64
22. Putilova IN, Balezin SA, Baranik UP (1960) Metallic corrosion inhibitors. Pergamon Press, New York, p 31
23. Gomma MK, Wahdan MH (1995) Mater Chem Phys 39:209
24. Schorr M, Yahalom J (1972) Corros Sci 12:867
25. Gomma GK, Wahdan MH (1995) Ind J Chem Technol 2:107
26. Orubite-Okorosaye K, Oforka NC (2004), J Appl Sci Environ 8:57
27. Atkins PW (1980) Chemisorbed and physisorbed species, a textbook of physical chemistry. University press, Oxford, p 936
28. Quraishi MA, Mideen AS, Khan MAW, Ajmal M (1994) Ind J Chem Tech 1:329
29. Ajmal M, Mideen AS, Quraishi MA (1994) Corros Sci 36:79
30. Houyi M, Chen S, Yin B, Zhao S, Liu X (2003) Corros Sci 45:867
31. Subramaniyam NC, Mayanna S (1985) Corros Sci 25:163
32. Quraishi MA, Jamal D, Saxena N (2005) Ind J Chem Tech. 12:225

Journal : 10800 | Dispatch : 21-7-2007 | Pages : 10
Article No. : 9379 | LE | TYPESET
MS Code : JACH K019-07 | CP | DISK

JCSE The Journal of Corrosion Science and Engineering
ISSN 1466-8858 Volume 10 Preprint 3 4 July 2006

Fatty acid thiosemicarbazides as corrosion inhibitors for Mild steel in Hydrochloric acid solution

M.A.Quraishi*,M.Z.A. Rafiquee, Nidhi Saxena, Sadaf Khan

Department of Applied Chemistry, Corrosion Research Laboratory, Faculty of Engineering & Technology, Aligarh Muslim University, Aligarh-202 002, India

* Corresponding: E-mail: maquraishi@rediffmail.com; Fax No. 0091+571+2700528

Abstract

Fattyacid thiosemicarbazides namely 2-Undecane-4-Phenylthiosemicarbazide(UPTS), 2-Pentadecane-4Phenylthiosemicarbazide(PPTS),2-Heptadecane-4Phenylthiosemicarbazide (HPTS), 2-Nonane-4 Phenylthiosemicarbazide (NPTS) were synthesized in the laboratory and their influence on the inhibition of corrosion of mild steel (MS) in aqueous solution containing 1N HCl was investigated by weight loss and potentiodynamic polarization techniques. The inhibition efficiency (IE) of these compounds was found to vary with concentration, temperature and immersion time. Good inhibition efficiencies (IE) were evidenced in the hydrochloric acid solution. The adsorption of these compounds was found to obey Langmuir adsorption isotherm. Scanning electron microscopy(SEM) of mild steels samples is performed to showed adsorption of inhibitors on metal surface. Various thermodynamic parameters were also calculated to investigate the mechanism of corrosion inhibition. Potentiodynamic polarization data showed that the compounds studied are mixed type inhibitors in the acid solution.

Keywords: Corrosion inhibitors; Thiosemicarbazide; Mild steel; Adsorbtion, Potentiodynamic polarization ; SEM

JCSE The Journal of Corrosion Science and Engineering
ISSN 1466-8858 Volume 10 Preprint 3 4 July 2006

Introduction

Corrosion of metals is major problems which causes heavy economic losses. Corrosion commonly occurs at metal surfaces in the presence of oxygen and moisture and involves electrochemical reactions. In acidic medium hydrogen evolution reactions predominates while in neutral medium reduction of oxygen takes places. Corrosion inhibitors reduce and prevent these reactions by adsorbtion on the metal surface and act by forming a barrier to oxygen and moisture, by complexing with metals ions or by removing corrodents from the environment,some of the inhibitors facilitate formation of passivating film on the metal surface. Many organic compounds are used as corrosion inhibitors in acidic environments in various industries [1-2]. Acid inhibitors has wide applications in the industrial field as a component in pretreatment composition, in cleaning solution for industrial equipments and in acidization of oil wells and in petrochemical plants [3].

Most of the effective organic inhibitors used in industry have heteroatoms such as O, N, S containing multiple bonds in their molecules through which they can adsorb on the metal surface [4-7]. The corrosion inhibiting property of these compounds is attributed to their molecular structure. The planarity (л) and lone pair of electrons present on heteroatom are the important structural features that determine the adsorption of these molecules on the metal surface. In continuation of earlier work on the development of acid corrosion inhibitors| [8-15], the present work includes the inhibiting behaviour of fatty acid thiosemicarbazides namely 2-Undecane-4-Phenylthiosemicarbazide(UPTS), 2- Nonane-4- Phenylthiosemicarbazi -de, 2-Heptadecane-4-Phenylthiosemicarbazide, 2- Heptadecane-4-Phenylthiosemi-carbazide.

Experimental

Material Preparation

Experiments were performed with cold rolled mild steel strips of size 2.0cm x 2.5cm x 0.2cm having composition, (wt%): 0.14%C, 0.35% Mn, 0.17%Si, 0.025%S, 0.03%P and remaining iron Fe as per standard methods [16]. The inhibitors were synthesized in the laboratory following the procedure described earlier [17]. Name, structural formules, melting points and molecular weight of the condensation products are given in Table 1.These inhibitors were characterized through their IR and NMR spectral data and their purity was confirmed by thin layer chromatography (TLC) .IR and NMR spectral data of most effective compound UPTS is mentioned in Table 1.

JCSE The Journal of Corrosion Science and Engineering
ISSN 1466-8858 Volume 10 Preprint 3 4 July 2006

Weight Loss Determination

Mild steel coupons of size 2.0cm x 2.5cm x 0.2cm were used. The specimens were degreased using acetone and finally dried. The cleaned specimens were weighed before and after the experiments. Weight loss studies were carried out at various temperatures ranging from 30 to 60^{0}C and for various immersion times from 3 to 24 hours. The aggressive solutions used were made of AR grade 35% HCl appropriate concentrations of acid were prepared using double distilled water. The concentration range of inhibitor employed was 100 to 500 ppm in the hydrochloric acid. The inhibition efficiency (%) of the inhibitors was calculated by using the following equation:

$$IE = \frac{CR_0 - CR_i}{CR_0} \times 100$$

Where
CR_0 = Corrosion rate of blank hydrochloric acid.
CR_i = Corrosion rate after adding inhibitors.

Potentiodynamic polarization studies

Potentiodynamic polarization studies were carried out using an EG & G Princeton Applied research (PAR) potentiostat / galvanostat (model 173), a universal programmer (model 175) and a X-Y recorder (model RE0089). A platinum foil was used as auxiliary electrode and a saturated calomel electrode (SCE) was used as reference electrode and mild steel was used as working electrode. All the experiments were carried out at temperature (30 ± 1 °C). Equilibrium time leading to steady state of the specimens was 30 minutes. Sweep rate in potentiodynamic experiment was 1mV/sec.

Scanning Electron Microscopy

Scanning electron microscope (SEM) Model No 435 VP LEO, was used to study the morphology of corroded surface in presence and absence of inhibitors. The specimens were thoroughly washed with double distilled water before putting on the slide. The photographs have been taken from that portion of specimen from where better information was obtained. They were photographed at 3000μ magnification. To understand the morphology of the steel surface in absence and presence of inhibitors, the following cases have been examined.

(i) Polished mild steel specimen
(ii) Mild steel specimen dipped in 1N HCl
(iii) Mild steel specimens dipped in 1N HCl containing 500 ppm concentration.

JCSE The Journal of Corrosion Science and Engineering
ISSN 1466-8858 Volume 10 Preprint 3 4 July 2006

Results and Discussion

Weight loss studies

Effect of Concentration on inhibition efficiency

The values of percentage inhibition efficiency (%IE) and corrosion rate (CR) obtained from weight loss method at different concentrations at 30°C are summarized in Table 2. It has been found that all of these compounds inhibit the corrosion of mild steel in HCl solution, at all concentrations used in this study i.e., 100 ppm –500 ppm. It has also been observed that the inhibition efficiency of these compounds increases with the increase in concentration of inhibitor variation as shown in Fig.1.

Effect of Temperature on inhibition efficiency

The variation of IE with solution temperature is shown in Fig. 2. It can be seen that IE for all inhibitors did not cause a significant change with an increase in temperature from 30°C to 60°C indicating that the inhibitive film formed on the metal surface is protective in nature at higher temperatures.

Effect of immersion time on inhibition efficiency

The variation of Inhibition efficiency in all four fatty acids thiosemicarbazides with immersion time is shown in Fig. 3. It is observed that no significant change in IE occurred with the increase in immersion time from 3h to 24h. This shows the persistency of the adsorbed fatty acid thiosemicarbazides over a longer test period.

Application of the principles of chemical kinetics to the results

Adsorption Isotherm studies

The degree of surface coverage (θ) for different concentration of inhibitors in 1N HCl at 30°C for 3 hour of immersion time has been evaluated from weight loss values. The datas were tested graphically by fitting to various isotherms. A straight line was obtained on plotting log (θ /1-θ) versus log C asshown in Fig.4, suggesting that the adsorption of these compounds in HCl on mild steel surface follows Langmuir's adsorption isotherm.

A plot of log θ /1-θ versus 1/T is given in Fig.5, the plot gives the values for calculating heat of adsorption (Q) with a slope (-Q/2.303R). The values for the heat of adsorption are depicted in Table 3. The lower values of heat of adsorption for these inhibitors shows physical nature of adsorption [18].

It has been reported by a number of authors [19-21] that in acid solution, the logarithm of the corrosion rate is a linear function with 1/T (Arrhenius equation):

JCSE The Journal of Corrosion Science and Engineering
ISSN 1466-8858 Volume 10 Preprint 3 4 July 2006

$$\text{Log (Rate)} = \frac{-E^{o}_{a}}{2.303\ RT} + A$$

where, E^{o}_{a} is apparent effective activation energy , R is general gas constant and A is Arrhenius pre exponential factor. A plot of log of corrosion rate obtained by weight loss measurement versus 1/T gave straight line as shown in Fig.6 The values of activation energy (E^{o}_{a}) obtained from the slope of the lines are given in Table 3 .An alternative formula of the Arrhenius equation is the transition state equation:

$$\text{Rate} = \frac{RT}{Nh} \exp\left(\frac{\Delta S^{o}}{R}\right) \exp\left(\frac{-\Delta H^{o}}{RT}\right)$$

where, h is the plank s constant , N the Avogadro s number , ΔS^{o} the entropy of activation, and ΔH^{o} the enthalpy of activation. A plot of log (rate/T) versus 1/T give a straight line (Fig.7) with a slope of ($-\Delta H^{o}$ /2.303 R) and an intercept of [(log(R/ Nh) +(ΔS^{o}/ 2.303 R)], from which the values of ΔS^{o} and ΔH^{o} were calculated and are listed in Table 3. The data shows that the thermodynamic activation function (E^{o}_{a}) for inhibited system are higher than those in the free acid solution except HPTS indicating that all inhibitors except HPTS are more effective at room temperature .The E^{o}_{a} value for HPTS is less than those in free acid indicating that inhibitor exhibit high efficiency at elevated temperature [22].The value of ΔH^{o} is more for all the inhibitors except HPTS indicating more energy barrier for the reaction in presence of inhibitor is attained [23].The lower value of ΔH^{o} for HPTS indicates less energy barrier for the reaction in presence of the inhibitor is attained. The entropy of activation ΔS^{o} in the absence and presence of the inhibitors are large and negative. This indicates that the activated complex in the rate determining step represents an association rather than a dissociation step, meaning that a decrease in disordering takes place on going from reactants to the activated complex [24]. Free energy of adsorption (ΔG_{ads}) was calculated using the following equations [25] are given in Table 3.

$$\Delta G_{ads} = - RT \ln (55.5\ K)$$

and K is given by:

$$K = \theta / C (1 - \theta)$$

where θ is degree of coverage on the metal surface, C is concentration of inhibitor in mole /l, K is equilibrium constant. It has been found that the values of ΔG_{ads} value is less than -40 k J/mol (-9.56 k Cal/mol) indicating that the thiosemicarbazides are physically adsorbed on the metal surface [26].

The negative value of ΔG_{ads} indicates the spontaneous adsorption of inhibitor on the surface of mild steel [27] .It was also found that the value of activation energy of the inhibited systems were lower than that of uninhibited system. Putilova [22] has reported that this type of inhibitor is effective at higher temperatures.

JCSE The Journal of Corrosion Science and Engineering
ISSN 1466-8858 Volume 10 Preprint 3 4 July 2006

Potentiodynamic Polarization Studies

The corrosion parameters such as E_{corr} , I_{corr} , IE and CR obtained from Fig. 8 are given in Table 4. It is observed that the presence of the thiosemicarbazides decreases I_{corr}, values. Maximum decrease in I_{corr}, was observed in case of UPTS. The trend of the IE was founds to be same as that of weight loss study. E_{corr} values do not show any significant change in presence of all the thiosemicarbazides in the acid solution suggesting that all these compounds are mixed type inhibitors (i.e., they retard the corrosion reaction by blocking both anodic and cathodic sites of the metal).

Scanning electron microscopy

It is seen in Fig 9 that the surface of mild steel immersed in inhibited solution is smoother than that in 1N HCl alone. These observations suggest that inhibitors form protective layer on the metal surface, which prevent attack of acid on metal surface.

Mechanism of corrosion inhibition

Inhibition of corrosion of mild steel in the acidic solutions by the fatty acid thiosemicarbazides can be explained on the basis of molecular adsorption. It is apparent from the molecular structures that these compounds are able to get adsorbed on the metal surface through π-electrons of aromatic ring and lone pair of electrons of N, O and S atoms, planarity π- electrons of a benzene ring and as a protonated species [28]. The presence of long hydrophobic chain also plays a role in IE by preventing acid solution away from metal surface. Among the compounds investigated in the present study, the order of IE has been found as follows:-

UPTS > NPTS > PPTS > HPTS
(C_{11}) (C_9) (C_{15}) (C_{17})

It has been observed that IE of the tested thiosemicarbazides increased with the increase in chain length up to C_{11}. A further increase in chain length up to C_{17} has been found to decrease the IE.

Conclusions

➢ The fatty acid thiosemicarbazides shows good performance as corrosion inhibitors in hydrochloric acid media. The order of inhibition efficiency (%) of thiosemicarbazides is UPTS > NPTS > PPTS > HPTS.

➢ All of the fatty acid thiosemicarbazides inhibit corrosion by adsorption mechanism and the adsorption of these compounds from acid solution follow Langmuir's adsorption isotherm.

➢ The Inhibition effiency increases with increasing inhibitor concentration, Inhibition effiency however did not change significantly with an increase in temperature and immersion time.

➢ The lower values of Heat of adsorption (Q) for these inhibitors shows physical nature of adsorption and lower values of ΔG_{ads} indicates that the inhibitors are physically adsorbed on the metal surface and negative value of ΔG_{ads} indicates the spontaneous adsorption of inhibitor on the surface of mild steel.

➢ Higher values of thermodynamic activation function (E^{o}_{a}) for inhibited system than those in the free acid solution except HPTS indicating that all inhibitors except HPTS are more effective at room temperature .The E^{o}_{a} value for HPTS is less than those in free acid indicating that inhibitor exhibit high efficiency at elevated temperature .

➢ The value of ΔH^{o} is more for all the inhibitors except HPTS indicating more energy barrier for the reaction in presence of inhibitor is attained .The lower value of ΔH^{o} for HPTS indicates less energy barrier for the reaction in presence of the inhibitor is attained.

➢ The entropy of activation ΔS^{o} in the absence and presence of the inhibitors are large and negative. This indicates that the activated complex in the rate determining step represents an association rather than a dissociation step.

➢ All the compounds examined acted as mixed inhibitors in HCl.

➢ Scanning electron microscopy studies shows that inhibitors prevent corrosion by adsorption on the metal surface.

JCSE The Journal of Corrosion Science and Engineering
ISSN 1466-8858 Volume 10 Preprint 3 4 July 2006

References:

1. Abd-El-Nabey, B. A.; Khamis, E.; Ramadan, M. S.; El-Gindy, A.; Corrosion , 52, 671 (1996)

2. Raman, A.; Labine, P.; Reviews on corros Inhib Sci Tech NACE International Houston, 2, 1 (1996)

3. Schmitt, G.; Br. Corros. J., 19, 165 (1984)

4. Quraishi, M. A.; Khan, M. A. W.; Ajmal, M.; Anti-Corros.Methods Mater, 43, 5 (1996)

5. Muralidharan, S.; Iyer, S. V.; Anti-Corros.Methods Mater, 44, 100 (1997)

6. Al-Andis, N.; Khamis, E.; Al-Mayouf, A.; AboulEnicm, H.; Corros. Prev Control, 42, 13 (1995)

7. Hammouti, B.; Aouniti, A.; Taleb, M.; Brighli, M.; Kertit, S.; Corrosion, 51, 441 (1995)

8. Quraishi, M. A.; Jamal, D.; Anti-Corros.Methods Mater, 47, 233 (2000)

9. Quraishi, M. A.; Jamal, D.; and Singh, R.; Corrosion, 58, 201 (2002)

10.Quraishi, M. A.; Ansari, F.; J.Am.Oil.Chem.Soc, 80, 7 (2003)

11. Quraishi, M. A.; Jamal, D.; Corrosion, 56, 156 (2000)

12. Quraishi, M. A.; Jamal, D.; Corrosion, 56, 983 (2000)

13. Quraishi, M. A.; Jamal, D.; Saeed, M. T.; J. Am. Oil. Chem.Soc, 77, 265 (2000)

14. Quraishi, M. A.; Jamal, D.; J.Am.Oil.Chem.Soc, 77,1107 (2000)

15 Quraishi, M. A.; Jamal, D.; Anti-Corros.Methods Mater, 47, 77 (2000)

16. ASTM, 'Metal Corrosion, Erosion and Wear' Annual Book of ASTM Standards, 0.3.02 G1-72 (1987)

17. ASTM, Standard Practice for Laboratory Immersion Corrosion Testing of Metals, Annual Book of Standards, G 31-72, 3.02 (1990)

18. Jha, L. J.; Ph.D Thesis "Studies of the Adsorption of amide derivative during acid during acid corrosion of pure iron & its characterization" 1990 111

19. Christopher, M. A. B.; Isabel, A. R. G.; and Jenny, P. S. M.; Corros.Sci, 36, 15 (1994)

JCSE The Journal of Corrosion Science and Engineering
ISSN 1466-8858 Volume 10 Preprint 3 4 July 2006

20. Breslin, C. B.; Carrol, W. M.; Corros. Sci, 34, 327 (1993)

21. Khedr, M. G. A.; Lashien, M. S.; Corros. Sci, 33, 137 (1992)

22. Puilova, I. N.; Balzin, S.A.; and Branik, U. P; "Mettalic corrosion inhibitors" Pergamon Press New york, 1960, 31.

23. Abd El Rehim, S. S.; Hassan, H. H.; and Amin, M. A.; Mat. Chem .Phys. 70, 64 (2001)

24. Gomma, M. K.; Wahdan, M. H., Mater. Chem. Phys., 39, 209 (1995)

25. Schorr, M.; Yahalom, J.; Corros. Sci, 12, 867 (1972)

26. Brinic, S.; Grubac, Z.; Babic, R.; and Metikos-Hukovic, M.; 8th Eur Sump Corros Inhib, Ferrara

27. Gomma, G. K.; Wahdan, M. H.; Ind. J. Chem. Technol, 2, 107 (1995)

28. Quraishi, M. A.; Khan, , M. A. W.; Ajmal, M.; Muralidharan, S.; and Iyer, S.V.; Br. Corros. J, 32, 72 (1997)

JCSE The Journal of Corrosion Science and Engineering
ISSN 1466-8858 Volume 10 Preprint 3 4 July 2006

Table 1 Name and molecular structures of the compounds used

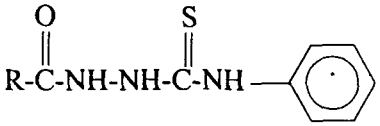

S. No	Structure	Designation & Abbreviation
1.	$R = CH_3(CH_2)_{10}$	2-Undecane-4-Phenyl thiosemicarbazide (UPTS)
2.	$R = CH_3(CH_2)_{14}$	2-Pentadecane-4-Phenyl thiosemicarbazide (PPTS)
3.	$R = CH_3(CH_2)_{16}$	2-Heptatadecane-4-Phenyl thiosemicarbazide (HPTS)
4.	$R = CH_3(CH_2)_8$	2- Nonane -4-Phenyl thiosemicarbazide (NPTS)

IR Spectral data (significant bands ν_{max} in cm^{-1} (KBr))

UPTS = 3280 (N - N), 2875 (CH_3), 2820 (CH_2 chain), 1618 (C = O), 1450 (C_6H_5), 1290 (Ar C - N), 1152 (C - N), 1020 (C - S).

NMR spectral data (δ $CDCl_3$)

UPTS = 1.38 (12 H, $(CH_2)_6$), 2.12 (2H, = CH - $\underline{C}H_2$), 2.38 (2H, $COCH_2$), 4.92 (1H, N - H), 5.19 (2H, $\underline{C}H_2$ = CH -), 5.97 (1 H, CH_2 - $\underline{C}H$ -), 7.59 (5 H, $C_6\underline{H}_5$), 9.18 (2H, NH - $N\underline{H}$), 9.52 (1 H, $\underline{H}N$ - C_6H_5).

JCSE The Journal of Corrosion Science and Engineering
ISSN 1466-8858 Volume 10 Preprint 3 4 July 2006

Table 2 Corrosion parameters for mild steel in 1N HCl in absence and presence of different concentrations of various inhibitors from weight loss measurement at 30 °C for 3 h.

Inhibitor conc (ppm)	Weight loss (mg)	IE (%)	CR (mmpy)
HCl	63.57	-	23.62
UPTS			
100	21.5	66.11	8.00
200	13.7	78.35	5.11
300	7.9	87.44	2.96
400	4.3	93.12	1.62
500	0.2	96.65	0.75
NPTS			
100	23.5	62.99	8.74
200	17.0	73.12	6.34
300	9.2	85.36	3.45
400	4.8	92.07	1.82
500	3.0	95.15	1.14
PPTS			
100	24.9	60.67	9.28
200	18.3	71.12	6.82
300	10.2	83.85	3.81
400	6.2	90.12	2.33
500	3.7	94.02	1.41
HPTS			
100	26.6	58.31	9.84
200	19.2	69.72	7.15
300	12.5	80.21	4.67
400	6.8	89.23	2.54
500	4.4	92.99	1.65

JCSE The Journal of Corrosion Science and Engineering
ISSN 1466-8858 Volume 10 Preprint 3 4 July 2006

Table 3 Thermodynamic activation parameters for mild steel in 1 HCl in absence and presence of inhibitors of 500 ppm concentration.

Inhibitors (500ppm)	E_a (KJ mol^{-1})	ΔH (KJ mol^{-1})	$-\Delta S$ (J mol/K^{-1})	$-\Delta G_{ad}$ (KJ mol^{-1})	-Q (KJ mol^{-1})
Blank	49.15	51.79	159.31	-	-
UPTS	75.23	77.88	198.56	39 75	28.72
NPTS	68.10	70.72	196.07	39.47	26.48
PPTS	58.32	60.95	195.31	38.88	19.78
HPTS	42.00	44.65	192.43	36.93	14.87

Table 4 Electrochemical polarization parameters for the corrosion of mild steel in 1N HCl containing 500 ppm inhibitors at 30 °C.

Inhibitor conc (ppm)	E_{corr} (mV)	I_{corr} ($mAcm^{-2}$)	IE (%)
HCl	-495	0.360	-
UPTS	-497	0.025	94.44
NPTS	-508	0.072	80.12
PPTS	-493	0.082	77.07
HPTS	-495	0.100	72.05

JCSE The Journal of Corrosion Science and Engineering
ISSN 1466-8858 Volume 10 Preprint 3 4 July 2006

CAPTION FOR FIGURES

Fig 1- Variation of inhibition efficiency with inhibitor concentration for 10-100 ppm concentration of inhibitors (▲,UPTS; O, NPTS ; •, PPTS; Δ,HPTS).

Fig 2- Variation of inhibition efficiency with solution temperature in 1N hydrochloric acid for 100 ppm concentration of inhibitors (▲,UPTS; O, NPTS ; •, PPTS; Δ,HPTS).

Fig 3- Variation of inhibition efficiency with immersion time in 1N hydrochloric acid for 100 ppm concentration of inhibitors (▲,UPTS; O, NPTS ; x, PPTS; Δ,HPTS).

Fig 4- Langmuir s adsorption isotherm plots for the adsorption of various inhibitors in 1N hydrochloric acid on the surface of mild steel (▲,UPTS; O, NPTS ; x, PPTS; Δ,HPTS).

Fig 5- Adsorption isotherm plot for log (θ /1- θ) versus 1/T(▲,UPTS; O,NPTS ; x, PPTS; Δ,HPTS).

Fig 6- Adsorption isotherm plot for log (CR) versus 1/T(▲,UPTS; O, NPTS ; x, PPTS; Δ,HPTS).

Fig 7- Adsorption isotherm plot for log (CR/T) versus 1/T(▲,UPTS; O, NPTS ; x, PPTS; Δ,HPTS).

Fig 8- Potentiodynamic polarization curves of mild steel in 1N hydrochloric acid containing 100 ppm concentrations of various thiosemicarbazides (1) Blank (2)HPTS (3) PPTS (4) NPTS (5) UPTS.

JCSE The Journal of Corrosion Science and Engineering
ISSN 1466-8858 Volume 10 Preprint 3 4 July 2006

(a)

(b)

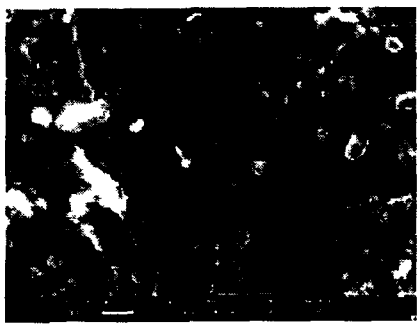

(c)

Fig 9 Scanning electron micrographs for mild steel surface in absence and presence of inhibitors (a) mild steel in 1N HCl (b) polished mild steel and (c) mild steel in presence of MBCT.

JCSE The Journal of Corrosion Science and Engineering
ISSN 1466-8858 Volume 10 Preprint 12 18 September 2006

Inhibitive Effect of Some New Triazole Derivatives on Mild Steel Corrosion in Formic and Acetic acid

M.A. Quraishi*, M.Z.A Rafiquee, Sadaf Khan and Nidhi Saxena

Corrosion Research Laboratory, Department of Applied Chemistry,

Faculty of Engineering & Technology, Aligarh Muslim University,

Aligarh-202 002, India

Abstract

Four organic inhibitors namely, 5-nonyl-4-phenyl-3-mercapto-1, 2,4-triazole (NPMT), 5-Undecyl-4-phenyl-3-mercapto-1, 2,4-triazole (UPMT), 5-Pentadecyl-4-phenyl-3-mercapto-1, 2,4-triazole (PPMT), 5-Heptadecyl-4-phenyl-3mercapto-1,2,4-triazole (HPMT) have been synthesized in the laboratory and their influence on the corrosion inhibition of mild steel (MS) in 20% formic acid and 20% acetic acid by weight loss and potentiodynamic polarization techniques were studied. Scanning electron microscopic study (SEM) was done to investigate the surface characterization of inhibited & uninhibited metal samples. The inhibition efficiency was found to vary with inhibitor concentration, immersion time, and acid concentration and solution temperature. Good inhibition efficiency (IE) was evidenced in both the acid solutions, even at concentration of 25 ppm. The adsorption of these compounds on the mild steel surface for both acids was found to obey langmuir's adsorption isotherm. The values of activation energy, free energy of adsorption, heat of adsorption, enthalpy of activation and entropy of activation were also calculated to elaborate the mechanism of corrosion inhibition. The potentiodynamic polarization data have shown that compounds studied are mixed type inhibitors. FT-IR & NMR Study were also done in order to confirm the composition of synthesised inhibitor.

* For correspondence (E-mail: maquraishi@rediffmail.com; Fax No. 0091+571+2700528)

JCSE The Journal of Corrosion Science and Engineering
ISSN 1466-8858 Volume 10 Preprint 12 18 September 2006

Introduction

Most of the researches on corrosion inhibition of metals have been done in mineral acids. Corrosion behaviour of iron and mild steel in organic acid solutions has attracted the attention of many investigators [1-3]. Mild steel is used in the fabrication of reaction vessels, storage tanks etc. by industries, which either manufacture or use organic acid as reactant. Organic acids rank among the most important chemicals in industry today. Rather than being used as final products, they serve as precursors to other chemicals. The reactive carboxyl group –COOH makes them a basic building block for many compounds such as drugs, pharmaceuticals, plastics and fibres.

Organic compounds containing heteroatoms such as O, N, S and multiple bonds in their molecules are of particular interest as they give better inhibition efficiency than those containing N or S atom alone [4-8]. A survey of literature reveals that corrosion inhibitors derived from triazoles constitute an important and potential class of corrosion inhibitors on mild steel in acidic medium [9-11]

In present investigation, the influence of four triazoles namely, 5-nonyl-4-phenyl-3-mercapto-1, 2,4-triazole (NPMT), 5-Undecyl-4-phenyl-3-mercapto-1, 2,4-triazole (UPMT), 5-Pentadecyl-4-phenyl-3-mercapto-1, 2,4-triazole (PPMT), 5-Heptadecyl-4-phenyl-3-mercapto-1, 2,4-triazole (HPMT) on corrosion inhibition of mild steel in 20% formic acid & 20% acetic acid have been reported.

Experimental

Material Preparation

AR grade formic and acetic acid (MERCK) and doubled distilled water were used for preparing test solutions of 20% formic acid and 20%acetic acid for all the experiments. The inhibitors were synthesized in the laboratory following the procedure described by Kittur et al. [12] and the compounds were characterized through their spectral data and their purity was confirmed by thin layer chromatography (TLC). Name & structural formulas of the condensation products are given in Table 1.

JCSE The Journal of Corrosion Science and Engineering
ISSN 1466-8858 Volume 10 Preprint 12 18 September 2006

FT-IR Spectroscopy

The FT-IR spectroscopic study was used to investigate the purity of the synthesized compound. The results are listed below:

i) 5-nonyl-4-phenyl-3mercapto-1,2,4-triazole (NPMT) - IR (KBr): 1734(C=N), 1410 (C–N), 2362 (S–H), 2848 (C–H), 925 (C_6H_5), 1234 (CH_3) cm^{-1}.

ii) 5-Undecyl-4-phenyl-3-mercapto-1,2,4-triazole (UPMT)- IR (KBr) 1606(C=N), 1313 (C–N), 1733 (S–H), 2984 (C–H), 999 (C_6H_5), 1252 (CH_3) cm^{-1}.

iii) 5-Pentadecyl-4-phenyl-3-mercapto-1,2,4-triazole (PPMT)- IR (KBr): 1640(C=N), 1311 (C–N), 2354 (S–H), 2911 (C–H), 915 (C_6H_5), 1203 (CH_3) cm^{-1}.

iv) 5-Heptadecyl-4-phenyl-3-mercapto-1,2,4-triazole (HPMT) - IR (KBr): 1558(C=N), 1315 (C–N), 2364 (S–H), 2850 (C–H), 917 (C_6H_5), 1203 (CH_3) cm^{-1}.

NMR Spectroscopy

NMR Spectral data ($\delta CDCl_3$)

7.388 (5H,C_6H_5), 1.180 (1H, SH), 0.983 (3H, CH_3), 2.245 (16H, $(CH_2)_8$)

Weight loss Determination

The mild steel samples having composition, (Wt %): 0.14% C, 0.35% Mn, 0.17% Si, 0.025% S, 0.03% P and balance Fe has been used for the experiment. The mild steel sample of size 2.0 cm × 2.0 cm ×0.025 cm were used for weight loss measurement studies. Weight loss measurement studies were carried out at various temperatures ranging from 30 to 60°C for various immersion times from 24 to 120 hrs. The experiments were performed as per ASTM method described previously [13]. The inhibition efficiency of the inhibitors was calculated by using the following equation: -

$$IE = \frac{CR_o - CR_i}{CR_o} \times 100 \qquad \text{------(1)}$$

where

CR_o = Corrosion rate of blank formic and acetic acid

CR_i = Corrosion rate after adding inhibitors.

JCSE The Journal of Corrosion Science and Engineering
ISSN 1466-8858 Volume 10 Preprint 12 18 September 2006

Electrochemical studies

For potentiodynamic polarization studies of mild steel strips of the above composition, coated with commercially available lacquer with an exposed area of 1.0 cm^2 were used and the experiments were carried out at temperature (30 ± 1 °C). Equilibrium time leading to steady state of the specimens was 30 minutes. Sweep rate in potentiodynamic experiment was 1mV/sec. Potentiodynamic polarization studies were carried out using an EG & G Princeton Applied research (PAR) potentiostat / galvanostat (model 173), a universal programmer (model 175) and a X-Y recorder (model RE0089). A platinum foil was used as auxiliary electrode and a saturated calomel electrode (SCE) was used as reference electrode. The CR was calculated using the following formula [14],

$$CR = \frac{0.13 \times I_{corr} \times EW}{D} \qquad \text{------ (2)}$$

where,

I_{corr} = Corrosion current density in $\mu A/cm^2$.

EW = Equivalent weight of the metal in gram.

D = Density of the metal in g/cm^3.

Scanning Electron Microscopy

Scanning electron microscope (SEM) Model No 435 VP LEO was used to study the morphology of corroded surface in presence and absence of inhibitors. The specimens were thoroughly washed with double distilled water before putting on the slide. The photographs have been taken from that portion of specimen from where better information was obtained. They were photographed at appropriate magnifications. To understand the morphology of the steel surface in absence and presence of inhibitors, the following cases have been examined.

i) Polished mild steel specimen

ii) Mild steel specimen dipped in 20% formic acid

iii) Mild steel specimens dipped in 20% formic acid containing 500ppm concentration of UPMT inhibitors.

JCSE The Journal of Corrosion Science and Engineering
ISSN 1466-8858 Volume 10 Preprint 12 18 September 2006

Results and Discussion

Weight loss studies

The values of percentage inhibition efficiency (%IE) and corrosion rate (CR) obtained from weight loss method at different concentrations at 30°C are summarized in Table 2. It has been found that all of these compounds inhibit the corrosion of mild steel in formic and acetic acid solution, at all concentrations used in this study i.e., 25ppm – 500 ppm. It has also been observed that the inhibition efficiency for all of these compounds increases with the increase in concentration variation as shown in Fig.1a & 1'a.

It is observed that the tested triazoles shows a decrease in the inhibition efficiency with the increase in the immersion time from 24 to 120 hours in formic as well as in acetic acid. This shows the persistency of the adsorbed triazole over a longer test period. Inhibition efficiency of all the compounds against the immersion time is shown in Fig.1b & 1'b.

The variation of IE with solution temperature is shown in Fig. 1c & 1'c. It can be seen that IE for compounds such as NPMT, UPMT, PPMT and HPMT increases with increase in temperature from 30°C to 60°C indicating that the inhibitive film formed on the metal surface is protective in nature up to 60°C. The effect of acid concentration of formic and acetic acid is shown in Fig. 1d & 1d'. With the increase in concentration of formic acid, the IE initially increases and attains maxima at 20%acid concentration and thereafter decreases on further increase in acid concentration to 30%. The IE decreases slightly with increase in acetic acid concentration.

The degree of surface coverage (θ) for different inhibitor concentrations in 20% formic acid and 20% acetic acid at 30°C over 24-hour immersion time was evaluated from weight loss values. The data were tested graphically by fitting to various isotherms. A plot of log (θ/1-θ) versus 1/T is shown in Figure 2a and 2'a. The plot gives the values of heat of adsorption (Q), which is determined from the slope (= -Q/2.303R). The values for the heat of adsorption are presented in Table 3. The values of heat of adsorption for the inhibitors in formic and acetic acid is found to be less than (-40kJ mol^{-1}); except for UPMT in formic acid. This indicates that all the inhibitors used except UPMT are adsorbed physically [15].

JCSE The Journal of Corrosion Science and Engineering
ISSN 1466-8858 Volume 10 Preprint 12 18 September 2006

It has been reported by a number of authors [16-18] that, in acid solution, the logarithm of the corrosion rate is a linear function of 1/T (Arrhenius equation):

$$\text{Log (Rate)} = \frac{-E_a^0}{2.303RT} + A \qquad \text{------ (3)}$$

where, E^o_a is the apparent activation energy, R the general gas constant and A the Arrhenius pre exponential factor. A plot of log (corrosion rate) versus 1/T gave straight lines as shown in Figure 2b and 2'b. The values of activation energy (E^o_a) obtained from the slope of the lines are given in Table 3. An alternative formula for the Arrhenius equation in the transition state equation:

$$\text{Rate} = \frac{RT}{Nh}\exp\left(\frac{\Delta S^0}{R}\right)\exp\left(-\frac{\Delta H^0}{RT}\right) \qquad \text{------ (4)}$$

where, h is the Plank constant, N the Avogadro's number, ΔS^o the entropy of activation, and ΔH^o the enthalpy of activation. A plot of log (CR/T) versus 1/T should give a straight line, (Figure 2c and 2c') with a slope of ($-\Delta H^o$ /2.303 R) and an intercept of [(log (R / Nh) + (ΔS^o/ 2.303 R)], from which the values of ΔS^o and ΔH^o were calculated and are listed in Table 3. The data show that the values of thermodynamic activation function (E^o_a) of the corrosion in mild steel in 20% formic acid and 20% acetic acid solution in the presence of the inhibitors are lower than those in the free acid solution, indicating that all the inhibitors exhibit high inhibition efficiency at elevated temperatures [19]. Such inhibitors are bound to the surface by specific adsorption forces or by chemisorption as a result of which a surface film of reaction product is formed [15]. The chemisorption process in the film formation with a strong attractive force is likely to be exothermic resulting in lowering of the activation energy [20]. The values of ΔH^o (Table 3) is in the order UPMT > NPMT > PPMT > HPMT which is an indicative of the existence of energy barrier at elevated temperature [19]. The values of activation ΔS^o in the absence and presence of the inhibitors are large and negative. This indicates that the activated complex in the rate determining step represents an association rather than a dissociation step, meaning that a decrease in disorder ness takes during the course of transition from

reactants to the activated complex [21]. The average value for free energy of adsorption (ΔG_{ads}), calculated using the following equations [22] are given in Table 3.

$\Delta G_{ads} = - RT \ln (55.5 K)$ ------ (5)

and K is given by:

$K = \theta/C (1 - \theta)$ ------ (6)

where, θ is degree of coverage on the metal surface, C is concentration of inhibitor in mol l^{-1}, K is equilibrium constant, R is a gas constant and T is temperature. It is found that the ΔG_{ads} values for the studied compound at higher temperature is less than -40 kJ mol^{-1} indicating that the triazoles are physically adsorbed on the metal surface except for a slight increase in ΔG_{ads} values for UPMT in formic acid, showing chemical adsorption [23].

The low and negative value of ΔG_{ads} indicates the spontaneous adsorption of inhibitor on the surface of mild steel [24]. It was also found that value of activation energy of the inhibited systems were lower than that of uninhibited system. Putilova [19] has suggested that this type of inhibitor is effective up to higher temperature.

The Plot of log (weight loss) versus Immersion time as shown in Figure (2d), gave a straight line indicating that it follows first order reaction. The value of rate constant is calculated by using the first order rate law [25].

$$k = \frac{2.303}{t} \log \frac{[A_o]}{[A]} \quad \text{------ (7)}$$

where $[A_o]$ is the initial mass of the metal and [A] is the mass corresponding to time t. The half-life ($t_{1/2}$) values were calculated using the relationship [26].

$t_{1/2} = 0.693/k$ ------ (8)

The values of rate constants and half-life ($t_{1/2}$) obtained from the above relations are summarized in Table 4. Half-life values were found to be constant at different immersion time .The order of effectiveness of inhibitors were observed as UPMT > NPMT > PPMT > HPMT in 20% formic acid and UPMT > NPMT > HPMT > PPMT in 20% acetic acid. The constant values of rate constant further confirmed that the corrosion of mild steel in

JCSE The Journal of Corrosion Science and Engineering
ISSN 1466-8858 Volume 10 Preprint 12 18 September 2006

20% formic acid and in 20% acetic acid in presence of different inhibitor follows first order kinetics.

Application of Adsorption isotherm

The mechanism of corrosion inhibition may be explained on the basis of adsorption behaviour of inhibitors [27]. The degrees of surface coverage (θ) for different inhibitor concentrations were evaluated from weight- loss data. Fitting of data to various isotherms was tested graphically. A plot of log θ /(1- θ) vs. log C shows a straight line (Figure 3 & 3') indicating that adsorption follows the Langmuir isotherm.

$$\theta/(1-\theta) = k\,C \exp(-G_{ads}/RT) \quad \text{------ (9)}$$

where G_{ads} is the free energy of adsorption and C is the inhibitor concentration.

Potentiodynamic polarization

The cathodic and anodic polarization curves of mild steel in 20% formic and 20%acetic acid in the absence and presence of different inhibitors at 500-ppm concentration at 28 ± 2 °C are shown in (Figure 4 & 4'). Electrochemical parameters such as corrosion current density (I_{corr}), corrosion potential (E_{corr}) and inhibition efficiency (IE) were calculated from Tafel plots and are given in Table 5. A maximum decrease in I_{corr} was observed for UPMT. It is also observed from Table 5 that (E_{corr}) values and Tafel slope constants b_a and b_c do not change significantly in inhibited solution as compare to uninhibited solution. It is seen from the results that triazoles do not shift E_{corr} values significantly thereby suggesting that they are mixed type inhibitors. This type of behaviour has been observed for mild steel in acid solution containing 2-hydrazino-6-methyl-benzothiazole [28].

Mechanism of corrosion inhibition

The corrosion of mild steel in non-aqueous and aqueous solution may occur in the following steps [29]:

$$Fe + HCOO \longrightarrow [Fe(HCOO)]_{ads} + e^- \quad \text{------ (10)}$$

$$[Fe(HCOO)]_{ads} \longrightarrow [Fe(HCOO)]^+ + e^- \quad \text{------ (11)}$$

$$[Fe(HCOO)]^+ + H^+ \rightleftharpoons Fe^+ + HCOOH \quad \text{------ (12)}$$

The evolution of hydrogen occurs due to the following cathodic reaction:

$$M + HCOOH + e^- \longrightarrow MH_{ads} + HCOO^- \quad \text{------(13)}$$

$$MH_{ads} + MH_{ads} \longrightarrow H_2 + M \quad \text{------(14)}$$

The adsorption of formate ions on the surface of iron is a prerequisite for the anodic dissolution to occur, thus the rate of corrosion should depend on the concentration of formate ion in the solution. The conductance of formic acid solution gradually increases in concentration range from 5% - 20%. As a result, the extent of adsorption of formate ion, as well as the rate of step (9) increases and consequently the rate of corrosion also increases.

The triazoles inhibit the corrosion by controlling both the anodic and cathodic reactions. In acidic solutions these compounds exist as protonated species. These protonated species adsorb on the cathodic sites of the mild steel and decrease the evolution of hydrogen. The adsorption on anodic sites occurs through the π- electrons of aromatic rings and lone pair of electrons of nitrogen and sulphur atoms [30].

Among the compounds investigated, the order of IE is:

UPMT > NPMT > PPMT > HPMT

(C_{11}) (C_9) (C_{15}) (C_{17})

UPMT gives the best performance as corrosion inhibitor. In general trend, the IE increases with increase in the chain length but it also decrease as we increase chain length after C_{11} due to decreased solubility and increased steric hindrance [31].

Conclusions

(i) The triazole derivatives showed good performance as corrosion inhibitors in formic acid and acetic acid media.

(ii) All of the four triazoles, inhibited corrosion by adsorption mechanism and the adsorption of these compounds from acid solution followed Langmuir's adsorption isotherm.

(iii) All the compounds examined acted as mixed inhibitors in formic and acetic acid solutions.

JCSE The Journal of Corrosion Science and Engineering
ISSN 1466-8858 Volume 10 Preprint 12 18 September 2006

References

[1] Teeple, H. O.; Corrosion, 8, 14 (1952)

[2] Constatinescu, E.; Heitz, E.; Corros. Sci. 16, 857 (1976)

[3] Sekine, I.; Chinda, A.; Corrosion, 40, 95 (1984)

[4] Muralidhara, S.; Quraishi, M.A.; Iyer, S. V. K.; Anti-Corros.Methods Mater, 44, 100 (1997)

[5] Quraishi, M.A.; Khan, M.A.W.; Ajmal, M.; Anti-Corros.Methods Mater, 43,5 (1996)

[6] Hammouti, B.; Aouniti, A.; Taleb, M.; Bright. M.; Kertit, S.; Corrosion, 51, 411 (1995)

[7] Andis, N, Al.; Khamis, E.; Mayouf, A, Al.; Enein, H. Aboul.; Corros. Prev. Cont. 42 (1995)

[8] Nabey, Abd. El.; Khammis, E.; Ramadan, M. Sh.; Gindy, A. El.; Corrosion, 52,671 (1996)

[9] Quraishi, M. A.; Ansari, F. A.; J Applied Electrochem, 33, 233 (2003)

[10] Quraishi, M. A.; Jamal, D.; J Applied Electrochem, 32, 425 (2002)

[11] Quraishi, M. A.; Sharma, H. K.; Bull Electrochem, 19, 535 (2003)

[12] Kittur, M. I. H.; Mahajanshetti, C. S.; J. Oil Tech. Assac. (India) 16, 49 (1984)

[13] ASTM, Standard Practice for Laboratory Immersion Corrosion Testing of Metals, Annual Book of Standards, G 31-72, 3.02 (1990).

[14] ASTM, Standard Practice for Calculation of Corrosion Rate and related Information from Electrochemical Measurements, Annual Book of Standards, G 102-89, 3.02 (1994).

[15] Jha, L.J.; Ph.D Thesis- (Studies of the Adsorption of amide derivative during acid corrosion of pure iron & its characterization), 1990, 111.

[16] Christopher, M.A.B.; Isabel, A.R.G.; Jenny, P.S.M.; Corros Sci, 36, 15 (1994)

[17] Breslin, C. B.; Carrol, W. M.; Corros Sci, 34, 327 (1993)

[18] Khedr, M. G. A.; Lashien, M. S.; Corros Sci, 33, 137 (1992)

[19] Putilova, I. N.; Balezin, S.A.; Baranik, Metallic Corrosion Inhibitors, (Pergamon Press New York), 31 (1960)

[20] Laidler, K.J.; Chemical kinetics, 3e, (Pearson Education Company), 247 (1984)

ISSN 1466-8858 Volume 10 Preprint 12 18 September 2006

[21] Gomma, M.K.; Wahdan, M.H.; Mater.Chem.Phys, 39, 209 (1995)

[22] Schorr, M.; Yahalom, J.; Corros Sci, 12 (1972) 867.

[23] Ateya, B.G.; Andouli, B.E.; Nizami, F.M.; Corros.Sci, 24, 509 (1984)

[24] Gomma, G.K.; Wahdan, M.H.; Ind J Chem Technol, 2, 107 (1995)

[25] Okorosaye, K.O.; Oforka, N.C.; J Appl.Sci.Environ, 8, 57 (2004)

[26] Atkins, P. W.; Chemisorbed and physisorbed species, a textbook of physical chemistry (University press oxford), 936 (1980)

[27] Quraishi, M. A.; Mideen, A.S.; Khan, M.A.W.; Ajmal, M.; Ind J Chem Tech.1 329 (1994)

[28] Ajmal M, Mideen A S & Quraishi M A, Corros Sci, 36 (1994) 79.

[29] Singh, M. M.; Gupta, A.; Mat.Chem.Phys. 46,15 (1996)

[30] Quraishi M A, Mideen A S, Khan M.A.W.; Ajmal M.; Indian J Chem Technol, 329 (1994)

[31] Li, P.; Tan, T. C.; Lee, J. Y.; Corrosion 53,186 (1997)

JCSE The Journal of Corrosion Science and Engineering
ISSN 1466-8858 Volume 10 Preprint 12 18 September 2006

Table 1.

Name, structures and molecular weights of the compounds used

S No	Structure	Designation and abbrevation
1.	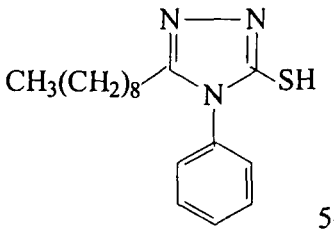	5-Nonayl- 4-Phenyl 3-mercapto-1,2,4 Triazole (NPMT)
2.	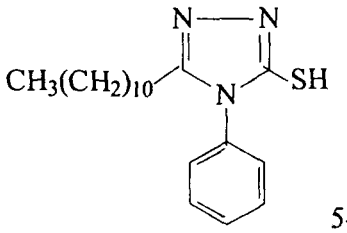	5-Undecyl- 4-Phenyl 3-mercapto1, 2,4 Triazole (UPMT)
3.	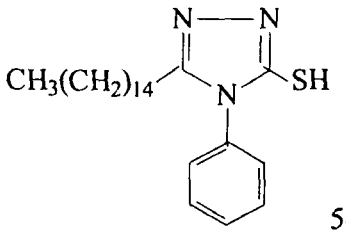	5-Pentadecyl- 4-Phenyl 3-mercapto1, 2,4 Triazole (PPMT)
4.	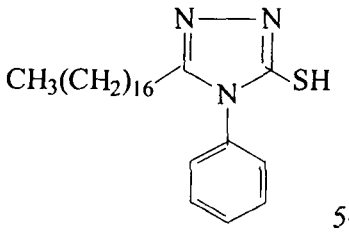	5-Heptadecyl- 4-Phenyl 3-mercapto1, 2,4 Triazole (HPMT)

JCSE The Journal of Corrosion Science and Engineering
ISSN 1466-8858 Volume 10 Preprint 12 18 September 2006

Table 2
Corrosion parameters for mild steel in aqueous solution of 20% formic acid and 20%acetic acid in absence and presence of different concentrations of various inhibitors from weight loss measurements at 30 °C for 24 h.

Inhibitor Conc. (ppm)	20% Formic acid Weight loss (mg)	IE (%)	CR (mmpy)	20% Acetic acid Weight loss (mg)	IE (%)	CR (mmpy)
Blank	308.21	-	14.31	150.36	-	6.97
UPMT						
25	23.53	92.36	1.09	11.51	92.34	0.53
50	14.94	95.18	0.69	9.37	93.76	0.44
100	9.76	96.83	0.45	8.72	94.20	0.41
300	6.01	98.05	0.28	7.12	95.26	0.33
500	3.26	98.94	0.15	5.75	96.17	0.27
NPMT						
25	30.10	90.23	1.39	14.42	90.40	0.67
50	18.98	93.84	0.88	12.29	91.82	0.57
100	13.67	95.56	0.65	10.13	93.26	0.47
300	9.18	97.02	0.43	9.30	93.81	0.43
500	5.57	98.19	0.26	8.16	94.57	0.38
PPMT						
25	33.15	89.24	1.54	19.14	87.26	0.89
50	25.78	91.63	1.19	15.73	89.53	0.73
100	17.93	94.18	0.83	12.83	91.46	0.59
300	10.10	96.72	0.47	10.59	92.95	0.49
500	8.87	97.15	0.41	8.97	94.03	0.42
HPMT						
25	43.96	85.73	2.04	22.05	85.19	1.03
50	35.24	88.56	1.64	19.79	86.83	0.92
100	23.60	92.34	1.09	17.40	88.42	0.81
300	16.48	94.65	0.76	13.88	90.76	0.65
500	9.76	96.83	0.45	12.74	91.50	0.59

JCSE The Journal of Corrosion Science and Engineering
ISSN 1466-8858 Volume 10 Preprint 12 18 September 2006

Table 3
Thermodynamic activation parameters for mild steel in 20% formic acid and 20%acetic acid in absence and presence of inhibitors of 500-ppm concentration.

Inhibitor concentration (ppm)	E_a (KJ mol^{-1})	ΔH (KJ mol^{-1})	$-\Delta S$ (J mol^{-1}K^{-1})	$-\Delta G_{ads}$ (KJ mol^{-1})	$-Q$ (KJmol^{-1})
20% Formic acid	18.51	25.53	226.31	-	-
UPMT	6.38	31.93	270.36	41.89	51.05
NPMT	9.57	12.76	262.69	39.09	25.53
PPMT	15.95	9.57	255.99	38.23	15.96
HPMT	16.59	7.66	253.12	37.97	6.38
20% Acetic acid	19.15	28.72	222.49	-	-
UPMT	15.95	12.76	260.78	37.80	21.06
NPMT	12.76	9.57	255.04	36.07	17.03
PPMT	10.85	5.11	250.25	36.25	14.68
HPMT	9.57	4.79	245.46	35.18	5.74

Table 4
Half-life (h) values for the corrosion of mild steel at different immersion time in 20% formic acid and 20% acetic acid in absence and presence of inhibitors of 500-ppm concentration at 30° C.

Inhibitor concentration (ppm)	k10^{-4}	$t_{1/2}$
20%Formic acid	6.23±0.0075	1112.36
UPMT	1.24±0.0002	5588.71
NPMT	1.64±0.0001	4233.35
PPMT	2.22±0.0002	3116.01
HPMT	2.90±0.0004	2387.18
20%Acetic acid	4.03±0.0004	1717.89
UPMT	1.67±0.0002	4162.16
NPMT	2.24±0.0005	3093.75
PPMT	5.91±0.0009	1172.58
HPMT	3.05±0.0003	2272.43

JCSE The Journal of Corrosion Science and Engineering
ISSN 1466-8858 Volume 10 Preprint 12 18 September 2006

Table 5
Electrochemical polarization parameters for the corrosion of mild steel in 20% formic acid and 20%acetic acid containing 500-ppm inhibitors at 30 °C.

Inhibitor concentration (ppm)	E_{corr} (mV)	I_{corr} (mA cm^{-2})	IE (%)	b_a ($mVdec^{-1}$)	b_c ($mVdec^{-1}$)
20%Formic acid	-416	0.350	-	68	104
UPMT	-420	0.0035	99.02	64	106
NPMT	-402	0.0051	98.54	60	100
PPMT	-423	0.0094	97.30	66	112
HPMT	-395	0.0154	95.60	70	120
20%Acetic acid	-402	0.240	-	60	100
UPMT	-406	0.005	97.90	52	96
NPMT	-390	0.039	94.70	54	92
PPMT	-412	0.034	93.90	58	104
HPMT	-418	0.024	90.83	56	98

JCSE The Journal of Corrosion Science and Engineering
ISSN 1466-8858 Volume 10 Preprint 12 18 September 2006

CAPTION FOR FIGURES

Fig. 1 —Variation of inhibition efficiency with (a) inhibitor concentration, (b) immersion time, (c) solution temperature, (d) acid concentration in 20% formic acid (1: UPMT; 2: NPMT; 3: PPMT; 4: HPMT)

Fig. 1' —Variation of inhibition efficiency with (a) inhibitor concentration, (b) immersion time, (c) solution temperature, (d) acid concentration in 20% acetic acid (1: UPMT; 2: NPMT; 3: PPMT; 4: HPMT)

Fig. 2— (a) Adsorption isotherm plot for log (θ /1- θ) versus 1/T; (b) Adsorption isotherm plot for log (CR) versus 1/T; (c) Adsorption isotherm plot for log (CR/T) versus 1/T; and (d) Half-life plot for log (weight loss) versus immersion time in 20% formic acid (1: UPMT; 2: NPMT; 3: PPMT; 4: HPMT; 5: Blank)

Fig. 2' — (a) Adsorption isotherm plot for log (θ /1- θ) versus 1/T; (b) Adsorption isotherm plot for log (CR) versus 1/T; (c) Adsorption isotherm plot for log (CR/T) versus 1/T; and (d) Half-life plot for log (weight loss) versus immersion time in 20% acetic acid (1: UPMT; 2: NPMT; 3: PPMT; 4: HPMT; 5: Blank)

Fig. 3 — Langmuir's adsorption isotherm plots for the adsorption of various inhibitors on the surface of mild steel in a) 20% formic acid b) 20% acetic acid. (1: UPMT; 2: NPMT; 3: PPMT; 4: HPMT; 5: Blank)

Fig. 4 — Potentiodynamic polarization curves for aluminium containing 500-ppm concentration of various azathiones in a) 20% formic acid b) 20% acetic acid. (1:Blank; 2: HPMT; 3: PPMT; 4: NPMT; 5: UPMT)

Fig. 5 — Scanning electron micrographs for
a) Polished mild steel b) Mild steel in 20% formic acid c) Mild steel in 20% formic acid + 500ppm UPMT

JCSE The Journal of Corrosion Science and Engineering
ISSN 1466-8858 Volume 10 Preprint 12 18 September 2006

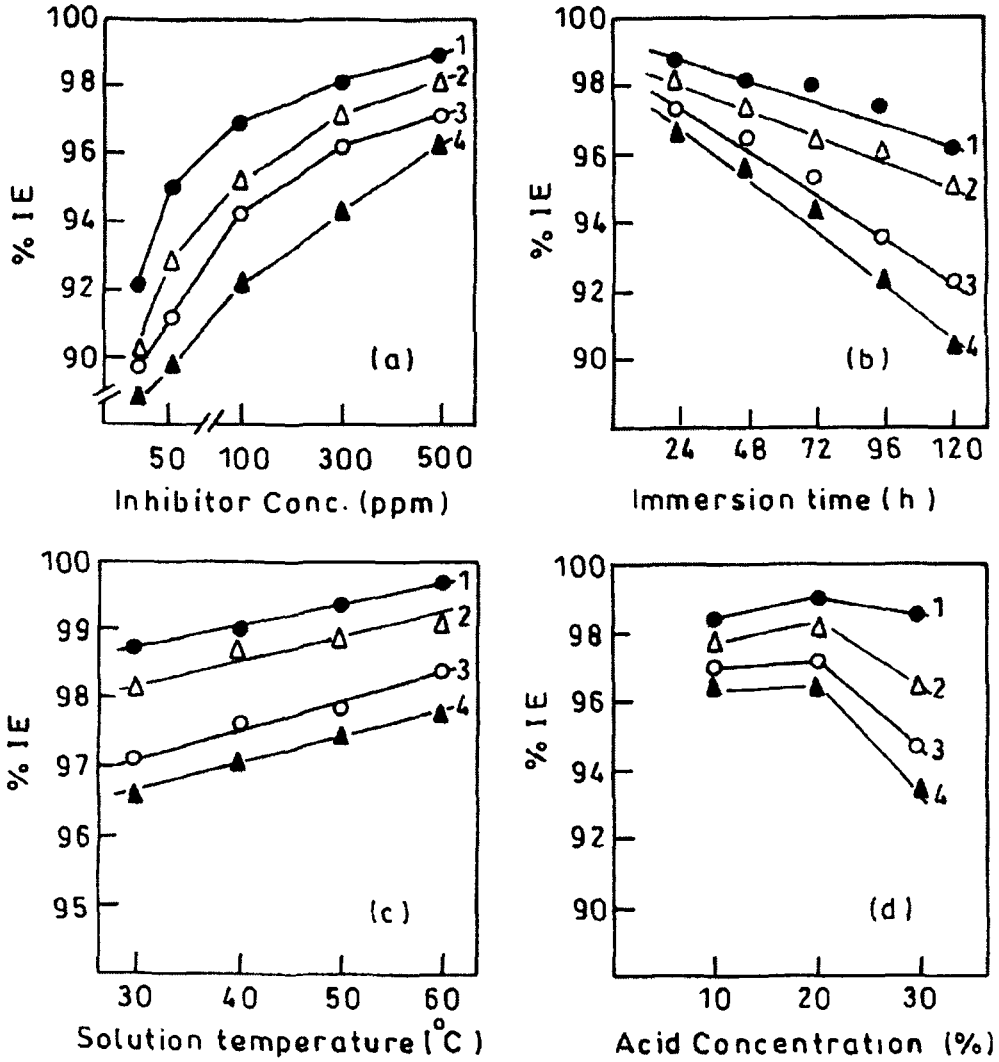

Fig. 1

JCSE The Journal of Corrosion Science and Engineering
ISSN 1466-8858 Volume 10 Preprint 12 18 September 2006

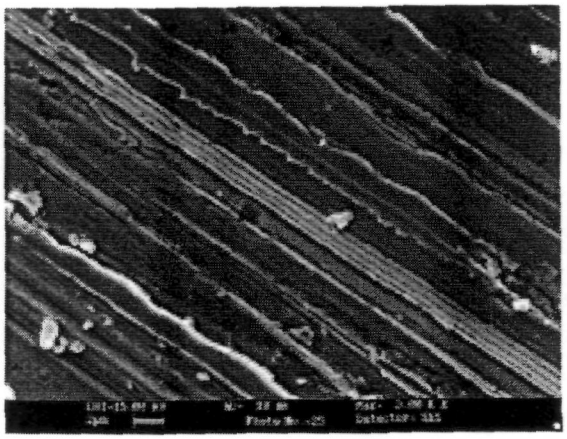

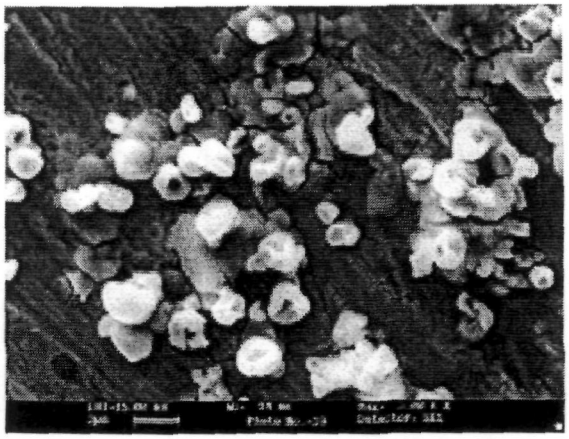

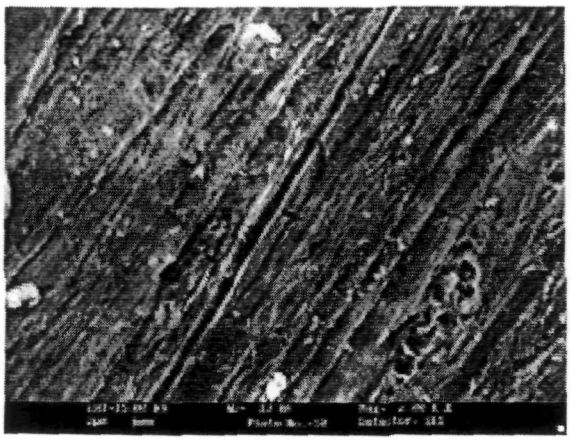

Scanning electron micrographs for
a) Polished mild steel b) Mild steel in 20% formic acid c) Mild steel in 20% formic acid + 500ppm UPMT

JCSE The Journal of Corrosion Science and Engineering
ISSN 1466-8858 Volume 10 Preprint 12 18 September 2006

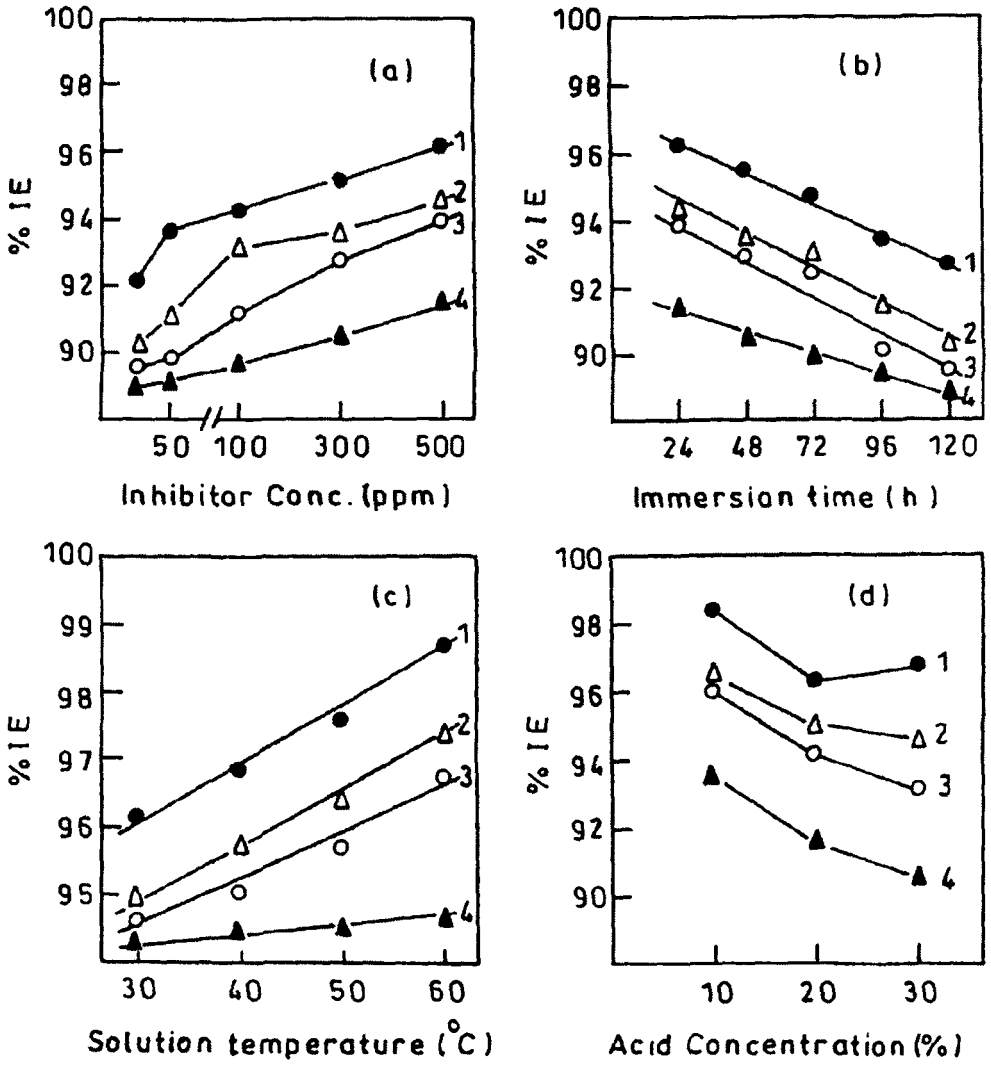

Fig.1'

JCSE The Journal of Corrosion Science and Engineering
ISSN 1466-8858 Volume 10 Preprint 12 18 September 2006

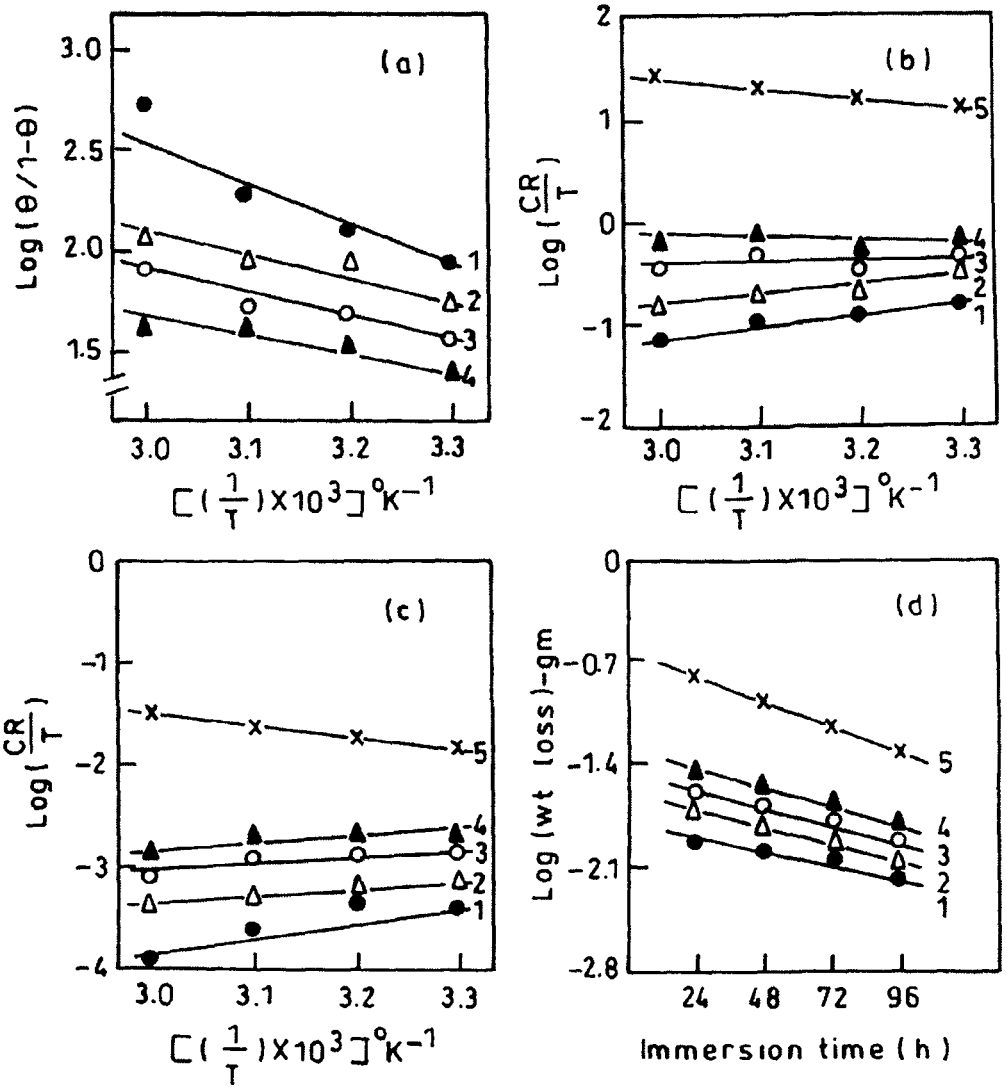

Fig. 2

JCSE The Journal of Corrosion Science and Engineering
ISSN 1466-8858 Volume 10 Preprint 12 18 September 2006

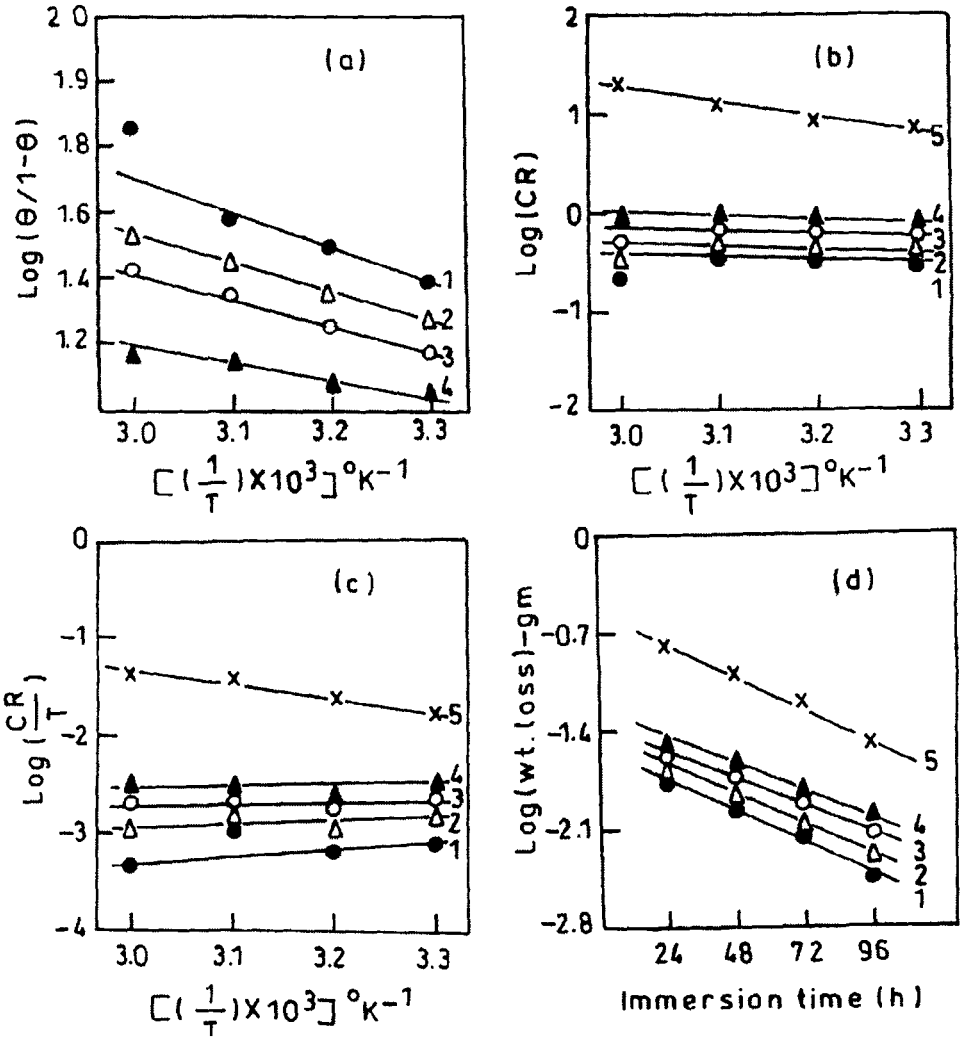

Fig. 2'

JCSE The Journal of Corrosion Science and Engineering
ISSN 1466-8858 Volume 10 Preprint 12 18 September 2006

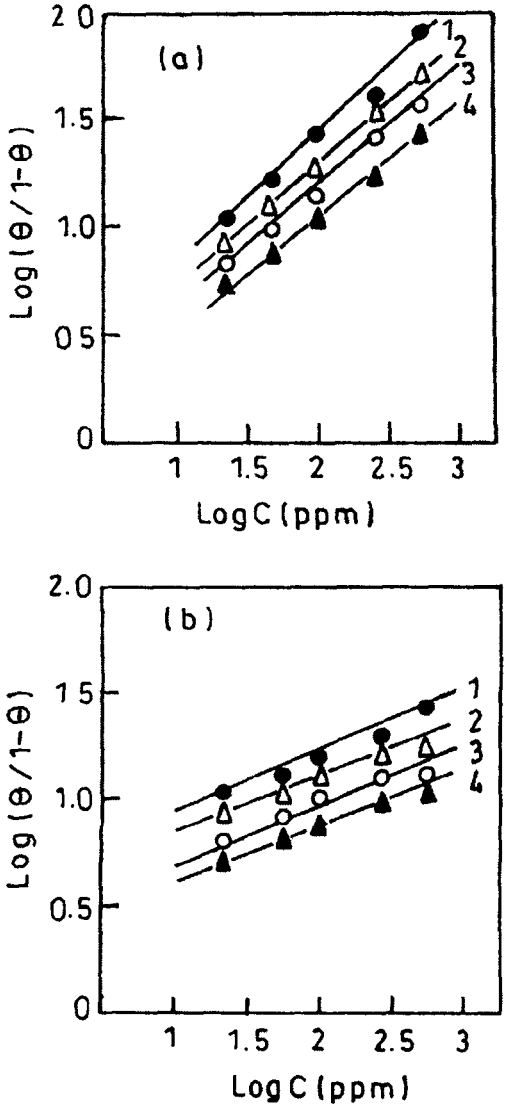

Fig. 3a & 3b

JCSE The Journal of Corrosion Science and Engineering
ISSN 1466-8858 Volume 10 Preprint 12 18 September 2006

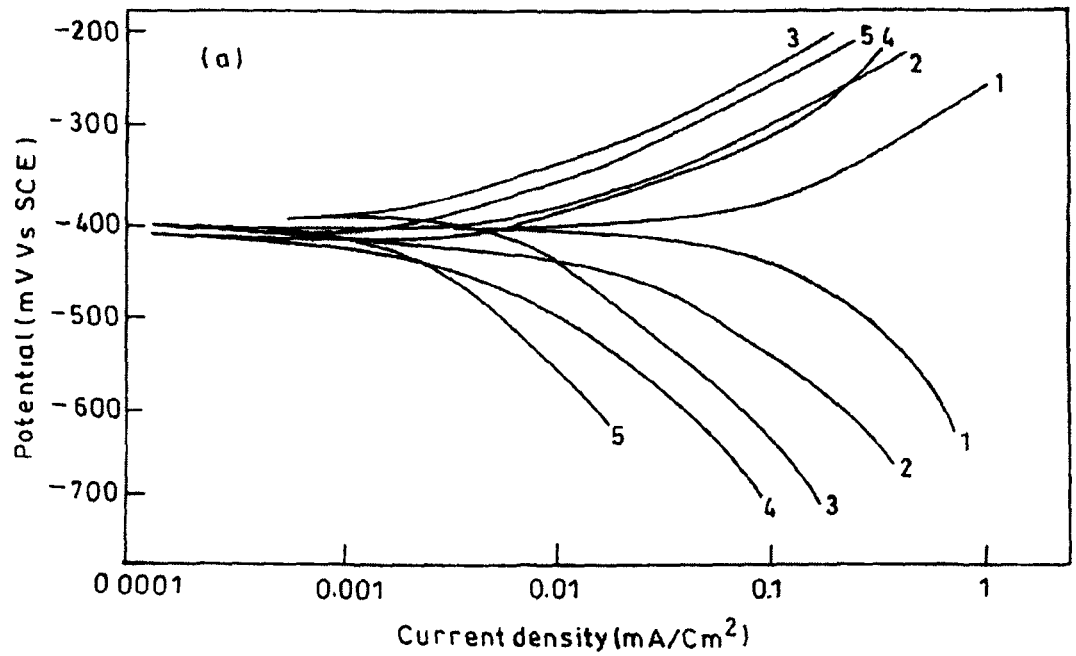

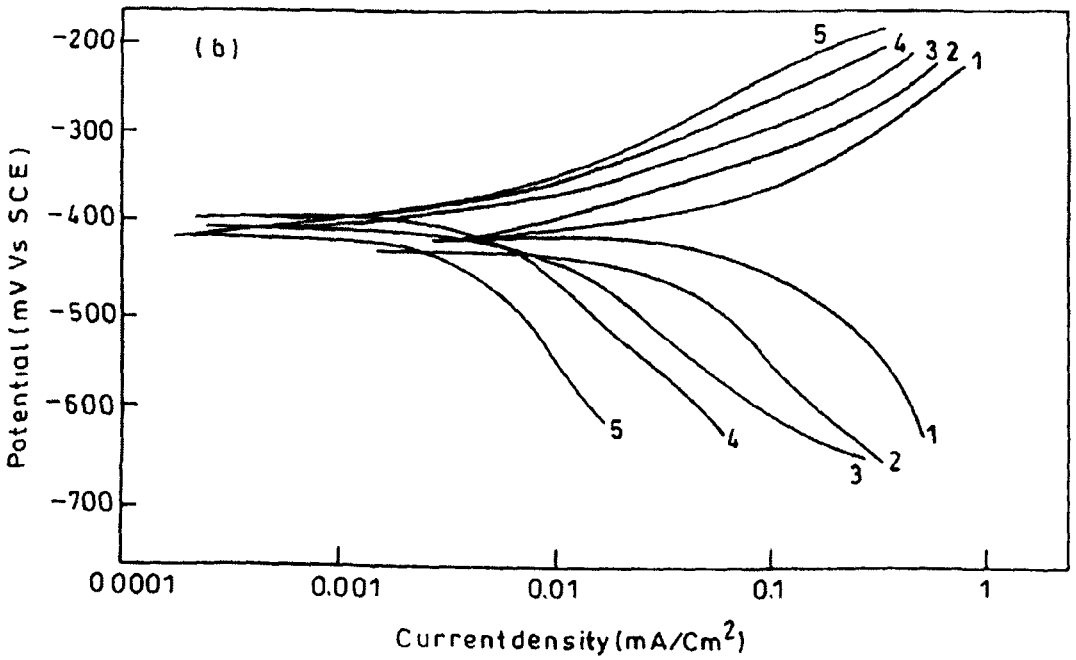

Fig. 4a & 4b